

N° d'ordre : 4250



THÈSE

Présentée à

L'UNIVERSITÉ DE BORDEAUX 1

ÉCOLE DOCTORALE DES SCIENCES CHIMIQUES

Par **DAKSHINAMOORTHY DEIVASAGAYAM**

Pour obtenir le grade de

DOCTEUR

Spécialité : Polymères

**TITANIUM COMPLEXES BASED ON AMINODIOL LIGAND FOR
RING OPENING POLYMERIZATION OF CYCLIC ESTERS**

Soutenue le 6 Avril 2011

Devant la commission d'examen formée de :

Mme S .M. Guillaume

M P.J. Lutz

M J.-J. Robin

M F. Peruch

M H. CRAMAIL

Chargé de recherche, CNRS, Rennes

Directeur de recherche, CNRS, Strasbourg

Professeur, Université Montpellier

Chargé de recherche, CNRS

Professeur, Université Bordeaux 1

Rapporteur

Rapporteur

Examineur

Examineur

Examineur

Acknowledgements

I would like to express my heart-felt gratitude to Prof. Yves GNANOU and Prof. Henri CRAMAIL for giving me an opportunity to do Ph.D in LCPO, University of Bordeaux. First and foremost, I would like to thank my research Supervisor Prof. Alain DEFFIEUX. He is a Senior Research Scientist and it was a privilege for me to work under his guidance. I would like to express my deepest gratitude to my research Supervisor Dr. Frédéric PERUCH for his enthusiastic guidance, inspiration, support and encouragement throughout the course of my research. I would also like to thank the members of Jury, Dr. S.M. Guillaume, Dr. P.J. Lutz, Prof. J.-J. Robin, Prof. H. Cramail for accepting to evaluate my thesis.

My sincere thanks to Mme. Catherine ROULINAT, Mme. Corinne GONÇALVES, Mme. Bernadette GUILLABERT and Mme. Nicole GABRIEL for their love and kind help in the administrative work. I am very much thankful to M. Michel SCHAPPACHER for his kind help in NMR and SEC techniques. I would also like to thank M. Nicolas GUIDOLIN for his kind help in SEC analysis. I thank M. Emmanuel IBARBOURE for his help in thermal analysis. I would also like to express my sincere thanks to M. Noël PINAUD, M. Jean-Michel LASNIER for their help in Homonuclear Decoupled NMR spectroscopic techniques. I am very grateful to Mme. Marie-Hélène LESCURE for her kind help in HPLC analysis. I would also like to thank Mme. Christelle ABSALON for her help in MALDI-TOF mass spectroscopic analysis.

I am highly indebted to my former colleagues Dr. G. Manickam, Dr. P. Sudhakar, Dr. Vijakrishna Kari, Dr. Karthikeyan for their wonderful help, encouragement and advices during the start of my research career in Indian Institute of Technology (IIT). I am extremely grateful to Dr. Palaskar, Dr. Arvind More, Dr. Harikrishna, Dr. Aurélie Boyer, Célia Nicolet, Dr. Maryline Costa for their help and creating good working atmosphere in the lab. I would like to express my special thanks to Dr. Bertrand HEURTEFEU for his timely help. I wish to thank all my research colleagues and friends in LCPO Dr. Mumtaz, Samira, Maréva, Stéphanie, Vincent, Julie, Maité, Na Liu, Chantal, Cédric, Dargie, Anne-laure, Dr. Gabriel, Reynaldo, Dr. Jean, Dr. Julien pinaud.

I would like to express my heartfelt gratitude to my friends, Logudurai, Karthikeyan, Srinivasan, Shanthi, Agalya, Sivakumar, Kavitha, Mathi, Tanuja, Kiran, Harikrishna, Anitha, Anand, Louise, Mythili, Bharani, Palaskar, Arun, Arvind for their support and help.

Last, but certainly not least, with great pleasure I would like to express my thanks to my parents, brothers and sisters for their love, support and encouragement throughout my life.

Dakshinamoorthy Deivasagayam

Dedication

This dissertation is dedicated to my beloved parents

DEIVASAGAYAM and SUSILA DEIVASAGAYAM

and also to my (late) Prof. G. SUNDARARAJAN

Abstract

A series of titanium isopropoxides complexes coordinated by *enantiopure*, *racemic*, *meso* and *diastereomeric* aminodiol ligands have been prepared and characterized by spectroscopic techniques. The complexes were tested as initiators for the ring opening polymerization (ROP) of cyclic esters such as L/*rac*-lactide, caprolactone, butyrolactone and trimethylene carbonate *via* coordination-insertion mechanism. In lactide polymerizations, all complexes showed significant activity both in solution at 70°C and in bulk at 130°C with a good control. The complex derived from *rac*-aminodiol ligand gave partially heterotactic polylactide in ROP of *rac*-lactide, whereas all other complexes yielded atactic polylactides. For caprolactone polymerizations, all complexes were found to be effective initiators under both solution and bulk conditions (up to 60% monomer conversion was reached within 10 min in bulk condition at 70°C), again with good control. Kinetic studies of ROP of lactides and caprolactone in solution conditions have been investigated and showed a first kinetic order in monomer. Significant activities were also observed for (ROP) of butyrolactone and trimethylene carbonate. Block copolymers of caprolactone and lactides were successfully synthesized with these catalytic systems by sequential polymerization techniques. The complexes were also tested as initiators for the production of random copolymers containing caprolactone and lactides and a reverse order of reactivity was observed between lactide and caprolactone compared to homopolymerization.

Résumé

Une série de complexes à base de titane porteurs de ligands aminodiols de différentes configuration (mélange de diastéréoisomère, *meso*, racémique ou chiral) ont été synthétisés et caractérisés par différentes techniques spectroscopiques. Ces complexes ont ensuite été utilisés comme amorceurs pour la polymérisation par ouverture de cycles de différents monomères hétérocycliques (L/*rac*-lactide, caprolactone, butyrolactone et triméthylène carbonate) *via* un mécanisme de coordination-insertion. Tous les complexes se sont révélés efficaces pour la polymérisation des lactides que ce soit en solution à 70°C ou en masse à 130°C avec un bon contrôle. Lors de la polymérisation du *rac*-lactide, le complexe porteur du ligand racémique a permis d'obtenir un polylactide partiellement heterotactique, alors que tous les autres complexes n'ont conduit qu'à des polymères atactiques. Tous les complexes se sont également révélés très actifs pour la polymérisation de la caprolactone aussi bien en solution qu'en masse à 70°C avec un bon contrôle. Des études cinétiques réalisées en solution ont permis de mettre en évidence un ordre cinétique unitaire en monomère. De bonnes activités ont également été obtenues pour la polymérisation de la butyrolactone et du triméthylène carbonate. De plus, le bon contrôle de ce type de la polymérisation a permis de synthétiser des copolymères à blocs du L/*rac*-lactide et de caprolactone. Enfin, la copolymérisation aléatoire de ces 2 monomères a permis de mettre en évidence une réactivité inversée par rapport aux réactions d'homopolymérisation.

Table of Contents

Description	Page No.
Abstract.....	1
List of Tables.....	9
List of Schemes.....	10
List of Figures.....	13
List of Abbreviations.....	18
General Introduction.....	23
CHAPTER 1 Literature Review	
1.1. Introduction.....	29
1.2. Synthesis of polyesters: some generalities.....	30
1.2.1. Step growth polymerization.....	30
1.2.2. Ring Opening Polymerization.....	31
1.2.2.1. Anionic Ring Opening Polymerization.....	32
1.2.2.2. Cationic Ring Opening Polymerization.....	32
1.2.2.3. Organocatalyzed and Enzymatic (ROP)	34
1.2.2.4. Coordination-Insertion Ring Opening Polymerization.....	36
1.3. Polylactide (PLA) and Polycaprolactone (PCL).....	39
1.3.1. Polylactide (PLA).....	39
1.3.1.1. Generalities on PLA.....	39
1.3.1.2. Stereochemistry and Microstructure of PLA.....	39
1.3.2. Polycaprolactone (PCL).....	42
1.4. Ring Opening Polymerization of cyclic esters with heteroleptic complexes.....	43
1.4.1. Stereoselective ROP of Lactide.....	43
1.4.1.1. Mechanism of Stereocontrol Polymerization of Lactide.....	43
1.4.1.2. Synthesis of Stereoblock PLA from <i>rac</i> -lactide.....	45
1.4.1.3. Synthesis of Heterotactic PLA from <i>rac</i> -lactide.....	47
1.4.2. Group (IV) Metal Complexes for ROP of Cyclic Esters.....	48
1.4.2.1. Bis(phenolate) Group 4 metal Complexes.....	48
1.4.2.2. (Di)amine bis(phenolate) Group 4 metal Complexes.....	52

1.4.2.3.	Amine tris(phenolate) Group 4 metal Complexes.....	59
1.4.2.4.	Titanatranes Group 4 metal Complexes.....	62
1.4.2.5.	Dialkanolamine Titanocanes and Spirobititanocane Complexes.....	64
1.4.2.6.	Sulfonamide ligands Group 4 metal Complexes.....	66
1.4.2.7.	Dithiodiolate ligands Group 4 metal Complexes.....	67
1.4.2.8.	Schiff base ligands Group 4 metal Complexes.....	68
1.4.3.	Comparitive studies of group (IV) metal complexes in ROP of ϵ -CL and Lactides.....	71
1.5.	Conclusion.....	72
1.6.	References.....	79

**CHAPTER 2 Synthesis and Characterization of Titanium alkoxide and
Halfsandwich Complexes based on Aminodiol Ligands**

2.1.	Introduction.....	87
2.2.	Results and Discussion.....	88
2.2.1.	Synthesis of aminodiol.....	88
2.2.2.	Separation of diastereomeric aminodiol.....	89
2.2.3.	^1H and ^{13}C NMR spectroscopy of ligands 1-4- H_2	89
2.2.4.	Synthesis of Titanium and Zirconium alkoxide Complexes.....	93
2.2.4.1.	Characterization of Titanium complex 1- $\text{Ti}(\text{O}^i\text{Pr})_2$	93
2.2.4.2.	Characterization of Titanium complex 2- $\text{Ti}(\text{O}^i\text{Pr})_2$	95
2.2.4.3.	Characterization of Titanium complex 3- $\text{Ti}(\text{O}^i\text{Pr})_2$	96
2.2.4.4.	Characterization of Titanium complex 4- $\text{Ti}(\text{O}^i\text{Pr})_2$	97
2.2.4.5.	Characterization of Zirconium complex 3- $\text{Zr}(\text{O}^t\text{Bu})_2$	99
2.2.5.	Synthesis and Characterization of Half-sandwich titanium complexes based on aminodiol ligands.....	100
2.2.6.	Synthesis and Characterization of Half-sandwich titanium complexes based on tetradentate aminotriol ligands.....	102
2.3.	Conclusion.....	105
2.4.	References.....	106

CHAPTER 3 Ring-Opening Polymerization of *L*-lactide and *rac*-lactide

3.1.	Introduction.....	109
3.2.	Results and Discussion.....	110
3.2.1.	Solution Polymerizations.....	110
3.2.1.1.	Polymerization of <i>L</i> -lactide and <i>rac</i> -lactide.....	110
3.2.1.2.	Poly(<i>L</i> / <i>rac</i> -lactide) characterization.....	113
3.2.1.2.1.	Determination of molecular weights by SEC with triple detection.....	113
3.2.1.2.2.	¹ H and ¹³ C NMR analysis.....	115
3.2.1.2.3.	MALDI-TOF mass spectrometry analysis....	118
3.2.1.2.4.	DSC analysis of PLLA and PDLLA.....	121
3.2.1.2.5.	Stereoselectivity of <i>rac</i> -LA polymerization with 1-4-Ti(O ^{<i>i</i>} Pr) ₂ complexes.....	121
3.2.1.3.	Kinetics studies of <i>L</i> / <i>rac</i> -lactide polymerization.....	126
3.2.2.	Bulk Polymerization.....	129
3.3.	Conclusion.....	133
3.4.	References.....	134

CHAPTER 4 Ring Opening Polymerization (ROP) of ϵ -Caprolactone, *rac*- β -Butyrolactone and Trimethylene Carbonate

4.1.	Ring Opening Polymerization of ϵ -caprolactone.....	139
4.1.1.	Introduction.....	139
4.1.2.	Results and Discussion.....	139
4.1.2.1.	Solution polymerization of ϵ -caprolactone.....	139
4.1.2.2.	Effect of [M]/[Ti] ratio.....	141
4.1.2.3.	Characterization of PCL.....	143
4.1.2.4.	Kinetic studies of ϵ -caprolactone polymerization.....	148
4.1.2.5.	Bulk polymerization of ϵ -caprolactone.....	152
4.2.	Ring Opening Polymerization of <i>rac</i> - β -Butyrolactone.....	154
4.2.1.	Introduction.....	154
4.2.2.	Results and Discussion.....	155

4.3.	Ring Opening Polymerization of Trimethylene carbonate.....	158
4.3.1.	Introduction.....	158
4.3.2.	Results and Discussion.....	158
4.3.2.1.	Solution polymerization of Trimethylene carbonate.....	159
4.3.2.2.	Bulk polymerization of Trimethylene carbonate.....	165
4.4.	Conclusion.....	166
4.5.	References.....	167

CHAPTER 5 Living Ring-Opening Block and Random copolymerization of ϵ -Caprolactone, L- and *rac*-Lactide

5.1.	Introduction.....	171
5.2.	Results and Discussion.....	174
5.2.1.	Diblock copolymer synthesis.....	174
5.2.1.1.	PCL- <i>block</i> -PLLA.....	174
5.2.1.2.	PLLA- <i>block</i> -PCL.....	177
5.2.1.3.	PDLLA- <i>block</i> -PCL.....	182
5.2.2.	Triblock copolymer synthesis.....	186
5.2.2.1.	PCL- <i>block</i> -PLLA- <i>block</i> -PCL.....	186
5.2.2.2.	PLLA- <i>block</i> -PCL- <i>block</i> -PLLA.....	189
5.2.3.	Random copolymerizations.....	192
5.3.	Conclusion.....	201
5.4.	References.....	202

CHAPTER 6 Experimental Section

6.1.	General Experimental Details.....	207
6.1.1.	Chemical Materials.....	207
6.1.2.	Purification of solvents.....	207
6.1.3.	Purification of Monomers.....	207
6.2.	Synthesis and Characterization of Ligands.....	208
6.2.1.	Synthesis and Characterization of Ligand 1-H ₂	208
6.2.2.	Synthesis and Characterization of Ligand 4-H ₂ , 2-H ₂ , 3-H ₂	208

6.2.3.	Synthesis and Characterization of Ligand 5-H ₃	210
6.2.4.	Synthesis and Characterization of Ligand 6-H ₂	211
6.3.	Synthesis and Characterization of Complexes.....	211
6.3.1.	Synthesis and Characterization of Titanium and Zirconium alkoxide complexes.....	211
6.3.1.1.	Synthesis and Characterization of complex 1-Ti(O ⁱ Pr) ₂	211
6.3.1.2.	Synthesis and Characterization of complex 2-Ti(O ⁱ Pr) ₂	211
6.3.1.3.	Synthesis and Characterization of complex 3-Ti(O ⁱ Pr) ₂	213
6.3.1.4.	Synthesis and Characterization of complex 4-Ti(O ⁱ Pr) ₂	214
6.3.1.5.	Synthesis and Characterization of complex 3-Zr(O ⁱ Pr) ₂	214
6.3.2.	Synthesis and Characterization of Half-sandwich Titanium complexes.....	215
6.3.2.1.	Synthesis and Characterization of complex 4-C _p TiCl[O,O,N]....	215
6.3.2.2.	Synthesis and Characterization of complex 4-C _p *TiCl[O,O,N]....	216
6.3.2.3.	Synthesis and Characterization of complex 6-C _p TiCl[O,O,N]....	217
6.4.	General procedure for solution polymerization.....	217
6.4.1.	Solution polymerization of Lactides.....	218
6.4.2.	Solution polymerization of ε-caprolactone	218
6.4.3.	Solution polymerization of β-Butyrolactone.....	219
6.4.4.	Solution polymerization of Trimethylene carbonate.....	219
6.5.	General procedure for Kinetic Studies on Lactide and ε-caprolactone polymerization.....	220
6.6.	Synthesis and Characterization of Block copolymers.....	220
6.6.1.	Synthesis of Poly(ε-caprolactone- <i>block-L</i> -lactide).....	220
6.6.2.	Synthesis of Poly(<i>L</i> -lactide- <i>block-ε</i> -caprolactone).....	221
6.6.3.	Synthesis of Poly(<i>DL</i> -lactide- <i>block-ε</i> -caprolactone).....	222
6.6.4.	Synthesis of Poly(TMC- <i>block-ε</i> -caprolactone).....	222
6.6.5.	Synthesis of Poly(ε-CL- <i>block-L</i> -LA- <i>block-ε</i> -CL).....	223
6.6.6.	Synthesis of Poly(<i>L</i> -LA- <i>block-ε</i> -CL- <i>block-L</i> -LA).....	224
6.7.	General procedure for Bulk polymerization.....	224

6.8.	Random copolymerization.....	225
6.8.1.	Synthesis of Poly(ϵ -caprolactone- <i>co</i> - <i>DL</i> -lactide).....	225
6.8.2.	Synthesis of Poly(ϵ -caprolactone- <i>co</i> - <i>L</i> -lactide).....	225
6.9.	Instrumentation and Characterization methods.....	226

GENERAL CONCLUSIONS.....231

List of Tables

Table 1.1.	Physical Properties of PCL.....	42
Table 1.2.	Ring Opening Polymerization of <i>L</i> -lactide in solution condition.....	73
Table 1.3.	Ring Opening Polymerization of <i>L</i> -lactide in bulk condition.....	74
Table 1.4.	Ring Opening Polymerization of <i>rac</i> -lactide in solution condition.....	75
Table 1.5.	Ring Opening Polymerization of <i>rac</i> -lactide in bulk condition.....	76
Table 1.6.	Ring Opening Polymerization of ϵ -CL in solution and bulk condition.....	78
Table 3.1.	Solution Polymerization of <i>L</i> -Lactide.....	111
Table 3.2.	Solution Polymerization of <i>rac</i> -Lactide.....	112
Table 3.3.	Tetrad Probabilities of PDLLA based on Bernoullian Statistics.....	122
Table 3.4.	First Order Propagation Rate Constant (K_{app}) for <i>L</i> / <i>rac</i> -LA (ROP).....	128
Table 3.5.	Bulk Polymerization of <i>L</i> -Lactide.....	129
Table 3.6.	Bulk Polymerization of <i>rac</i> -Lactide.....	130
Table 4.1.	Solution Polymerization of ϵ -Caprolactone.....	140
Table 4.2.	Polymerization of ϵ -caprolactone at different [M]/[Ti] ratio using 4-Ti(O ⁱ Pr) ₂	141
Table 4.3.	First Order Propagation Rate Constant (K_{app}) for ϵ -CL polymerization.....	149
Table 4.4.	Bulk Polymerization of ϵ -caprolactone.....	153
Table 4.5.	Bulk polymerization of TMC using initiator 4-Ti(O ⁱ Pr) ₂	165
Table 5.1.	Synthesis of Diblock copolymer PCL- <i>block</i> -PLLA.....	174
Table 5.2.	Synthesis of Diblock copolymer PLLA- <i>block</i> - PCL.....	178
Table 5.3.	Synthesis of Diblock copolymer PDLLA- <i>block</i> -PCL.....	183
Table 5.4.	Synthesis of Triblock copolymer PCL- <i>b</i> -PLLA- <i>b</i> -PCL.....	186
Table 5.5.	Synthesis of Triblock copolymer PLLA- <i>b</i> -PCL- <i>b</i> -PLLA.....	189
Table 5.6.	Copolymerization of ϵ -CL and <i>D,L</i> -Lactide with 4-Ti(O ⁱ Pr) ₂ in Solution.....	193
Table 5.7.	Copolymerization of ϵ -CL and <i>D,L</i> -Lactide with 4-Ti(O ⁱ Pr) ₂ in Bulk.....	199

List of Schemes

Scheme 1.1.	Lactic acid and Glycolic acid and their derived homo and copolymers	29
Scheme 1.2.	Structure of ϵ -caprolactone, Lactide and Glycolide	30
Scheme 1.3.	Synthesis of aliphatic polyesters by step growth Polycondensation	31
Scheme 1.4.	ROP of unsubstituted lactones, lactides and glycolides	31
Scheme 1.5.	Anionic ROP Mechanism	32
Scheme 1.6.	Proposed pathway for cationic ROP of Lactide	33
Scheme 1.7.	Proposed activated monomer pathway for cationic ROP of Lactide	33
Scheme 1.8.	Bifunctional activated mechanism using hydrogen bonding thiourea catalyst	34
Scheme 1.9.	Plausible Mechanism for the Nucleophilic ROP of Lactide	35
Scheme 1.10.	Mechanism of Lipase-Catalyzed Polymerization of Lactones	35
Scheme 1.11.	Structure of tin(II)octanoate, aluminum(III)isopropoxide, zinc(II)lactate	36
Scheme 1.12.	Coordination-Insertion Mechanism for lactide polymerization using metal alkoxide catalyst	37
Scheme 1.13.	Schematic representations for the transesterification side reactions.....	38
Scheme 1.14.	Stereoisomers of Lactides	40
Scheme 1.15.	Microstructures of polylactides	41
Scheme 1.16.	Stereoselective complexes for ROP of <i>rac</i> -lactide.....	45
Scheme 1.17.	Proposed Mechanism of Stereoblock PLA from <i>rac</i> -lactide.....	46
Scheme 1.18.	Stereoselective complexes for heterotactic ROP of <i>rac</i> -LA	47
Scheme 1.19.	Bis(phenolate) titanium complexes	49
Scheme 1.20.	Formation of 2 polymeric chains for 1 molecule of catalyst during ROP of ϵ -CL	49
Scheme 1.21.	Titanium based Heterobimetallic complexes based on bulky Bis(phenolates)	52

Scheme 1.22.	Tetradentate amine bis(phenolate) ligands and the corresponding complexes.....	53
Scheme 1.23.	Dianionic tetradentate amine bis(phenolate)titanium Complexes	56
Scheme 1.24.	Synthesis and interconversion of mononuclear and dinuclear titanium complexes.....	57
Scheme 1.25.	Dianionic tridentate amine bis(phenolate)titanium complexes.....	59
Scheme 1.26.	Amino tris(phenolate) Group 4 metal alkoxide complexes.....	59
Scheme 1.27.	Titanatranes alkoxide complexes	62
Scheme 1.28.	Mono, di and trinuclear titanium alkoxide complexes	63
Scheme 1.29.	Titanocanes and Spirotitanocene complexes for ROP of ϵ -CL.....	65
Scheme 1.30.	Sulfonamide supported Group4 metal complexes.....	66
Scheme 1.31.	Dithiodiolate ligand Group 4 metal complexes	67
Scheme 1.32.	Schiff base ligands Group 4 metal complexes	68
Scheme 2.1.	Titanium alkoxide complexes of different symmetry based on aminodiol ligands	88
Scheme 2.2.	Synthesis of <i>chiral</i> (1-H ₂) and <i>diastereomeric</i> (4-H ₂) aminodiol....	88
Scheme 2.3.	Diastereomers of aminodiol.....	89
Scheme 2.4.	Synthesis of Titanium Alkoxide Complexes 1-4-Ti(O ⁱ Pr) ₂	93
Scheme 2.5.	Synthesis of complex 3-Zr(O ^t Bu) ₂ from <i>meso</i> -aminodiol-3H ₂	99
Scheme 2.6.	Synthesis of titanium half-sandwich complexes based on aminodiol ligands.....	100
Scheme 2.7.	Synthesis of titanium half-sandwich complexes 6-C _p TiCl[O,O,O,N] based on tetradentate dianionic ligand.....	103
Scheme 3.1.	Titanium alkoxide complexes.....	110
Scheme 3.2.	Solution Polymerization of <i>L</i> -lactide using 1-4-Ti(O ⁱ Pr) ₂	110
Scheme 3.3.	Solution Polymerization of <i>rac</i> -lactide using 1-4-Ti(O ⁱ Pr) ₂	112
Scheme 3.4.	Transesterification side reactions by coordination insertion mechanism.....	119
Scheme 3.5.	Structures of possible tetrads of Poly(<i>rac</i> -lactide).....	122

Scheme 3.6.	Preparation of Heterotactic PLA using the catalyst 2-Ti(O ⁱ Pr) ₂ in toluene at 70°C.....	124
Scheme 4.1.	Titanium alkoxide complexes.....	139
Scheme 4.2.	Schematic representation of formation of two growing polymer chains per molecule of the catalyst.....	147
Scheme 4.3.	Proposed mechanism of ε-caprolactone polymerization <i>via</i> coordination-insertion mechanism.....	147
Scheme 4.4.	Possible modes of ROP of β-butyrolactone (BBL) for anionic/“coordination-insertion” processes (Nu = nucleophile, [M] = metal); (a) Acyl-oxygen cleavage and (b) Alkyl oxygen cleavage.....	154
Scheme 4.5.	Microstructures of Poly(3-hydroxybutyrate) (PHB).....	155
Scheme 4.6.	ROP of <i>rac</i> -β-butyrolactone (BBL) using 1-Ti(O ⁱ Pr) ₂ in toluene at 70°C.....	155
Scheme 4.7.	Elimination reactions of PHBs by metal catalysts.....	156
Scheme 4.8.	Ring Opening Polymerization of TMC initiated with 4-Ti(O ⁱ Pr) ₂ in toluene at 70°C.....	159
Scheme 4.9.	Ring Opening modes of Trimethylene carbonate.....	159
Scheme 4.10.	Sequential synthesis of block copolymer PTMC- <i>b</i> -PCL.....	161
Scheme 5.1.	Sequential polymerization of LA and CL accompanied by the bimolecular transesterification.....	172
Scheme 5.2.	Schematic representation of sequential diblock and triblock copolymer synthesis.....	173
Scheme 5.3.	Copolymerization of ε-caprolactone with <i>D,L</i> -Lactide using the initiator 4-Ti(O ⁱ Pr) ₂	193

List of Figures

Figure 1.1.	Schematic representation of the single site catalysis of the form L_nM-OR	38
Figure 1.2.	Life Cycle of PLA.....	39
Figure 2.1.	HPLC traces of <i>diastereomeric</i> aminodiol.....	89
Figure 2.2.	1H -NMR spectrum of <i>diastereomeric</i> aminodiol 4- H_2	90
Figure 2.3.	1H -NMR spectrum of <i>meso</i> aminodiol 3- H_2	91
Figure 2.4.	1H -NMR spectrum of <i>racemic</i> aminodiol 2- H_2	91
Figure 2.5.	1H -NMR spectrum of <i>Chiral</i> aminodiol 1- H_2	91
Figure 2.6.	^{13}C -NMR spectrum of <i>diastereomeric</i> aminodiol 4- H_2	92
Figure 2.7.	^{13}C -NMR spectrum of <i>meso</i> aminodiol 3- H_2	92
Figure 2.8.	^{13}C -NMR spectrum of <i>racemic</i> aminodiol 2- H_2	92
Figure 2.9.	1H -NMR spectrum of 1- $Ti(O^iPr)_2$	94
Figure 2.10.	^{13}C -NMR spectrum of 1- $Ti(O^iPr)_2$	94
Figure 2.11.	1H -NMR) spectrum of 2- $Ti(O^iPr)_2$	95
Figure 2.12.	^{13}C -NMR spectrum of 2- $Ti(O^iPr)_2$	96
Figure 2.13.	1H -NMR spectrum of 3- $Ti(O^iPr)_2$	97
Figure 2.14.	^{13}C -NMR spectrum of 3- $Ti(O^iPr)_2$	97
Figure 2.15.	1H -NMR spectrum of 4- $Ti(O^iPr)_2$	98
Figure 2.16.	^{13}C -NMR spectrum of 4- $Ti(O^iPr)_2$	98
Figure 2.17.	1H -NMR spectrum of 3- $Zr(O^iBu)_2$	100
Figure 2.18.	1H NMR spectrum of complex 4- $C_pTiCl[O,O,N]$	101
Figure 2.19.	1H NMR spectrum of complex 4- $C_p^*TiCl[O,O,N]$	102
Figure 2.20.	1H NMR spectrum of <i>diastereomeric</i> aminotriol 5- H_3	103
Figure 2.21.	1H NMR spectrum of <i>diastereomeric</i> aminodiol 6- H_2	104
Figure 2.22.	1H NMR spectrum of complex 6- $C_pTiCl[O,O,O,N]$	105
Figure 3.1.	SEC Chromatogram of PDLLA prepared using 4- $Ti(O^iPr)_2$ with $[M]/[Ti] = 100$	114
Figure 3.2.	SEC Chromatogram of PLLA (Table 3.1, entry 4).....	114
Figure 3.3.	1H NMR spectrum of PLLA prepared using 4- $Ti(O^iPr)_2$	115
Figure 3.4.	1H NMR spectrum of PDLLA prepared using 4- $Ti(O^iPr)_2$	116

Figure 3.5.	^{13}C NMR spectrum of PLLA prepared using 4-Ti(O ⁱ Pr) ₂	117
Figure 3.6.	^{13}C NMR spectrum of PDLLA prepared using 4-Ti(O ⁱ Pr) ₂	117
Figure 3.7.	MALDI-TOF mass spectrum of PLLA prepared using 1-Ti(O ⁱ Pr) ₂ in toluene solution at 70°C.....	119
Figure 3.8.	MALDI-TOF mass spectrum of PDLLA prepared using 1-Ti(O ⁱ Pr) ₂ in toluene solution at 70°C with [M]/[Ti] = 50.....	121
Figure 3.9.	DSC thermograms of (a) PLLA and (b) PDLLA prepared using 1-Ti(O ⁱ Pr) ₂ in toluene at 70°C with [M]/[Ti] = 100.....	121
Figure 3.10.	$^{13}\text{C}\{^1\text{H}\}$ NMR spectrum of the methine and carbonyl region of PDLLA obtained by using 1-4-Ti(O ⁱ Pr) ₂ at 70°C in toluene.....	123
Figure 3.11.	Homonuclear decoupled ^1H NMR spectrum of the methine region of PDLLA prepared with 2-Ti(O ⁱ Pr) ₂ at 70°C.....	124
Figure 3.12.	Homonuclear decoupled ^1H NMR spectrum of the methine region of PDLLA prepared with 1, 3 & 4-Ti(O ⁱ Pr) ₂ at 70°C.....	125
Figure 3.13.	First order kinetic plot for <i>L</i> -LA consumption vs time using 1-Ti(O ⁱ Pr) ₂	127
Figure 3.14.	First order kinetic plot for <i>rac</i> -LA consumption vs time using 1-Ti(O ⁱ Pr) ₂	127
Figure 3.15.	Plots of $M_n(\text{theory})$, $M_n(\text{SEC})^*$ and PDI vs conversion for the polymerization of <i>L</i> -LA using catalyst 1-Ti(O ⁱ Pr) ₂	128
Figure 3.16.	Plots of $M_n(\text{theory})$, $M_n(\text{SEC})^*$ and PDI vs conversion for the polymerization of <i>rac</i> -LA using catalyst 1-Ti(O ⁱ Pr) ₂	129
Figure 3.17.	$^{13}\text{C}\{^1\text{H}\}$ NMR spectrum of the methine and carbonyl region of PDLLA obtained by using 1-4-Ti(O ⁱ Pr) ₂ at 130°C.....	131
Figure 3.18.	Homonuclear decoupled ^1H NMR spectrum of the methine region of PDLLA prepared with 1-4-Ti(O ⁱ Pr) ₂ at 130°C.....	132
Figure 4.1.	Plot of $M_n(\text{theory})$, $M_n(\text{SEC})^*$ and PDI as a function of [M]/[Ti] ratio at 70°C in toluene using 4-Ti(O ⁱ Pr) ₂	142
Figure 4.2.	SEC overlay of PCL obtained at different [M]/[Ti] mole ratio.....	142
Figure 4.3.	^1H NMR spectrum of PCL prepared using 4-Ti(O ⁱ Pr) ₂ at 70°C and [M]/[Ti] = 50.....	143

Figure 4.4.	^{13}C NMR spectrum of PCL prepared using $4\text{-Ti}(\text{O}^i\text{Pr})_2$ at 70°C and $[\text{M}]/[\text{Ti}] = 50$	144
Figure 4.5.	SEC chromatogram of PCL prepared using $4\text{-Ti}(\text{O}^i\text{Pr})_2$ at 70°C ($[\text{M}]/[\text{Ti}] = 50$).....	145
Figure 4.6.	SEC chromatogram of PCL prepared using $4\text{-Ti}(\text{O}^i\text{Pr})_2$ at 25°C ($[\text{M}]/[\text{Ti}] = 300$).....	145
Figure 4.7.	MALDI-TOF-MS of PCL prepared using $4\text{-Ti}(\text{O}^i\text{Pr})_2$ at 70°C and $[\text{M}]/[\text{Ti}] = 50$	146
Figure 4.8.	DSC analysis of PCL prepared using $4\text{-Ti}(\text{O}^i\text{Pr})_2$ at 70°C and $[\text{M}]/[\text{Ti}] = 50$	148
Figure 4.9.	First order kinetic plot for $\epsilon\text{-CL}$ consumption vs time using $4\text{-Ti}(\text{O}^i\text{Pr})_2$ at 25°C & 70°C	149
Figure 4.10.	Plot for $\epsilon\text{-CL}$ consumption vs time using $4\text{-Ti}(\text{O}^i\text{Pr})_2$ at 25°C and 70°C	150
Figure 4.11.	Plots of M_n (theory), M_n (SEC)* and PDI vs Conversion for the polymerization of $\epsilon\text{-CL}$ using catalyst $4\text{-Ti}(\text{O}^i\text{Pr})_2$ at 25°C	151
Figure 4.12.	Plots of M_n (theory), M_n (SEC)* and PDI vs Conversion for the polymerization of $\epsilon\text{-CL}$ using catalyst $4\text{-Ti}(\text{O}^i\text{Pr})_2$ at 70°C	151
Figure 4.13.	Two-stage polymerization of $\epsilon\text{-CL}$ initiated by $4\text{-Ti}(\text{O}^i\text{Pr})_2$ in toluene at 70°C	152
Figure 4.14.	^1H NMR spectrum of PHB prepared using $1\text{-Ti}(\text{O}^i\text{Pr})_2$ in toluene at 70°C	156
Figure 4.15.	^{13}C NMR spectrum of PHB prepared using $1\text{-Ti}(\text{O}^i\text{Pr})_2$ in toluene at 70°C	157
Figure 4.16.	a) Carbonyl region, b) Methylene region, c) Methyl region of the $^{13}\text{C}\{^1\text{H}\}$ NMR spectra of PHBs prepared by ROP of <i>rac</i> -BBL.....	158
Figure 4.17.	^1H NMR spectrum of PTMC prepared using $4\text{-Ti}(\text{O}^i\text{Pr})_2$ in toluene at 70°C	160
Figure 4.18.	^{13}C NMR spectrum of PTMC prepared using $4\text{-Ti}(\text{O}^i\text{Pr})_2$ in toluene at 70°C	161

Figure 4.19.	SEC traces of PTMC and the corresponding PTMC- <i>b</i> -PCL copolymer prepared using 4-Ti(O ⁱ Pr) ₂ in toluene at 70°C.....	162
Figure 4.20.	¹ H NMR spectrum of PTMC- <i>b</i> -PCL prepared using 4-Ti(O ⁱ Pr) ₂ in toluene at 70°C.....	163
Figure 4.21.	¹³ C NMR spectrum of PTMC- <i>b</i> -PCL prepared using 4-Ti(O ⁱ Pr) ₂ in toluene at 70°C.....	163
Figure 4.22.	DSC thermograms of PTMC and PTMC- <i>b</i> -PCL.....	164
Figure 4.23.	Plot of M _n (theory), M _n (SEC)* and PDI as a function of [M]/[Ti] ratio for ROP of TMC in melt at 100°C.....	166
Figure 5.1.	SEC traces of PCL and the corresponding PCL- <i>block</i> -PLLA copolymer prepared using 1-Ti(O ⁱ Pr) ₂ (Table 5.1, Entry 1).....	175
Figure 5.2.	¹ H NMR spectrum of PCL- <i>block</i> -PLLA copolymer synthesized using 1-Ti(O ⁱ Pr) ₂	176
Figure 5.3.	¹³ C NMR spectrum of PCL- <i>block</i> -PLLA copolymer synthesized using 1-Ti(O ⁱ Pr) ₂	176
Figure 5.4.	DSC analysis of PCL- <i>block</i> -PLLA copolymer synthesized using 1-Ti(O ⁱ Pr) ₂	177
Figure 5.5.	SEC traces of PLLA and the corresponding PLLA- <i>block</i> -PCL copolymer prepared using 1-Ti(O ⁱ Pr) ₂ (Table 5.2, Entry 1).....	179
Figure 5.6.	Triple chromatogram of PLLA- <i>block</i> -PCL copolymer prepared using 1-Ti(O ⁱ Pr) ₂	179
Figure 5.7.	¹ H NMR spectrum of PLLA- <i>block</i> -PCL copolymer synthesized using 1-Ti(O ⁱ Pr) ₂	180
Figure 5.8	¹³ C NMR spectrum of PLLA- <i>block</i> -PCL copolymer synthesized using 1-Ti(O ⁱ Pr) ₂	181
Figure 5.9.	DSC analysis of PLLA- <i>block</i> -PCL copolymer prepared using 1, 3, 4-Ti(O ⁱ Pr) ₂	182
Figure 5.10.	SEC traces of PDLLA and the corresponding PDLLA- <i>block</i> -PCL copolymer prepared using 4-Ti(O ⁱ Pr) ₂	183
Figure 5.11.	¹ H NMR spectrum of PDLLA- <i>block</i> -PCL copolymer synthesized using 2-Ti(O ⁱ Pr) ₂	184

Figure 5.12. ^{13}C NMR spectrum of PDLLA- <i>block</i> -PCL copolymer synthesized Using 2-Ti(O ⁱ Pr) ₂	185
Figure 5.13. DSC analysis of PDLLA- <i>block</i> -PCL copolymer prepared using 2-Ti(O ⁱ Pr) ₂	185
Figure 5.14. SEC traces of PCL, PCL- <i>b</i> -PLLA and the corresponding PCL- <i>b</i> -PLLA- <i>b</i> -PCL triblock copolymer.....	187
Figure 5.15. ^1H NMR spectrum of PCL- <i>block</i> -PLLA- <i>block</i> -PCL triblock copolymer...	187
Figure 5.16. ^{13}C NMR spectrum of PCL- <i>block</i> -PLLA- <i>block</i> -PCL triblock copolymer...	188
Figure 5.17. DSC analysis of PCL- <i>block</i> -PLLA- <i>block</i> -PCL triblock copolymer.....	189
Figure 5.18. SEC traces of PLLA, PLLA- <i>b</i> -PCL, and the corresponding PLLA- <i>b</i> -PCL- <i>b</i> -PLLA triblock copolymer.....	190
Figure 5.19. ^1H NMR spectrum of PLLA- <i>block</i> -PCL- <i>block</i> -PLLA triblock copolymer.....	191
Figure 5.20. ^{13}C NMR spectrum of PLLA- <i>block</i> -PCL- <i>block</i> -PLLA triblock copolymer.....	191
Figure 5.21. DSC analysis of PLLA- <i>block</i> -PCL- <i>block</i> -PLLA copolymer.....	192
Figure 5.22. ^1H NMR spectrum of PCL- <i>co</i> -PDLLA (run 2, table 5.6).....	194
Figure 5.23. ^1H NMR spectrum of ϵ - and α -methylene protons of PCL- <i>co</i> -PDLLA of run 1 (a), run 2 (b), run 3 (c) in Table 5.6.....	195
Figure 5.24. ^{13}C NMR spectrum of PCL- <i>co</i> -PDLLA of run 1 (a), run 2 (b), run 3 (c) in Table 5.6 (CL = caprolactone unit, LA = Lactide unit).....	196
Figure 5.25. ^1H NMR spectrum of PCL- <i>co</i> -PLLA (run 4, table 5.6).....	197
Figure 5.26. ^{13}C NMR spectrum carbonyl carbon of PCL- <i>co</i> -PLLA (run 4, table 5.6).....	197
Figure 5.27. DSC thermograms of PCL- <i>co</i> -PDLLA (Table 5.6, run 1) and PCL- <i>co</i> -PLLA (Table 5.6, run 4) in solution condition.....	198
Figure 5.28. ^{13}C NMR spectrum of PCL- <i>co</i> -PDLLA of run 1 (a), run 2 (b), run 3 (c) in Table 5.7 (CL = caprolactone unit, LA = Lactide unit).....	199
Figure 5.29. DSC thermograms of PCL- <i>co</i> -PDLLA copolymers (Table 5.7, run 1, 2, 3) in bulk condition.....	200

List of Abbreviations

A	Activity
BBL	β -Butyrolactone
CL	Caprolactone
ϵ -CL	ϵ -Caprolactone
CEM	Chain End control Mechanism
C _p	Cyclopentadienyl
C _p *	Pentamethyl cyclopentadienyl
D-LA	D-lactide
D,L-LA	D,L-lactide
DCM	Dichloromethane
DSC	Differential Scanning Calorimetry
GPC	Gel Permeation Chromatography
HPLC	High Pressure Liquid Chromatography
<i>i</i>	<i>isotactic</i>
i-Pr	Isopropyl
K _{app}	Apparent rate constant
L _n	Ligand
LS	Light Scattering
LA	Lactide
L-LA	L-lactide
L _{CL}	Average sequence length of the caproyl unit
L _{LA}	Average sequence length of the lactidyl unit
M	Metal
M _n	Number average molecular weight
M _w	Weight average molecular weight
MALDI-TOF	Matrix Assisted Laser Desorption Induced-Time of Flight
M.W	Molecular weight
MWD	Molecular Weight Distribution
meso-LA	meso-lactide
N _c	Number of polymer chains

NHCs	N-Heterocyclic carbenes
O ^t Bu	tert-butoxy
OR	Alkoxide
PLA	Poly(lactide)
PLLA	Poly(L-lactide)
PDLLA	Poly(D,L-lactide)
PGA	Polyglycolide
PLGA	Poly(lactide-co-glycolide)
PTMC	Poly(trimethylene carbonate)
PHB	Poly(3-hydroxybutyrate)
PHAs	Poly(3-hydroxyalkanoates)
PDI	Polydispersity index
P _r	Probability of racemic linkage
P _m	Probability of meso linkage
β-PL	β-propiolactone
RI	Refractive Index
ROP	Ring Opening Polymerization
rac-LA	racemic-lactide
SEC	Size Exclusion Chromatography
SEM	Enantiomorphic Site Control Mechanism
TfOH	Trifluoromethane sulfonic acid
TfOMe	Methyl triflate
T _m	Melting temperature
T _g	Glass transition temperature
T _c	Crystallization temperature
THF	Tetrahydrofuran
TMC	Trimethylene carbonate
Visco	Viscometry
δ-VL	δ-valerolactone

General Introduction

General Introduction

Plastic materials derived from petrochemical feed stocks are widely used nowadays in our daily life in all domestic and industrial appliances. World wide production of plastics is estimated to be over 240 million tons per year.¹ Plastic consumption is expected to increase by over 5% per year, with experts setting the annual plastic consumption in 2016 over 400 million tons.² Poly-olefins, with poly(ethylene) (LDPE, LLDPE and HDPE) and poly(propylene) is widely dominating the plastic production. However, these poly(olefins) raises two different issues: (i) The main resources for poly(olefins) production are expensive fossil fuels, which can contribute to 80% of total production cost (ii) These non-renewable resources suffer from a lack of biodegradability in nature that makes them environmentally unfriendly. For example, poly(ethylene) plastic bags can take up to 400 years to degrade in landfill sites.³ Thus, such high demand of fossil fuels and an environmental awareness requires a new alternative to conventional polyolefins. It is for these reasons that the production and utilization of biodegradable aliphatic polyesters from renewable resources is of increasing interest.

Polyesters play a predominant role as biodegradable plastics due to their potentially hydrolysable ester bonds. Among the polyesters, poly(lactide), poly(ϵ -caprolactone) and copolymers thereof are among the most studied polymers, and their biocompatibility makes them ideal for use in numerous biomedical and pharmaceutical applications.⁴⁻⁷ In 1954, Dupont patented a high-molecular weight PLA and since then many companies started to commercialize PLA. Currently, Nature works LLC is one of the leading manufacturers of lactic acid based products under the trade name of (Nature-Works PLA[®]), used for plastics or packaging applications, and of the Ingeo[™] poly(rac-lactide) based fibres used in specialty textiles and fiber applications. Poly(ϵ -caprolactone) is produced by companies such as Solvay Interlox (CAPA[®]), Dow Union Carbide (Tone[®]) and Daicel (Placel[®]).

These polyesters can be produced by different polymerization techniques: polycondensation, anionic polymerizations, cationic polymerizations, enzymatic polymerization and coordination-insertion polymerization.^{8,9} Among these, coordination complexes based on metals with empty *p*, *d* or *f* orbitals enables the synthesis of high molecular weight polyesters *via* coordination-insertion mechanism. Stannous octoate is the most widely used catalysts in the production of PLA industrially.⁷ Homogenous metal complexes containing ancillary ligand enables the production of high molecular weight polymers with good control and narrow polydispersity, well defined end groups as well as stereoregular polymers. A wide range of metal complexes have been studied for the ROP of cyclic esters.¹⁰⁻¹³ Nevertheless, the study of new metal complexes that

catalyze cyclic esters polymerization *via* a coordination-insertion mechanism is still an important topic for both academia and industry.

Thesis Overview: Among the variety of initiators/catalyst derived from different metal groups that have been developed so far for the ROP of cyclic esters, only a limited number of investigations are reported on the group 4 metal complexes.¹⁴⁻¹⁷ Among various metal complexes, the production of stereoregular polymer by group 4 metal complexes is limited. Therefore, exigent need to find out potential group 4 metal catalysts for ROP is of interest. The motivation of the research presented here was to synthesize new group 4 metal complexes and study their effect on the ROP of cyclic esters. To this end, we were interested in group 4 metal alkoxide complexes supported by new aminodiol ligands. Such well defined complexes can then be examined for ROP of cyclic esters.

This manuscript is divided into six chapters:

Chapter 1 presents a literature review on the recent advances in the ROP of lactides and lactones using metal complexes as initiators. This chapter is subdivided into different sections. The first section describes the different synthetic routes to synthesize biodegradable polymers, by focusing on different ROP mechanisms. The next section describes the general characteristics of PLA and PCL. Finally, the last section describes the stereoselective polymerization of lactide and the coordination-insertion ROP of cyclic esters with Group (IV) metal complexes that have been developed so far in the literature.

Chapter 2 describes the synthesis and characterization of aminodiol ligands as well as titanium and zirconium alkoxide complexes obtained from the reaction of the suitable metal precursor with the respective aminodiol ligands. This chapter also describes the synthesis and characterization of Half-sandwich titanium complexes using the same aminodiol ligands, this type of complexes being act as potent catalysts for the syndiotactic styrene polymerization.

Chapter 3 begins with a short introduction on PLA synthesis using metal catalysts as initiators. Next section discusses the catalyst/initiator efficiency for ROP of *L*-LA and *rac*-LA in solution condition followed by structural characterization of polymers by different techniques (SEC with triple detection, ¹H & ¹³C NMR spectroscopy, MALDI-TOF mass spectrometry, DSC). The stereoselectivity of the catalyst for ROP of *rac*-lactide is also discussed briefly. Finally, polymerization kinetic studies in solution conditions followed by discussion about solvent free polymerization performed at higher temperature are described.

Chapter 4 presents the ROP of lactones and carbonates with titanium alkoxide complexes. This chapter is subdivided into three different sections and each section starts with a small introduction. In the first section, results for the ROP of ϵ -CL in different polymerization conditions (solution and bulk), polymer characterization and kinetics studies are discussed. Next section describes the preliminary results obtained for the ROP of β -butyrolactone and finally the last section discusses the results obtained for the ROP of trimethylene carbonate.

Chapter 5 begins with a short introduction about importance of block copolymers in the biomedical field. Next section discusses about block copolymer (diblock and triblock) synthesis of ϵ -CL and LA by sequential polymerization techniques using titanium alkoxide complexes as initiators. Structural characterization of all polymers by different techniques (SEC with triple detection, ^1H & ^{13}C NMR spectroscopy, DSC) are described. A study of random copolymerization of ϵ -CL and LA in different polymerization condition (solution and bulk) and the structural characterization of the copolymers is finally presented.

Chapter 6 summarizes the materials, general experimental techniques, Instrumentation and characterization details of ligands, complexes and polymers.

References

- [1] Plastics Europe, *The Compelling Facts About Plastics*, **2008**.
- [2] Bjacek, P. *Oil Gas J.*, **2008**, 106, 40.
- [3] Guttag, A. US patent 1994/5346929, 1994.
- [4] Chiellini, E.; Solaro, R. *Adv. Mater.*, **1996**, 8, 305.
- [5] Woodruff, M. A.; Hutmacher, D.W. *Prog. Polym. Sci.* **2010**, 35, 1217.
- [6] Nair, L. S.; Laurencin, C. T. *Prog. Polym. Sci.* **2007**, 32, 762.
- [7] Nampoothiri, K. M.; Nair, N. R.; John, R. P. *Bioresour. Technol.* **2010**, 101, 8493.
- [8] Jérôme, C.; Lecomte, P. *Advanced Drug Delivery Reviews*. **2008**, 60, 1056.
- [9] Labet, M.; Thielemans, W. *Chem. Soc. Rev.* **2009**, 38, 3484.
- [10] Williams, C. K. *Chem. Soc. Rev.* **2007**, 36, 1573.
- [11] Dechy-Cabaret, O.; Martin-Vaca, B.; Bourissou, D. *Chem. Rev.* **2004**, 104, 6147.
- [12] Kamber, N. E.; Jeong, W.; Waymouth, R. M.; Pratt, R. C.; Lohmeijer, B. G. G.; Hedrick, J. L. *Chem. Rev.* **2007**, 107, 5813.
- [13] Arbaoui, A.; Redshaw, C.; *Polym. Chem.* **2010**, 1, 801.
- [14] Chmura, A. J.; Davidson, M. G.; Jones, M. D.; Lunn, M. D.; Mahon, M. F.; Johnson, A. F.; Khunkamchoo, P.; Roberts, S. L.; Wong, S. S. F. *Macromolecules*. **2006**, 39, 7250.
- [15] Chmura, A. J.; Davidson, M. G.; Frankis, C. J.; Jones, M. D.; Lunn, M. D. *Chem. Commun.* **2008**, 1293.
- [16] Zelikoff, A. L.; Kopilov, J.; Goldberg, I.; Coates, G. W.; Kol, M. *Chem. Commun.* **2009**, 6804.
- [17] Sergeeva, E.; Kopilov, J.; Goldberg, I.; Kol, M. *Inorg. Chem.* **2010**, 49, 3977.

CHAPTER 1
Literature Review

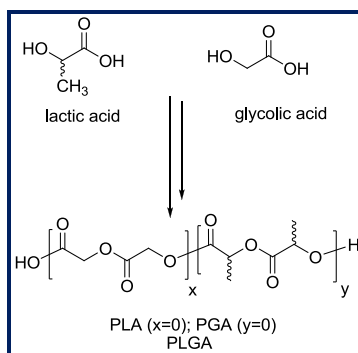
Chapter 1

Literature Review

1.1. Introduction

Among the commercial synthetic polymers, polyolefins are by far the most important class of materials since 1940s, due to the factors governed by monomer availability and cost, synthetic ease and excellent properties.¹ Despite the numerous advantages of these polymers two drawbacks remains to be solved, namely the use of non renewable resources in their production and the ultimate fate of these large scale commodity polymers. The extensive use of these polymers has created important problem; despite increasing popularity of plastic recycling, disposal of these non-degradable materials has led to serious environmental pollution.

In order to overcome these problems a wealth of research has been focused on the biodegradable polymers and the spectacular advances achieved over the last 30 years in the synthesis, manufacture, and the processing of these materials have given rise to a broad range of applications from the packaging to more sophisticated biomedical devices.^{2,3} Of the variety of biodegradable polymers known, linear aliphatic polyesters are more particularly attractive. Among them, polylactide (PLA, derived from Lactic acid-LA), polyglycolide (PGA, derived from glycolic acid-GA) and poly(lactide-co-glycolide) (known as PLGA) are the most studied in the literature (Scheme 1.1).⁴ These are both biodegradable (the aliphatic polyesters backbone is sensitive to hydrolysis) and bioassimilable (hydrolysis releases lactic acids and glycolic acids-nontoxic compounds that are eliminated or assimilated via the Krebs cycle).^{5,6} These types of polyesters have raised increasing interest for biomedical applications over the last few decades owing to their biodegradable, biocompatible and permeable properties important features such as biodegradation rate, bioadherence, hydrophilicity, glass transition temperature and crystallinity rely on the availability of suitable synthetic process.³



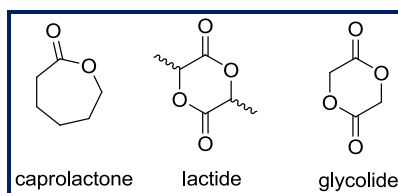
Scheme 1.1. Lactic acid and Glycolic acid and their derived homo and copolymers.

In this chapter, we present an overview on the recent advances in the ring opening polymerization (ROP) of cyclic esters such as lactides and lactones using metal complexes as initiators (other monomers are not described in this review due to limited studies). In the first section, we will discuss the synthetic strategies of these biodegradable polymers by focusing on different ROP mechanisms which allow generally quite good control of the polymer characteristics (i.e. predictable molecular weight, narrow molecular weight distribution). In the next section, general characteristics of poly(lactides) and poly(lactones) will be presented. The last section focuses on the stereoselective polymerization of lactide and its mechanisms and the coordination-insertion ROP of lactide and lactones with Group (IV) metal complexes that have been developed over the past few years or so. In this section, the group 4 metal catalysts will be classified by the nature of their ancillary ligands.

1.2. Synthesis of polyesters: some generalities

Aliphatic polyesters such as poly(ϵ -caprolactone), poly(lactide),⁷ and poly(glycolide)³ can be prepared by two different polymerization techniques.

- (i) Step growth polymerization or polycondensation
- (ii) Ring Opening Polymerization (ROP) of lactones, lactide and glycolide (Scheme 1.2).

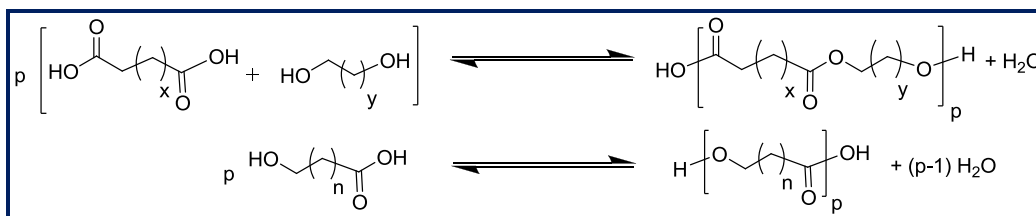


Scheme 1.2. Structure of ϵ -caprolactone, Lactide and Glycolide.

1.2.1. Step growth polymerization

The step growth polymerization technique relies on the condensation reaction of hydroxy acids (AB monomer) or of mixtures of diacids and diols (AA + BB monomers) (Scheme 1.3). Although these polycondensation techniques allow to synthesize a broader range of polymer structures than ROP through a higher accessibility of monomers involved, they present many drawbacks:

- Conversion is limited due to water formation yielding to equilibrium in esterification reactions. As a consequence, very high temperatures are required in order to eliminate water and thus to go to high conversions and high molar mass polymer.
- In the case of monomers (AA + BB), if the stoichiometry is not perfect, conversion will also decrease and only oligomers will be obtained.
- This method will not be developed in this chapter.

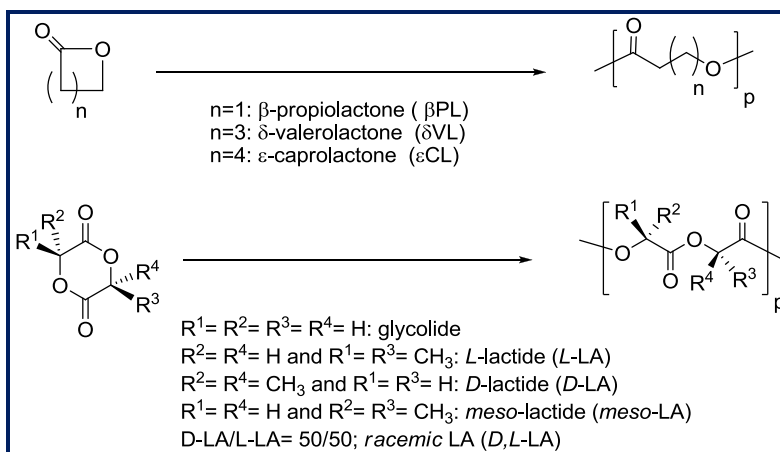


Scheme 1.3. Synthesis of aliphatic polyesters by step growth polycondensation.

1.2.2. Ring Opening Polymerization

The polymerization of lactide and lactones by ring opening polymerization (ROP) overcomes the limitations obtained from step growth polycondensation. Thus, ROP is the most convenient and efficient method to synthesize polyesters and allows a better control over the polymerization process, in terms of molar mass, dispersity, polymer chain ends and tacticity. High molar mass polyesters can be easily prepared under mild conditions from lactide and lactones of different ring size substituted or not by functional groups (Scheme 1.4).^{4,8,9}

Ring strain is the most important factor affecting the ring opening polymerization of cyclic ester monomers.¹⁰ For the lactone series, ring strain and thermodynamic polymerizability increases with increasing ring size from five to seven, while for the lactide series, polymerizability decreases with increasing substitution on the α -carbon. The ROP of lactones and lactides can occur through five polymerization methods: anionic, cationic, organocatalytic, enzymatic and “coordination-insertion” mechanism using metal catalyst initiators. The polymer formed from these methods could be easily functionalized with one chain end originating from the termination reaction and one terminus end capped with a functional group originating from the initiator. By altering the catalyst or initiator and the termination reaction, the nature of the functional groups can be varied to fit the application of the polymer.

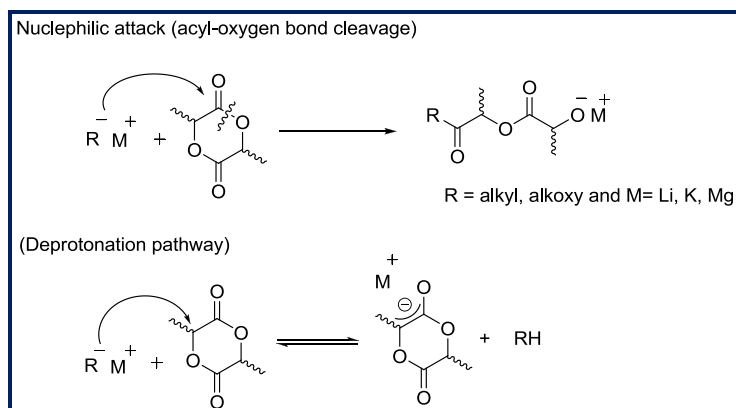


Scheme 1.4. ROP of unsubstituted lactones, lactides and glycolides.

1.2.2.1. Anionic Ring Opening Polymerization ⁵

From a mechanistic point of view, anionic ROP of cyclic esters has been demonstrated to occur *via* acyl-oxygen cleavage, the initiation steps can occur either by the nucleophilic attack of a negatively charged initiator on the carbon of the carbonyl function or by attack of anionic species (initiator) on the carbon atom (deprotonation) adjacent to the acyl-oxygen resulting in a linear polyester. The propagating species is negatively charged and is counter balanced with a positive ion. The two different initiation steps are easily differentiated by the end group analysis from the NMR, since the deprotonation pathway can be easily identified by the absence of initiator fragments, whereas the acyl-oxygen cleavage pathway can be identified from the ester end groups derived from the alkoxide initiators (Scheme 1.5, same for lactones).

The main drawback of this method is the occurrence of intramolecular transesterification side reactions also called “back biting” in the latter stages of polymerization. As a consequence, polymerizations have to be stopped before completion to avoid side reactions and generally, only low molar mass polymers are thus obtained.

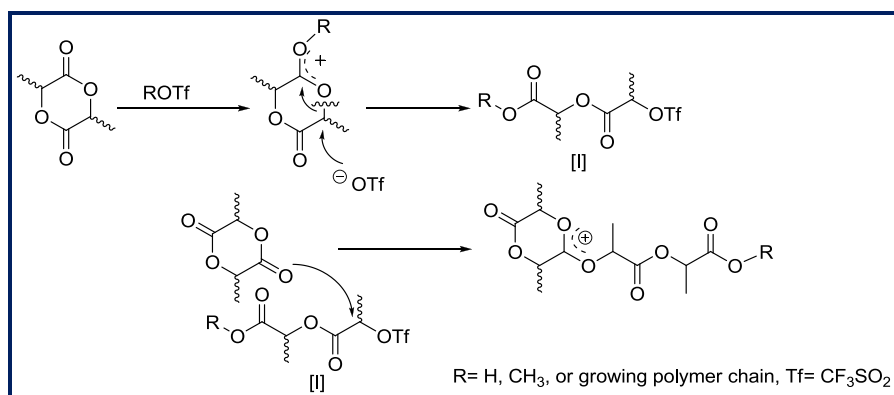


Scheme 1.5. Anionic ROP Mechanism.

1.2.2.2. Cationic Ring Opening Polymerization ¹¹

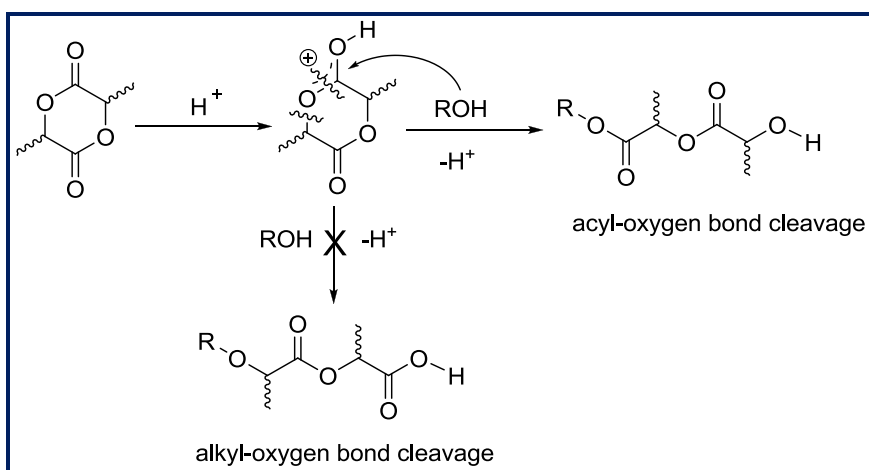
The cationic ROP of lactides and lactones has been achieved using alkylating agents, acylating agents, Lewis acids, and protic acids. Kricheldorf and co-workers screened a variety of acidic compounds, among them trifluoromethane sulfonic acid (triflic acid, HOTf) and methyl triflate (MeOTf) proved to be useful initiators for the cationic ROP of LA.^{12,13} End group analysis of the polymer by ¹H NMR indicates methyl ester end groups when (MeOTf) is used as initiator, suggesting that the polymerization occurs *via* cleavage of alkyl-oxygen bond rather than the acyl-oxygen bond. A two step propagation mechanism was proposed involving activation of the monomer by methylation with (MeOTf) followed by S_N2 attack on the triflate anion on the positively charged LA with inversion of configuration. Propagation was proposed to proceed by nucleophilic attack by LA on the activated cationic chain end with inversion in

configuration, leading to net retention of the configuration (Scheme 1.6). Similar kind of mechanism has been proposed for the ROP of ϵ -caprolactone by Khanna *et al.*¹⁴ and Stridsberg *et al.*¹⁵



Scheme 1.6. Proposed pathway for cationic ROP of Lactide.

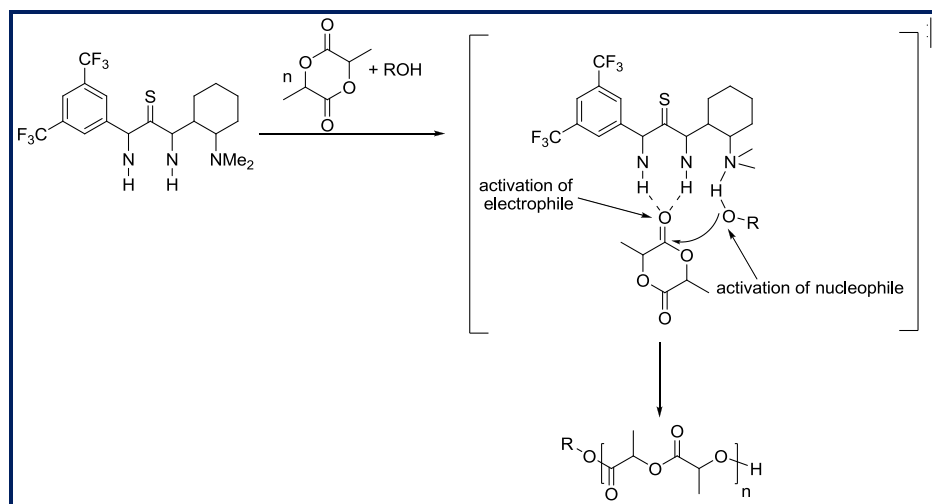
Recently, Bourissou *et al.* reported the controlled cationic polymerization of LA using a combination of the triflic acid (as the catalyst) and a protic reagent (water or an alcohol) as an initiator.¹⁶ The polymerization proceeds *via* an “activated cationic polymerization mechanism” as described by Penczek,¹⁷ where the acid would activate the cyclic ester monomer and the alcohol would be the initiator of the polymerization. Polymerization is, therefore, thought to proceed by protonation of LA by triflic acid followed by nucleophilic attack of the initiating alcohol or that of the growing polymer chain, as shown in Scheme 1.7. Analysis of the polymer by ¹H NMR indicates isopropyl ester chain ends and suggest that polymerization proceeds by acyl bond cleavage, not by alkyl bond cleavage. Similar kind of mechanism has been proposed for the ROP of ϵ -caprolactone by Kim *et al.*¹⁸ and Endo.¹⁹



Scheme 1.7. Proposed activated monomer pathway for cationic ROP of Lactide.

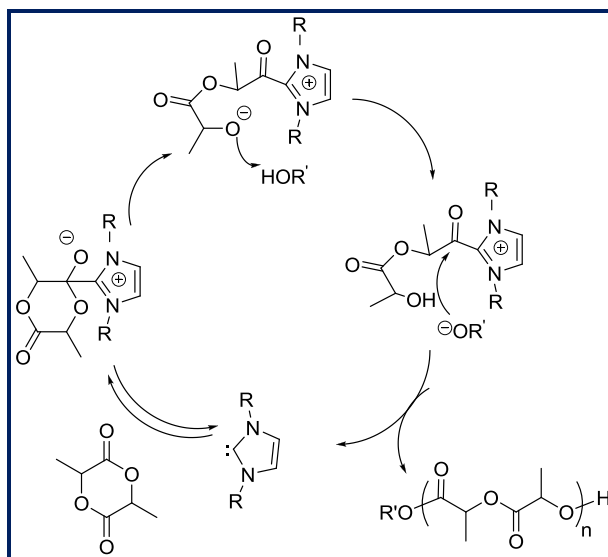
1.2.2.3. Organocatalyzed and Enzymatic (ROP)^{11,20}

In recent years, metal free catalysts for the ROP of heterocyclic monomers revealed particularly interesting as the resulting polymers are not contaminated by metallic residues and are thus more suitable for biomedical applications, for example. In this metal free approach; amines, phosphines, carbenes, thioureas, acts as activators of the chain end and/or the monomer (Scheme 1.8). The bifunctional activation of both the monomer and the initiator/chain end is a very effective strategy for the controlled ROP of cyclic esters. One particular example for ROP of lactides includes thiourea based bifunctional catalyst containing both electrophile activating thiourea and nucleophile activating amine. The mechanistic and theoretical studies revealed the hydrogen-bonding capabilities of a thiourea and an amine, making them suitable for the bifunctional activation of both the electrophilic monomer, and the nucleophilic alcohol respectively in ROP.²¹



Scheme 1.8. Bifunctional activated mechanism using hydrogen bonding thiourea catalyst.

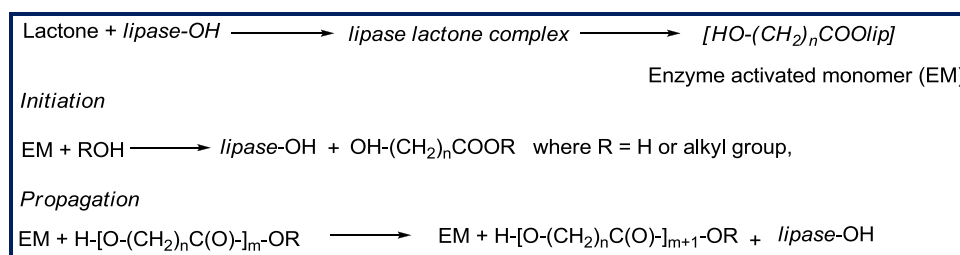
N-Heterocyclic carbenes (NHCs) are another class of potent neutral bases and nucleophiles used as activator for the (ROP) of lactides and lactones.^{11,22-24} The polymerization is proposed to proceed *via* a "Monomer Activated Mechanism" involving the formation of zwitterionic intermediates by the attack of the nucleophile (NHCs) on the carbonyl carbon of the lactide and lactones, followed by ring opening of the tetrahedral intermediate to generate the acylimidazolium alkoxide zwitterions. Protonation of the alkoxide of the zwitterion by the initiating or chain-end terminated alcohol generates an alkoxide that esterifies the acylimidazolium to generate the open chain ester and the carbene (Scheme 1.9). Compelling evidence of nucleophilic mechanism in the ROP of LA was provided in an attempt to generate zwitterionic ring-opening polymerization of lactide from the (NHCs) in the absence of alcohol initiators. These mechanistic studies led to the new strategy to generate cyclic polylactides.



Scheme 1.9. Plausible Mechanism for the Nucleophilic ROP of Lactide.

The enzymatic polymerizations also appear as an alternative technique for producing metal-free polyesters. Kobayashi,²⁵ and Knani²⁶ first reported in 1993 the enzymatic bulk and solution ROP of ϵ -CL with the enzyme *Candida Antarctica* Lipase B. Generally, enzymes catalyse reactions with high enantio- and regio-selectivity and even under mild reaction conditions (i.e. temperature, pressure, pH, etc.)

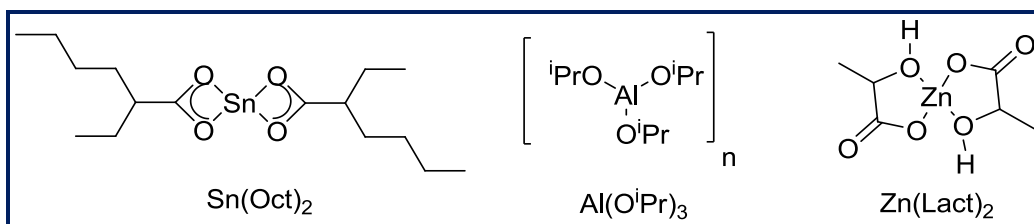
The lipase catalyzed polymerization of lactones is believed to proceed by an activated monomer mechanism. The key step is the reaction of the catalytic active serine residue of the enzyme with the cyclic ester leading to the formation of the acyl-enzyme intermediate. This intermediate reacts with water or alcohol to regenerate the enzyme and a ω -hydroxycarboxylic acid or ester (Scheme 1.10). In the next propagation step, nucleophile attack of the terminal hydroxyl group of the propagating polymer on the acyl-enzyme intermediate leads to the addition of one more unit to the chain and regeneration of the enzyme. More insights into the mechanism of lipase-catalyzed ROP of lactones are discussed in details in the review written by Kobayashi.²⁷ Further advances in enzymatic ROP have been made and the polymerization of different monomers has been studied and reviewed in the literatures.^{6,11,28,29}



Scheme 1.10. Mechanism of Lipase-Catalyzed Polymerization of Lactones.

1.2.2.4. Coordination- Insertion Ring Opening Polymerization

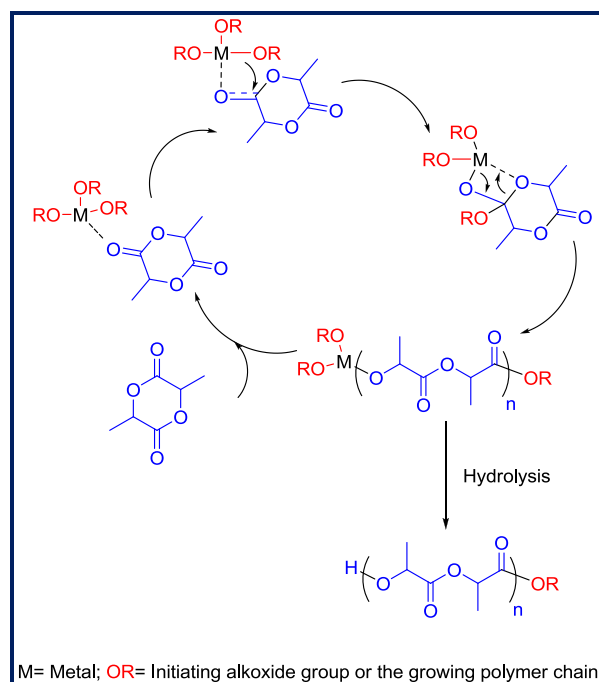
Coordination insertion ring opening polymerization has been extensively used for the preparation of aliphatic polyesters with well defined microstructure and architecture. The covalent metal alkoxides and carboxylates with vacant “d” orbitals act as coordination initiators and not as anionic initiators in this polymerization. The first generations of metal initiators are mainly constituted by simple homoleptic metal complexes. Tin(II)octanoate $[\text{Sn}(\text{Oct})_2]$, aluminum(III)isopropoxide $\text{Al}(\text{O}^i\text{-Pr})_3$, zinc(II)lactate $[\text{Zn}(\text{Lact})_2]$ are the most widely used complexes (Scheme 1.11).³⁰



Scheme 1.11. Structure of tin(II)octanoate, aluminum(III)isopropoxide, zinc(II)lactate.

$\text{Sn}(\text{Oct})_2$ is commercially available, easy to handle, soluble in most of the organic solvents. It is highly active in melt polymerization condition (140-180°C, typical reaction times requires few minutes to hours). $\text{Al}(\text{O}^i\text{-Pr})_3$ also proved to be an efficient catalyst and has been mostly used for mechanistic studies, its activity being less than that of $\text{Sn}(\text{Oct})_2$ due to some kind of aggregation phenomenon (i.e. due to the presence of equilibrium between the tetramer and trimer structure of $\text{Al}(\text{O}^i\text{-Pr})_3$).³¹ Zinc(II) lactate is a potential non toxic catalyst, commercially available, and its activity is in the range of $\text{Al}(\text{O}^i\text{-Pr})_3$.³² These first generation metal initiators have been widely used for the controlled ring opening polymerization of cyclic esters and brought important contributions for the mechanism understanding. In 1971, Dittrich and Schulz were the first to suggest a three step coordination insertion mechanism for the ROP of cyclic esters.³³ Kricheldorf *et al.*³⁴ and Teyssie *et al.*³⁵ demonstrated the first experimental proof for such a mechanism in the $\text{Al}(\text{O}^i\text{-Pr})_3$ initiated polymerization of lactide.

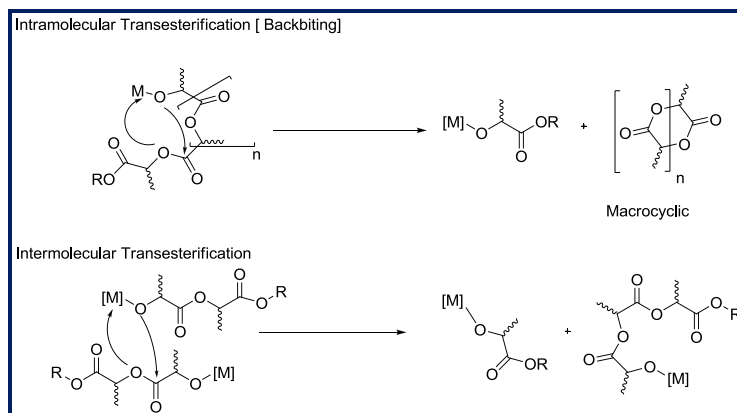
The coordination-insertion mechanism of lactide polymerization involves the coordination of the monomer to the Lewis-acidic metal center (Scheme 1.12), which enhances the electrophilicity of the carbonyl group and the nucleophilicity of the alkoxide (OR) group. The monomer is then inserted into one of the metal alkoxide bonds *via* nucleophilic addition of OR group on the carbonyl carbon, followed by ring opening *via* acyl oxygen cleavage. The chain propagation continues by the subsequent monomer addition. Hydrolysis of the metal alkoxide bonds leads to a polymer chain having a hydroxyl end group and the other chain end is encapped with an isopropyl ester.



Scheme 1.12. Coordination-Insertion Mechanism for lactide polymerization using metal alkoxide catalyst.

However, although tin, aluminum and zinc based catalytic systems proved to be quite convenient (in terms of activity, polymerization control and mechanism) for the polymerization of cyclic esters, such homoleptic metal alkoxide complexes,⁵ may sometimes present several drawbacks:

- Multiple nuclearities: The presence of multiple active metal sites present in the catalyst structure can initiate more than one growing polymer chain from each metallic center and the control of molecular weight distribution is complicated by the clustered form of these active species (i.e. the exact nature of active site is not always very well known because of possible aggregation).
- Homoleptic nature of these species results in detrimental side reactions such as transesterification that can occur both intramolecularly (also called backbiting, leading to macrocyclic structure and shorter chains) and intermolecularly (chain redistributions) (Scheme 1.13). These side reactions lead to polymer with broader molecular weight distributions and unpredictable molecular weight. The extent of these transesterification reactions depends on the polymerization temperature and the type of metallic initiator.^{36,37} For example with $\text{Sn}(\text{Oct})_2$, these side reactions occurs at the very beginning of the polymerization leading to broad molecular weight distributions, (PDI values around 2) whereas these side reactions occurs at high or even complete monomer conversion with $\text{Al}(\text{O}^i\text{Pr})_3$ leading to lower PDI (less than 1.5).



Scheme 1.13. Schematic representations for the transesterification side reactions.

In order to overcome all these problems, well defined catalysts bearing supporting ligands was developed to control the structure of the corresponding heteroleptic complexes. Therefore, this second generation of catalytic systems, namely so called single site catalysts, attracted interests in order to achieve better control, activity, and selectivity of the polymerization.

Single-site metal catalysts for olefins have provided some of the most spectacular advances in controlled polymerization in recent years and have made available a plethora of new materials.³⁸ Thereby some of these catalysts lead to controlled polymerization, namely, a process involving minimal chain transfer, combined with fast initiation. Such process may be defined as a “living” polymerization that lead to polymers of predetermined molecular weights (achieved by the specific monomer/catalyst ratio chosen) and narrow molecular weight distributions (M_w/M_n approaching 1.0).

Single site catalysts dedicated to cyclic esters (ROP) are of the form L_nM-OR , where the alkoxide group (OR) is capable of propagation, M is the active metal center, and L_n are ancillary ligands that are not directly involved in the polymerization but can tune the properties of the metal center and minimize the aggregation process and side reactions (Figure 1.1). These catalysts are conceptually different from typical homoleptic catalysts of the form $M(OR)_n$, which do not possess a permanent ancillary ligand.

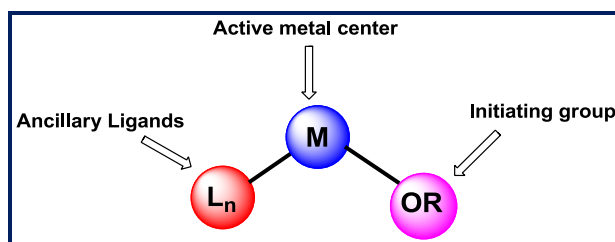


Figure 1.1. Schematic representation of the single site catalysis of the form L_nM-OR .

1.3. Polylactide (PLA) and Polycaprolactone (PCL)

1.3.1. Polylactide (PLA)

1.3.1.1. Generalities on PLA

Poly(lactic acid) or Polylactide (PLA) is a biodegradable, biocompatible, thermoplastic, aliphatic polyester derived from 100% renewable resources such as corn, sugar beets, and dairy products, because PLA is biodegradable and its degradation products are non toxic, it has found numerous applications in the biomedical field such as absorbable stitches, resorbable medical implants, disposable degradable plastic articles, scaffolds for tissue engineering,³⁹ and matrixes for controlled drug release of pharmaceuticals.⁴⁰ More recently, applications of PLA as a substitute for the traditional thermoplastics derived from fossil fuels, e.g., in packaging films, are being developed.³⁰ Large scale manufacturers are very keen to PLA because of its renewable and easy biodegradable properties. Life cycle of PLA is shown in Figure 1.2.⁴¹ Copolymerization of lactide with other monomers like glycolide or lactones can significantly enhance the properties and broaden the use of polylactide.^{42,43} A wide range of degradation rates, physical and mechanical properties, can be reached by varying its molecular weights and composition in the copolymers.

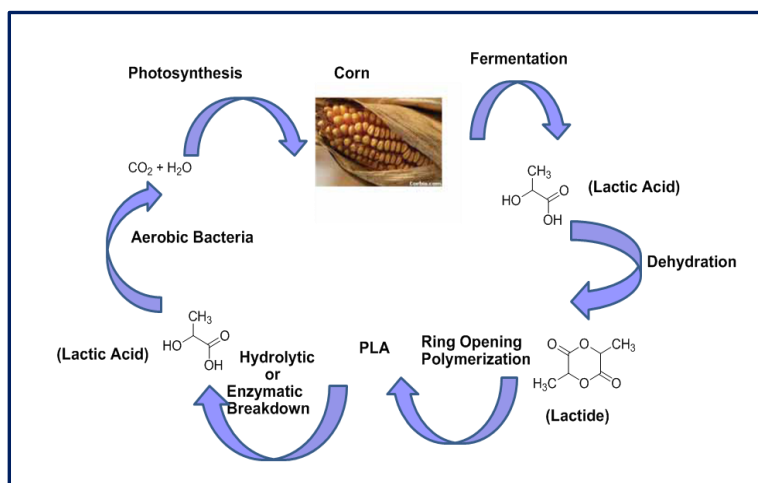
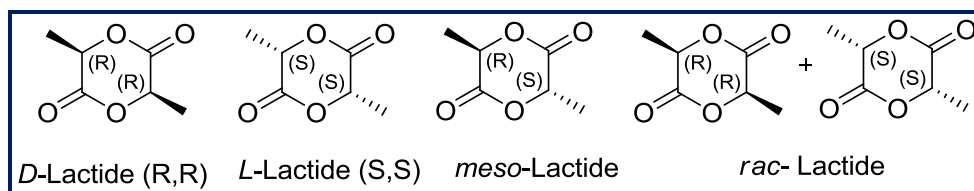


Figure 1.2. Life Cycle of PLA.

1.3.1.2. Stereochemistry and Microstructures of PLA

PLAs prepared from ring opening polymerization of lactide (LA), a cyclic diester of lactic acid by metal catalysts can exhibit different microstructures, since the monomer lactide (LA) have different stereoisomers, *RR*, *SS*, and *RS*. An *RR* configuration is referred to as *D*-lactide, *SS* is referred to as *L*-lactide, and *RS* is referred to as *meso*-lactide, as shown in Scheme 1.14. A mixture of equal amounts of *D* and *L*-lactide is referred to as *racemic* or *DL*-lactide.

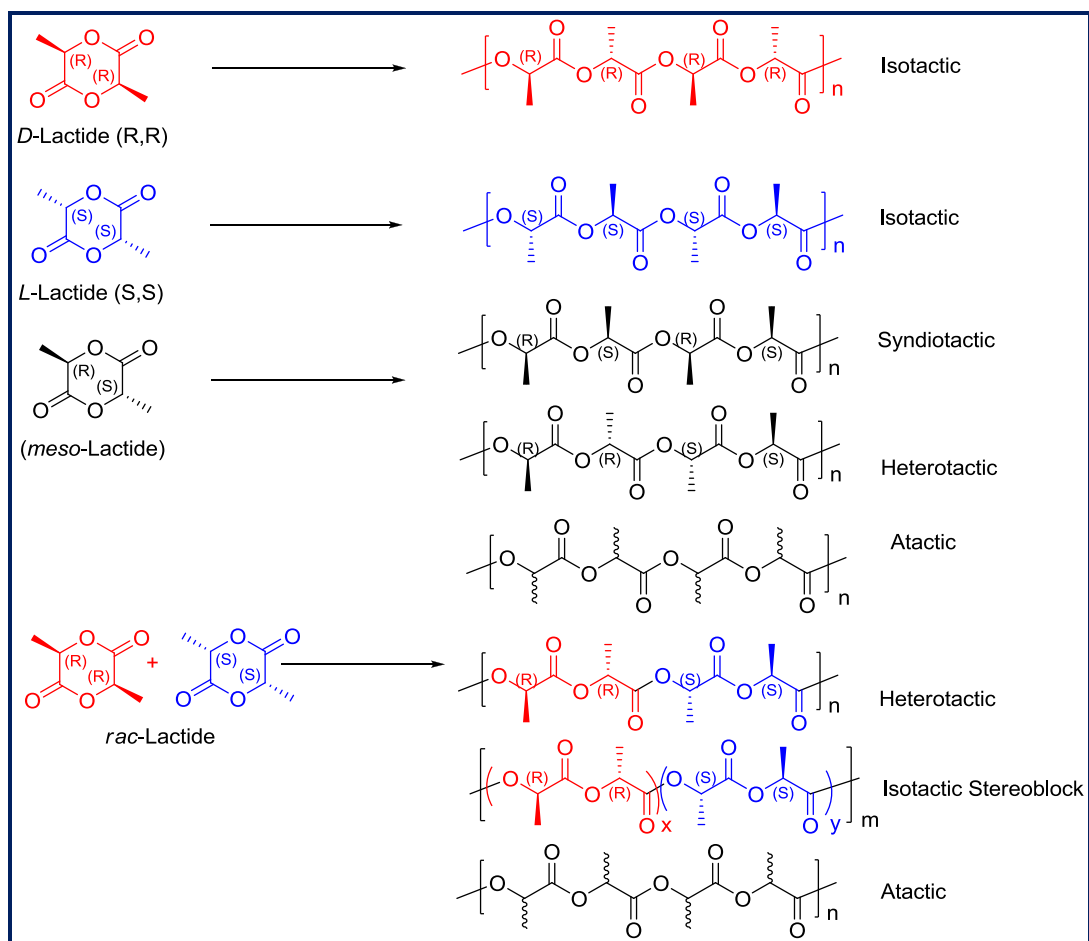
The properties of PLA, such as melting temperature, crystallinity, and mechanical strength are affected by the polymer microstructure and its molecular weight. For example homopolymers of *L*-LA or *D*-LA has a melting temperature (T_m) of 170-183°C and a glass transition temperature (T_g) of 55-65°C while homopolymer of *DL*-LA (*rac*-LA) has (T_g) of 59°C^{44,45} and poly(*L*-LA)/poly(*D*-LA) stereocomplexes have melting temperatures of 230°C.⁴⁶



Scheme 1.14. Stereoisomers of Lactides.

Microstructures of the resulting polymer is highly dependent on the type of monomer employed as well as the polymerization conditions (Scheme 1.15).⁴⁷

- Isotactic poly lactides either poly(*L*-LA) or poly(*D*-LA), containing sequential stereocenters of the same relative configuration are prepared from enantiomerically pure *L*- and *D*-LA respectively.
- Syndiotactic polymers namely poly(*meso*-lactide) contains sequential stereocenters of opposite configuration prepared from the *meso*-lactide by using a stereoselective catalyst.
- Heterotactic poly lactides contain regular alternation of *L*- and *D*-lactide units along the polymer chain afforded from the polymerization of *rac*-lactide or *meso*-lactide.
- Stereoblock PLA contains alternating blocks of *D*- and *L*-lactides in the main chain afforded from the *rac*-lactide by using stereoselective catalyst.⁴⁸
- Amorphous atactic polymers are afforded from the polymerization of *rac*-lactide or *meso*-lactide with non stereoselective catalysts aluminium tris-(alkoxide)^{31,35} or tin bis(carboxylate).⁴⁹ These atactic polymers possess random placements of $-RR-$ and $-SS-$ stereosequences for *rac*-lactide and $-RS-$ and $-SR-$ stereosequences for *meso*-lactide.
- The stereosequence distribution in poly lactide is usually determined by NMR spectroscopy through inspection of the methine and / or carbonyl regions (¹³C NMR and homonuclear decoupled ¹H NMR). The stereoselectivities are classically quantified by P_r and P_m values associated with the probabilities of racemic and meso linkage between the monomer units, respectively.⁵⁰⁻⁵³
- These types of stereoregular polymers should be achievable using well characterized, discrete single site catalytic systems. Several groups have reported the formation of both heterotactic ((*RRSS*)_n) and isotactic stereoblock ((*RR*)_n(*SS*)_m) by well controlled metal alkoxide catalyzed ROP of *rac*-lactide.⁵⁴



Scheme 1.15. Microstructures of polylactides.

The stereoselective ring-opening polymerization (ROP) of racemic lactide has received considerable attention in recent years in industry as well as in academia because the stereoblock poly(*rac*-LA) with a high isotacticity has a melting temperature ($\sim 230^{\circ}\text{C}$) higher than that of the commercially available homochiral poly(*L*-lactide) ($\sim 170^{\circ}\text{C}$) and could be a practical material superior to the homochiral poly(*L*-lactide).³¹ Isotactic PLA can be obtained by sequential polymerization of (*R,R*)-lactide or (*S,S*)-lactide with an achiral, living initiator. However, this strategy suffers from the fact that (*R,R*)-lactide is much more expensive than (*S,S*)-lactide. An alternative approach is to employ a more selective catalyst to affect the kinetic resolution of *rac*-lactide (i.e., a catalyst with a propagation rate constant for the preferred enantiomer that is much higher than the corresponding rate constant for the unpreferred enantiomer).

1.3.2. Polycaprolactone (PCL)

Nomenclature of Lactones: Lactones are generally named according to the precursor acid molecule, for example (propio 3 carbon, valero 5 carbon, capro 6 carbon) with a *-lactone* suffix and a Greek letter prefix that specifies the number of carbons in the heterocyclic ring, i.e. the distance between the –OH and the –COOH group alongside backbone. The first carbon after the carbon in the –COOH group on the parent compound is labeled as α , the second will be labeled as β , third carbon as γ , fourth carbon as δ , fifth carbon as ϵ etc.

In the family of synthetic biodegradable polymers, poly(ϵ -caprolactone) (PCL), is a linear aliphatic polyester composed of hexanoate repeating units, hydrophobic and semicrystalline with a degree of crystallinity which can reach 69%.⁵⁵ The physical, thermal and mechanical properties of PCL depend on its molecular weight and its degree of crystallinity. The main physical properties of PCL reported in the literature are shown in Table 1.1.

Table 1.1. Physical Properties of PCL

Properties	Range	Ref.
Number average molecular weight ($M_n/g\ mol^{-1}$)	530-630 000	-
Melting temperature ($T_m/^\circ C$)	56-65	56,41,58
Glass transition temperature ($T_g/^\circ C$)	(-65)-(-60)	41,58
Decomposition temperature ($^\circ C$)	350	57
Density ($\rho/g\ cm^{-3}$)	1.145	56
Inherent viscosity ($\eta_{inh}/cm^3\ g^{-1}$)	100-130	59
Intrinsic viscosity ($\eta/cm^3\ g^{-1}$)	0.9	55
Tensile strength (σ/MPa)	4-785	59,41,58
Young modulus (E/GPa)	0.21-0.44	59
Elongation at break ($\epsilon /\%$)	20-120	59,41,58

PCL biodegrades within several months to several years depending upon the molecular weight, degree of crystallinity and the condition of degradation.^{41,56,57,60-63} Microorganisms are able to completely biodegrade PCL in the nature.⁵⁶ Nevertheless, if PCL can be enzymatically degraded in the environment, it cannot be degraded enzymatically in the body.⁴¹ PCL is one of the most widely used aliphatic linear polyesters in the biomedical field as scaffolds in tissue engineering,^{57,60,63} in long term drug delivery systems,^{58,62} but also in microelectronics,⁶⁴ and in packaging,⁴¹ due to its properties of controlled degradability, miscibility with few polymers and biocompatibility.

PCL is synthesized by ring opening polymerization of ϵ -caprolactone with different metal based catalytic systems, enzymes, organic compounds and inorganic acid.⁶⁵ Tin(II) 2-ethylhexanoate is the most widely used catalyst for the polymerization of ϵ -caprolactone both in academia and industries. However, all tin compounds are cytotoxic and they cannot be used for the production of polyesters for pharmaceutical or biomedical applications. In contrast, metal alkoxides complexes of rare earth metals were proposed recently as the most active and nontoxic catalyst for the living ROP of cyclic esters under relatively mild experimental conditions.^{66,67} Polymers with high molecular weight and low dispersity can be easily prepared using these catalytic systems, but they are probably too expensive for a significant interest in industry.

1.4. Ring Opening Polymerization of Cyclic Esters with Heteroleptic complexes

1.4.1. Stereoselective ROP of Lactide

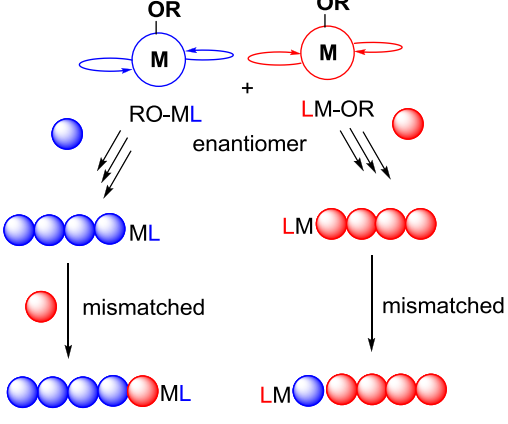
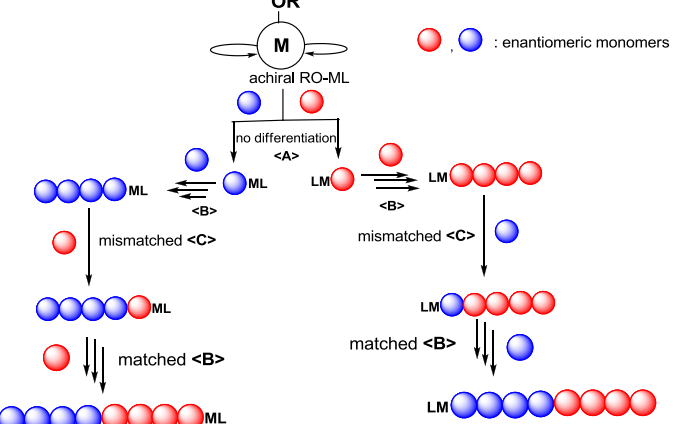
As already mentioned in section 1.3.1.2, the stereoselective ROP of lactides has received a lot of attention in the recent years. In the following paragraphs, after presenting the mechanisms that can regulate the stereoselectivity, we will summarize the results described in the literature concerning the synthesis of stereocontrolled PLA.

1.4.1.1. Mechanism of Stereocontrol Polymerization of Lactide

Two mechanisms are generally proposed for stereocontrolled polymerization: (a) Enantiomorphic site control mechanism and (b) Chain end control mechanism

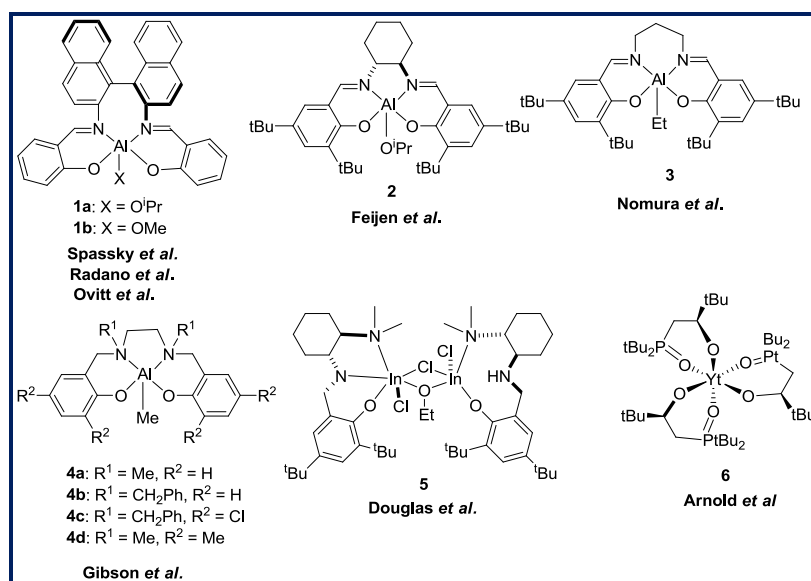
(a) Enantiomorphic site control mechanism (SEM): In this mechanism, the chirality of the catalyst defines the stereochemistry of the subsequent monomer insertion during chain propagation.

(b) Chain end control mechanism (CEM): In this mechanism, stereochemistry of the last inserted monomer in the growing polymer chain influences which enantiomeric form of the monomer is incorporated next.

Site control mechanism (SEM)	Chain End control Mechanism (CEM)
	
<p>1. In this mechanism, the complex has a chiral environment that is constructed by the ligand around the metal center and can consistently be able to differentiate one enantiomer of lactide from the other as represented in the above scheme for the (ROP) of <i>rac</i>-LA with the <i>rac</i>-catalyst.</p>	<p>1. In this mechanism, both the metal complex and the ligand are achiral. In contrast to SEM the initiation occurs without enantiomeric differentiation of the racemic monomer (<A>) as represented in the above scheme for the (ROP) of <i>rac</i>-lactide with the achiral-catalyst.</p>
<p>2. The insertion of the wrong monomer could occur at the active polymer chain end.</p>	<p>2. The insertion of the mismatched monomer could occur (<C>), the monomer with the same chiral sense as that of the propagating chain end continues.</p>
<p>3. Under this mechanism, (ROP) of <i>rac</i>- and <i>meso</i> lactide can lead to <i>Isotactic</i> and <i>Syndiotactic</i>^a polymer respectively.</p> <p>^a Assuming no polymer exchange occur</p>	<p>3. In this mechanism, polymerization of <i>rac</i>-lactide lead to <i>Isotactic</i> or <i>Heterotactic</i> polymer and <i>meso</i>-lactide lead to <i>Syndiotactic</i> or <i>heterotactic</i> polymer.</p>

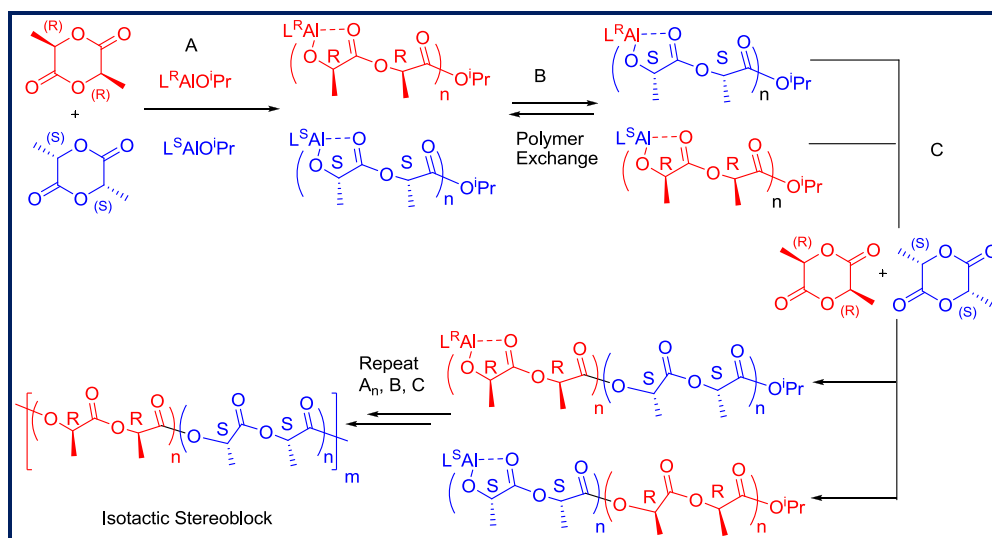
1.4.1.2. Synthesis of Stereoblock PLA from *rac*-lactide

Spassky *et al.*⁶⁸ were the first to demonstrate that Schiff-base (SALEN type) aluminum complexes are highly selective initiators for the polymerization of racemic lactide (*rac*-LA). As early as 1996, his group reported the kinetic resolution of enantiomers of lactides in the polymerization of *rac*-LA by using aluminum methoxide complex (**1b**) bearing a chiral binaphthyl Schiff-base ligand (Scheme 1.16). The chiral nature of the catalyst led to the highly selective ring-opening of (*R,R*)-LA to give isotactic PLA through an enantiomorphic site-control mechanism; the (*S,S*)-LA was left largely unreacted. At 70°C, the catalyst exhibited a 20:1 preference for the polymerization of (*R,R*)-LA over (*S,S*)-LA ($k_{RR} / k_{SS} = 20$), high monomer conversion leads to a highly crystalline stereoblock copolymer with higher T_m (187°C) than an optically pure PLA (due to crystalline structure of the stereocomplex different from that of the “homopolymer”).



Scheme 1.16. Stereoselective complexes for ROP of *rac*-lactide.

Radano *et al.*⁶⁹ and Ovitt *et al.*^{48,70} reported the polymerization of *rac*-LA with *rac*-(SalBinap)AlOⁱPr complex (**1**) yielded highly crystalline, predominantly isotactic polymer ($T_m = 179-191^\circ\text{C}$). Detailed microstructure investigation allowed them to propose polymer exchange mechanism for the formation of stereoblock PLA with alternating blocks of (*R*)- and (*S*)-LA in the main chain (Scheme 1.17). This mechanism involves the predominant ring opening reaction of each enantiomer of the catalyst **1**-(*R*) and **1**-(*S*) with (*R*) and (*S*)-lactide respectively step (A). Eventually, due to the modestly higher activation energy of reacting with the disfavored lactide stereoisomer, polymer exchange occurs and the other enantiomer of lactide is incorporated in steps (B,C). At this point, propagation resumed with the favored lactide stereoisomer, creating a stereoblock structure (Scheme 1.17).



Scheme 1.17. Proposed Mechanism of Stereoblock PLA from *rac*-lactide.

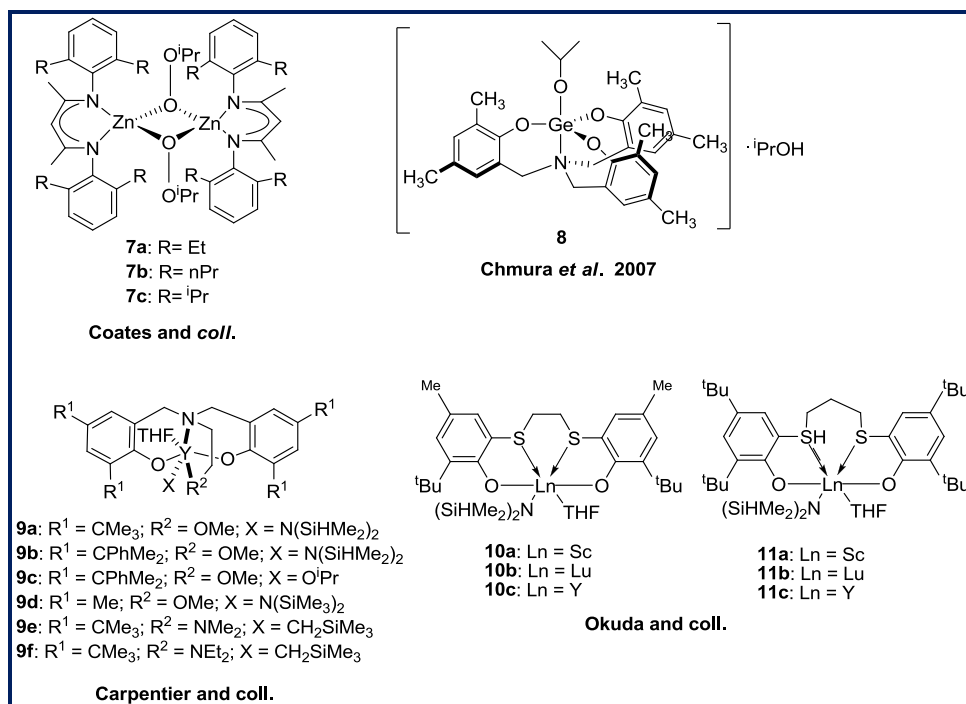
Feijen and *coll.*⁷¹ succeeded in the synthesis of crystalline PLAs ($T_m = 183.5^\circ\text{C}$) with long isotactic sequences in toluene or solvent free polymerization of *rac*-lactide by using chiral aluminum complex (**2**) based on (*R,R*)-cyclohexane diamine Schiff base ligands (Scheme 1.16). In comparison with Spassky's catalyst, this one preferentially polymerized (*S,S*)-LA over (*R,R*)-LA ($k_{SS}/k_{RR} = 14$). In both cases, chiral ligand induces the enantiomorphic site control mechanism during chain propagation. Nomura *et al.*⁷² reported an aluminum-achiral ligand complex (**3**) (Scheme 1.16) that was able to polymerize *rac*-LA to form PLA stereocomplex ($T_m = 170\text{--}192^\circ\text{C}$) *via* chain-end control mechanism.

Gibson *et al.*⁷³ reported aluminum complexes based on aminophenoxide ligands (designated as SALAN, a saturated version of Schiff-base SALEN ligand) and found that subtle changes in the ligand periphery dramatically influenced the stereochemistry of the resulting polymer. In particular complexes **4a** & **4b** (Scheme 1.16) with unsubstituted phenoxide units of the SALAN ligand produced isotactic PLAs, whereas the complexes **4c** & **4d** with substituted phenoxide units of the SALAN moiety produced heterotactic PLAs. It was also demonstrated that the substituents R^1 attached to the nitrogen atoms changes the tacticity of the polymer. For example, the benzylamine derivative **4b** affords higher isotacticity ($P_m = 0.79$) than its methylamine analogue **4a** ($P_m = 0.68$). Further advances has been made recently by Douglas *et al.*⁷⁴ who reported that the *racemic*-alkoxy bridged dinuclear indium complex **5** (Scheme 1.16) produces moderate isotactic PLAs ($P_m = 0.59$), whereas the enantiopure catalyst **5** produces polymer with decreased activity and enantioselectivity ($P_m = 0.43$), thereby highlighting the importance of a site-control mechanism.

Recently, Arnold *et al.*⁷⁵ reported the C_3 -symmetric yttrium complex **6** (Scheme 1.16) containing racemic mixture of two homochiral (R,R,R) and (S,S,S) complexes. This complex was used as a new class of effective initiator for the polymerization of *rac*-LA and produces high isotactic PLAs ($P_m = 0.81$) even at high monomer conversions and high molecular weights ($M_n = 200000 \text{ g}\cdot\text{mol}^{-1}$).

1.4.1.3. Synthesis of Heterotactic PLA from *rac*-lactide

Preparation of heterotactic polylactide from the polymerization of *rac*-lactide results from the alternate incorporation of (R,R)- and (S,S)-LA during the chain propagation *via* chain end control mechanism. Coates and *coll.*⁷⁶ reported a new class of β -diiminate dinuclear achiral complexes **7a-7c** (Scheme 1.18) that were found to act as single site living initiators for the polymerization of *rac*-lactide affording highly heterotactic PLA. Interestingly substituents on the β -diiminate ligand exert a significant influence on the rate and stereoselectivity of the polymerization. For example complex **7c** (isopropyl group substituted) exhibited the highest activity and stereoselectivity ($P_r = 0.90$). Changing the ligand substitution from isopropyl to ethyl groups in complex **7a** resulted in a decrease in heterotacticity ($P_r = 0.79$). Similarly substitution with *n*-propyl groups lowers the heterotacticity ($P_r = 0.76$). Recently Chmura *et al.*⁷⁷ reported single site germanium complex **8** (Scheme 1.18) derived from C_3 -symmetric amine(trisphenolate) ligand. This complex has shown higher activity and heterotactic-enriched PLA ($P_r = 0.82$) in bulk conditions at higher temperature (130°C).



Scheme 1.18. Stereoselective complexes for heterotactic ROP of *rac*-LA.

Well defined rare-earth metal (i.e. yttrium, lanthanum and neodymium) complexes **9a-9f** supported by amine-bis(phenolate) ligands were also investigated recently by Carpentier and *coll.*⁷⁸ Okuda and *coll.*⁷⁹ also reported several lanthanoid complexes **10** and **11** supported by 1, ω -dithiaalkanediy-bridged bis(phenolate) ligands. These complexes have shown to be excellent initiators for the heterotactic PLAs formation and have been reviewed recently by C.M. Thomas.⁵⁴ However, few studies have been reported so far on the utilization of Group (IV) metal (Ti, Zr, Hf) complexes as initiators for the stereoselective polymerization of *rac*-lactide. Further studies of these types of metal complexes as an initiator for stereoselective ROP of *rac*-lactide will be discussed in details in the later section of this chapter.

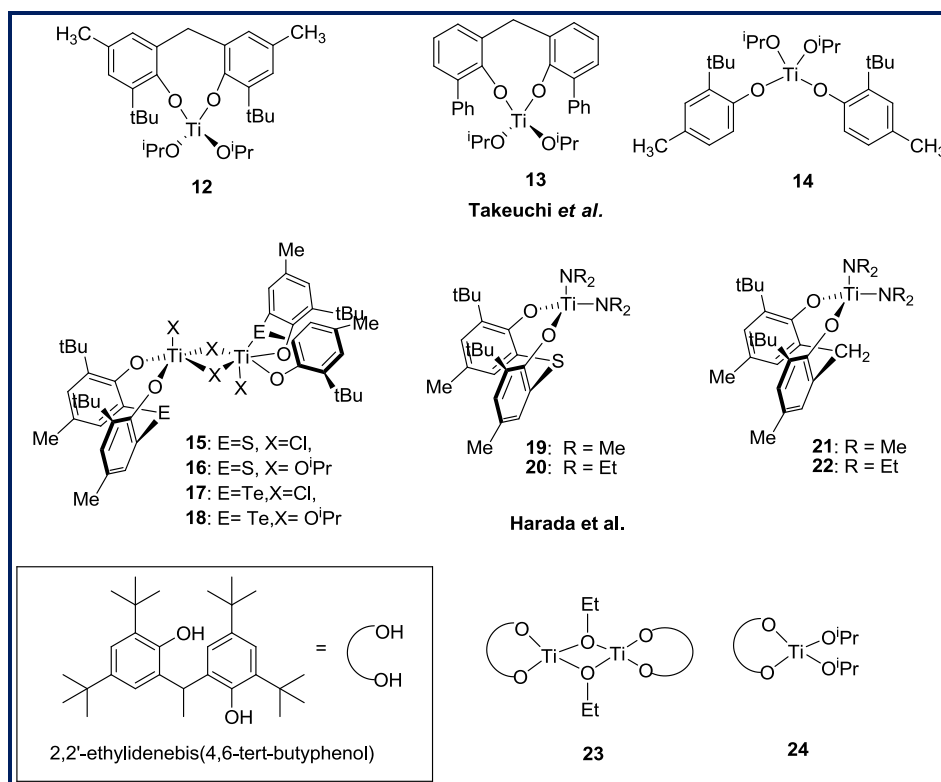
1.4.2. Group (IV) Metal Complexes for ROP of Cyclic Esters

Ring Opening Polymerization of cyclic esters such as lactide and ϵ -caprolactone with a wide variety of catalytic systems based on tin, aluminum, zinc, magnesium, iron, lanthanide and lithium organometallic complexes containing initiating groups such as amides, carboxylates, and alkoxides has been extensively studied over the past few decades.^{5,80} Despite the fact that some excellent initiators have been reported for the polymerization of lactides in the literatures, the search for new catalysts that generate well defined PLA polymers are still important.

Heteroleptic Group (IV) metal complexes are a relatively new addition to the arsenal of cyclic esters ROP catalysts. These complexes are generally derived from different types of chelating ligands and the influence of the catalyst structures on the activities and the physical properties of the polymer are studied. Among the transition metals, Group (IV) metal complexes have exhibited good control over the polymerization process, featuring reasonably fast initiation and minimal side reactions and this one leads to polymers of well-defined and predictable molecular weight (M_n) and narrow dispersity values (M_w/M_n). Polymers with heterotactic enrichment of monomers have also been reported in the literature for the polymerization of *rac*-LA. The role of Group (IV) metal (Ti, Zr, and Hf) complexes in ROP of cyclic esters is reviewed in the following section of this chapter.

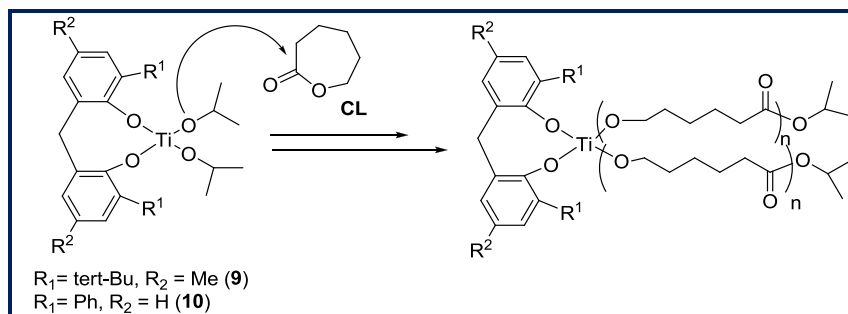
1.4.2.1. Bis (phenolate) Group 4 metal Complexes

It is well known that non-metallocene complexes of Group (IV) metals based on bis(phenolate) ligands, are highly active initiators for the polymerization of α -olefins and styrene.^{81,82} Takeuchi *et al.*⁸³ were the first to report the living polymerization of ϵ -caprolactone using titanium complexes with bulky bis(phenolate) ligands (Scheme 1.19).



Scheme 1.19. Bis(phenolate) titanium complexes.

Complexes **12**, **13**, and **14** having different phenolate substitution were tested as initiators for the ROP of ϵ -caprolactone. Complex **12** showed higher activity when the polymerization was carried out in dichloromethane at 25°C, for monomer to initiator mole ratio of 100, complete conversion was achieved within 5 h and the obtained polymer exhibited narrow molecular weight distribution ($M_w/M_n = 1.15$) and a number-average molecular mass (M_n) of 6500 g.mol⁻¹. The degree of polymerization (DP_n) of the polymer was almost half of the monomer-to-initiator mole ratio, suggesting the formation of two polymeric chains from every molecule of **12** (Scheme 1.20).



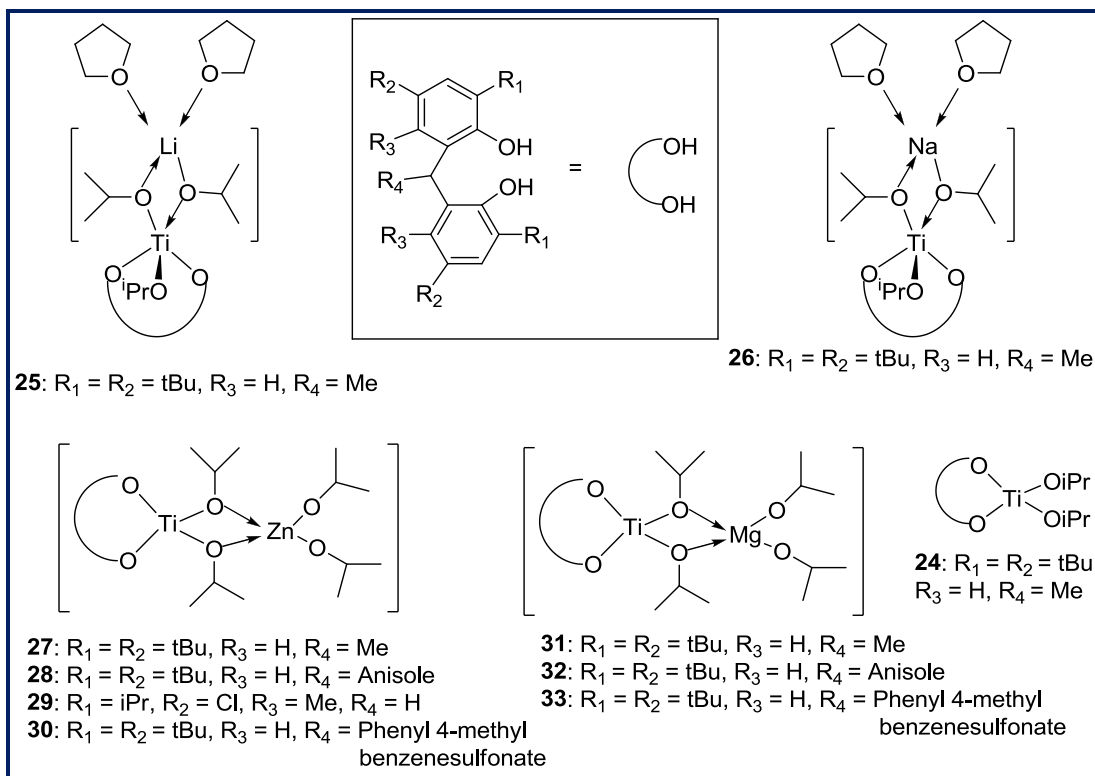
Scheme 1.20. Formation of 2 polymeric chains for 1 molecule of catalyst during ROP of ϵ -CL.

Complex **13** with less bulky ligand showed lower activity (100% conversion in 75 h) with narrower molecular weight distribution ($M_n = 5600 \text{ g.mol}^{-1}$; $M_w/M_n = 1.10$). Complex **14** having non bridged hindered phenols, showed rapid monomer conversion (100% in 7 h) but the polymer had a broader molecular weight distribution ($M_n = 6300 \text{ g mol}^{-1}$, $M_w/M_n = 1.47$). These results suggested that the complex derived from bridged bulky bis(phenolate) ligands is more effective than sterically unhindered ligands in the ROP of ϵ -CL.

Harada and *coll.*⁸⁴ in 2002 reported the titanium complexes **15-18** having Sulfur and Tellurium bridged chelating bis(phenolate) ligands for the ROP of cyclic esters such as ϵ -caprolactone, *L*-LA, and δ -valerolactone. The titanium dichloride complexes **15** and **17** having the sulfur and tellurium bridged bis(phenolate) ligands respectively, permit the ROP of ϵ -CL in toluene at 100°C without any pre-initiator (propylene oxide). These results are in sharp contrast to the titanium dichloride complex having methylene bridged bis(phenolate) ligands reported by Takeuchi *et al.*⁸³ in which the titanium dichloride complex were active for ϵ -CL only after the addition of propylene oxide (formation of chloro titanium monoalcoholate species which in turn initiate the ϵ -CL polymerization). These results indicate that the coordination of sulfur or tellurium to the metal center plays an important role in the catalyst activity. Complex **17** (containing Te bridged ligand) showed a better controlled polymerization of *L*-LA compare to that of complex **15** having the sulfur bridged ligands. The ^1H NMR of the poly-(ϵ -CL) obtained from the titanium alkoxide complex **18** (Tellurium bridged ligand) showed hydroxyl and isopropyl ester chain ends, suggesting that the initiation of the polymerization occurs *via* the isopropoxides groups of the complex. However, these complexes were hardly soluble in toluene and in order to improve the solubility of these complexes, a series of bis(dialkylamido) titanium complexes **19-22** having a sulfur or methylene bridged bis(phenolate) ligands was reported by the same group and utilized for ROP of ϵ -CL and *L*-LA with a $[\text{M}]/[\text{Ti}]$ ratio of 200.⁸⁵ Complex **20** having the sulfur bridged bis(phenolate) ligand with an amido initiating group catalyzed polymerization of ϵ -CL (90% conversion in 32 h) with a controlled molecular weight distribution ($M_n = 18,800 \text{ g.mol}^{-1}$, $M_w/M_n = 1.31$) whereas titanium dichloro complex **15** gave 100% yield in 6 h with a broad molecular weight distribution ($M_w/M_n = 2.28$). The polymerization of ϵ -CL with complex **22** having the methylene bridged bis(phenolate) ligand, led to 91% conversion within 8 h with a high molecular weight ($M_n = 56,200 \text{ g.mol}^{-1}$) and relatively broader molecular weight distribution ($M_w/M_n = 1.60$). In the ^1H NMR spectrum of the polymer obtained, resonances corresponding to $\text{N-CH}_2\text{-CH}_3$ end groups are present. This indicates that the initiation occurs through the insertion of a first monomer into the titanium-nitrogen bond yielding a titanium alkoxide that will permit the propagation.

Sobota and *coll.*⁸⁶ reported bis(aryloxo) alkoxo titanium complexes **23** and **24** (Scheme 1.19) having 2,2'-ethylidene bis(4,6-tert-butylphenol) as an ancillary ligand for the ROP of *L*- and *rac*-LA in toluene at 70°C with a monomer to initiator ratio of 100. Monomeric complex **24** showed higher activity (98% conversion within 1h 12 min) with M_n of 18,000 g.mol⁻¹ and M_w/M_n of 1.08 than for dimeric complex **23** (90% conversion in 2.5 h). This difference in activity reported probably due to the fact that coordination of lactide to the dimeric complex, this later must break into monomeric complex which is the actual active species. Activity of these complexes was higher compared to the titanium complexes reported by Harada *et al.* mentioned previously. These complexes were also found to be good initiator for controlled polymerization of *rac*-LA with high degree of heterotactic addition.

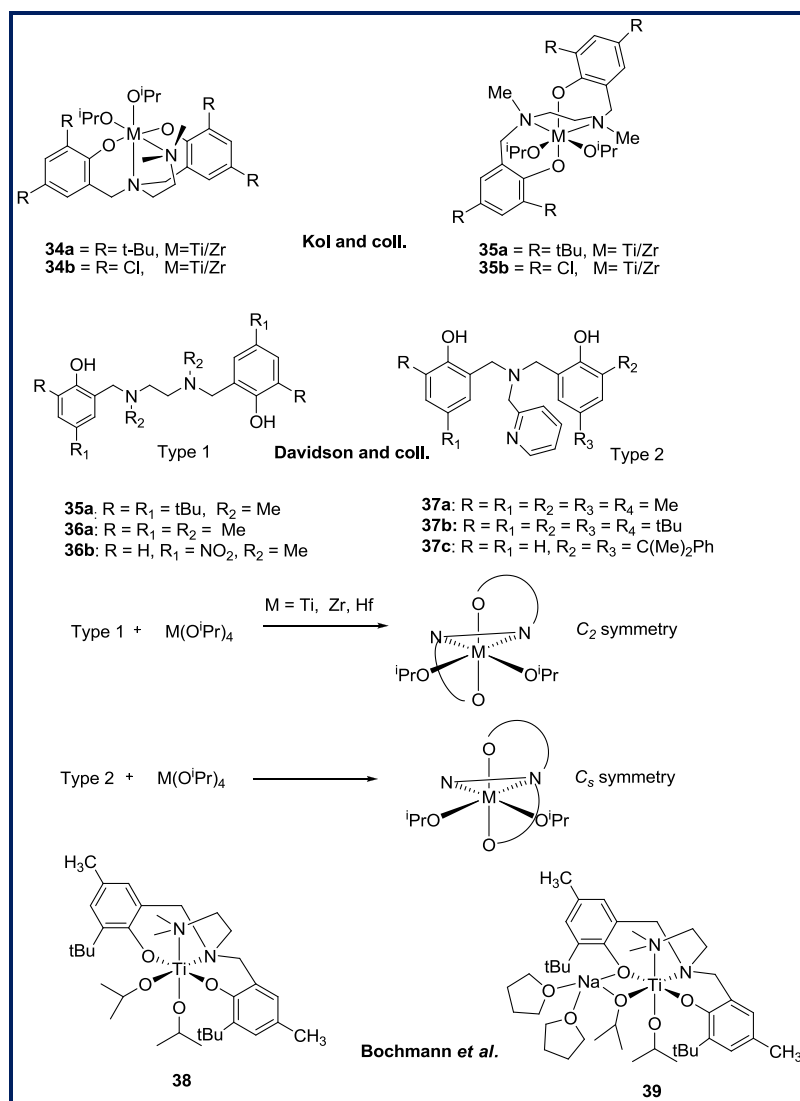
Very recently Chen *et al.* reported titanium based heterobimetallic complexes **25-33** (Scheme 1.21) supported by sterically protected bis(phenolate) ligands and subsequently varying the other metal with Li, Na, Mg, and Zn. These complexes were tested as initiators for ROP of *L*-LA.⁸⁷ Polymerization was carried out in toluene at 30°C to 70°C (these complexes are stable in toluene within this temperature range and remain intact during the course of polymerization process). At 30°C, bimetallic complexes **25** (Ti-Li) (74% conversion in 94 h) and **26**(Ti-Na) (80% conversion in 94 h) having the same ligand substitution showed very similar activities. In contrast when the magnesium was introduced in place of (Li) or (Na) in complex **31** (Ti-Mg) the polymerization rates was drastically enhanced (89% conversion in 3.5 h at 30°C). More interestingly the reaction rate was further increased when the Mg was replaced with Zn in complex **27**(Ti-Zn) (91% conversion in 0.5 h at 30°C). This has been reported probably due to the difference in electronic configurations and charge density of Zn and Mg. It is known that the charge density of Mg is higher than that of Zn, resulting in a stronger Mg-OR bond and therefore making it more difficult to cleave the Mg-O bond causing decreases in the polymerization rate. Monometallic titanium complex **24** with the same ligand system showed lower activity (76% conversion in 94 h at 30°C). In the case of complex **28** (Ti-Zn) polymerization was completed within 30 min, whereas the complex **32** (Ti-Mg) bearing the same ligand substitution showed very less activity (13% conversion in 1 h). When the methyl group was replaced with methylphenylsulfonyl group, the reactivity of complexes **30**(Ti-Zn) (93% conversion in 0.25 h at 30°C) and **33**(Ti-Mg) (95% conversion in 1h at 30°C) increased due to the electron donating ability of the methylphenylsulfonyl group. The reactivity decreases in the order **30** > **28** > **27** > **29** for (Ti-Zn) complexes and **33** > **32** > **31** for (Ti-Mg) complexes, indicating that the electron donating substituent plays a vital role in polymerization activity.



Scheme 1.21. Titanium based Heterobimetallc complexes based on bulky Bis(phenolates).

1.4.2.2. (Di)amine bis(phenolate) Group (IV) metal Complexes

Group (IV) metal complexes derived from several families of tetradentate di- and trianionic amine bis(phenolate) ligands has been reported earlier in the literature for α -olefin polymerization.^{88,89} Since these ligands exhibit a variety of wrapping modes around group IV transition metals, they present the ability to tune the metal geometry as well as electronic and steric parameters by changing their structure and substitution pattern. In this connection Kol and *coll.* reported a series of titanium and zirconium alkoxide complexes **34** and **35** (Scheme 1.22) supported by dianionic tetradentate amine bis(phenolate) ligands of different families, for the ROP of *L*-lactide.⁹⁰ The isopropoxo titanium complexes were synthesized by reacting the respective ligand with $Ti(O^iPr)_4$, whereas the zirconium complexes were synthesized by reacting the respective ligand with monomeric $Zr(CH_2Ph)_4$ or $Zr(NMe_2)_4$ and the respective intermediate complexes were treated with 2 equiv of isopropyl alcohol to yield the zirconium isopropoxide complexes. Ti and Zr complexes **34** (**a,b**) having an amine-bis(phenolate) ligand bearing a dimethylamino side arm donor feature C_s symmetry in solution, whereas Ti and Zr complexes **35** (**a,b**) having a diamine-bis(phenolate) ligand feature C_2 symmetry.



Scheme 1.22. Tetradentate amine bis(phenolate) ligands and the corresponding complexes.

Polymerizations were carried out in neat monomer at 130°C with a [M]/[I] ratio of 300. These studies revealed that complexes Ti(OⁱPr)₂ **34a** ($A = 0.25 \text{ g}_{\text{pol}} \text{ mmol}_{\text{cat}}^{-1} \text{ h}^{-1}$; $M_n = 7000 \text{ g} \cdot \text{mol}^{-1}$; PDI = 1.28) and Ti(OⁱPr)₂ **35a** ($A = 0.23 \text{ g}_{\text{pol}} \text{ mmol}_{\text{cat}}^{-1} \text{ h}^{-1}$; $M_n = 5400 \text{ g} \cdot \text{mol}^{-1}$; PDI = 1.11) corresponding to two different ligand families with a same phenolate ligand substitution (t-Bu) showed similar activities, molecular weights and narrow molecular weight distributions. Similarly, complexes Ti(OⁱPr)₂ **34b** ($A = 0.09 \text{ g}_{\text{pol}} \text{ mmol}_{\text{cat}}^{-1} \text{ h}^{-1}$; $M_n = 4000 \text{ g} \cdot \text{mol}^{-1}$; PDI = 1.21) and Ti(OⁱPr)₂ **35b** ($A = 0.11 \text{ g}_{\text{pol}} \text{ mmol}_{\text{cat}}^{-1} \text{ h}^{-1}$, $M_n = 6800 \text{ g} \cdot \text{mol}^{-1}$; PDI = 1.18) of two different ligand families featuring the same phenolate substituent (Cl) showed similar activities. The molar mass observed from the SEC corresponds to two polymer chains grown per metal center. Again, zirconium complexes of isomeric ligands bearing the same phenolate substituent but belonging to

different families showed similar activities. However, in contrast to titanium series, the activity of the zirconium complexes **34b** ($32.4 \text{ g}_{\text{pol}}\text{mmol}_{\text{cat}}^{-1}\text{h}^{-1}$) and **35b** ($27.0 \text{ g}_{\text{pol}}\text{mmol}_{\text{cat}}^{-1}\text{h}^{-1}$) were 10-20 times higher than those of the other pair of complexes **34a** ($1.7 \text{ g}_{\text{pol}}\text{mmol}_{\text{cat}}^{-1}\text{h}^{-1}$) and **35a** ($2.2 \text{ g}_{\text{pol}}\text{mmol}_{\text{cat}}^{-1}\text{h}^{-1}$). These results suggested that the structural effects on reactivity were more pronounced in the zirconium series relative to the titanium series. It has also been observed that the activity of zirconium complex is considerably higher than that of the corresponding titanium complex. The ratio of zirconium-to-titanium activities was ca. 10-fold for the complexes $\text{M}(\text{O}^i\text{Pr})_2$ **34a** and $\text{M}(\text{O}^i\text{Pr})_2$ **35a** ($\text{M} = \text{Zr}, \text{Ti}$) bearing the tert-butyl substitution on the ligand, but reached more than 200 fold for complexes $\text{M}(\text{O}^i\text{Pr})_2$ **34b** and $\text{M}(\text{O}^i\text{Pr})_2$ **35b** ($\text{M} = \text{Zr}, \text{Ti}$) bearing the chloro substitution on the ligand. For example $\text{Zr}(\text{O}^i\text{Pr})_2$ **34b** showed higher activity ($32.4 \text{ g}_{\text{pol}}\text{mmol}_{\text{cat}}^{-1}\text{h}^{-1}$), whereas $\text{Ti}(\text{O}^i\text{Pr})_2$ **34b** exhibited very less activity ($0.09 \text{ g}_{\text{pol}}\text{mmol}_{\text{cat}}^{-1}\text{h}^{-1}$). This difference in activity is reported probably due to the less crowded and larger atomic radius of Zr metal center, which may allow facile approach of monomer for coordination as compare to the Ti metal center.

A subsequent work reported by Davidson and *coll.*⁹¹ considered the same kind of ligand framework and prepared a series of Ti, Zr, and Hf alkoxide complexes **36-37** (Scheme 1.22) supported by two types of amine bisphenolate ligands. Structural characterization by X-ray diffraction revealed two classes of six-coordinate complexes, depending upon the ligand type (pseudo- C_s or pseudo- C_2). These complexes allow the controlled ROP of cyclic esters (LA and ϵ -CL) with predictable molecular weight and low dispersity. The Ti(IV) and Zr(IV) complexes were screened for the ROP of ϵ -CL at room temperature in toluene ($[\text{M}]/[\text{I}] = 100$; time 24 h). Complex $\text{Ti}(\text{O}^i\text{Pr})_2$ **35a** (ligand of type 1 with the bulkiest group in ortho position of the phenoxide) was found to polymerize ϵ -CL (yield 99%, $M_n = 3800 \text{ g}\cdot\text{mol}^{-1}$) with broad molecular weight distribution ($M_w/M_n = 2.60$), whereas all other titanium complexes (**36**) of these ligands series were found to be inactive. Ti(IV) complexes of type 2 ligands (**37**) also proved to be inactive under the same reaction condition.

For Zr(IV) complexes of type 1 ligands, the opposite trend was observed, complex $\text{Zr}(\text{O}^i\text{Pr})_2$ **36a** (ligand with less bulky group in ortho position of the phenoxide) polymerizes ϵ -CL with moderate activity, in a more controlled manner (yield 99%, $M_n = 12,000 \text{ g}\cdot\text{mol}^{-1}$, $M_w/M_n = 1.59$). Under the same experimental condition, $\text{Zr}(\text{O}^i\text{Pr})_2$ **35a** was found to be less active (yield 10%, $M_n = 900 \text{ g}\cdot\text{mol}^{-1}$, $M_w/M_n = 1.27$). A similar trend was observed for Zr(IV) complexes of type 2 ligands with the more bulky $\text{Zr}(\text{O}^i\text{Pr})_2$ **37b** being inactive and the less bulky $\text{Zr}(\text{O}^i\text{Pr})_2$ **37a** being highly active and exhibiting well controlled polymerization (yield 99%, $M_n = 13,800 \text{ g}\cdot\text{mol}^{-1}$, $M_w/M_n = 1.35$). The type 2 complex $\text{Zr}(\text{O}^i\text{Pr})_2$ **37a** containing a pyridyl group, found to be more active (50% conversion in 2 h) than the type 1 complex $\text{Zr}(\text{O}^i\text{Pr})_2$ **36a** (50% conversion in 6 h) and these results can be rationalized by the structural differences between the type1 and

type 2 complexes. For the latter, one N-donor atom are part of the labile side arm donor whereas for type 1, both N-donors are part of the ligand backbone and are consequently less labile.

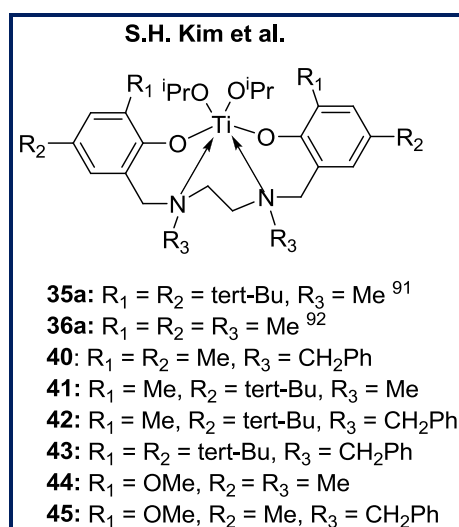
These complexes were also tested as initiators for the ROP of *L*-LA ($[M]/[Ti] = 100$, 2 h, 110°C; toluene = 10 mL). All titanium complexes were found to be inactive except $Ti(O^iPr)_2$ **35a** and even in this case only modest conversion was achieved (20% yield, $M_n = 550 \text{ g}\cdot\text{mol}^{-1}$, $M_w/M_n = 1.43$). For zirconium, whereas complexes containing bulky ligands $Zr(O^iPr)_2$ **37b** and $Zr(O^iPr)_2$ **37c** were found to be inactive, complexes containing less bulky ligands lead to well controlled polymerization with high activity, for example $Zr(O^iPr)_2$ **36a** (99% yield, $M_n = 10800 \text{ g}\cdot\text{mol}^{-1}$, $M_w/M_n = 1.08$) and $Zr(O^iPr)_2$ **37a** (99% yield, $M_n = 10800 \text{ g}\cdot\text{mol}^{-1}$, $M_w/M_n = 1.13$).

All these complexes were also tested as initiators for the ROP of *rac*-LA under melt condition ($[M]/[I] = 300$; 130°C; 2 h) and solution condition ($[M]/[I] = 100$; 110°C; 2 h, toluene = 10 mL). Complexes $Zr(O^iPr)_2$ **36a** and $Zr(O^iPr)_2$ **37a** showed significant conversion in solution condition, whereas all other complexes were found to be inactive under this condition. However, all titanium complexes were found to be active under melt condition except $Ti(O^iPr)_2$ **35a** and they all produce atactic PLA. Comparison of molecular weight of the polymer produced from the initiators under melt condition ($Ti(O^iPr)_2$ **36a**, $M_n = 33,000 \text{ g}\cdot\text{mol}^{-1}$; $M_w/M_n = 1.64$) and ($Hf(O^iPr)_2$ **36a**, $M_n = 14,100 \text{ g}\cdot\text{mol}^{-1}$; $M_w/M_n = 1.54$) containing the same ligand, showed the molecular weight of the Hf-initiated polymer is approximately half of the Ti-initiated polymer. This is consistent with initiation and propagation of polymer chains occurring at both isopropoxide sites for Hf but at only one site for Ti initiator. However Zr and Hf initiators derived from bulky ligands produced high molecular weight polymers, which is consistent with the formation of one polymer chains per metal center.

Stereoselective polymerization of *rac*-LA was achieved using Zr and Hf complexes under melt and solution conditions in contrast to the titanium complexes. The zirconium complexes $Zr(O^iPr)_2$ **36a** and $Zr(O^iPr)_2$ **37a** both formed isotactically enriched PLA ($P_r/P_m = 0.25/0.75$) and ($P_r/P_m = 0.4/0.6$) respectively, where P_r/P_m is the stereoselective parameter (P_r = probability of racemic linkage; P_m = probability of meso linkage) observed from the 1H homonuclear decoupled NMR spectrum.⁵⁰⁻⁵³ Type 1 ligands showed greater selectivity than the type 2 ligands, this difference in selectivity by chain end control mechanism may be accounted to their structural differences in their metal complexes (i.e. type 1 ligands after coordination with metal center (Zr) exhibit pseudo C_2 symmetry chiral complexes and type 2 ligands exhibit nonchiral pseudo C_s symmetry). The origin of stereoselectivity in both Zr and Hf complexes as compare to Ti complex explained by the minor variation in the coordination chemistry of Group (IV) metals (i.e. both Zr and Hf metals favors higher coordination number than Ti).

Titanium alkoxide complexes were found to be less active than Zr and Hf complexes towards ROP because of their high positive charges and strong Π bond effect between Ti and alkoxides and consequent decrease of the rate of polymerization. To overcome this problem, Bochmann *et al.*⁹² developed new heterobimetallic complex of titanium-sodium supported by a multidentate amino bis(phenolate) ligand (Scheme 1.22) for the ROP of ϵ -caprolactone in toluene at 60°C. The reactivity studies were shown that monometallic complex **38** exhibited lower activity than bimetallic complex **39** (complete conversion of 200 equiv of monomer in 2 h). Increases in reactivity are probably due to the coordination of sodium metal reducing the electron density on alkoxo Ti-O bond and therefore decreases Π donor ability.

Kim *et al.*⁹³ recently reported a series of titanium isopropoxide complexes **40-45** based on tetradentate salan-type ligands with benzyl or methyl substituents on bridging nitrogen atoms, and studied the ROP of *L*-LA (Scheme 1.23) and discussed about the electronic and steric effect on the activity and polymer properties.

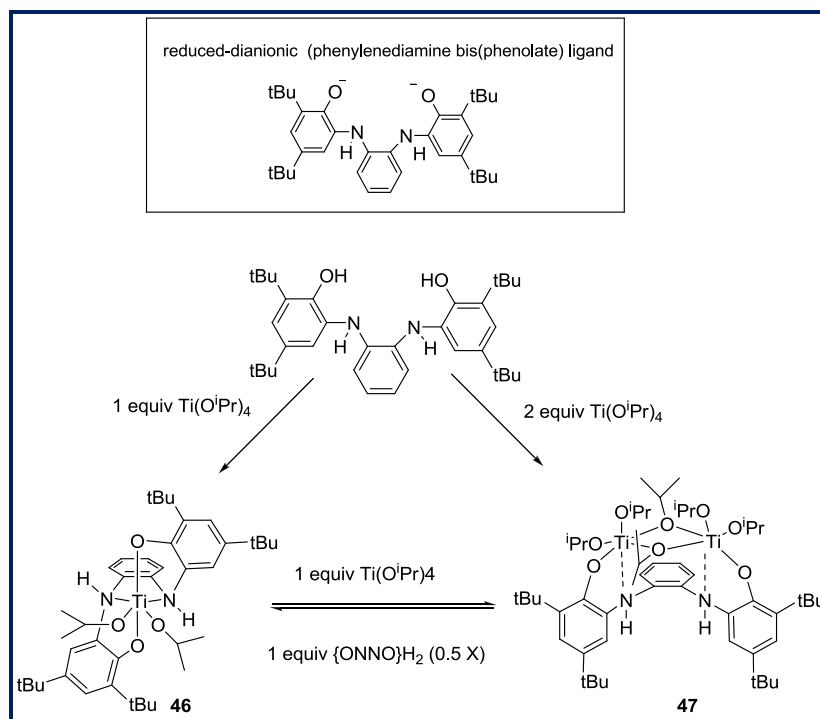


Scheme 1.23. Dianionic tetradentate amine bis(phenolate)titanium complexes.

The polymerization was carried out both in bulk and solution (toluene) condition at 130°C with a [LA]/[Ti] ratio of 300 (6 h). Under the bulk polymerization conditions all complexes **40-45** gave PLA with 81-89% conversion. In the solution polymerization conditions, they produce PLA with 59-67% conversion, which represents 40% decrease in yield as compare to bulk condition. All pairs of complexes bearing the same substituent at aryl rings but different groups on bridging nitrogen showed very similar activities both under the bulk and in the solution polymerization condition. In contrast a clear difference in molecular weight and PDI values was observed between the two complexes of the same pair. For example complex **41** produced PLA with ($M_n = 13,200$ g.mol⁻¹ and $M_w/M_n = 1.15$) whereas the complex **42** produced PLA with ($M_n = 27,700$

$\text{g}\cdot\text{mol}^{-1}$ and $M_w/M_n = 1.30$) indicating that the complex featuring the N-benzyl substituted ligand produce polymer with high molecular weight which is close to the expected M_n value of $36,000 \text{ g}\cdot\text{mol}^{-1}$ assuming one polymer chain from each metal center.

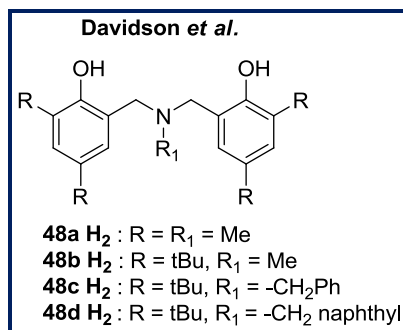
More interestingly Kol and *coll.* recently described a new type of tetradentate phenylenediamine bis(phenolate) ligand for Group (IV) metal complexes.⁹⁴ It is known in the literature that tetradentate diamine bis(phenolate) ligands when coordinated to group 4 metals exhibited a tetra anionic form or an oxidized-dianionic form, in both of which the N-donors are sp^2 - hybridized, thus the [ONNO] donor array adopts a planar geometry. The more "typical" reduced-dianionic form featuring sp^3 - hybridized N-donors, was reported for the first time by this group. Mononuclear $[\{\text{ONNO}\}\text{Ti}(\text{O}^i\text{Pr})_2]$ **46** and dinuclear complexes $[\{\mu\text{-ONNO}\}\{\text{Ti}(\mu\text{-O-}i\text{-Pr})(\text{O-}i\text{-Pr})_2\}_2]$ **47** were prepared by reacting the ligand precursor $\{\text{ONNO}\}$ and the metal precursor $\text{Ti}(\text{O}^i\text{Pr})_4$ in a proper reactant ratio (Scheme 1.24). In both types of complexes, the ligand binds in the reduced dianionic form. The reaction between the ligand precursor and $\text{Zr}(\text{O-}i\text{-Pr})_4(i\text{-PrOH})$ did not lead to a mononuclear complex even with a 1:1 reactant ratio. Instead a dinuclear complex $[\{\mu\text{-ONNO}\}\{\text{Zr}(\mu\text{-O-}i\text{-Pr})(\text{O-}i\text{-Pr})_2\}_2]$ was isolated. However by employing the bulkier metal precursor $\text{M}(\text{O-t-Bu})_4$ ($\text{M} = \text{Ti}, \text{Zr}$), the mononuclear complexes $[\{\text{ONNO}\}\text{M}(\text{O-t-Bu})_2]$ were formed exclusively.



Scheme 1.24. Synthesis and interconversion of mononuclear and dinuclear titanium complexes.

All these complexes were used as initiators for the polymerization of *L*- and *rac*-LA in neat monomer at 130°C with [M]/[I] ratio of 300. The dinuclear complexes showed very low activity and polymerization of *rac*-LA produced atactic PLA. More interestingly mononuclear titanium complexes [{ONNO}Ti(O^{*i*}Pr)₂] **46** and [{ONNO}Ti(O-*t*-Bu)₂] were considerably more active than the corresponding zirconium and hafnium complex, and this is the first report of titanium complex exhibiting a higher activity than the corresponding Zr and Hf complexes. In addition, *rac*-LA was consumed much faster than the *L*-LA by both Ti and Zr complexes. For example 300 equiv of *L*-LA were not completely consumed by [{ONNO}Ti(O-*t*-Bu)₂] in 1 h, whereas 300 equiv. of *rac*-LA were almost completely consumed within 1 min. The higher activity towards *rac*-LA is consistent with a hetero-specific stereoselectivity. The Zr complex led to higher degree of heterotacticity relative to the Ti complex. Degree of heterotacticity increased when the polymerization is performed at lower temperature, the highest degree of heterotactic enchainment ($P_r = 87\%$) being obtained at 75°C with [{ONNO}Zr(O-*t*-Bu)₂]. The molecular weights of the polymer obtained from *L*-LA were considerably lower than the calculated values due to non-living polymerization. For *rac*-LA, molecular weights of the polymer obtained from the zirconium catalyst approached the calculated values, whereas the Ti catalyst led to lower molecular weight due to two growing chains on the metal center.

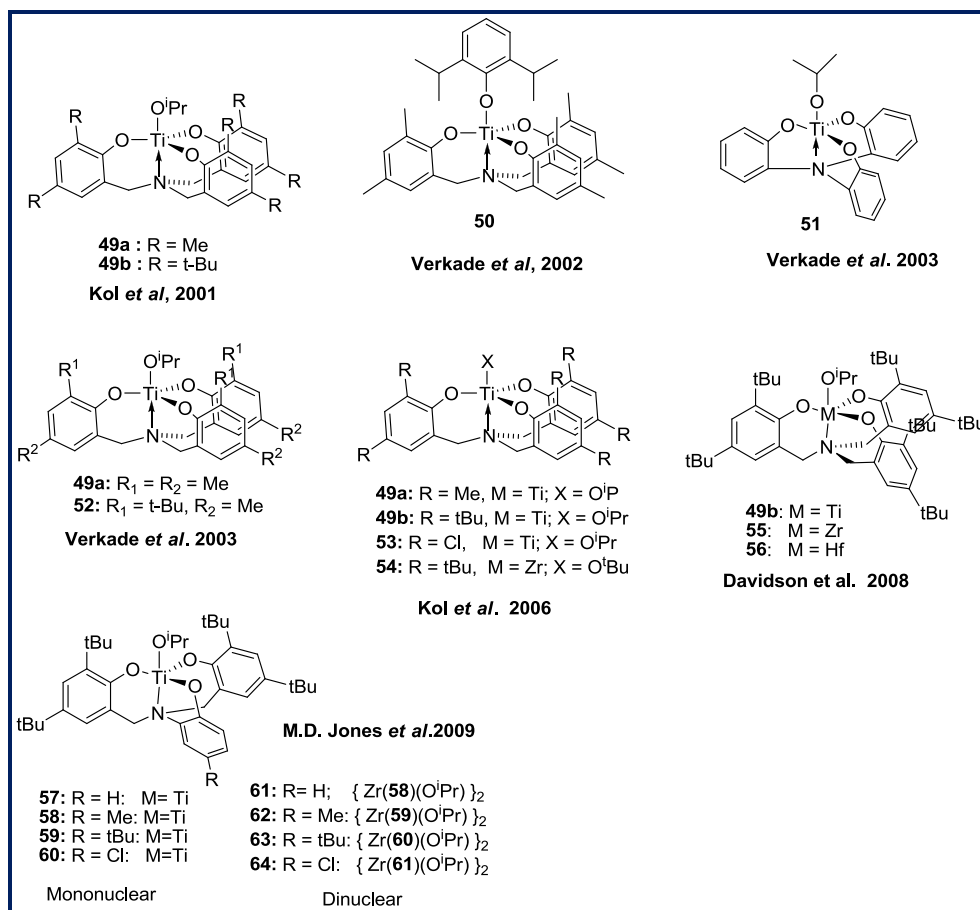
Davidson *et al.*⁹⁵ reported a series of Group (IV) metal complexes based on tridentate amine bis(phenolate) ligands (Scheme 1.25). Ligand **48a**-H₂ having less bulky substitution on the phenolate was reacted with Ti(O^{*i*}Pr)₄ in a 1:1 mole ratio to produce a mixture of mono and disubstituted complexes [Ti(**48a**)(O^{*i*}Pr)₂ and Ti(**48a**)₂]. Attempts to isolate the monomeric complex from this mixture were unsuccessful. Related zirconium and hafnium complexes were prepared in an analogous manner. Steric bulk of the ligands has been increased (**48b**, **48c**, **48d**) in order to favor the formation of mono-substituted complexes. For Zr and Hf metals only disubstituted complexes could be isolated. In contrast, mono-substituted titanium complexes Ti(O^{*i*}Pr)₂(**48b**), Ti(O^{*i*}Pr)₂(**48c**), Ti(O^{*i*}Pr)₂(**48d**) could be isolated. These mono-substituted titanium complexes were used as initiators for the ROP of ϵ -CL in toluene at 20°C with [M]/[Ti] ratio of 100 during 24 h. All complexes were active for the controlled polymerization of ϵ -CL with excellent conversions and low dispersity values (example, for complex Ti(O^{*i*}Pr)₂(**48d**), >99% conversion, $M_n = 11400 \text{ g}\cdot\text{mol}^{-1}$, $M_w/M_n = 1.08$).



Scheme 1.25. Dianionic tridentate amine bis(phenolate)titanium complexes.

1.4.2.3. Amine tris(phenolate) Group 4 metal Complexes

Amine tris(phenolate) ligand has recently received considerable interest in metal coordination chemistry for its ability to stabilize well-defined monomeric complexes for a wide range of reactive metal centers.^{96,97} In 2001, for the first time, Kol *et al.*⁹⁸ synthesized and characterized amine tris (phenolate) titanium complexes **49** (Scheme 1.26).



Scheme 1.26. Amino tris(phenolate) Group 4 metal alkoxide complexes.

Subsequently Verkade *et al.*⁹⁹ reported the amine tris(phenolate) titanium alkoxide complex **50** (Scheme 1.26) which possesses the bulky di-ⁱPr-phenolate as an initiating group as compare to complex **49a**. Polymerization of *L/rac*-LA was carried out using this complex under bulk condition at 130°C (24 h) with a monomer to initiator ratio of 300. Moderate activity for both *L*-LA (69% yield; $M_n = 19400 \text{ g}\cdot\text{mol}^{-1}$; $M_w/M_n = 1.51$) and *rac*-LA (68% yield; $M_n = 16000 \text{ g}\cdot\text{mol}^{-1}$; $M_w/M_n = 1.43$) has been observed. However, polymerization of *rac*-LA leads to atactic polymer.

Further advances have been made by the same group who reported complexes **51**, **52** and **49a** (Scheme 1.26) having different bulkiness for the ROP of *L*- and *rac*-LA under bulk (solvent free) as well as in solution (toluene) condition at 130°C.¹⁰⁰ Complex **51** revealed to be a highly active catalyst for *L*- and *rac*-LA polymerization under bulk condition. For example, in bulk conditions, with complex **51**, *L*-LA is polymerized with a 95% yield in 4 h exhibiting $M_n = 80800 \text{ g}\cdot\text{mol}^{-1}$ and $M_w/M_n = 2.00$ while initiator **49a** was significantly less active (55% yield in 4 h; $M_n = 52000 \text{ g}\cdot\text{mol}^{-1}$; $M_w/M_n = 1.46$) and initiator **52** was even worse (26% yield in 14 h; $M_n = 28400 \text{ g}\cdot\text{mol}^{-1}$; $M_w/M_n = 1.35$). The activity of these complexes for *rac*-LA also decreases in the same order **51** > **49a** > **52**. No stereoselectivity was observed for *rac*-LA polymerization. In solution condition (toluene, at 130°C), initiator **51** showed moderate activity for *L*-LA (68% yield in 24 h; $M_n = 11100 \text{ g}\cdot\text{mol}^{-1}$; $M_w/M_n = 1.66$) while **49a** and **52** did not show any catalytic activity. This report also established that increasing steric bulk on the titanium in **49a** and **52** particularly in the region above the equatorial plane can block the titanium ligation in the coordination insertion step.

A subsequent report by Kol and *coll.*⁹⁰ considered the same ligand framework by varying the substituents on the phenolate rings of the ligands (Scheme 1.26). Pentacoordinate titanium complexes **49a**, **53**, and **49b** were prepared in quantitative yield by reaction of $\text{Ti}(\text{O}^i\text{Pr})_4$ with the requisite proteo ligand, while the reaction of $\text{Zr}(\text{O}^i\text{Pr})_4 \cdot i\text{PrOH}$ led to a zwitterionic bis(homoleptic) complex.¹⁰¹ Pentacoordinate Zirconium complex **54** was prepared by reacting the ligand with the bulky $\text{Zr}(\text{O}-t\text{-Bu})_4$ precursor, whereas less bulky ligands led to undefined products. All these complexes were used as initiators for the ROP of *L*-LA under bulk condition at 130°C and the activity was found to be less than that previously reported by Verkade *et al.* Titanium complexes **49a** and **53** showed similar activity, whereas complex **49b** showed lower activity due to bulky substituents. Most significantly, the activity of the zirconium complex **54** ($A = 6.6 \text{ g}_{\text{pol}} \text{ mmol}_{\text{cat}}^{-1} \text{ h}^{-1}$; $M_n = 24200 \text{ g}\cdot\text{mol}^{-1}$; $M_w/M_n = 1.31$) was considerably higher than that of the corresponding titanium complexes **49b** bearing the same ligand substituents ($A = 0.38 \text{ g}_{\text{pol}} \text{ mmol}_{\text{cat}}^{-1} \text{ h}^{-1}$; $M_n = 12500 \text{ g}\cdot\text{mol}^{-1}$; $M_w/M_n = 1.29$) and complexes **49a** ($A = 0.91 \text{ g}_{\text{pol}} \text{ mmol}_{\text{cat}}^{-1} \text{ h}^{-1}$; $M_n = 18100 \text{ g}\cdot\text{mol}^{-1}$; $M_w/M_n = 1.44$) and **53** ($A = 1.10 \text{ g}_{\text{pol}} \text{ mmol}_{\text{cat}}^{-1} \text{ h}^{-1}$; $M_n = 17600 \text{ g}\cdot\text{mol}^{-1}$; $M_w/M_n = 1.32$) bearing less bulky ligand substituents. These results suggest that activity was found to depend strongly on the metal, the coordination number around the metal, and the phenolate substituents.

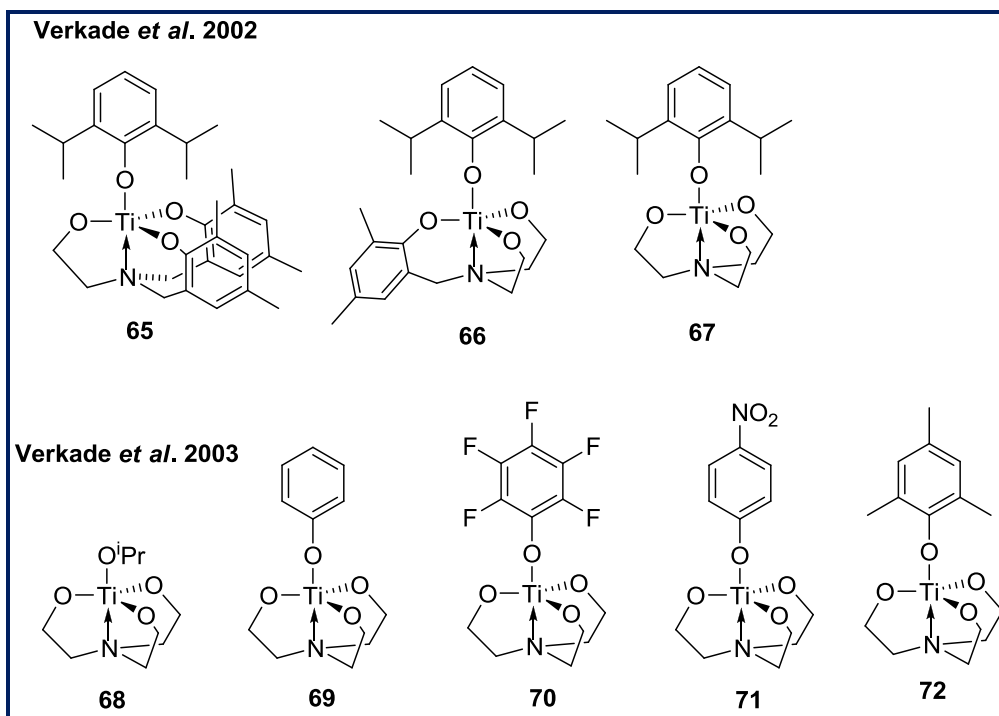
Further advances for this type of ligand have been made recently by Davidson *et al.*¹⁰² who reported Group 4 metal (Ti, Zr, Hf) complexes **49b**, **55**, and **56** (Scheme 1.26) bearing bulky amine tris(phenolate) ligands. Titanium complex **49b** used as initiator for ROP of *rac*-LA, under bulk polymerization condition (130°C; [M]/[I] = 300) showed moderate activity (50% yield in 0.5 h ; $M_n = 37100 \text{ g}\cdot\text{mol}^{-1}$; $M_w/M_n = 1.38$) but analysis of microstructure of the resulting polymers showed atactic PLA, whereas zirconium complex **55** (78% yield in 0.1 h ; $M_n = 32300 \text{ g}\cdot\text{mol}^{-1}$; $M_w/M_n = 1.22$) and hafnium complex **56** (95% yield in 0.5 h ; $M_n = 71150 \text{ g}\cdot\text{mol}^{-1}$; $M_w/M_n = 1.19$) showed higher activity than Ti complex **49b**. For Zr and Hf complexes, high degree of stereocontrol, the degree of heterotactic enrichment being $P_r = 0.96$ and $P_r = 0.88$ respectively was observed. Such high activity and stereoselectivity have never been achieved before for any initiator under solvent free condition. Indeed, the highest selectivity was reported by Nomura *et al.* under similar condition using an aluminium salen complex (130°C; [M]/[I] = 300; 30 min, 25% yield, $P_r = 0.84$).¹⁰³ It has been proposed that changes in stereoselectivity from Ti to (Zr / Hf) could be due to the minor differences in the coordination mode of the growing polymer chain to the metal center, and it has also been proposed that for complexes **55** and **56**, inversion of axial chirality during chain propagation can lead to alternation stereochemistry at the metal center and therefore heterotactic selectivity can occur *via* a dynamic enantiomeric site control mechanism as observed for Ge complex.⁷⁷

Recently, Jones *et al.*¹⁰⁴ reported Group 4 metal complexes with different amine phenolate ligands **57-64** (Scheme 1.26). All titanium complexes **57-60** have shown to be monomeric by X-ray crystallography, whereas zirconium analogues **61-64** have been isolated as dimeric species. These complexes have been tested for the ROP of *rac*-LA under both solution (toluene) and bulk conditions. Both the Ti(IV) and Zr(IV) complexes were active for the ROP of *rac*-LA (except complex **59**) in toluene at 80°C. Zr(IV) complexes showed a high degree of control as shown from the lower molecular weight distribution ($M_n = 13000\text{-}28000 \text{ g}\cdot\text{mol}^{-1}$; $M_w/M_n = 1.30$ to 1.34) compared to Ti(IV) complexes ($M_n = 11000\text{-}23000 \text{ g}\cdot\text{mol}^{-1}$; $M_w/M_n = 1.14$ to 2.07). However, polymerization with Ti complex **57** is highly controlled, affording a narrow molecular weight distribution ($M_w/M_n = 1.14$). Interestingly, Zr(IV) complexes yield only slight degree of heterotacticity ($P_r = 0.6$, Complex **63** and **64**) and this is in sharp contrast to the related C_3 symmetric complexes **55**, reported by Davidson *et al.* as discussed previously, which afforded PLA with a great degree of heterotacticity ($P_r = 0.96$) even under bulk condition. This indicates the subtlety of the environment of the metal to control the stereoselectivity for the ROP of *rac*-LA.⁷³ In bulk polymerization condition, all complexes were found to be active including complex **59**. Ti(IV) complexes **57** and **59** afforded polymer with low polydispersity indexes $M_w/M_n = 1.09$ and $M_w/M_n = 1.06$ respectively. Zr(IV) complexes were again more active than the Ti(IV) complexes in bulk condition. Complex (Zr) **61** maintained higher activity (99% conversion in 15 min at 130°C), whereas complex **57**

(Ti) showed moderate activity (74% conversion in 120 min at 130°C). However, the polymerization initiated with (Ti) complexes is not well controlled due to the broad and unpredictable range of molecular weights.

1.4.2.4. Titanatranes Group 4 metal Complexes

Titanatrane (Titanium + atrane skeleton of the ligand) group 4 metal complex have received considerable interest because of their applications in olefin polymerization.¹⁰⁵ Atrane ligands contain a neutral nitrogen atom that facilitates coordination in a chelate fashion when necessary by providing the metal with additional electron density. Kim and Verkade⁹⁹ reported for the first time the use of Titanium(IV)alkoxide complexes with titanatranes containing different sizes for the ROP of *L*- and *rac*-LA under bulk condition (Scheme 1.27). All the complexes **65-67** were prepared by reacting $\text{Ti}(\text{O}^i\text{Pr})_4$ with 1 equiv of 2,6-di-*i*-Pr-phenol and 1 equiv of the corresponding ligand precursor.

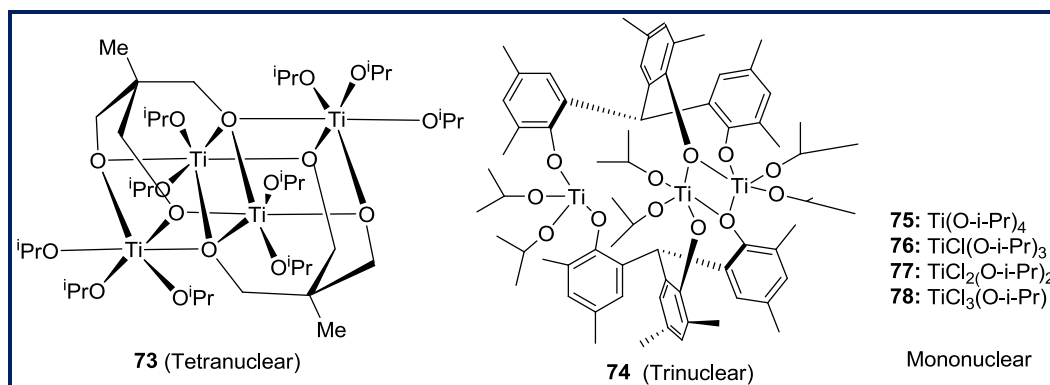


Scheme 1.27. Titanatranes alkoxide complexes.

The polymerization was carried out in neat monomer at 130°C with [LA]/[Ti] ratio of 300 during 24 h. Polymerization results suggest that molecular weight, PDI, and activity are highly affected by the nature of the tetradentate ligand. Polymerization activity and dispersity value increases with respect to increase in the number of five-membered rings in tetradentate ligand from complexes **65-67**. However, polymerization of *rac*-LA leads to atactic PLA for all complexes.

The same group has also synthesized several other type of titanatrane (**68-72**, Scheme 1.27) in a one pot reaction containing $\text{Ti}(\text{O}^i\text{Pr})_4$, triethanolamine, and the appropriate phenol.¹⁰⁰ Complex **68** exhibited monomeric form in solution and dimeric form in the solid state. These complexes have been tested as initiator for the ROP of *L*- and *rac*-LA under both bulk and solution conditions. Bulk polymerization was carried out at 130°C with a $[\text{M}]/[\text{Ti}]$ ratio of 300 at different reaction time (2 h to 15 h). All these complexes **68-72** were shown to be effective initiators and afforded polymer with narrow molecular weight distribution at low monomer conversion (80%), but showed bimodal distribution by SEC at conversion greater than 90% due to prominent transesterification side reactions. Under this condition, the polymers obtained from *rac*-LA were atactic. However, better polymerization control was achieved when the polymerization were carried out in toluene at 70°C. Among these, complex **68** was shown to be an effective initiator (70% conversion in 36 h, $M_n = 28,000 \text{ g}\cdot\text{mol}^{-1}$, $M_w/M_n = 1.03$), whereas at higher temperature (130°C), the PDI value increases from 1.03 to 1.35 with a decrease in polymer yield. The same trend was also observed for other complexes **69-72**. These results suggest that at higher polymerization temperatures, transesterification reactions are more prevalent by titanatrane complexes.

Tetranuclear titanium complex **73** (Scheme 1.28) was also synthesized by Verkade and used as initiator for ROP of *L*- and *rac*-LA.¹⁰⁶ Complex **73** was synthesized by reacting one equivalent of 1,1,1-tris(hydroxymethyl)ethane and excess of $\text{Ti}(\text{O}^i\text{Pr})_4$ in THF solution. Bulk polymerization of LA was carried out at 130°C with a $[\text{LA}]/[\text{Ti}]$ ratio of 300. Almost complete conversion was reached within 30 min ($M_n = 13300 \text{ g}\cdot\text{mol}^{-1}$; $M_w/M_n = 1.86$) and longer polymerization times (12 h) increased the molecular weight distribution ($M_n = 15000 \text{ g}\cdot\text{mol}^{-1}$; $M_w/M_n = 2.33$) indicating that complex **73** is thermally unstable and probably generates multinuclear initiating species under this condition.



Scheme 1.28. Mono, di and trinuclear titanium alkoxide complexes.

Solution polymerizations were carried out in toluene at 70°C and 130°C during 24 h with different [LA]/[Ti] ratio. Polymers with a controlled molecular weight distribution ranging from 1.33 to 1.55 and reasonably good conversion (60 to 99 % yield) were obtained. The ¹H NMR spectrum of PLA obtained from complex **73** in solution showed hydroxyl as well as i-Pr ester chain terminus, suggesting that initiation of LA takes place into a Ti-OⁱPr bond. Besides, the experimentally determined molecular weights are consistent with the formation of two growing polymer chain per metal centre.

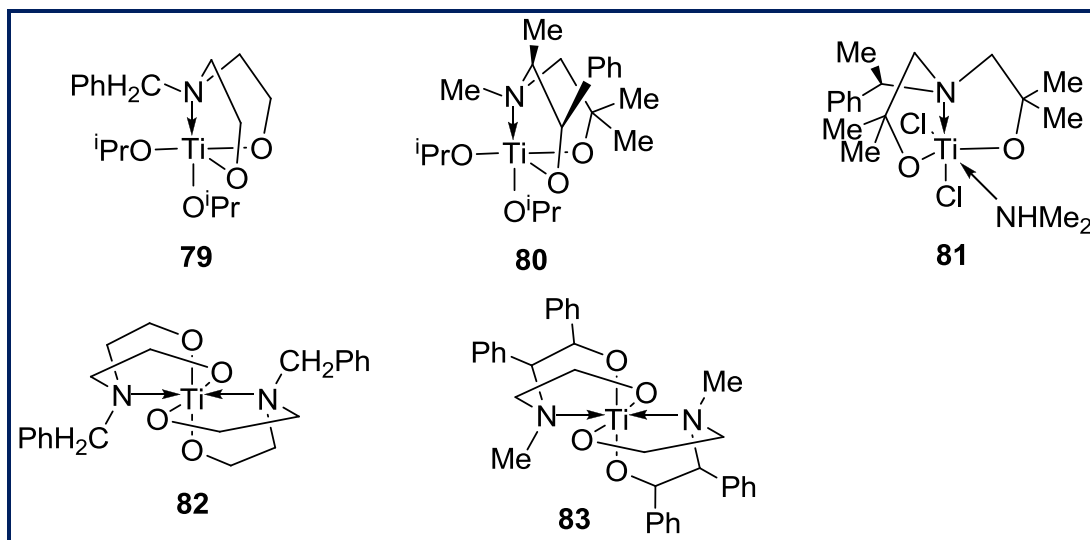
Trinuclear titanium isopropoxide complex **74** (Scheme 1.28) was synthesized by reacting one equivalent of tris(2-hydroxy-3,5-dimethylphenyl)methane and excess Ti(OⁱPr)₄ in THF solution.¹⁰⁷ Complex **74** was also tested as initiator for the ROP of *L*- and *rac*-LA in toluene at 130°C with a [LA]/[Ti] ratio of 200. Polymerization results suggest that 90% conversion was reached within 12 h and low PDI values ranging from 1.12 to 1.36 were observed. The controlled nature of the polymerization was shown by the linear increase of molecular weight with respect to monomer conversion.

Mononuclear titanium complexes (**75-78**)¹⁰⁰ (Scheme 1.28) were also tested as initiator for the ROP of *L*- and *rac*-LA under bulk as well as in solution condition at 130°C or 70°C with a [LA]/[Ti] ratio of 300 and 200 at different reaction time 2 h to 15 h. Complexes **76-78** were prepared by the reaction of **75** with the appropriate amount of TiCl₄ in pentane at room temperature. In solution polymerization of *L*-LA, complex **75** showed reasonably good yield (85% in 24 h) and the observed molecular weight from SEC ($M_n = 14300 \text{ g}\cdot\text{mol}^{-1}$) are consistent with the formation of four polymer chains per metal center with broader molecular weight distribution ($M_w/M_n = 2.01$). On the other hand, moderate yield and controlled molecular weight distributions ranging from 1.1 to 1.2 has been observed for the complexes **76-78** when the number of chlorine atoms in the respective complex increases. The methine region in the homonuclear decoupled ¹H NMR spectrum of poly(*rac*-LA) derived from complexes **76** and **77** displays more intense *sis* and *isi* tetrads peaks and these observation are consistent with a heterotactic-biased poly(*rac*-LA).

1.4.2.5. Dialkanolamine Titanocanes and Spirobititanocane Complexes

Titanium complexes of dialkanolamine ligands has been used as a potential catalyst for olefin polymerization and syndiotactic styrene polymerization.^{108,109} Recently, Kostjuk and co-workers reported titanium complexes **79-83** (Scheme 1.29) titanocanes and spirobititanocanes based on dialkanolamine ligands as initiators for ROP of ϵ -caprolactone under mild reaction temperature in bulk.¹¹⁰

Titanium complexes **79-81** (titanocanes) were prepared by the reaction of one equivalent of the corresponding dialkanolamine ligands with the same equivalent of metal precursor $\text{Ti}(\text{O}^i\text{Pr})_4$, whereas Spirotitanocanes complexes **82** and **83** were prepared by the reaction of $\text{Ti}(\text{O}^i\text{Pr})_4$, with two equivalents of the corresponding ligands.



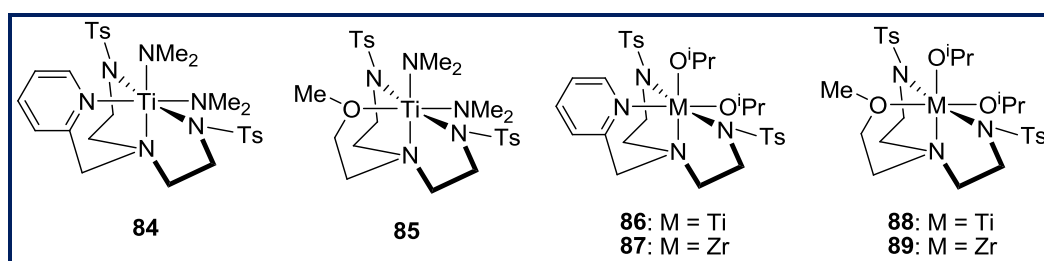
Scheme 1.29. Titanocanes and Spirotitanocane complexes for ROP of ϵ -CL.

The polymerization was carried out in toluene at 80°C with a $[\text{M}]/[\text{Ti}]$ ratio of 300. The molecular weights of polymer obtained from complexes **79** and **80** correspond to two growing polymer chains per metal center. Complex **80** produced polymers with considerably narrow molecular weight distribution ($M_w/M_n < 1.2$ up to 80% conversion) compare to that of polymer obtained from complex **79** derived from non-substituted dialkanolamine ligand ($M_w/M_n \sim 1.5$). In contrast, polymers obtained from the complex **81** exhibited high molecular weight (M_n up to $30,000 \text{ g}\cdot\text{mol}^{-1}$) indicating that only one polymer chain grows from the metal center, but with rather broader MWD ($M_w/M_n \sim 1.8$). The activity of the catalyst decreased in the order of **79** > **80** > **81**.

Activity of spirobititanocanes **82** and **83** found to be less than that of corresponding titanocanes **79** and **80**. As in the case of titanocanes, the spirobititanocane **82** with less bulky substituents induced faster polymerization than **83**. High molecular weight PCL ($M_n \leq 70,000 \text{ g}\cdot\text{mol}^{-1}$) with reasonable MWD ($M_w/M_n \leq 1.6$) are obtained with spirobititanocane complexes. These studies highlighted that the steric and electronic modification of the active site using bulky electronic rich multidentate ligands suppressed the undesirable side reactions; moreover the coordination of the nitrogen atom to the titanium also played a key role in the catalyst activity.

1.4.2.6. Sulfonamide ligands Group 4 metal Complexes

Group 4 metal complexes supported on bi- and tridentate bis(sulfonamide) ligands have been reported for a variety of catalytic transformation reaction over the past 15 years.¹¹⁰⁻¹¹⁴ Sulfonamide-supported ROP catalyst based on aluminum complexes have also been reported in the literature.^{115,116} Mountford *et al.* reported the first group 4 metal sulfonamide complexes for the ROP of ϵ -caprolactone and *rac*-LA.¹¹⁷ The bis(amide) complexes **84**, **85** (Scheme 1.30) were easily prepared under mild conditions by protonolysis reactions of the respective ligands with 1 equiv of $\text{Ti}(\text{NMe}_2)_2$ in benzene, whereas the bis(isopropoxide) complexes **86-89** were prepared under drastic condition by the reaction of appropriate ligands with excess of $\text{Ti}(\text{O}^i\text{Pr})_4$ for Ti complexes **86**, **88** and with $\text{Zr}(\text{O}^i\text{Pr})_4 \cdot \text{HO}^i\text{Pr}$ for Zr complexes **87**, **89**.

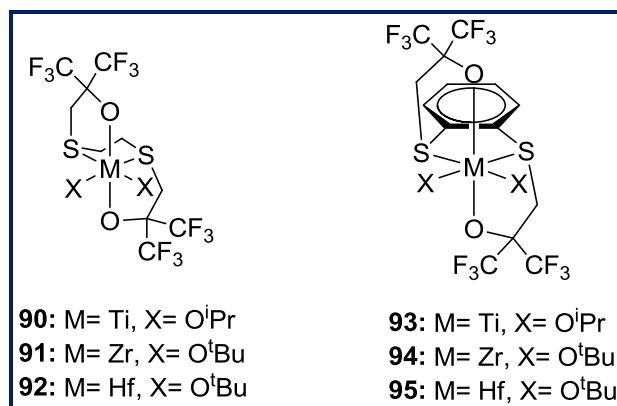


Scheme 1.30. Sulfonamide supported Group 4 metal complexes.

All these complexes were tested as initiators for the ROP of ϵ -CL in toluene at 100°C with $[\text{M}]/[\text{I}]$ ratio of 100. Moderate activity and poor control of molecular weight distribution has been observed for titanium bis(amide) complexes **84** (97% yield in 12 h; $M_w/M_n = 1.91$; $M_n = 12,990 \text{ g}\cdot\text{mol}^{-1}$ (value calculated from the SEC using the Mark-Houwink corrections^{118,119}) and **85** (95% yield in 22 h; $M_n = 14,260 \text{ g}\cdot\text{mol}^{-1}$; $M_w/M_n = 1.60$). However M_n observed from SEC are consistent with the formation of one polymer chain grown per metal center. More interestingly, titanium bis(isopropoxide) analogue complexes **86** (93% yield in 9 h; $M_n = 5720 \text{ g}\cdot\text{mol}^{-1}$; $M_w/M_n = 1.80$) and **88** (87% yield in 1 h; $M_n = 6390 \text{ g}\cdot\text{mol}^{-1}$; $M_w/M_n = 1.39$) were more active, and also gave a clear switch from one to two polymer chains per metal center. The zirconium analogue complexes **87** and **89** were shown to have a similar activity than Ti complexes and formed two polymer chains per metal center. Moreover, the PDI values ($M_w/M_n \leq 1.19$) indicated a better control than the Ti complexes. It was also found that activity of both Ti and Zr complexes bearing an OMe donor (**88** and **89**) were higher compared to the catalyst bearing a pyridyl donor ligand (**86** and **87**). The polymerization of *rac*-LA was also carried out with complex **89** in toluene at 70°C with $[\text{LA}]/[\text{Zr}]$ of 100 until 95% conversion (6.5 h). Polymers with low PDI value (1.14) were produced but were atactic, observed M_n value suggests two polymer chains were grown per metal center. Surprisingly, when the polymerization was carried out in bulk condition (130°C in 30 min, $[\text{M}]/[\text{Zr}] = 300$), polymers with higher M_n (42,430 $\text{g}\cdot\text{mol}^{-1}$, $M_w/M_n = 1.49$) were formed which is consistent with the formation of only one polymer chain per metal center.

1.4.2.7. Dithiodiolate ligands Group 4 metal complexes

Titanium complexes of {OSSO} type derived from dithiodiphenolate anionic chelating ligands have been reported in the literature for the isospecific polymerization of styrene.^{120,121} Scandium complexes based on these type of ligands has been successfully used for the heteroselective polymerization of *rac*-LA.⁷⁹ Kol and *coll.* recently reported the dithiodiolate group 4 metal complexes **90-95** bearing ligands with aliphatic or aromatic carbon bridge between the two sulfur atom (Scheme 1.31).¹²² They have been used as initiator for the ROP of *L*-LA in melt condition 130°C and *rac*-LA polymerization in the bulk (at 130°C; 142-144°C) and solution conditions at 75°C.

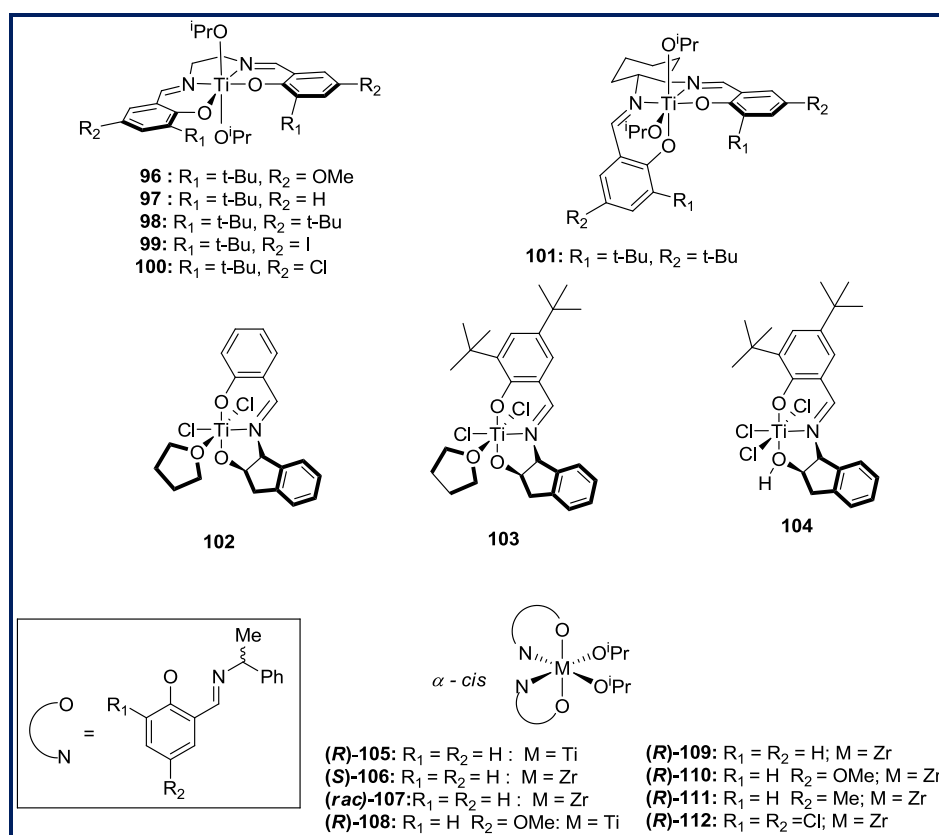


Scheme 1.31. Dithiodiolate ligand Group 4 metal complexes.

Polymerization studies revealed that the activity and stereoselectivity varied depending on the metal, whereas the nature of bridge between the two sulfur donors was found to be less significant. Titanium complexes **90** and **93** were found to be less active and gave atactic PLA for polymerization carried out in neat monomer (*rac*-LA) at 144°C. Higher activities and heterotacticity were observed for the analogues Zr and Hf complexes **91**, **94**, **92**, **95**. Interestingly, for the bulk polymerization conditions, hafnium complex **95** consumed 300 equiv of *rac*-LA within 1 min and 3000 equiv within 5 min, and this was found to be the highest active initiator among the group 4 metal complexes reported so far in the literature.^{94,102,117} The degree of heterotacticity was found to be higher in toluene at lower temperature 75°C ($P_r = 0.76-0.89$) than in bulk condition (0.48-0.73). The highest degree of heterotacticity (89%) was observed for Zr complex **94** and all these complexes were found to be active for polymerization of *L*-LA as well. Reasonably controlled molecular weight distribution ($M_w/M_n = 1.17-1.75$) was observed for all the polymerization.

1.4.2.8. Schiff base ligands Group 4 metal complexes

Schiff base ligands are considered “privileged ligands” since stereogenic centers or other elements of chirality (planes, axes) can be introduced in the synthetic design and could be able to coordinate with many different metals and to stabilize them in various oxidation states enabling the use of large variety of useful catalytic transformations.¹²³ Aluminium complexes derived from tetradentate schiff base (SALEN) ligands were particularly well studied for the ROP of lactides. These studies revealed that the polymerization activity, tacticity and molecular weight control dependent upon the diimine backbone and the aryl substituents, particularly the rate of polymerization is enhanced for complexes containing electron-withdrawing substituent attached to the phenoxy donors.¹²⁴



Scheme 1.32. Schiff base ligands Group 4 metal complexes.

Gibson *et al.* investigated the Ti-salen complexes (**96-101**) as initiator for the ROP of lactides.¹²⁵ Titanium (IV) bis(alkoxide) complexes **96-100** (Scheme 1.32) bearing ligands with different substitution on the phenolate ring, were synthesized by reacting the appropriate ligands with Ti(OⁱPr)₄ in Et₂O. Structure of complexes **96-100** with (1,2-ethylenediimine) backbone adopts a trans planar geometry as shown from NMR studies, whereas complex **101** with (cyclohexanedimine) backbone adopts a β -cis geometry as shown from the NMR as well as from X-ray structure analysis.

These complexes were tested as initiators for the ROP of *rac*-LA in toluene at 70°C. All complexes were found to be active, affording polymers with narrow molecular weight distribution (M_w/M_n value in the range of 1.11 to 1.21) and observed M_n values indicating that only one PLA chain propagates from each titanium center. Complex **96**, featuring electron-donating methoxy substituents, found to be more active than the other complexes. Surprisingly, the kinetic data revealed that complexes **99** and **100**, containing electron-withdrawing substituents **I** and **Cl** at the para position of the salen aryl rings respectively, presented lower activity, which is in sharp contrast to the salen aluminum initiators for which halide substituents in the para position of the aryl rings enhanced the activities.¹²⁴ Complex **101** was found to be the less active initiator, reported could be due to the nature of the diamino linkages in the ligand backbone. Homonuclear decoupled ¹H NMR spectrum of polymers showed only moderate heterotacticity with this catalytic system.

Subsequently Kim *et al.* synthesized a new type of di- and trichlorotitanium complexes **102-104** (Scheme 1.32) supported on chiral tridentate Schiff base ligands, derived from (1*R*,2*S*)-(-)-1-aminoindanol. These catalysts were used as initiator for the ROP of *L*-LA in toluene at 100°C with different [M]/[Ti] mole ratio.¹²⁶ Even though these complexes does not contain a “normal” initiating groups such as alkoxide or amide, they were able to polymerize lactide in a controlled manner (dispersity values in the range of 1.17 to 1.33). Activities of these complexes were shown to be reasonably good (50 to 86 % yield in 10 h). End group analysis of polymer by MALDI-TOF mass spectrometry and ¹H NMR suggests that initiation occurs through the insertion of *L*-LA into the titanium chloride bond. The observed molecular weights of the polymers obtained from the complexes **102** to **104** are consistent with the formation of two polymer chains from each metal center. The attempted synthesis of stereoblock PLA from *rac*-LA using a racemic analogue of catalyst **104** leads to dominantly atactic PLA but with an increased isotactic portion of 45%.

Further advances in this type of ligand systems have been made by Davidson and co-workers for the stereoselective ROP of *rac*-LA.¹²⁷ Complexes **105-112** were synthesized by reacting enantiomerically pure (*R*)- or (*S*)- or (*racemic*)- Schiff base ligands with the suitable metal precursor. The X-ray structures of complexes **108**, **109**, **111** exhibited pseudo-octahedral six-coordinated metal complexes and adopted α -*cis* geometry around the metal center. Polymerization of *rac*-LA were carried out in toluene at 80°C, with a [M]/[I] ratio of 100 for 2 h and in bulk condition at 130°C, with a [M]/[I] ratio of 300 for 0.5 h. At 80°C, all titanium complexes were found to be inactive under these conditions, whereas all zirconium complexes showed reasonable and similar level of activity (35 to 43 % yields with M_n value in the range of 9000 to 17000 g.mol⁻¹). Molecular weights are consistent with the propagation of only one polymer chain per metal center, and low molecular weight distribution (M_w/M_n in the range of 1.12 to 1.23) indicating a controlled polymerization.

Besides, similar heterotactic selectivity ($P_r \sim 0.7$) was observed for all complexes, suggesting that neither the chirality nor the nature of the ligand substitution significantly influenced the activity or selectivity of the complexes. These results suggest that the chain end control mechanism operates in the chain propagation. At low temperature (20°C), all Zr complexes were found to be active (45% yield in 24 h) and lead to controlled polymerization (M_w/M_n in the range of 1.08 to 1.12). Surprisingly, moderate heterotacticity (0.68%) was observed even under the presence of water (1 equiv) in the polymerization medium. These results suggest that the presence of water is not critically detrimental to polymerization initiated by zirconium Schiff based alkoxide complexes. Under solvent free conditions, both titanium and zirconium complexes were found to be active. However, Ti initiators yielded only atactic PLA, whereas Zr initiators produced PLA with reasonable stereoselectivity even under these demanding conditions ($P_r = 0.70-0.76$). The robust nature of the zirconium complexes **109**, **110**, **111** was deduced from experiments conducted in melt using unsublimed *rac*-lactide, all initiators giving PLA with similar molecular weights, low molecular weight distribution and good stereocontrol. For example the polymer obtained from the complex **109** shows 91% yield in 0.5h with M_n of 21150 g mol^{-1} ; $M_w/M_n = 1.11$ and ($P_r = 0.69$).

1.4.3. Comparative studies of group (IV) metal complexes in ROP of ϵ -CL and Lactides

The role of group 4 heteroleptic metal complexes in the ring opening polymerization of cyclic esters such as ϵ -caprolactone and Lactides, so far studied in the literature has been discussed briefly in the above sections. Comparison of activity, polymer molecular weight, dispersity and stereoselectivity of group 4 metal (Ti, Zr, Hf) complexes derived from the different type of ligand systems are summarized in the following tables (1.2 to 1.6) in order to understand more easily about the nature of different metal complexes and activity under different polymerization conditions.

Comparative studies of ROP of L-LA in solution condition as observed from table 1.2. From this table, we could able to infer that, among group 4 metal complexes, heterobimetallic complex (Ti- Zn) based on bis-(phenolate) ligand were shown to be the most active even at low temperature (30°C) as compared to any other mono-metallic complexes. Zirconium complexes derived from amine bis(phenolate) were shown more active as compared to the analogue titanium complex at higher temperature (110°C). All complexes derived from Schiff based ligands, atrane ligands (titanatranes) showed moderate activity at different polymerization temperature under these conditions. However, from this table we could also be able to observe that few titanium complexes derived from amine tris(phenolate) ligands were shown to be inactive under solution polymerization conditions.

Polymerization of L-LA in bulk condition has been compared in table 1.3. From this table we observe that most of the complexes were shown to be active as compared to solution polymerization conditions. Among these, zirconium complexes derived from amine bis(phenolate) ligand (entry 4 & 5) were shown to be more active as compared to all other complexes. Surprisingly, more bulky titanium complex derived from the similar kind of ligand systems were found to be more active and lead to controlled polymerization as compared to the corresponding zirconium analogue complex (entry 8 & 9). Mononuclear titanium complexes were also shown to have higher activity but rather broader molecular weight distribution (entry 17-19). Tetranuclear titanium complex also shows higher activity (entry 15). All other complexes exhibited moderate to high activity under these polymerization conditions.

Polymerization of rac-LA in solution condition has been compared in table 1.4. From this table we observe that group 4 metal complexes derived from different ligand systems have been reported as efficient initiators in the ROP of rac-LA. Recently reported complexes based on dithiodiolate ligand system were found to be more active catalysts along with good heterotactic stereoselectivity than all other complexes (entry 18 & 19). Moreover, few zirconium complexes based on amine bis(phenolate) ligands were also found to be efficient initiators along with good isotactic selectivity even at higher temperature (entry 1-3). All other complexes showed moderate activity and stereoselectivity under this condition. From this comparative study we could also be able to observe that only few titanium complexes were found to be stereoselective catalysts compared to Zr & Hf complexes.

Polymerization of rac-LA in bulk condition has been compared in table 1.5. From this table we observe that most of the complexes were shown to be more active initiators under this condition than in solution condition. More interestingly, Zr & Hf complexes derived from dithiodiolate ligand systems were found to be one of the most active initiators at high temperature with a good heterotactic selectivity (entry 26, 27, 30). Few other bulky metal complexes derived from amine bis(phenolate) ligand system were also found to be very active initiator and it is note worthy that in this case, Ti complex is more active than Zr & Hf complexes derived from the same ligands (entry 7-9). Zirconium complex derived from the amine tris(phenolate) ligand system showed to be more active with higher heterotactic selectivity ($P_r = 0.96$) even at high temperature (entry 13). Complexes derived from Schiff base ligands were also found to be efficient initiators along with good heterotactic stereoselectivity (entry 31-37). All other complexes were also found to be efficient initiators under these polymerization conditions.

Polymerization of ϵ -caprolactone using different metal complexes under solution and bulk polymerization conditions is compared in table 1.6. Very few group 4 metal complexes have been reported in the literature for ROP of ϵ -CL as compared to lactide polymerization. Among these, few amine bis(phenolate) and sulfonamide based complexes were shown to be active catalyst under solution polymerization at low and high temperatures. All other metal complexes were shown to have low to moderate activity in ϵ -CL polymerization.

1.5. Conclusion

Poly lactides (PLA), Polylactones and other related polyesters are polymers of significant interest in the biomedical field due to their biodegradable, biocompatible, and permeable properties. Ring-opening polymerization (ROP) of cyclic esters is the major polymerization method employed to synthesize these polymers. This method involves different type of mechanism namely anionic, cationic, organocatalyzed & enzymatic and coordination-insertion. Recently significant advances have been made in coordination insertion (ROP) by using well defined organometallic complexes as initiators. Particularly, promising results have been obtained over the past few years in the area of stereoselective ring opening polymerization of lactides that can lead to iso- or heterospecificity of the polymer. In this chapter, the application of well defined group 4 metal complexes supported by a variety of ligands in ROP of lactide and ϵ -caprolactone were reviewed. Among group 4 metal complexes Zr and Hf complexes, were shown to have higher activity and stereoselectivity for ROP of lactides than titanium complexes which produced mostly atactic polymers. However, very few Zr and Hf metal complexes have been reported in the literature for stereoselective polymerization of lactides as compare to other group metal complexes. Although, enormous amount of research have been dedicated to ROP initiating systems and processes, the number of active, productive and selective group 4 metal complexes initiators remains limited. This might be improved by designing more reactive and new initiating systems by using different ligands.

Table 1.2. Ring Opening Polymerization of *L*-lactide in solution condition.^a

Entry	Type of ligand	Catalyst	[M]/[I]	T(°C)	A ^b	M _n ^c (g.mol ⁻¹)	PDI ^c	N _c ^d	ref
1	Bis-(phenolate)	30-Ti (Zn)	100	30	52.8	7700	1.29	2	87
2		33-Ti (Mg)	100	30	4.6	-nd-	-nd-	-nd-	87
3	Amine bisphenolate	35a-Ti	100	110	1.4	550	1.43	-nd-	91
4		36a-Zr	100	110	7.1	10800	1.08		91
5		41-Ti	300	130	4.87	7100	1.15	2	93
6		42-Ti	300	130	4.80	8600	1.30	2	93
7	Amine trisphenolate	51-Ti	300	130	1.25	11000	1.66	-nd-	100
8		49a-Ti	300	130	0	-nd-	-nd-	-nd-	100
9		52-Ti	300	130	0	-nd-	-nd-	-nd-	100
10	Titanatranes	68-Ti	300	130	1.45	25400	1.35	-nd-	100
11		68-Ti	300	70	0.69	28000	1.03	-nd-	100
12		73-Ti	300	70	1.67	11300	1.50	-nd-	106
13		74-Ti	200	130	1.94	25400	1.35	-nd-	107
14	Schiff base ligands	103-Ti	200	100	2.32	9300	1.26	2	126
15		104-Ti	200	100	2.47	12400	1.25	2	126

^a Polymerization condition: solvent: Toluene, ^b Activity in terms of g_{poly}mmol_{cat}⁻¹h⁻¹, ^c Determined by SEC in THF using polystyrene as reference, ^d Number of polymer chains grown from each metal center.

Table 1.3. Ring Opening Polymerization of *L*-lactide in bulk condition.^a

Entry	Type of ligand	Catalyst	[M]/[I]	A ^b	M _n ^c (g.mol ⁻¹)	PDI ^c	N _c ^e	ref
1	Amine bisphenolate	34a-Ti	300	0.25	7000	1.28	2	90
2		34a-Zr	300	1.7	11900	1.19	2	90
3		35a-Zr	300	2.2	11300	1.17	2	90
4		34b-Zr	300	32.4	14300	1.56	2	90
5		35b-Zr	300	27	14600	1.53	2	90
6		41-Ti	300	6.2	13200	1.19	2	93
7		42-Ti	300	6.42	27700	1.51	-nd-	93
8		46-Ti(O^tBu)₂	300	20.64	3539 ^d	1.13	-nd-	94
9		46-Zr(O^tBu)₂	300	0.66	2343 ^d	1.28	-nd-	94
10	Amine trisphenolate	50-Ti	300	1.24	19400	1.51	-nd-	99
11		51-Ti	300	10.27	80800	2.00	-nd-	100
12		49b-Ti	300	0.38	12500	1.29	2	90
13		54-Zr	300	6.6	24200	1.31	2	90
14	Titanatranes	67-Ti	300	1.78	25400	1.75	-nd-	99
15		70-Ti	300	9.94	63200	1.44	-nd-	100
16		73-Ti	300	3.6	15000	2.33	2	106
17	Mononuclear	76-Ti	300	17.08	27600	1.47	-nd-	100
18		77-Ti	300	19.89	19900	1.85	-nd-	100
19		78-Ti	300	20.32	60900	1.31	-nd-	100

^a Polymerization condition: solvent: Toluene, temperature = 130°C. ^b Activity in terms of g_{poly}mmol_{cat}⁻¹h⁻¹, ^c Determined by SEC in THF using polystyrene as reference, ^d Molecular weights determined from SEC using the appropriate Mark-Houwink corrections. ^e Number of polymer chains grown from each metal center.

Table 1.4. Ring Opening Polymerization of *rac*-lactide in solution condition.^a

Entry	Type of ligand	Catalyst	[M]/[I]	T (°C)	A ^b	M _n ^c (g.mol ⁻¹)	PDI ^c	P _r ^d	P _m ^d	ref
1	Amine bisphenolate	36a-Zr	100	110	7.13	9150	1.17	0.25	0.75	91
2		37a-Zr	100	110	7.13	7900	1.11	0.4	0.6	91
3		37c-Zr	100	110	5.40	8650	1.10	0.4	0.6	91
4	Amine trisphenolate	51-Ti	300	130	1.15	13300	1.34	-nd-	-nd-	100
5		59-Ti	100	80	0	-nd-	-nd-	-nd-	-nd-	104
6		63-Zr	100	80	0.58	28700	1.26	0.6	-nd-	104
7		60-Ti	100	80	0.57	23100	2.06	0.5	-nd-	104
8		64-Zr	100	80	0.59	13100	1.32	0.6	-nd-	104
9	Titanatranes	68-Ti	300	50	0.46	13200	1.09	-nd-	-nd-	100
10		73-Ti	100	70	0.46	7200	1.22	-nd-	-nd-	106
11		74-Ti	200	130	2.36	12100	1.16	-nd-	-nd-	107
12	Mononuclear	76-Ti	200	70	1.04	16300	1.07	-nd-	-nd-	100
13		77-Ti	200	70	1.36	5200	1.08	-nd-	-nd-	100
14		78-Ti	300	130	0.86	37000	1.20	-nd-	-nd-	100
15	Sulfonamide	89-Zr	100	70	2.08	8290	1.14	-nd-	-nd-	117
16	Dithiodiolate	91-Zr	300	75	2.88	11600	1.19	0.79	-nd-	122
17		92-Hf	300	75	6.30	9000	1.30	0.76	-nd-	122
18		94-Zr	300	75	23.2	12000	1.75	0.89	-nd-	122
19		95-Hf	300	75	25.9	9300	1.44	0.8	-nd-	122
20	Schiff base ligands	96-Ti	100	70	0.56	22000	1.19	0.56	-nd-	125
21		98-Ti	100	70	0.50	14230	1.21	0.53	-nd-	125
22		100-Ti	100	70	0.33	11540	1.19	0.51	-nd-	125
23		101-Ti	100	70	0.34	9210	1.11	0.54	-nd-	125
24		109-Zr	100	80	2.88	14200	1.12	0.70	-nd-	127
25		109-Zr	100	20	0.41	13400	1.08	0.74	-nd-	127
26		110-Zr	100	80	2.95	17000	1.16	0.7	-nd-	127
27		110-Zr	100	20	0.32	11300	1.12	0.76	-nd-	127

Table 1.5. Ring Opening Polymerization of *rac*-lactide in bulk condition.^a

Entry	Type of ligand	Catalyst	[M]/[I]	T (°C)	A ^b	M _n ^c (g.mol ⁻¹)	PDI ^c	P _r ^d	P _m ^d	ref
1	Amine bisphenolate	36a-Ti	300	130	16.08	33000	1.64	0.5	0.5	91
2		36a-Zr	300	130	11.95	6050	1.47	0.3	0.7	91
3		36a-Hf	300	130	14.78	14100	1.54	0.3	0.7	91
4		37a-Ti	300	130	16.09	32700	1.38	0.5	0.5	91
5		37a-Zr	300	130	9.78	4400	1.27	0.45	0.55	91
6		37c-Zr	300	130	2.17	1700	1.42	0.35	0.65	91
7		46-Ti(O^tBu)₂	300	130	3245	14423 ^e	1.56	0.61	-	94
8		46-Zr(O^tBu)₂	300	130	112.5	8484 ^e	1.65	0.72	-	94
9		46-Hf(O^tBu)₂	300	130	147.2	13043 ^e	1.38	0.55	-	94
10	Amine trisphenolate	50-Ti	300	130	1.21	16000	1.43	-	-	99
11		51-Ti	300	130	10.16	96000	2.02	-	-	100
12		49b-Ti	300	130	43.47	37100	1.38	0.5	-	102
13		55-Zr	300	130	336.9	32300	1.22	0.96	-	102
14		55-Hf	300	130	82.6	71150	1.19	0.88	-	102
15		59-Ti	300	130	11.02	18700	1.06	0.5	-	104
16		63-Zr	300	130	171.1	41800	1.46	0.6	-	104
17	Titanatranes	67-Ti	300	130	1.72	33600	1.97	-	-	99
18		68-Ti	300	130	2.59	119200	2.55	-	-	100
19		71-Ti	300	130	2.73	82700	1.72	-	-	100
20		73-Ti	300	130	79	11900	1.55	-	-	106
21	Mononuclear	76-Ti	300	130	16.2	23800	1.60	-	-	100
22		77-Ti	300	130	19.4	28400	1.23	-	-	100
23		78-Ti	300	130	20.1	68600	1.42	-	-	100
24	Sulfonamide	89-Zr	300	130	77.7	42430	1.49	-	-	117

Table 1.5. continued.....

Entry	Type of ligand	Catalyst	[M]/[I]	T (°C)	A ^b	M _n ^c (g.mol ⁻¹)	PDI ^c	P _r ^d	P _m ^d	ref
25	Dithiodiolate	90-Ti	300	144	43.8	7600	1.17	0.48	-	122
26		91-Zr	300	144	1178.3	17200	1.35	0.71	-	122
27		92-Hf	300	142	1381.3	19500	1.26	0.68	-	122
28		93-Ti	300	144	78.96	2800	1.19	0.52	-	122
29		94-Zr	300	144	417.7	16100	1.43	0.73	-	122
30		95-Hf	300	142	2357	9200	1.43	0.7	-	122
31	Schiff base ligands	105-Ti	300	130	77.7	25500	1.20	0.5	-	127
32		109-Zr	300	130	83.8	40400	1.72	0.68	-	127
33		106-Zr	300	130	77.7	48300	2.45	0.70	-	127
34		107-Zr	300	130	82	45900	1.75	0.68	-	127
35		110-Zr	300	130	71.7	59000	1.77	0.68	-	127
36		111-Zr	300	130	74.3	68000	1.39	0.73	-	127
37		112-Zr	300	130	82.08	91900	1.69	0.69	-	127

^a Polymerization condition: solvent: Toluene for solution polymerization, no solvent (Bulk condition). ^b Activity in terms of g_{poly}/mmol_{cat}⁻¹h⁻¹, ^c Determined by SEC in THF using polystyrene as reference. ^d P_r and P_m (probability of racemic and meso linkages) calculated from ¹H homonuclear decoupled NMR analysis. ^e Molecular weights determined from SEC using the appropriate Mark-Houwink corrections.

Table 1.6. Ring Opening Polymerization of ϵ -CL in solution and bulk condition.^a

Entry	Type of ligand	catalyst	[M]/[I]	T(°C)	solvent	A ^b	M _n ^c (g.mol ⁻¹)	PDI ^c	N _c ^e	ref
1	Bis-(phenolate)	12-Ti	100	25	DCM	2.28	6500	1.15	2	83
2		13-Ti	100	25	DCM	0.15	5600	1.10	2	83
3		15-Ti	100	100	none	3.53	62200	2.07	-nd-	84
4		15-Ti	100	100	toluene	3.8	72300	2.28	-nd-	84
5		17-Ti	100	100	none	1.04	45100	1.65	-nd-	84
6		17-Ti	100	100	toluene	-nd-	-	-	-nd-	84
7		18-Ti	100	100	none	1.61	37900	1.43	-nd-	84
8		18-Ti	100	100	toluene	-nd-	-	-	-nd-	84
9		20-Ti	200	100	toluene	0.64	18800	1.31	-nd-	85
10		22-Ti	200	100	toluene	2.6	56200	1.60	-nd-	85
11	Amine bisphenolate	35a-Ti	100	20	toluene	0.47	3800	2.60	-nd-	91
12		36a-Zr	100	20	toluene	0.47	12000	1.59	-nd-	91
13		35a-Zr	100	20	toluene	0.047	900	1.27	-nd-	91
14		37a-Zr	100	20	toluene	0.47	13800	1.35	-nd-	91
15		38-Ti	200	60	toluene	-nd-	-	-	-	92
16		39-Ti	200	60	toluene	10.81	32000	2.5	-nd-	92
17		48b-Ti	100	20	toluene	0.47	11000	1.24	-nd-	95
18		48c-Ti	100	20	toluene	0.47	14300	1.11	-nd-	95
19		48d-Ti	100	20	toluene	0.47	11400	1.08	-nd-	95
20	Titanatranes	68-Ti	200	70	toluene	0.84	17600	1.10	-nd-	100
21	Mononuclear	76-Ti	175	70	toluene	0.64	15800	1.06	-nd-	100
22	Sulfonamide	84-Ti	100	100	toluene	0.92	12990 ^d	1.91	1	117
23		85-Ti	100	100	toluene	0.48	14260 ^d	1.60	1	117
24		86-Ti	100	100	toluene	1.16	5720 ^d	1.80	2	117
25		87-Zr	100	100	toluene	10.3	5180 ^d	1.19	2	117
26		88-Ti	100	100	toluene	9.84	6390 ^d	1.39	2	117
27		89-Zr	100	100	toluene	10.45	7700 ^d	1.18	2	117

^a Polymerization condition: solvent: Toluene. ^b Activity in terms of $g_{\text{poly}} \text{mmol}_{\text{cat}}^{-1} \text{h}^{-1}$, ^c Determined by SEC in THF using polystyrene standards. ^d Molecular weights determined from SEC using the appropriate Mark-Houwink corrections. ^e Number of polymer chains grown from each metal center.

1.6. References

- [1] Heurtefeu, B.; Bouilhac, C.; Cloutet, E.; Taton, D.; Deffieux, A.; Cramail, H. *Prog. Polym. Sci.* **2011**, 36, 89.
- [2] Woodruff, M. A.; Hutmacher, D. W. *Prog. Polym. Sci.* **2010**, 35, 1217.
- [3] Nair, L. S.; Laurencin, C. T. *Prog. Polym. Sci.* **2007**, 32, 762.
- [4] Jérôme, C.; Lecomte, P. *Advanced Drug Delivery Reviews.* **2008**, 60, 1056.
- [5] Dechy-Cabaret, O.; Martin-Vaca, B.; Bourissou, D. *Chem. Rev.* **2004**, 104, 6147.
- [6] Albertsson, A.-C.; Varma, I. K. *Biomacromolecules.* **2003**, 4, 1466.
- [7] Gupta, A. P.; Kumar, V. *Eur. Polym. J.* **2007**, 43, 4053.
- [8] Lou, X.; Detrembleur, C.; Jérôme, R. *Macromol. Rapid. Comm.* **2003**, 24, 161.
- [9] Williams, C. K. *Chem. Soc. Rev.* **2007**, 36, 1573.
- [10] Saiyasombat, W.; Molly, R.; Nicholson, T. M.; Johnson, A. F.; Ward, I. M. *Polymer.* **1998**, 39, 5581.
- [11] Kamber, N. E.; Jeong, W.; Waymouth, R. M.; Pratt, R. C.; Lohmeijer, B. G. G.; Hedrick, J. L. *Chem. Rev.* **2007**, 107, 5813.
- [12] Kricheldorf, H. R.; Dunsing, R. *Makromol. Chem.* **1986**, 187, 1611.
- [13] Kricheldorf, H. R.; Kreiser, I. *Makromol. Chem.* **1987**, 188, 1861.
- [14] Khanna, A.; Sudha, Y.; Pillai, S.; Rath, S. *J. Mol. Model.* **2008**, 14, 367.
- [15] Stridsberg, K. M.; Ryner, M.; Albertsson, A.-C. *Adv. Polym. Sci.* **2002**, 157, 41.
- [16] Bourissou, D.; Martin-Vaca, B.; Dumitrescu, A.; Graullier, M.; Lacombe, F. *Macromolecules.* **2005**, 38, 9993.
- [17] Penczek, S. *J. Polym. Sci., Part A: Polym. Chem.* **2000**, 38, 1919.
- [18] Kim, M. S.; Seo, K. S.; Khang, G.; Lee, H. B. *Macromol. Rapid Commun.* **2005**, 26, 643.
- [19] Endo, T. in *Handbook of Ring-Opening Polymerization*, ed. Dubois, P.; Coulembier, O.; Raquez, J.-M. Wiley-VCH, Weinheim, **2009**, 53.
- [20] Kiesewetter, M. K.; Shin, E. J.; Hedrick, J. L.; Waymouth, R. M. *Macromolecules.* **2010**, 43, 2093.
- [21] Dove, A. P.; Pratt, R. C.; Lohmeijer, B. G. G.; Waymouth, R. M.; Hedrick, J. L. *J. Am. Chem. Soc.* **2005**, 127, 13798.
- [22] Connor, E. F.; Nyce, G. W.; Myers, M.; Mock, A.; Hedrick, J. L. *J. Am. Chem. Soc.* **2002**, 124, 914.
- [23] Nyce, G. W.; Glauser, T.; Connor, E. F.; Mock, A.; Waymouth, R. M.; Hedrick, J. L. *J. Am. Chem. Soc.* **2003**, 125, 3046.
- [24] Dove, A. P.; Pratt, R. C.; Lohmeijer, B. G. G.; Culkin, D. A.; Hagberg, E. C.; Nyce, G. W.; Waymouth, R. M.; Hedrick, J. L. *Polymer.* **2006**, 47, 4018.
- [25] Uyama, H.; Kobayashi, S. *Chem. Lett.* **1993**, 1149.
- [26] Knani, D.; Gutman, A. L.; Kohn, D. H.; *J. Polym. Sci., Part A: Polym. Chem.* **1993**, 31, 1221.
- [27] Kobayashi, S. *Macromol. Symp.* **2006**, 240, 178.
- [28] Varma, I. K.; Albertsson, A. C.; Rajkhowa, R.; Srivastava, R. K. *Prog. Polym. Sci.* **2005**, 30, 949.
- [29] Gross, R. A.; Kumar, A.; Kalra, B. *Chem. Rev.* **2001**, 101, 2097.
- [30] Drumright, R. E.; Gruber, P. R.; Henton, E. *Adv. Mater.* **2000**, 12, 1841.

- [31] Kowalski, A.; Duda, A.; Penczek, S. *Macromolecules*. **1998**, 31, 2114.
- [32] Kricheldorf, H. R.; Damrau, D. O. *Macromol. Chem. Phys.* **1997**, 198, 1753.
- [33] Dittrich, W.; Schulz, R. C. *Angew. Makromol. Chem.* **1971**, 15, 109.
- [34] Kricheldorf, H. R.; Berl, M.; Scharnagl, N. *Macromolecules*. **1988**, 21, 286.
- [35] Dubois, P.; Jacobs, C.; Jérôme, R.; Teyssie, P. *Macromolecules*, **1991**, 24, 2266.
- [36] Kricheldorf, H. R.; Berl, M.; Scharnagl, N. *Macromolecules*. **1988**, 21, 286.
- [37] Baran, J.; Duda, A.; Kowalski, A.; Szymanski, R.; Penczek, S. *Macromol. Symp.* **1997**, 123, 93.
- [38] Domski, G. J.; Rose, J. M.; Coates, G. W.; Bolig, A. D.; Brookhart, M. *Prog. Polym. Sci.* **2007**, 32, 30.
- [39] Dorgan, J. R.; Lehermeier, H. J.; Palade, L. I.; Cicero, J. *Macromol. Symp.* **2001**, 175, 55.
- [40] Vert, M. *Macromol. Symp.* **2000**, 153, 333.
- [41] Ikada, Y.; Tsuji, H. *Macromol. Rapid. Commun.* **2000**, 21, 117.
- [42] Xiong, C. D.; Cheng, L. M.; Xu, R. P.; Deng, X. M. *J. Appl. Polym. Sci.* **1995**, 55, 865.
- [43] Chen, X.; McCarthy, S. P.; Gross, R. A. *Macromolecules*. **1998**, 31, 662.
- [44] Middleton, J. C.; Tipton, A. J. *Biomaterials*. **2000**, 21, 2335.
- [45] Coulembier, O.; Degée, P.; Hedrick, J. L.; Dubois, P. *Prog. Polym. Sci.* **2006**, 31, 723.
- [46] Biela, T.; Duda, A.; Penczek, S. *Macromolecules*. **2006**, 39, 3710.
- [47] Zhong, Z.; Dijkstra, P. J.; Feijen, J. *J. Am. Chem. Soc.* **2003**, 125, 11291.
- [48] Ovitt, T. M.; Coates, G. W. *J. Am. Chem. Soc.* **2002**, 124, 1316.
- [49] Kowalski, A.; Duda, A.; Penczek, S. *Macromolecules*. **2000**, 33, 689.
- [50] Thakur, K. A. M.; Kean, R. T.; Hall, E. S.; Kolstad, J. J.; Lindgren, T. A.; Doscotch, M. A.; Siepmann, J. I.; Munson, E. J. *Macromolecules*. **1997**, 30, 2422.
- [51] Thakur, K. A. M.; Kean, R. T.; Hall, E. S.; Kolstad, J. J.; Munson, E. J. *Macromolecules*. **1998**, 31, 1487.
- [52] Kasperczyk, J. E. *Macromolecules*. **1995**, 28, 3937.
- [53] Kasperczyk, J. E. *Polymer*. **1996**, 37, 201.
- [54] Thomas, C. M. *Chem. Soc. Rev.* **2010**, 39, 165.
- [55] Iroh, J. O. in *Polymer Data Handbook*, ed. J. E. Mark, Oxford University Press, New York, **1999**, 361.
- [56] Gross, R. A.; Kalra, B. *Science*, **2002**, 297, 803.
- [57] Lam, C. X. F.; Teoh, S. H.; Hutmacher, D. W. *Polymer.Int.*, **2007**, 56, 718.
- [58] Sinha, V. R.; Bansal, K.; Kaushik, R.; Kumria, R.; Trehan, A. *Int. J. Pharm.* **2004**, 278, 1.
- [59] Birminghampolymers, *Chemical&Physicalproperties*, <http://www.birminghampolymers.com/>.
- [60] Pena, J.; Corrales, T.; Izquierdo-Barba, I.; Doadrio, A. L.; VAllet-Regi, M. *Polym. Degrad. Stab.* **2006**, 91, 1424.
- [61] Joshi, P.; Madras, G. *Polym. Degrad. Stab.* **2008**, 93, 1901.
- [62] Chen, D. R.; Bei, J. Z.; Wang, S. G. *Polym. Degrad. Stab.* **2000**, 67, 455.
- [63] Jenkins, M. J.; Harrison, K. L.; Silva, M. M. C. G.; Whitaker, M. J.; Shakesheff, K. M.; Howdle, S. M. *Eur. Polym. J.* **2006**, 42, 3145.
- [64] Hedrick, J. L.; Magbitang, T.; Connor, E. F.; Glauser, T.; Volksen, W.; Hawker, C. J.; Lee, V. Y.; Miller, R. D. *Chem. Eur. J.*, **2002**, 8, 3308.

- [65] Labet, M.; Thielemans, W. *Chem. Soc. Rev.* **2009**, 38, 3484.
- [66] Palard, I.; Schappacher, M.; Soum, A.; Guillaume, S. M. *Polym Int.* **2006**, 55, 1132.
- [67] Hodgson, L. M.; Platel, R. H.; White, A. J. P.; Williams, C. K. *Macromolecules.* **2008**, 41, 8603.
- [68] Spassky, N.; Wisniewski, M.; Pluta, C.; LeBorgne, A. *Macromol. Chem. Phys.* **1996**, 197, 2627.
- [69] Radano, C. P.; Baker, G. L.; Smith, M. R. *J. Am. Chem. Soc.* **2000**, 122, 1552.
- [70] Ovitt, T. M.; Coates, G. W.; *J. Polym. Sci., Part A: Polym. Chem.* **2000**, 38, 4686.
- [71] Zhong, Z.; Feijen, P. J. *Angew. Chem., Int. Ed.* **2002**, 41, 4510.
- [72] Nomura, N.; Ishii, R.; Akakura, M.; Aoi, K. *J. Am. Chem. Soc.* **2002**, 124, 5938.
- [73] Hormnirun, P.; Marshall, E. L.; Gibson, V. C.; White, A. J. P.; Williams, D. J. *J. Am. Chem. Soc.* **2004**, 126, 2688.
- [74] Douglas, A. F.; Patrick, B. O.; Mehrkhodavandi, P. *Angew. Chem., Int. Ed.* **2008**, 47, 2290.
- [75] Arnold, P. L.; Buffet, J. C.; Blaudeck, R. P.; Sujecki, S.; Blake, A. J.; Wilson, C. *Angew. Chem., Int. Ed.* **2008**, 47, 6033.
- [76] Chamberlain, B. M.; Cheng, M.; Moore, D. R.; Ovitt, T. M.; Lobkovsky, E. B.; Coates, G. W. *J. Am. Chem. Soc.* **2001**, 123, 3229.
- [77] Chmura, A. J.; Davidson, M. G.; Frankis, C. J.; Jones, M. D.; Lunn, M. D.; Bull, S. D.; Mahon, M. F. *Angew. Chem., Int. Ed.* **2007**, 46, 2280.
- [78] Amgoune, A.; Thomas, C. M.; Roisnel, T.; Carpentier, J.-F. *Chem.-Eur. J.* **2006**, 12, 169 and references therein.
- [79] Ma, H.; Spaniol, T. P.; Okuda, J. *Angew. Chem., Int. Ed.* **2006**, 45, 7818.
- [80] Whitelaw, E. L.; Jones, M. D.; Mahon, M. F. *Inorg. Chem.* **2010**, 49, 7176 and references there in.
- [81] Van der Linden, A.; Schaverien, C. J.; Meijboom, N.; Ganter, C.; Orpen, A. G. *J. Am. Chem. Soc.* **1995**, 117, 3008.
- [82] Sernetz, F. G.; Mulhaupt, R.; Fokken, S.; Okuda, J. *Macromolecules.* **1997**, 30, 1562.
- [83] Takeuchi, D.; Nakamura, T.; Aida, T. *Macromolecules.* **2000**, 33, 725.
- [84] Takashima, Y.; Nakayama, Y.; Watanabe, K.; Itono, T.; Ueyama, N.; Yasuda, A. H.; Harada, A. *Macromolecules.* **2002**, 35, 7538.
- [85] Takashima, Y.; Nakayama, Y.; Hirao, T.; Yasuda, H.; Harada, A. *J. Organomet. Chem.* **2004**, 689, 612.
- [86] Ejfler, J.; Kobyłka, M.; Jerzykiewicz, L. B.; Sobota, P. *J. Mol. Catal. A: Chem.* **2006**, 257, 105.
- [87] Chen, H. Y.; Liu, M. Y.; Sutar, A. K.; Lin, C. C. *Inorg. Chem.* **2010**, 49, 665.
- [88] Tshuva, E. Y.; Groysman, S.; Goldberg, I.; Kol, M.; Goldschmidt, Z. *Organometallics.* **2002**, 21, 662.
- [89] Segal, S.; Goldberg, I.; Kol, M. *Organometallics.* **2005**, 24, 200.
- [90] Gendler, S.; Segal, S.; Goldberg, I.; Goldschmidt, Z.; Kol, M. *Inorg. Chem.* **2006**, 45, 4783.
- [91] Chmura, A. J.; Davidson, M. G.; Jones, M. D.; Lunn, M. D.; Mahon, M. F.; Johnson, A. F.; Khunkamchoo, P.; Roberts, S. L.; Wong, S. S. F. *Macromolecules.* **2006**, 39, 7250.

- [92] Sarazin, Y.; Howard, R. H.; Hughes, D. L.; Humphrey, S. M.; Bochmann, M. *Dalton Trans.* **2006**, 340.
- [93] Kim, S. H.; Lee, J.; Kim, D. J.; Moon, J. H.; Yoon, S.; Oh, H. J.; Do, Y.; Ko, Y. S.; Yim, J. H.; Kim, Y. *J. Organomet. Chem.* **2009**, 694, 3409.
- [94] Zelikoff, A. L.; Kopilov, J.; Goldberg, I.; Coates, G. W.; Kol, M. *Chem. Commun.* **2009**, 6804.
- [95] Chmura, A. J.; Davidson, M. G.; Jones, M. D.; Lunn, M. D.; Mahon, M. F. *Dalton Trans.* **2006**, 887.
- [96] Kawaguchi, H.; Matsuo, T. *J. Organomet. Chem.* **2004**, 689, 4228.
- [97] Chandrasekaran, A.; Day, R. O.; Holmes, R. R. *J. Am. Chem. Soc.* **2000**, 122, 1066.
- [98] Kol, M.; Shamis, M.; Goldberg, I.; Goldschmidt, Z.; Alfi, S.; Hayut-Salant, E. *Inorg. Chem. Commun.* **2001**, 4, 177.
- [99] Kim, Y.; Verkade, J. G. *Organometallics.* **2002**, 21, 2395.
- [100] Kim, Y.; Jnaneshwara, G. K.; Verkade, J. G. *Inorg. Chem.* **2003**, 42, 1437.
- [101] Davidson, M. G.; Doherty, C. L.; Johnson, A. L.; Mahon, M. F. *Chem. Commun.* **2003**, 1832.
- [102] Chmura, A. J.; Davidson, M. G.; Frankis, C. J.; Jones, M. D.; Lunn, M. D. *Chem. Commun.* **2008**, 1293.
- [103] Ishii, R.; Nomura, N.; Kondo, T. *Polym. J.* (Tokyo, Jpn), **2004**, 36, 261.
- [104] Whitelaw, E. L.; Jones, M. D.; Mahon, M. F.; Kociok-Kohn, G. *Dalton. Trans.* **2009**, 9020.
- [105] Gurubasavaraj, P. M.; Nomura, K. *Organometallics.* **2010**, 29, 3500.
- [106] Kim, Y.; Verkade, J. G. *Macromol. Rapid. Commun.* **2002**, 23, 917.
- [107] Kim, Y.; Verkade, J. G. *Macromol. Symp.* **2005**, 224, 105.
- [108] Lavanant, L.; Toupet, L.; Lehmann, C. W.; Carpentier, J.-F. *Organometallics.* **2005**, 24, 5620.
- [109] Vasilenko, I. V.; Kostjuk, S. V.; Zaitsev, K. V.; Nedorezova, P. M.; Lemenovskii, D. A.; Karlov, S. S. *Polym Sci Ser B.* **2010**, 52, 136.
- [110] Piskun, Y. A.; Vasilenko, I. V.; Kostjuk, S. V.; Zaitsev, K. V.; Zaitseva, G. S.; Karlov, S. S. *J. Polym. Sci., Part A: Polym. Chem.* **2010**, 48, 1230.
- [111] Lütjens, H.; Nowotny, S.; Knochel, P. *Tetrahedron: Asymmetry.* **1995**, 6, 2675.
- [112] Pritchett, S.; Gantzel, P.; Walsh, P. J. *Organometallics.* **1999**, 18, 823.
- [113] Ackermann, L.; Bergman, R. G.; Loy, R. N. *J. Am. Chem. Soc.* **2003**, 125, 11956.
- [114] Padmanabhan, S.; Sundararajan, G. *J. Polym. Sci., Part A: Polym. Chem.* **2006**, 44, 4006.
- [115] Wu, J.; Pan, X.; Tang, N.; Lin, C.-C. *Eur. Polym. J.* **2007**, 43, 5040.
- [116] Zhao, J.; Song, H.; Cui, C. *Organometallics.* **2007**, 26, 1947.
- [117] Schwarz, A. D.; Thompson, A. L.; Mountford, P. *Inorg. Chem.* **2009**, 48, 10442.
- [118] Alfred, R.; Howard, L. W. H. *J. Polym. Sci., Part A: Polym. Chem.* **1972**, 10, 217.
- [119] John, R. D.; Jay, J.; Daniel, M. K.; Sukhendu, B. H.; Bradford, R. L.; Matthew, H. H. J. *Polym. Sci., Part B: Polym. Phys.* **2005**, 43, 3100.
- [120] Capacchione, C.; Proto, A.; Ebeling, H.; Mülhaupt, R.; Möller, K.; Spaniol, T. P.; Okuda, J. *J. Am. Chem. Soc.* **2003**, 125, 4964.
- [121] Beckerle, K.; Manivannan, R.; Lian, B.; Meppelder, G. J. M.; Spaniol, G. T. P.; Ebeling, H.; Pelascini, F.; Mülhaupt, R.; Okuda, J. *Angew. Chem., Int. Ed.* **2007**, 46, 4790.

- [122] Sergeeva, E.; Kopilov, J.; Goldberg, I.; Kol, M. *Inorg. Chem.* **2010**, 49, 3977.
- [123] Cozzi, P. G. *Chem. Soc. Rev.* **2004**, 33, 410.
- [124] Cameron, P. A.; Jhurry, D.; Gibson, V. C.; White, A. J. P.; Williams, D. J. S. *Macromol. Rapid. Commun.* **1999**, 20, 616.
- [125] Gregson, C. K. A.; Blackmore, I. J.; Gibson, V. C.; Long, N. J.; Marshall, E. L.; White, A. J.P. *Dalton Trans.* **2006**, 3134.
- [126] Lee, J.; Kim, Y.; Do, Y. *Inorg. Chem.* **2007**, 46, 7701.
- [127] Chmura, A. J.; Cousins, D. M.; Davidson, M. G.; Jones, M. D.; Lunn, M. D.; Mahon, M. F. *Dalton Trans.* **2008**, 1437.

CHAPTER 2

**Synthesis and Characterization of Titanium alkoxide and
Half sandwich Complexes based on Aminodiol Ligands**

CHAPTER 2

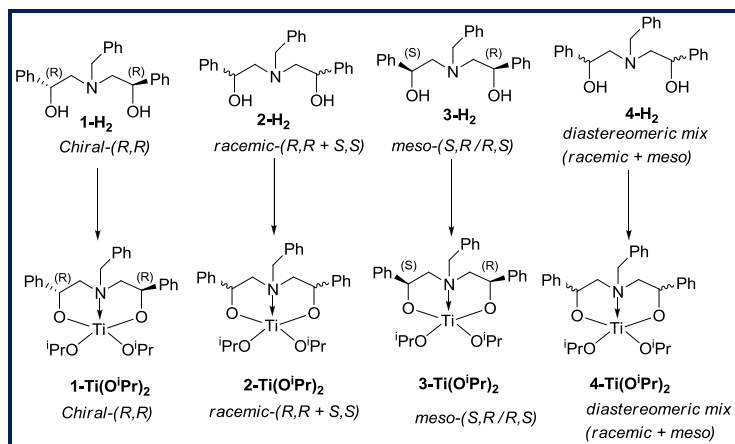
Synthesis and Characterization of Titanium alkoxide and Half sandwich Complexes based on Aminodiol Ligands

2.1. Introduction

Organometallic group 4 metal complexes containing heteroatom-bridged diaryloxy ligands $\{\text{OZO}\}^{2-}$ (e.g., Z = N or S) have been reported as promising catalysts for α -olefin polymerization. Indeed the bridged hetero atom when coordinated to the metal center can produce stereochemically rigid framework essential for the formation of stereoregular polymers and can also provide increased stabilization of reactive electron deficient metal center.¹⁻³ Titanium complexes based on dialkanolamine ligands have already been used for the polymerization of α -olefin and styrene and presented moderate activity and syndiospecificity.⁴ Further development of this type of group 4 metal complexes has been focused on the ring opening polymerization of cyclic esters. Titanium alkoxide complexes with different trialkanolamines, atranes ligands were briefly investigated in the ring opening polymerization of *L*- and *rac*-lactide.⁵⁻⁷ Recently titanium complexes of dialkanolamine ligands has been reported for ROP of ϵ -caprolactone.⁸

As already discussed in chapter 1, catalysts introduced in the last decade for the ROP of lactides (including metal complexes of polydentate ligands) enable the synthesis of stereoregular PLA from *rac*-LA.⁹⁻¹⁴ The extent of the stereoregularity of polymers depends not only on the transition metal but also on the structural parameters of the ligands such as chirality, rigidity, and steric bulk surrounding the center metal atom.

It has also been reported in the literature that titanium dichloride complexes derived from aminodiol ligands (dialkanolamine) having different symmetry can polymerize 1-hexene. The symmetry of the complexes played a key role in dictating the activity and also the stereoregularity of the polymers.¹⁵⁻¹⁶ In this connection, it was proposed to utilize titanium alkoxide complexes (**1-4-Ti(OⁱPr)₂**) containing aminodiol ligands (**1-4-H₂**) of different symmetry (Scheme 2.1). Ligand 1-H₂ is enantiomerically pure (*R,R*), giving a C₂ symmetry to complex **1-Ti(OⁱPr)₂**. Ligand 2-H₂ is the *racemic* form (*R,R* + *S,S*) of 1-H₂ to give complex **2-Ti(OⁱPr)₂**. Ligand 3-H₂ is *meso* form (*S,R* or *R,S*) to yield complex **3-Ti(OⁱPr)₂**. Ligand 4-H₂ is a diastereomeric mixture of both *racemic* and *meso* form yielding to complex **4-Ti(OⁱPr)₂**. These complexes will be used as more promising initiators for ROP of cyclic esters due to their greater chemical and structural flexibility. The presence of chiral center in the ligand backbone could also play a key role in the stereoselective polymerization of *rac*-LA. These points will be developed in the following chapters.

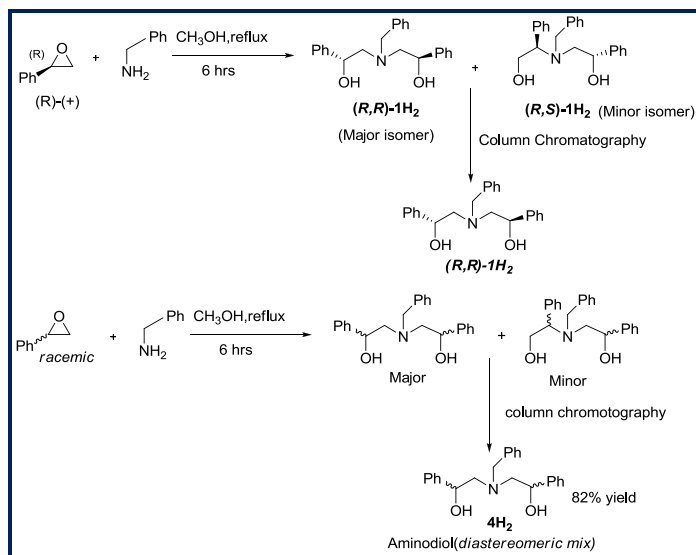


Scheme 2.1. Titanium alkoxide complexes of different symmetry based on aminodiol ligands.

2.2. Results and Discussion

2.2.1. Synthesis of aminodiol

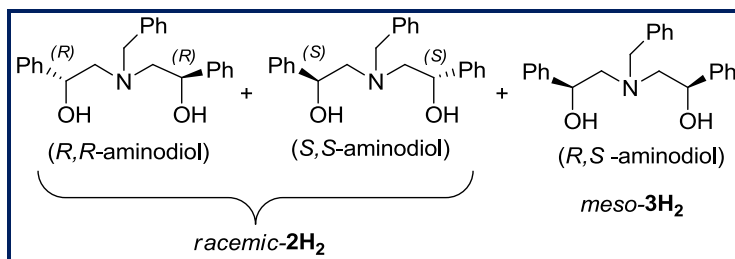
Aminodiol ligands were synthesized according to the literature procedure.^{15,16} The chiral C_2 -symmetric aminodiol was synthesized by the reaction of benzylamine with 2 equivalents of enantiomerically pure (*R*)-(+)-styrene oxide under reflux condition in methanol, whereas the diastereomeric mixture of aminodiol was obtained by the reaction of benzylamine with *racemic* styrene epoxide (Scheme 2.2). The C_2 symmetric aminodiol was isolated as the major isomer (Yield: 85 %) after purification by flash column chromatography. The diastereomeric aminodiols were obtained as a syrupy colorless liquid after column chromatography (Yield: 82%).



Scheme 2.2. Synthesis of *chiral* (**1-H₂**) and *diastereomeric* (**4-H₂**) aminodiol.

2.2.2. Separation of diastereomeric aminodiols

The diastereomeric aminodiols contain a mixture of *racemic* and *meso* ligands (Scheme 2.3) that could be separated by semi-preparative HPLC using CH₃OH : H₂O (80:20) mixture. The HPLC traces of the separated aminodiols are shown in Figure 2.1. The mixture gave two peaks while the separated ones showed only one peak. The ¹H-NMR spectroscopy suggests that the peak 1 and peak 2 corresponds to *meso* and *racemic* ligands respectively.



Scheme 2.3. Diastereomers of aminodiols.

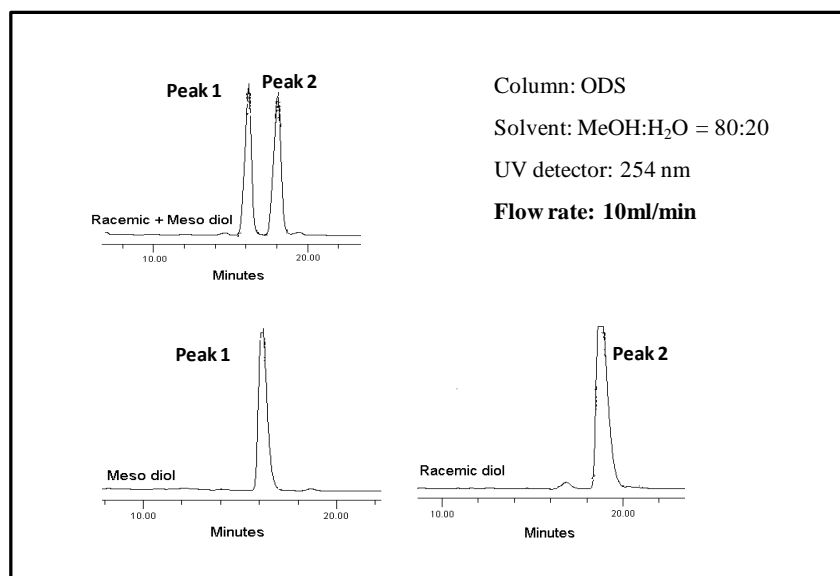


Figure 2.1. HPLC traces of *diastereomeric* aminodiols.

2.2.3. ¹H and ¹³C NMR spectroscopy of ligands 1-4-H₂

¹H-NMR spectrum of ligand **4-H₂** (*diastereomeric*) is presented on Figure 2.2. The four methylene protons of N-CH₂ appeared at 2.68 to 2.80 ppm as a multiplet. The methine proton of O-CH-Ph appeared at 4.58 ppm as two doublet of doublet. The benzylic protons (N-CH₂-Ph; *racemic ligand*) appeared at 3.59 and 3.72 ppm as two different doublets and an additional singlet also appeared at 3.83 ppm (N-CH₂-Ph; *meso ligand*), while other signals in the aromatic region appeared as multiplet.

$^1\text{H-NMR}$ spectrum of ligand **3-H₂** (*meso*) is presented on Figure 2.3. The two different methylene protons of N-CH₂ appeared at 2.62 and 2.67 ppm as separate doublet of doublets. The methine proton of O-CH-Ph appeared at 4.56 ppm as discrete doublet of doublet. Benzylic protons (N-CH₂-Ph) appeared at 3.70 ppm as singlet. The phenyl protons appear as multiplet. This spectrum also shows the pure *meso* ligand isolated from the HPLC separation.

$^1\text{H-NMR}$ spectrum of ligand **2-H₂** (*racemic*) is presented on Figure 2.4. The four methylene protons of N-CH₂ appeared at 2.62 to 2.74 ppm as a multiplet. The methine proton of O-CH-Ph appeared at 4.65 ppm as discrete doublet of doublet. Two different diastereotropic benzylic protons (N-CH₂-Ph) appeared at 3.59 and 3.86 ppm as two different doublets. The protons corresponding to the phenyl appeared as a multiplet in the aromatic region. On this spectrum, the absence of singlet peak at 3.83 ppm as compare to the *diastereomeric* ligand suggest the pure *racemic* ligand obtained after HPLC separation of mixture of ligands. Similar kind of spectrum was also observed for enantiomerically pure ligand **1-H₂** (Figure 2.5).

$^{13}\text{C-NMR}$ spectrum of all the ligands **4,3,2-H₂** with proper assignments presented in figures 2.6 to 2.8. The spectrum of diastereomeric aminodiols **4-H₂** was shown in figure 2.6 displays the two pairs of peaks corresponds to the (CH₂-N) and (N-CH₂-Ph) due to the presence of diastereomeric mixture of two different ligands *racemic* and *meso*, whereas the spectrum of all other ligands presents a single peak in the same region.

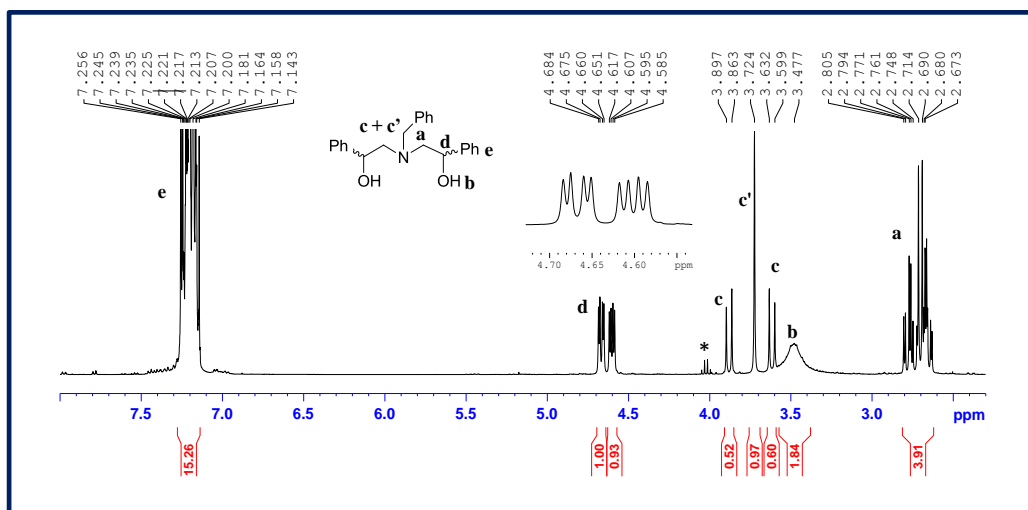


Figure 2.2. $^1\text{H-NMR}$ spectrum of diastereomeric aminodiols **4-H₂**.

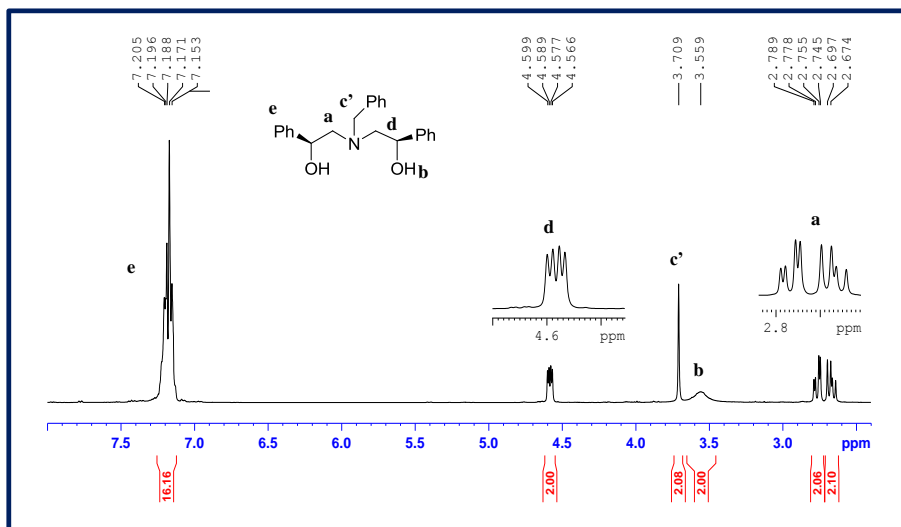


Figure 2.3. ¹H-NMR spectrum of meso aminodiol **3-H₂**.

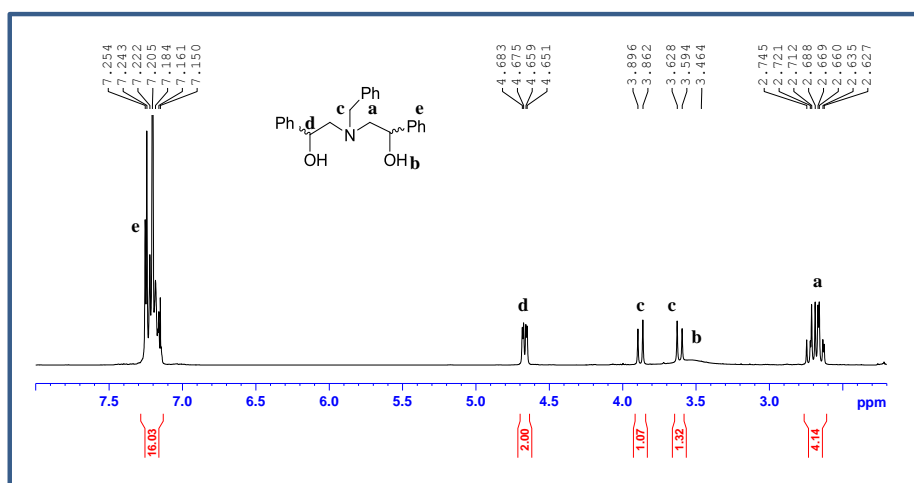


Figure 2.4. ¹H-NMR spectrum of racemic aminodiol **2-H₂**.

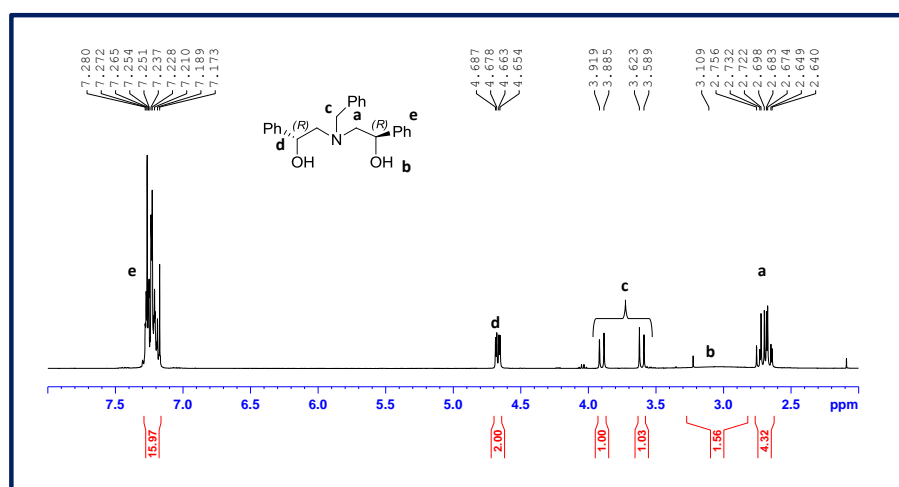


Figure 2.5. ¹H-NMR spectrum of Chiral aminodiol **1-H₂**.

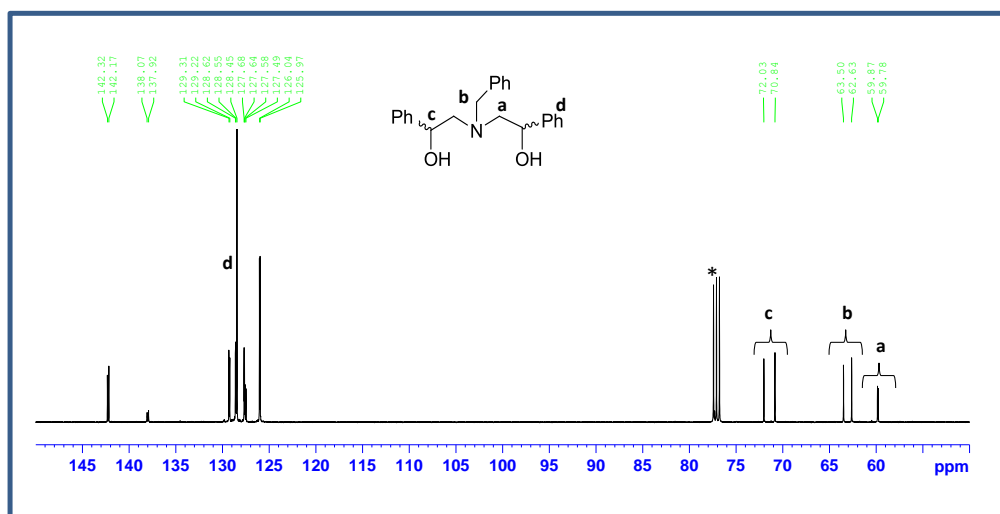


Figure 2.6. ¹³C-NMR spectrum of *diastomeric* aminodiol 4-H₂.

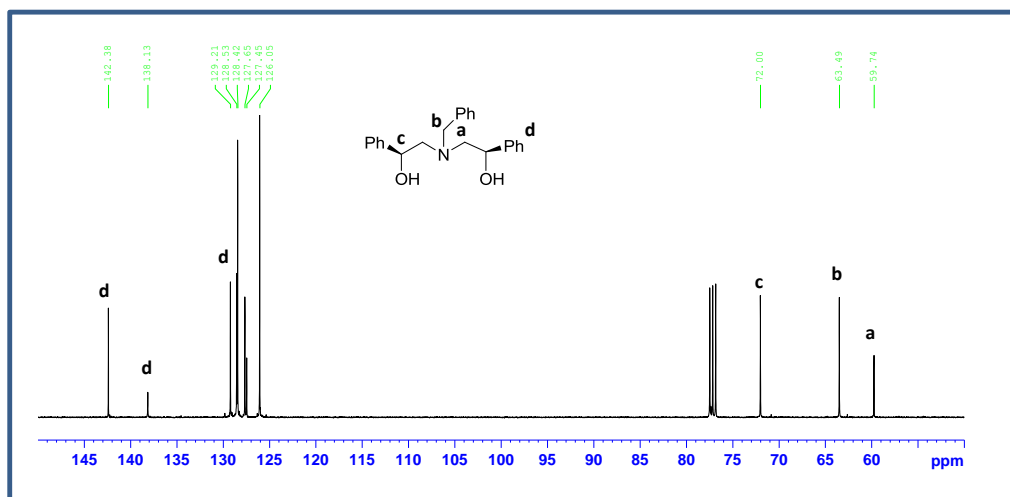


Figure 2.7. ¹³C-NMR spectrum of *meso* aminodiol 3-H₂.

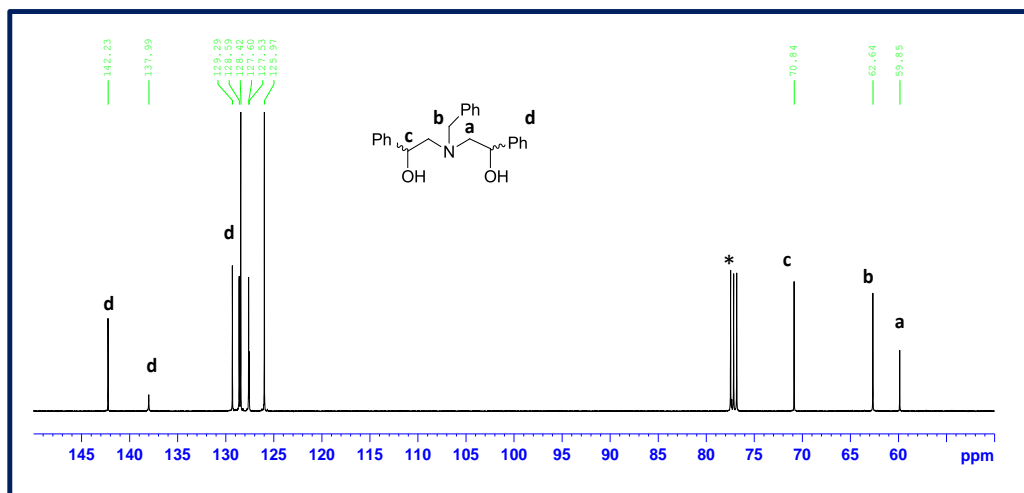
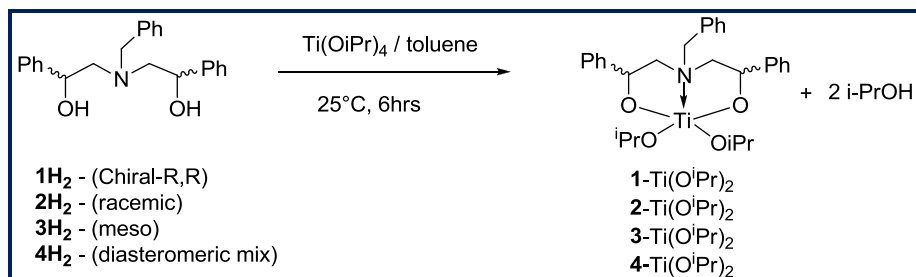


Figure 2.8. ¹³C-NMR spectrum of *racemic* aminodiol 2-H₂.

2.2.4. Synthesis of Titanium and Zirconium alkoxide Complexes

Monomeric titanium complexes **1-4-Ti(OⁱPr)₂** were prepared by the reaction of one equivalent of the metal precursor Ti(OⁱPr)₄ with the same equivalent of the corresponding ligand precursor as shown in Scheme 2.4. The synthesis was performed in dry toluene at room temperature (25°C) for a period of 6 hours. Solvent evaporation under vacuum from the reaction mixture afforded the complexes as yellow crystalline solid in good isolated yield (70-85%). All complexes are air and moisture sensitive, soluble in common organic solvents such as dichloromethane (DCM), tetrahydrofuran (THF), toluene and even in non-polar solvents such as pentane and hexane. These complexes can be stored for months under an inert atmosphere without decomposition. All complexes were fully characterized by ¹H & ¹³C NMR spectroscopy. However, all our attempts to obtain single-crystal XRD of these complexes, failed.



Scheme 2.4. Synthesis of Titanium Alkoxide Complexes 1-4-Ti(OⁱPr)₂.

2.2.4.1. Characterization of Titanium complex 1-Ti(OⁱPr)₂

As mentioned above enantiomerically pure ligand **1-H₂** upon reaction with metal precursor Ti(OⁱPr)₄ in toluene afforded a crystalline yellow solid as complex **1-Ti(OⁱPr)₂**. The complex was then characterized by ¹H & ¹³C NMR spectroscopy.

The ¹H NMR of the complex **1-Ti(OⁱPr)₂** (Figure 2.9) showed signals at 1.17-1.32 ppm and 4.70 ppm with an integral ratio of 12:2, which are attributed to the methyl and methine protons of the isopropoxide ligand respectively. Notably, the isopropoxide methyl protons appeared as four different doublets, indicating that the four methyl groups are chemically inequivalent. In addition, the methine protons of the ligand **1-H₂** moiety in **1-Ti(OⁱPr)₂** are well resolved into two different chemical environments as doublet of doublets. The -CH-Ph protons display downfield chemical shift at 5.48 and 5.87 ppm in comparison to the free ligand. In addition the signals corresponding to benzylic protons appeared around 0.5 ppm downfield shift from 3.58 to 4.13 ppm and the methylene protons shifted downfield (≈ 0.17 ppm) from 2.64 to 2.81 ppm. The aromatic protons appeared as a multiplet in the region 7.24-7.32 ppm. From this observation, the appearance of downfield shift of protons in the complexes in comparison to the ligands indicates the coordination of titanium onto to the ligand moiety.

^{13}C NMR spectrum of **1-Ti(OⁱPr)₂** is presented in Figure 2.10. The spectrum showed the four resonances for the methyl groups of the isopropoxide ligand at 26.01 to 26.57 ppm, and two resonances for the methine carbon appeared at 80.49 & 80.73 ppm again indicating the inequivalent chemical environment of the two isopropoxide ligand in the complex.

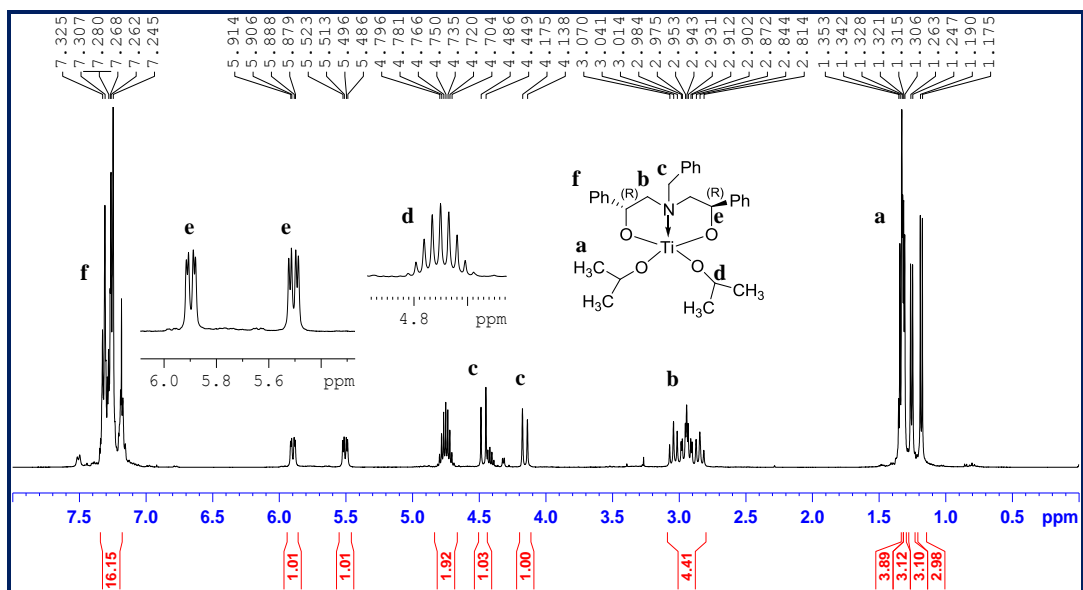


Figure 2.9. $^1\text{H-NMR}$ spectrum of **1-Ti(OⁱPr)₂**.

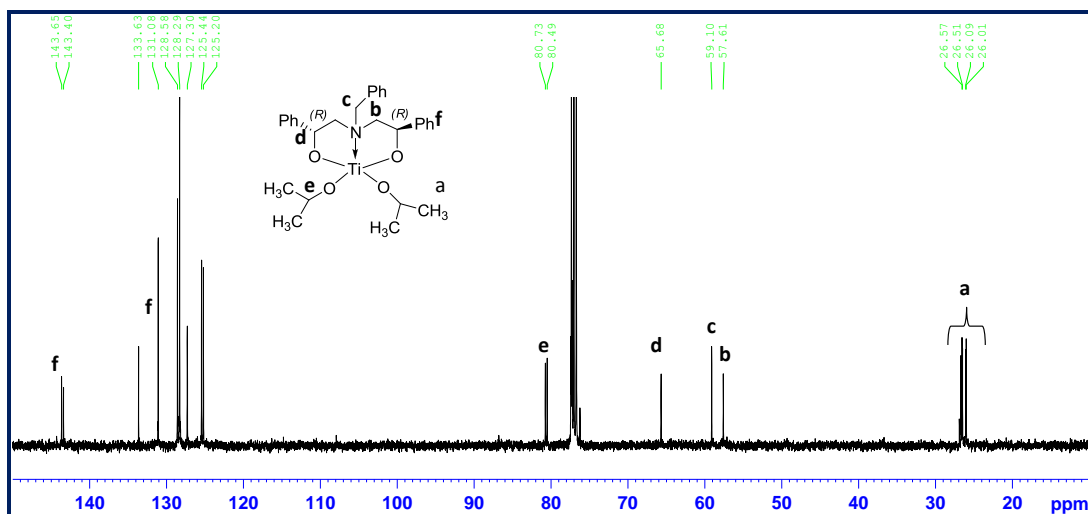


Figure 2.10. $^{13}\text{C-NMR}$ spectrum of **1-Ti(OⁱPr)₂**.

2.2.4.2. Characterization of Titanium complex $2\text{-Ti}(\text{O}^i\text{Pr})_2$

The racemic aminodiol ligand **2-H₂** upon reaction with metal precursor $\text{Ti}(\text{O}^i\text{Pr})_4$ in toluene afforded a crystalline yellow solid as complex $2\text{-Ti}(\text{O}^i\text{Pr})_2$. The complex was then characterized by ^1H & ^{13}C NMR spectroscopy.

The ^1H NMR of the complex $2\text{-Ti}(\text{O}^i\text{Pr})_2$ (Figure 2.11) benzylic proton showed around ≈ 0.5 ppm downfield shift from 3.59 to 4.13 ppm as compare to the ligand and the methylene protons shifted downfield (≈ 0.2 ppm) from 2.62 to 2.80 ppm as multiplet, and the methine protons shifted downfield (≈ 1.2 ppm) from 4.65 ppm to 5.48 & 5.87 ppm as two discrete doublet of doublets. The isopropoxide methyl protons appeared as four different doublets, from 1.17 to 1.34 ppm, and the two methine protons corresponding to isopropoxide ligand appeared as septets at 4.70 ppm. As in the case of complex $1\text{-Ti}(\text{O}^i\text{Pr})_2$, the methyl and methine protons of isopropoxide ligand were shown to be chemically inequivalent, as well as the appearance of downfield shift of protons, indicative of complex formation.

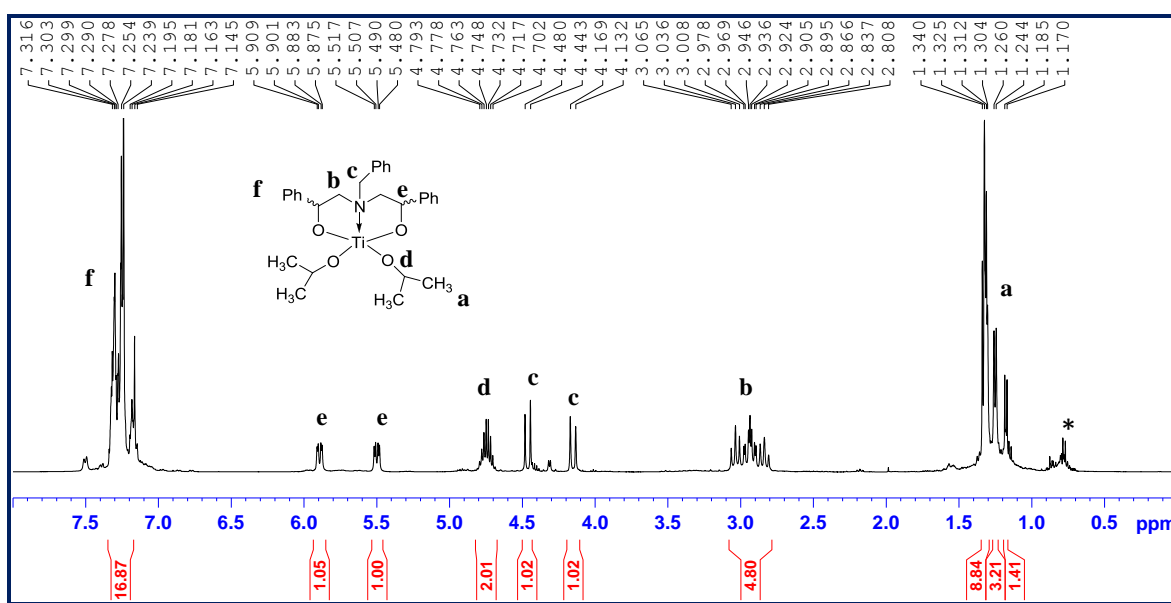


Figure 2.11. ^1H -NMR spectrum of $2\text{-Ti}(\text{O}^i\text{Pr})_2$.

^{13}C NMR spectrum of $2\text{-Ti}(\text{O}^i\text{Pr})_2$ is presented in Figure 2.12, the peaks corresponding to methyl and the methine carbons of isopropoxide ligand appeared from the region at 26.01-26.70 ppm and 80.50, 80.74 ppm respectively. The peaks corresponding to methylene, methine, benzylic and the phenyl carbon also appear and have been assigned as **b**, **c**, **d** and **f**.

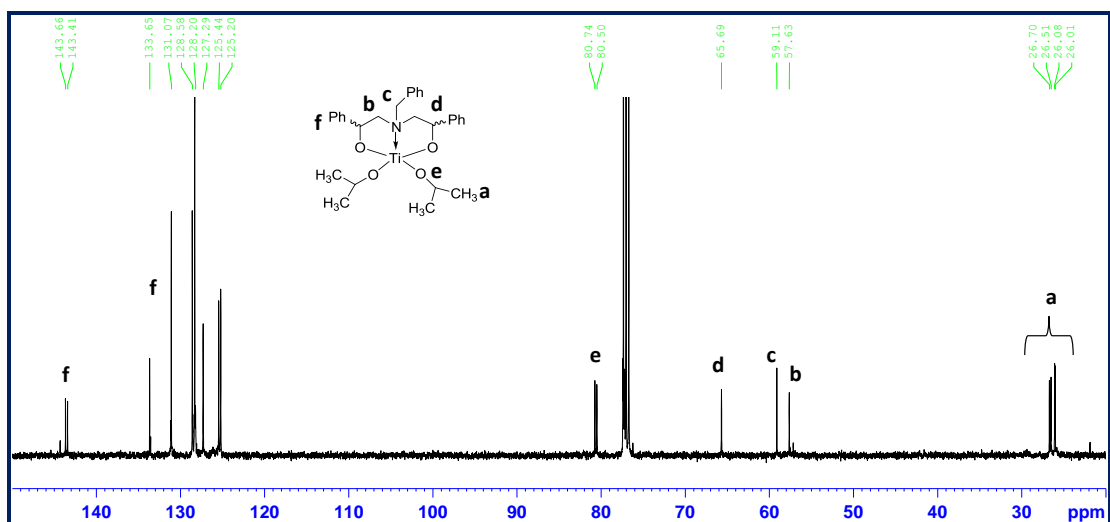


Figure 2.12. ^{13}C -NMR spectrum of $2\text{-Ti}(\text{O}^i\text{Pr})_2$.

2.2.4.3. Characterization of Titanium complex $3\text{-Ti}(\text{O}^i\text{Pr})_2$

The *meso* aminodiols ligand 3-H_2 upon reaction with metal precursor $\text{Ti}(\text{O}^i\text{Pr})_4$ in toluene afforded a crystalline yellow solid as complex $3\text{-Ti}(\text{O}^i\text{Pr})_2$. The complex was then characterized by ^1H & ^{13}C NMR spectroscopy.

In the ^1H NMR of the complex $3\text{-Ti}(\text{O}^i\text{Pr})_2$ (Figure 2.13) benzylic proton showed around ≈ 0.7 ppm downfield shift from 3.7 to 4.42 ppm and the methylene protons appeared as two discrete doublet of doublets at 2.49 and 3.45 ppm. The two methine protons ($-\text{CH}-\text{Ph}$) showed downfield shift ≈ 1.26 ppm from 4.56 to 5.82 ppm as doublet of doublets. The methyl and methine protons of the isopropoxide ligand appeared as two different doublets at 1.36, 1.46 ppm and two different septets at 4.76, 4.89 ppm respectively with an integral ratio of 12:2. Notably, the isopropoxide methyl protons appeared as two different doublets, indicating that two methyl groups of one pair is chemically equivalent, and the methine protons appeared as two different septets, and this is in sharp contrast to the spectrum observed in the complexes $1\text{-Ti}(\text{O}^i\text{Pr})_2$ and $2\text{-Ti}(\text{O}^i\text{Pr})_2$, indicating that the complex may exist as C_s symmetry in the solution.

^{13}C NMR spectrum of $3\text{-Ti}(\text{O}^i\text{Pr})_2$ is presented in Figure 2.14 with proper assignments. The spectrum displays the peaks corresponding to both the methyl and the methine carbon of the isopropoxide ligand in addition to the peaks due to the methylene, methine, benzylic and phenyl carbon as observed from the ligand 3-H_2 .

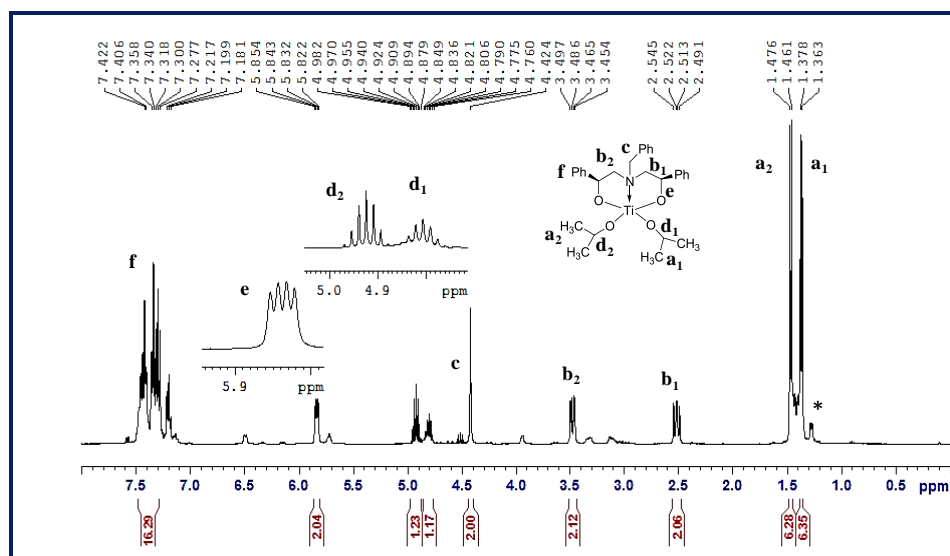


Figure 2.13. $^1\text{H-NMR}$ spectrum of $3\text{-Ti}(\text{O}^i\text{Pr})_2$.

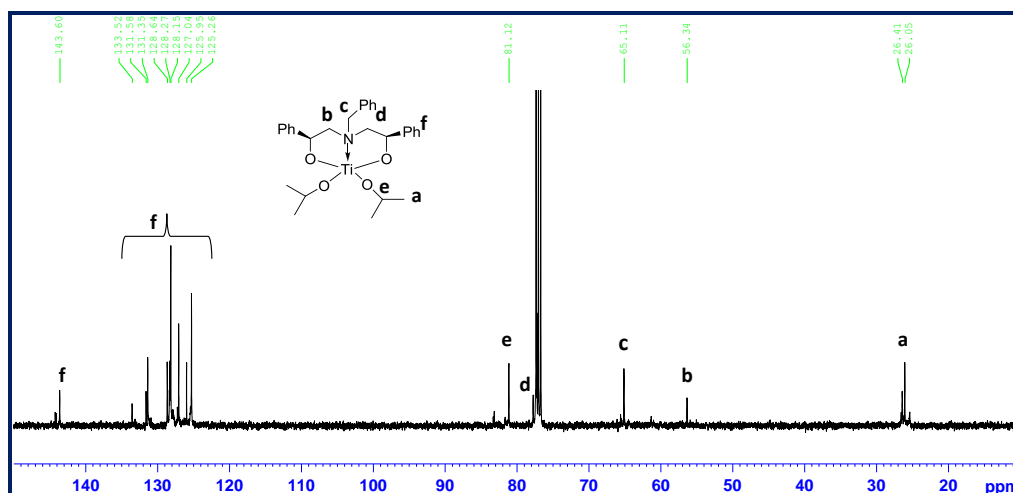


Figure 2.14. $^{13}\text{C-NMR}$ spectrum of $3\text{-Ti}(\text{O}^i\text{Pr})_2$.

2.2.4.4. Characterization of Titanium complex $4\text{-Ti}(\text{O}^i\text{Pr})_2$

The diastereomeric aminodiol ligand 4-H_2 upon reaction with metal precursor $\text{Ti}(\text{O}^i\text{Pr})_4$ in toluene afforded a crystalline yellow solid as complex $4\text{-Ti}(\text{O}^i\text{Pr})_2$. The complex was then characterized by ^1H & ^{13}C NMR spectroscopy.

The ^1H NMR of the complex $4\text{-Ti}(\text{O}^i\text{Pr})_2$ (Figure 2.15) showed the resonance corresponding to the four different methyl groups of the isopropoxide ligand as doublets at 1.17-1.37 ppm, and the methine protons appeared as two different septets at 4.70 to 4.83 ppm, four methylene protons appeared as two discrete doublet of doublets and multiplet in the region at 2.39 to 3.39 ppm. The peaks corresponding to the benzylic protons appeared downfield shift at 4.13 to 4.48 ppm and the two methine protons appears as multiplet at 5.48 to 5.89 ppm.

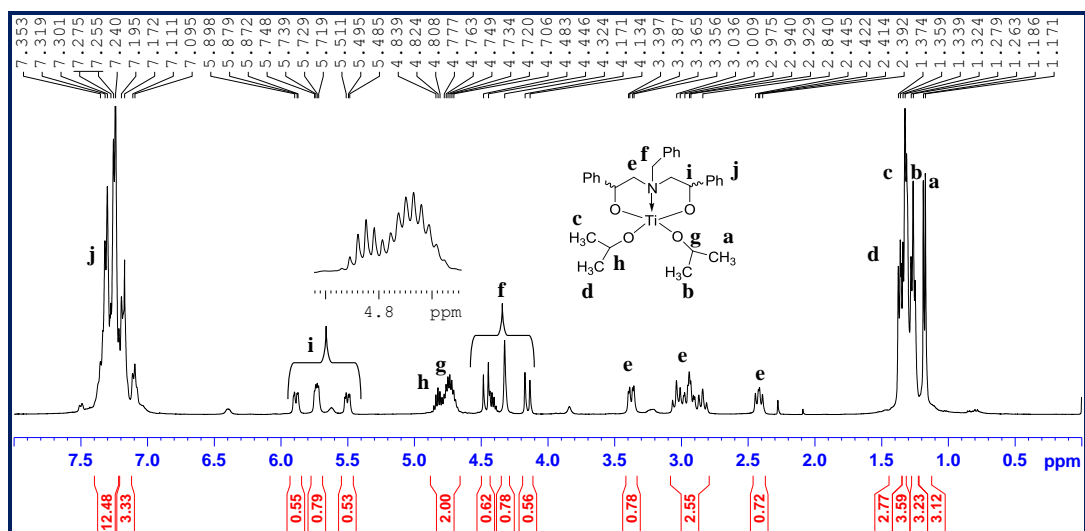


Figure 2.15. $^1\text{H-NMR}$ spectrum of $4\text{-Ti}(\text{O}^i\text{Pr})_2$.

^{13}C NMR spectrum of $4\text{-Ti}(\text{O}^i\text{Pr})_2$ is presented in (Figure 2.16). The spectrum displays the peaks corresponding to both the methyl and methine carbon of the isopropoxide ligand. The resonance due to the methylene and the methine carbon appears as a pairs of singlet and the resonance due to the benzylic carbon appears as a single peak. Both ^1H & ^{13}C NMR spectrum indicates that the complex exhibited two different structural isomers (*meso* and *racemic*) existing in solution in equal proportions.

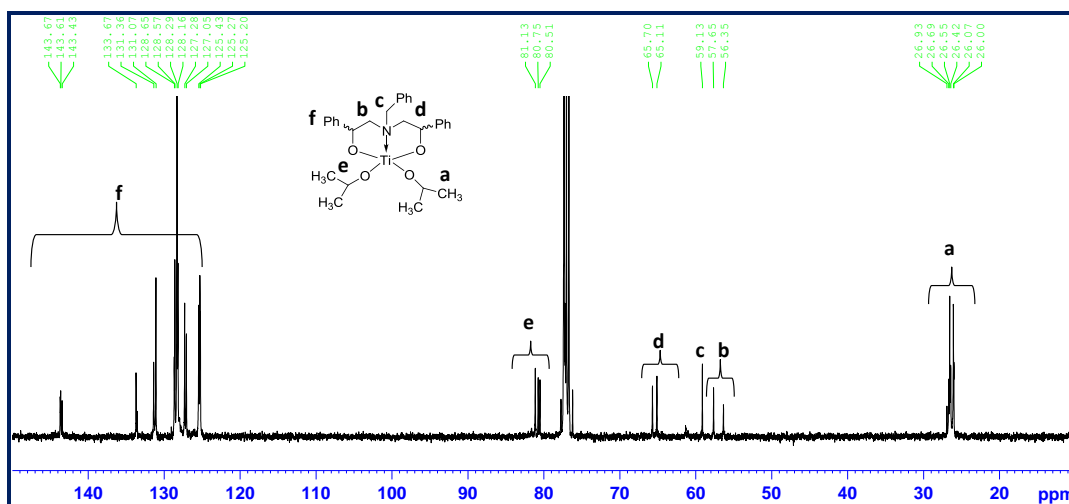
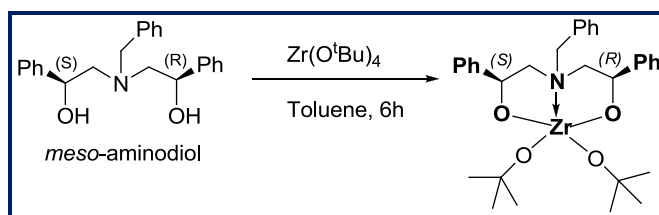


Figure 2.16. $^{13}\text{C-NMR}$ spectrum of $4\text{-Ti}(\text{O}^i\text{Pr})_2$.

2.2.4.5. Synthesis and Characterization of Zirconium complex 3-Zr(O^tBu)₂

It is described in the literature that zirconium complexes act as efficient initiators for the ring opening polymerization of cyclic esters. The structure-activity relationship was studied and compared with the Ti metal center with the same set of ligand backbone and was described briefly in chapter 1.¹⁷⁻²⁴ We also tried to explore the possibility to use aminodiols as the ligating backbone on zirconium. Attempts to prepare the 1-4-Zr(OⁱPr)₂ complexes with Zr(OⁱPr)₂.ⁱPrOH under various conditions led to undefined products. Nevertheless the corresponding monomeric **3-Zr(O^tBu)₂** complex were prepared successfully by reacting 1:1 equivalent of the bulky metal precursor Zr(O^tBu)₄ with the same equivalent of the corresponding (*meso*-aminodiols) precursor as shown in Scheme 2.5.



Scheme 2.5. Synthesis of complex **3-Zr(O^tBu)₂** from *meso*-aminodiols-3H₂.

The synthesis was performed in dry toluene at room temperature (25°C) for a period of 6 hours, followed by the removal of solvents under vacuum from the reaction mixture affording the complex as crystalline yellow solid in good isolated yield (75%). The complex was fully characterized by ¹H NMR spectroscopy.

.Characterization of 3-Zr(O^tBu)₂ by ¹H NMR spectroscopy

The ¹H NMR spectrum of the complex 3-Zr(O^tBu)₂ is presented on Figure 2.17. The signal at 2.55-3.32 ppm (multiplet) corresponds to the methylene protons (**a**). The methyl protons of the tert-butoxide ligand appeared as three different singlets and one doublet at 0.62, 0.91, 1.15, 1.21 ppm as proton (**b**). The signals at 4.19-5.34 ppm as four different doublets correspond to the benzylic protons. The signals at 5.96 to 6.41 ppm (doublet of doublets) correspond to the methine protons (**d**) and the phenyl protons appear as a multiplet in the region 7.11-7.7 ppm. The appearance of downfield shift of proton was observed in the complex as compare to the ligand due to the coordination of Zr onto the ligand. Peaks corresponding to the benzylic proton (doublets) in the complex are in contrast to those observed in the ligand (singlet).

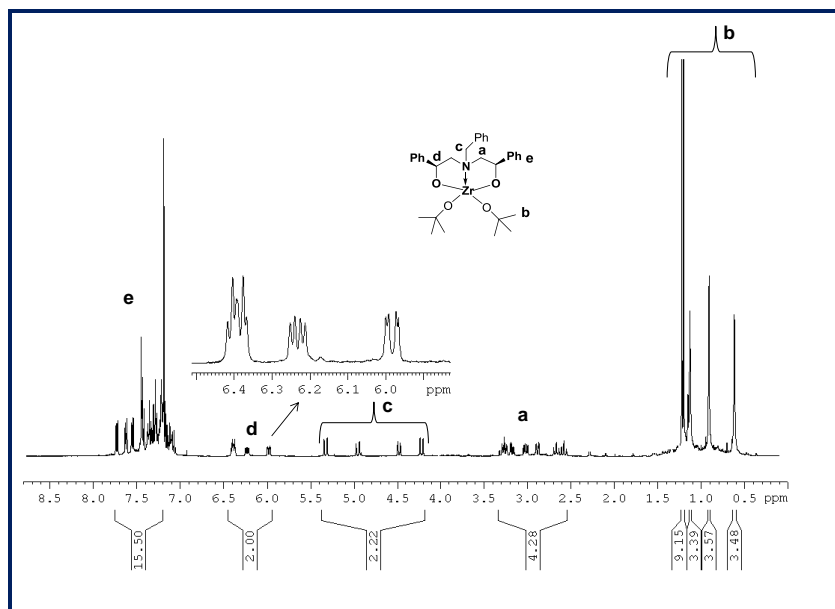
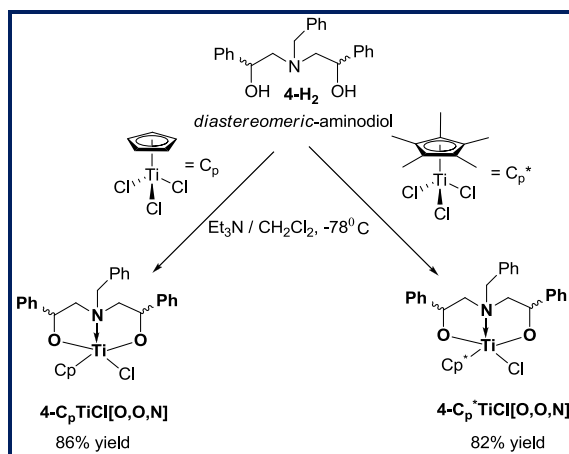


Figure 2.17. $^1\text{H-NMR}$ spectrum of **3-Zr(O^tBu)₂**.

2.2.5. Synthesis and Characterization of Half-sandwich titanium complexes based on aminodiols ligands

A general synthetic route for new titanium complexes **4-C_pTiCl[O,O,N]** and **4-C_p*TiCl[O,O,N]** is outlined in Scheme 2.6. The complexes were prepared from the literature procedure,²⁵ by reacting the diastereomeric aminodiols ligand (**4-H₂**) with the same equivalent of the C_pTiCl₃ or C_p*TiCl₃ in the presence of excessive triethylamine in dichloromethane giving, after workup, the complexes in good isolated yield. The complexes are soluble in toluene and methylene chloride but insoluble in hydrocarbon solvents, such as hexane and pentane.



Scheme 2.6. Synthesis of titanium half-sandwich complexes based on aminodiols ligands.

The chemical structure of the complexes was established from the $^1\text{H-NMR}$ spectroscopy. The ^1H NMR spectrum of the complex $4\text{-C}_p\text{TiCl}[\text{O},\text{O},\text{N}]$ is shown in Figure 2.18 and compared to the corresponding ligand 4-H_2 . ^1H NMR spectrum of the complex display well-defined resonances with the expected integrations.

In comparison to the free ligand precursor, all signals in the complex are shifted downfield, which is a consequence of the complexation with the Lewis acidic titanium metal. The spectra display the resonance signals of the methine proton $\text{OCH}(\text{Ph})$ at 5.3-5.9 ppm (doublets) which have been shifted downfield by 0.8-1.25 ppm in comparison to the free ligand (corresponding resonances at 4.56-4.65 ppm). The resonance signal corresponding to the benzylic protons ($\text{N-CH}_2\text{Ph}$) appeared at 4.05-4.34 ppm, shifted downfield by 0.4-0.48 ppm when compared to the free ligands (resonances at 3.59-3.86 ppm), while the resonance signals corresponding to the methylene protons (N-CH_2) are displayed at 2.6-3.2 ppm shifted downfield by 0.4 ppm in comparison to the free ligand (resonances signals at 2.6-2.7 ppm). This suggests that a strong bond is formed between the titanium atom and the oxygen atoms of the ligand, and a weak bond is formed between the titanium and the nitrogen atom of the ligand. The resonances corresponding to the (C_p) appeared at 6.3-6.5 ppm as three different singlets and the phenyl protons in the aromatic region appeared at 7.18-7.35 ppm as multiplet.

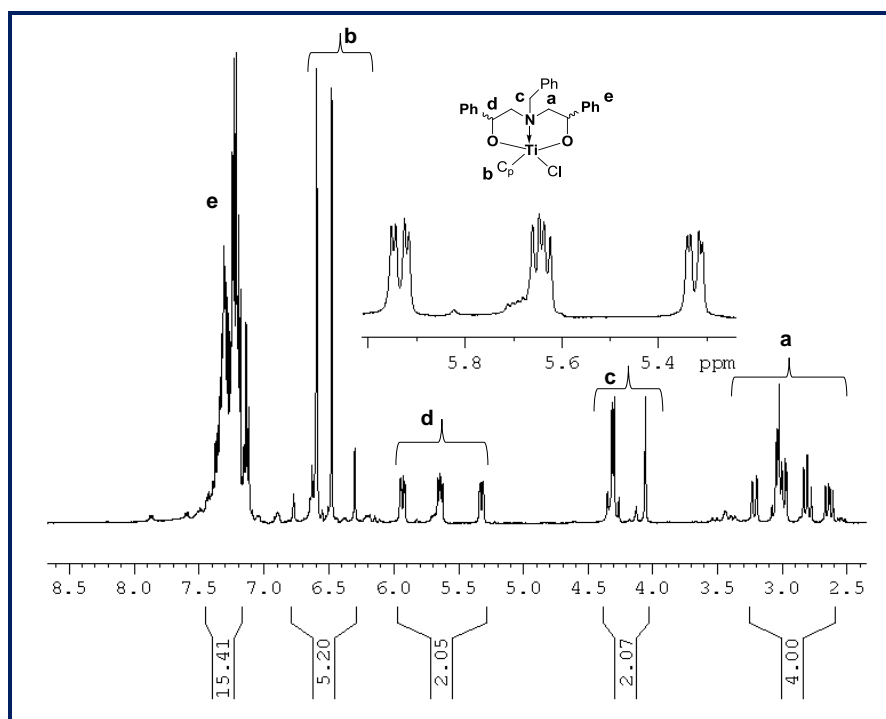


Figure 2.18. ^1H NMR spectrum of complex $4\text{-C}_p\text{TiCl}[\text{O},\text{O},\text{N}]$.

The ^1H NMR spectrum of the complex $4\text{-C}_p^*\text{TiCl}[\text{O},\text{O},\text{N}]$ is shown in Figure 2.19. The spectrum displays well defined peaks with the expected integrations. The resonance signals corresponding to the methine proton is displayed at 5.64-6.12 ppm (shifted downfield by 1.08-1.47 ppm in comparison to the ligand), while the signals corresponding to the methylene protons appear at 2.83-3.3 ppm (shifted small downfield of 0.23 ppm), and the signals corresponding to the benzylic proton displayed at 4.10-4.71 ppm (shifted downfield by 0.51-0.85 ppm). This result suggests the coordination of the Lewis acidic titanium metal to the ligand. The downfield shift is greater for the methine (CH-Ph) resonance than that of benzylic (N-CH₂Ph) resonance suggesting a strong bond between O atom and Ti atom and a weak interaction between the N atom and the Ti atom upon complexation. The presence of new resonance signals (singlet) at 2.30 and 2.35 ppm corresponding to the (C_p^*) moiety also confirms the formation of complex. The signal in the aromatic region 7.24-7.61 ppm (multiplet) corresponds to the phenyl protons.

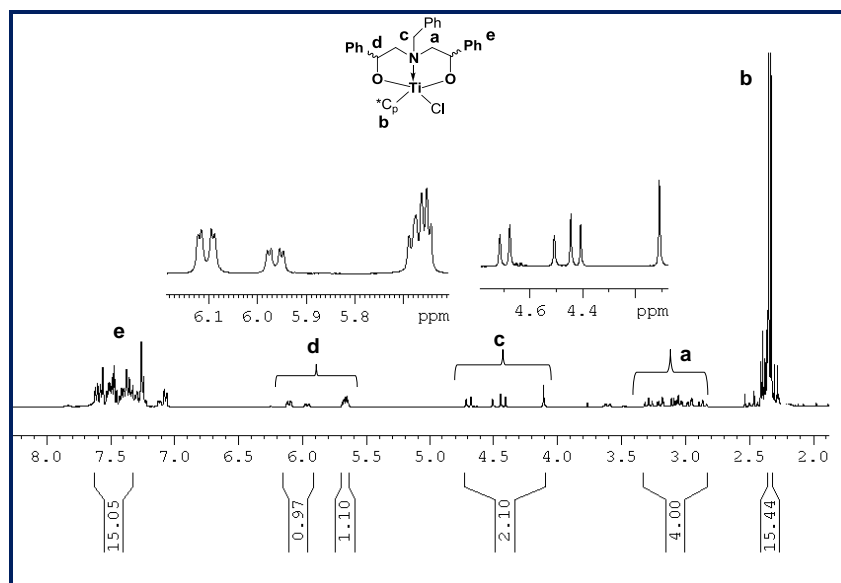
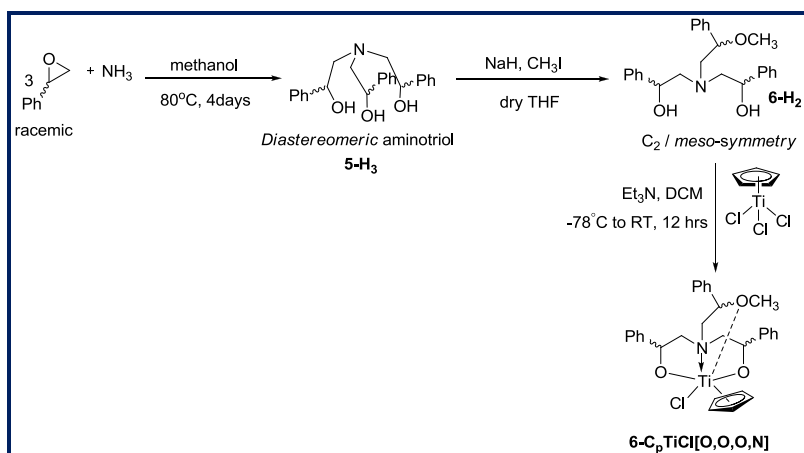


Figure 2.19. ^1H NMR spectrum of complex $4\text{-C}_p^*\text{TiCl}[\text{O},\text{O},\text{N}]$.

2.2.6. Synthesis and Characterization of half-sandwich titanium complex based on tetradentate aminotriol ligand.

A new type of half-sandwich titanium complex containing tetradentate dianionic ligand has also been prepared and characterized by ^1H NMR. The synthesis of the ligand and the corresponding complex is outlined in Scheme 2.7. The Aminotriol ligand was synthesized as a diastereomeric mixture (containing (C_3) and (C_s) symmetry) by reacting 3 equiv. of *racemic* styrene oxide with 1 equiv. of NH_3 in methanol.^{26,27} Upon methylation with one equiv. of NaH and CH_3I , the aminotriol ligand gave the diastereomeric aminodiols (containing (C_2) and (*meso*) symmetry).

Titanium complex was prepared by reacting the aminotriol ligand [O,O,O,N] with the same equivalent of the C_pTiCl_3 in the presence of excessive triethylamine in dichloromethane.



Scheme 2.7. Synthesis of titanium half-sandwich complexes **6-C_pTiCl[O,O,O,N]** based on tetradentate dianionic ligand.

The 1H NMR spectrum of the aminotriol ligand **5-H₃** (Figure 2.20) displays a signal at 2.61-2.90 ppm (multiplet) corresponding to the enantiotopic methylene protons (N-CH₂-) and signals at 4.65-4.85 ppm (two doublet of doublet) due to the Ph-CH-O methine protons. The resonance signal at 4.30 ppm (singlet) is due to the hydroxyl protons and the phenyl protons appear as a multiplet in the aromatic region at 7.23-7.38 ppm.

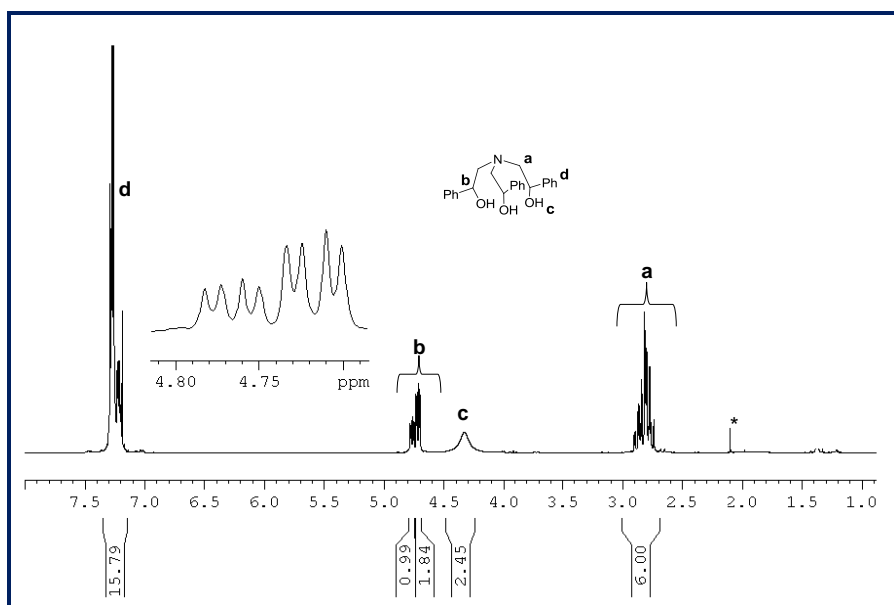


Figure 2.20. 1H NMR spectrum of diastereomeric aminotriol **5-H₃**.

The diastereomeric aminodiol ligand **6-H₂** prepared from the aminotriol **5-H₃** was characterized by ¹H NMR (Figure 2.21). The spectrum also displays the same kind of resonance signals for the methylene, hydroxyl and the phenyl protons, while the resonance signals at 4.35-4.45 ppm (multiplet) and 4.69-4.83 ppm (multiplet) correspond to the (CH-PhOMe) and (CH-PhO) methine protons respectively. The methyl protons of the (OMe) display a signal at 3.32-3.37 ppm as three different singlets.

The titanium complex 6-C_pTiCl[O,O,O,N] was characterized by ¹H NMR spectroscopy (Figure 2.22). Well defined resonance peaks with expected integrations are observed. The methine protons (CH-PhOMe) appear at 4.44-4.57 ppm (multiplet) shifted downfield by 0.1-0.12 ppm, while the other methine proton (CH-PhO) display a resonance at 5.44-5.99 ppm (multiplet) shifted downfield by 0.75-1.16 ppm in comparison to the free ligand. The methylene (CH₂N) and methyl (OMe) protons appears together in the region 2.55-3.58 as multiplet. This indicates that the coordination of titanium to the O atom of the ligand is stronger than the other coordinating heteroatom (OCH₃ & NCH₂). The presence of new resonance signals (singlet) at 6.46, 6.49, 6.5 ppm corresponding to the (C_p) moiety also confirms the formation of the complex. The phenyl protons resonances appear at 7.22-7.37 ppm.

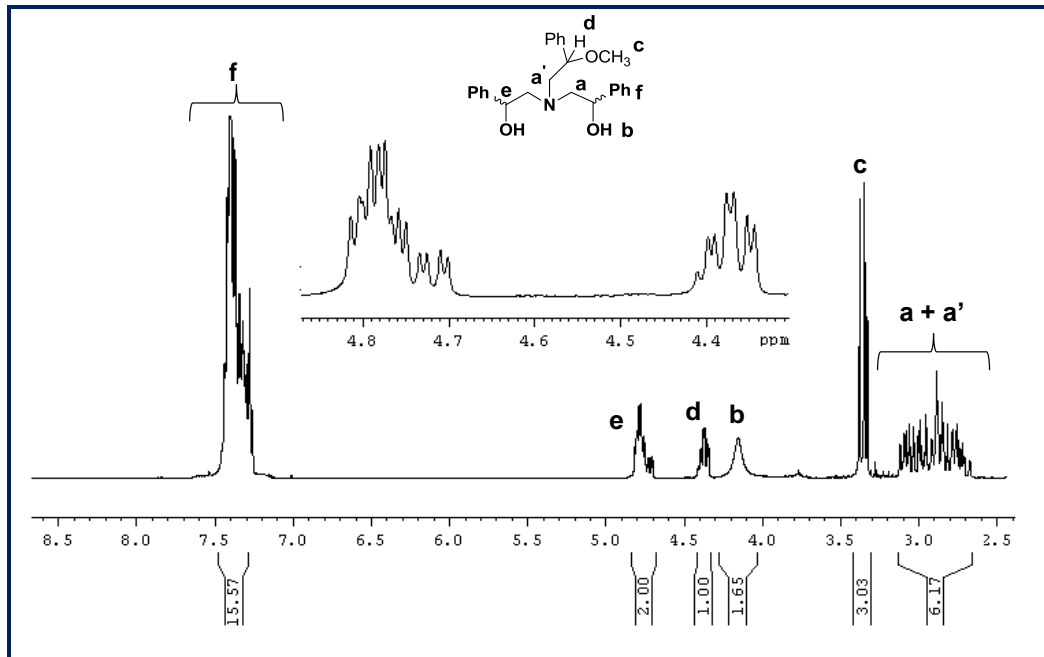


Figure 2.21. ¹H NMR spectrum of *diastereomeric* aminodiol **6-H₂**.

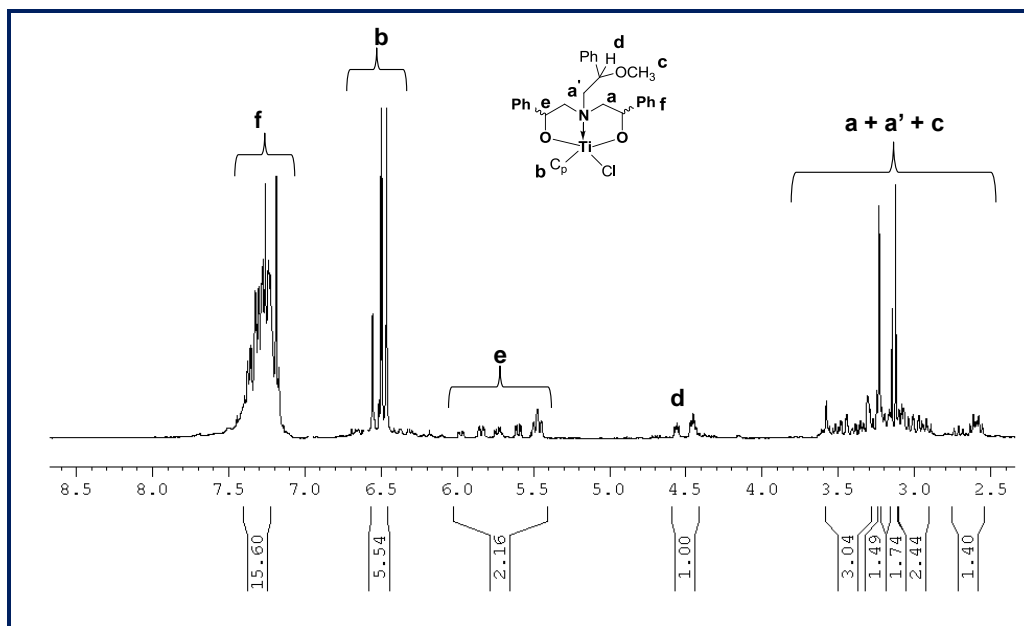


Figure 2.22. ^1H NMR spectrum of complex $6\text{-C}_p\text{TiCl}[\text{O},\text{O},\text{O},\text{N}]$.

2.3. Conclusion

A new type of titanium dialkoxide complexes supported by an enantiomerically pure, *racemic*, *meso* and diastereomeric aminodiol ligands were easily prepared under mild conditions by reacting the ligands with the metal precursor $\text{Ti}(\text{O}^i\text{Pr})_4$. Prepared complexes were characterized by ^1H & ^{13}C NMR spectroscopy. These complexes were used as initiator for the ring opening polymerization of cyclic esters, this will be discussed in the following chapters. Attempt to synthesize the zirconium isopropoxide analogue complexes lead to un-defined products, whereas the zirconium tert-butoxide complex derived from the *meso* ligand was easily prepared by using the bulky metal precursor $\text{Zr}(\text{O}^t\text{Bu})_4$. Using the same ligand system, tridentate half sandwich titanium complexes have also been synthesized by using the metal precursor (C_pTiCl_3 and $\text{C}_p^*\text{TiCl}_3$). The same types of complexes derived from other tetradentate ligand system have also been prepared. These half-sandwich complexes can be used as catalysts for the syndiospecific styrene polymerization.

2.4. References

- [1] Zaitsev, K. V.; Karlov, S. S.; Selina, A. A.; Oprunenko, Yu. F.; Churakov, A. V.; Neumüller, B.; Howard, J. A. K.; Zaitseva, G. S.; *Eur. J. Inorg. Chem.* **2006**, 1987.
- [2] Zaitsev, K. V.; Bermeshev, M. V.; Samsonov, A. A.; Oprunenko, Yu. F.; Churakov, A. V.; Howard, J. A. K.; Karlov, S. S. G.; Zaitseva, S. *New. J. Chem.* **2008**, 32, 1415.
- [3] Lavanant, L.; Toupet, L.; Lehmann, C. W.; Carpentier, J.- F. *Organometallics.* **2005**, 24, 5620.
- [4] Vasilenko, I. V.; Kostjuk, S. V.; Zaitsev, K. V.; Nedorezova, P. M.; Lemenovskii, D. A.; Karlov, S. S. *Polym Sci Ser B.* **2010**, 52, 136.
- [5] Kim, Y.; Verkade, J. G. *Organometallics.* **2002**, 21, 2395.
- [6] Kim, Y.; Jnaneshwara, G. K.; Verkade, J. G. *Inorg. Chem.* **2003**, 42, 1437.
- [7] Kim, Y.; Verkade, J. G. *Macromol Symp.* **2005**, 224, 105.
- [8] Piskun, Y. A.; Vasilenko, I. V.; Kostjuk, S. V.; Zaitsev, K. V.; Zaitseva, G. S.; Karlov, S. S. *J. Polym. Sci., Part A: Polym. Chem.* **2010**, 48, 1230.
- [9] Spassky, N.; Wisniewski, M.; Pluta, C.; Le Borgne, A. *Macromol. Chem. Phys.* **1996**, 197, 2627.
- [10] Ovitt, T. M.; Coates, G. W. *J. Polym. Sci., Part A: Polym. Chem.* **2000**, 38, 4686.
- [11] Radano, C. P.; Baker, G. L.; Smith, M. R. *J. Am. Chem. Soc.* **2000**, 122, 1552.
- [12] Ovitt, T. M.; Coates, G. W. *J. Am. Chem. Soc.* **2002**, 124, 1316.
- [13] Zhong, Z.; Dijkstra, P.J.; Feijen, J. *J. Am. Chem. Soc.* **2003**, 125, 11291.
- [14] Nomura, N.; Ishii, R.; Yamamoto, Y.; Kondo, T. *Chem.–Eur. J.* **2007**, 13, 4433.
- [15] Manivannan, R.; Sundararajan, G. *Macromolecules.* **2002**, 35, 7883.
- [16] Keren, E.; Sundararajan, G. *J. Polym. Sci., Part A: Polym. Chem.* **2007**, 45, 3599.
- [17] Zelikoff, A. L.; Kopilov, J.; Goldberg, I.; Coates, G. W.; Kol, M. *Chem. Commun.* **2009**, 6804.
- [18] Schwarz, A. D.; Thompson, A. L.; Mountford, P. *Inorg. Chem.* **2009**, 48, 10442.
- [19] Ning, Y.; Zhang, Y.; Rodriguez-Delgado, A.; Chen, E. Y.-X. *Organometallics.* **2008**, 27, 5632.
- [20] Chmura, A. J.; Cousins, D. M.; Davidson, M. G.; Jones, M. D.; Lunn, M. D.; Mahon, M. F. *Dalton Trans.* **2008**, 1437.
- [21] Chmura, A. J.; Davidson, M. G.; Frankis, C. J.; Jones, M. D.; Lunn, M. D.; *Chem. Commun.* **2008**, 1293.
- [22] Gendler, S.; Segal, S.; Goldberg, I.; Goldschmidt, Z.; Kol, M. *Inorg. Chem.* **2006**, 45, 4783.
- [23] Chmura, A. J.; Davidson, M. G.; Jones, M. D.; Lunn, M. D.; Mahon, M. F.; Johnson, A. F.; Khunkamchoo, P.; Roberts, S. L.; Wong, S. S. F. *Macromolecules.* **2006**, 39, 7250.
- [24] Chmura, A. J.; Davidson, M. G.; Jones, M. D.; Lunn, M. D.; Mahon, M. F. *Dalton Trans.* **2006**, 887.
- [25] Hong, Y.; Mun, S.-D.; Lee, J.; Do, Y.; Kim, Y. *J. Organomet. Chem.* **2008**, 693, 1945.
- [26] Sudhakar, P.; Amburose, C. V.; Sundararajan, G.; Nethaji, M. *Organometallics*, **2004**, 23, 4462.
- [27] Sudhakar, P.; Sundararajan, G. *Macromol. Rapid Commun.* **2005**, 26, 1854.

CHAPTER 3
Ring-Opening Polymerization of *L*-lactide and *rac*-lactide

CHAPTER 3

Ring-Opening Polymerization of *L*-lactide and *rac*-lactide

3.1. Introduction

Poly(lactic acid) (PLA) is a biodegradable polymer derived from bio-renewable resources such as corn, sugar beets, and dairy products. It has found widespread applications as a commodity plastic¹ and as a biomedical material.² In order to increase the range of potential application of these polymers, PLAs with defined and controlled physical and mechanical properties are required.

PLAs are generally prepared from the ring opening polymerization (ROP) of the cyclic ester monomer lactide (LA). The production of PLAs by ROP includes anionic, cationic, organocatalytic, enzymatic and coordination insertion mechanisms. Among these, the method using metal based initiators has received considerable attention in recent years, both in academia and industry, since it enables control of the molecular weight and tacticity of the polymer, which affects its mechanical properties and its tendency to degrade.^{3,4} Polymerization of *L*-LA leads to isotactic PLA, while polymerization of *rac*-LA can lead to atactic, heterotactic, stereoblock, or stereocomplex PLA as determined by the type of catalyst employed.⁵ Therefore a large number of investigation has been directed towards the synthesis of efficient metal based initiators and their reactivity studies.

Well defined single site alkoxide complexes introduced in the last decade have shown significant improvement for the synthesis of stereoregular polymer from the *rac*-LA polymerization.⁵ The catalyst activity and stereoregularity of the polymer depend on the metal employed, as well as the structural parameters of the chelating ligands (including chirality, rigidity and steric bulk). For example, predominantly isotactic PLA could be obtained with aluminum complexes bearing tetradentate Schiff base (salen) ligands.⁶ Isotactic stereoblock PLA were also obtained with aluminum salen⁷⁻⁹ and aluminum aminophenoxide complexes.^{10,11} Heterotactic PLA were obtained with zinc, calcium and magnesium complexes.¹²⁻¹⁴ Coates *et al.* have used aluminum, yttrium, zinc and magnesium based complexes in the polymerization of *meso* and *rac*-LA that leads to syndiotactic and isotactic stereoblock polymer respectively.¹⁵⁻¹⁸

Group (IV) metal complexes are less explored for the ROP of lactides. Some of them revealed to be very active but only modest stereoselectivity were observed in the *rac*-lactide polymerization.¹⁹⁻²⁹ These Group (IV) metal (Ti, Zr, Hf) complexes with different ligands have been described in the chapter 1.

Despite the fact that some excellent initiators have been reported for the polymerization of lactides, the search for new catalyst that generate well defined poly(lactides) remains of keen interest. Previously, Sundararajan *et al.* have reported the titanium dichloride complexes derived from an aminodiol ligand, as active catalyst for the 1-Hexene polymerization, and found that subtle changes in the symmetry of the ligand periphery changes the stereospecificity of poly(1-hexene).³⁰

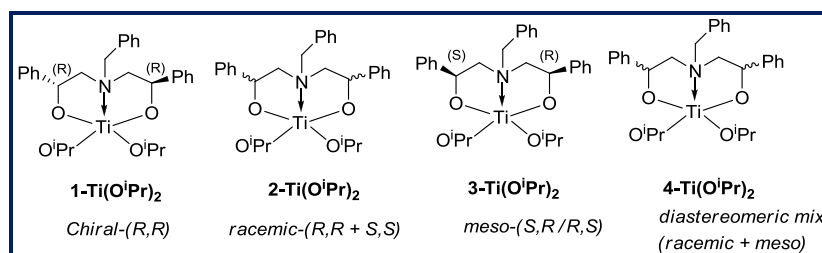
To further explore the use of aminodiol ligands for the development of stereoselective Group (IV) metal complexes for the ROP of *rac*-LA, we reported a new type of titanium alkoxide complex of aminodiol ligand having different symmetry, and their abilities in the ring opening polymerization of *L*-LA and *rac*-LA. Very recently, Piskun *et al.* reported the titanium complexes based on dialkanolamine ligands for ROP of ϵ -caprolactone.³¹

3.2. Results and Discussion

3.2.1. Solution Polymerizations

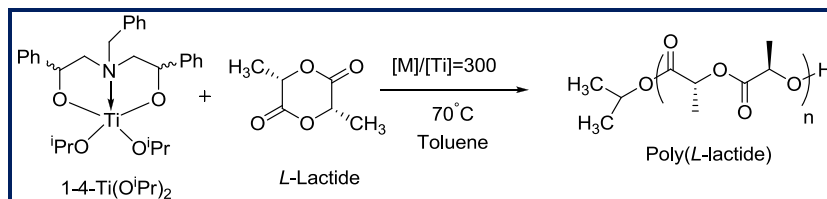
3.2.1.1. Polymerization of *L*-lactide and *rac*-lactide

The titanium complexes 1-4-Ti(O^{*i*}Pr)₂ shown in Scheme 3.1 were tested as initiators for the ring opening polymerization of *L*-LA and *rac*-LA.



Scheme 3.1. Titanium alkoxide complexes.

We aimed at unraveling the effect of the structural parameters, i.e. nature of the ligand, on the activity and stereoselectivity of the corresponding catalysts. To start, the optically pure monomer (*L*-LA) was preferred because it is expected to lead to an isotactic polymer, independently of the catalyst being used. Preliminary polymerization experiments were conducted in toluene at 70°C, with a monomer to initiator ratio of 300 (Scheme 3.2). Results are summarized in Table 3.1.



Scheme 3.2. Solution polymerization of *L*-lactide using 1-4-Ti(O^{*i*}Pr)₂.

Table 3.1. Solution polymerization of *L*-Lactide ^a

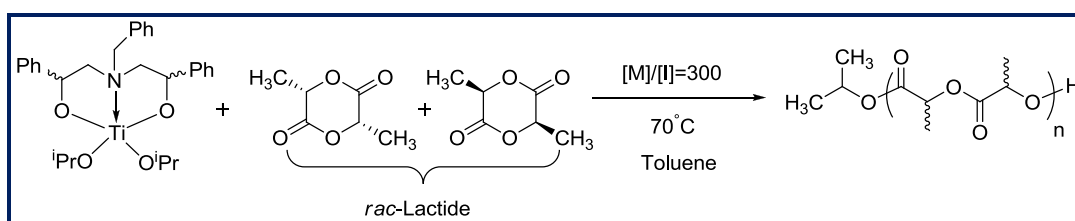
Entry	Catalyst	Conv (%) ^b	M _n (NMR) ^c (g.mol ⁻¹)	M _n (theory) ^d (g.mol ⁻¹)	M _n (SEC) ^e (g.mol ⁻¹)	M _n (SEC) ^f (g.mol ⁻¹)	PDI ^e
1	1-Ti(O ⁱ Pr) ₂	96.4	27360	20910	30480	17680	1.60
2	2-Ti(O ⁱ Pr) ₂	94.7	28410	20510	45650	26480	1.34
3	3-Ti(O ⁱ Pr) ₂	>99	27020	21660	35660	20680	1.36
4	4-Ti(O ⁱ Pr) ₂	>99	22170	21660	28870	16740	1.31

^a Polymerization conditions: 1g of (*L* - LA), temperature = 70°C, [M]/[Ti]= 300, solvent: toluene = 15 mL, polymerization time = 22 h. ^b Conversion determined by ¹H NMR via the integration of the methine resonance peak of LA and the polymer. ^c Calculated from ¹H NMR analysis by integration of the end group of the isopropoxide at 1.24 ppm and the backbone resonance at 5.1 ppm. ^d M_n(theory) was calculated from the formula ((M.W of LA) × (conversion / 100) × [LA]) / 2×[Ti] + 60 (End group). ^e Determined from SEC (in THF) relative to polystyrene standards. ^f Determined from SEC (in THF) relative to polystyrene standards and corrected by Mark-Houwink correction factor of 0.58.³²

All complexes were found to be active under these polymerization conditions with similar monomer conversion (>95%) in 22 h, and showed reasonably controlled molecular weight distribution in the range of 1.31 to 1.60. The relatively narrow PDI values support controlled polymerization catalysis. However, the PDIs of the polymer obtained from the chiral complex 1-Ti(OⁱPr)₂ were broader (PDI = 1.60) when compared to the other complexes. This broadening of PDIs may be indicative of trans-esterification side reaction occurring at high monomer conversion (available monomer concentration is less favorizing side reactions) during the polymerization process. The observed polymer molecular weight from SEC showed a higher value, due to the lower solution state volume of PLA relative to polystyrene standards used for the calibration. Duda *et al.* suggested that in order to obtain the correct values of PLAs, the experimental value obtained by the SEC traces using polystyrene standards has to be multiplied by the Mark-Houwink correction factor of 0.58 for PLA.³² Thus the M_n value obtained after applying correction factor was in close agreement with the theoretical ones (calculated on the assumption that two Ti-OⁱPr initiates the polymerization). For example, polymer obtained from the complex 3-Ti(OⁱPr)₂ (Table 3.1, Entry 3), showed M_n (SEC)^f = 20680 g.mol⁻¹ which is in close agreement with M_n (theory) = 21660 g.mol⁻¹. However, molecular weight determined from the NMR showed higher value compare to the M_n (theory), which may be due to the inconsistency in determination of molecular weight by NMR due to low intensity of end group protons as compare to the polymer methine protons.

Activity of these complexes was comparable to some of the previously reported titanium alkoxide complexes^{33,34} and was found to be higher than other previously reported titanium alkoxide complexes bearing triethanolamine ligands (70% of monomer conversion in 36 h, under the same polymerization conditions).²⁰

All complexes were further tested for the polymerization of *rac*-lactide in solution (toluene) at 70°C in order to assess the possible stereocontrol of the initiators (Scheme 3.3). Results are summarized in Table 3.2. All complexes were found to be efficient initiators and a complete monomer conversion was reached in 22 h, except for complex 1-Ti(O^{*i*}Pr)₂ which showed only 72% monomer conversion. Relatively narrow polydispersities (PDI = 1.18 -1.52) were observed for all complexes indicating controlled polymerizations.



Scheme 3.3. Solution polymerization of *rac*-lactide using 1-4-Ti(O^{*i*}Pr)₂.

Table 3.2. Solution polymerization of *rac*-Lactide^a

Entry	Catalyst	Conv (%) ^b	M _n (NMR) ^c (g.mol ⁻¹)	M _n (theory) ^d (g.mol ⁻¹)	M _n (SEC) ^e (g.mol ⁻¹)	M _n (SEC) ^f (g.mol ⁻¹)	PDI ^e	P _r ^g
1	1-Ti(O ^{<i>i</i>} Pr) ₂	72	21710	15620	18620	10800	1.18	0.58
2	2-Ti(O ^{<i>i</i>} Pr) ₂	>99	26090	21460	27830	16140	1.28	0.65
3	3-Ti(O ^{<i>i</i>} Pr) ₂	98	31300	21250	21230	12310	1.53	0.50
4	4-Ti(O ^{<i>i</i>} Pr) ₂	>99	20990	21460	14920	8650	1.42	0.58

^a Polymerization conditions: 1g of (*rac* - LA), temperature = 70°C, [M]/[Ti] = 300, solvent: toluene = 15 mL, polymerization time = 22 h. ^b Conversion determined by ¹H NMR via the integration of the methine resonance peak of LA and the polymer. ^c Calculated from ¹H NMR (CDCl₃) analysis by integration of the end group of the isopropoxide at 1.24 ppm and the backbone resonance at 5.1 ppm. ^d M_n (theory) was calculated from the formula ((M.W of LA) × (conversion / 100) × [LA]) / 2 × [Ti] + 60 (End group). ^e Determined from SEC (in THF) relative to polystyrene standards, no correction factor employed. ^f Determined from SEC (in THF) relative to polystyrene standards and corrected by Mark-Houwink correction factor of 0.58.³² ^g P_r (probability of racemic linkage) calculated from ¹H Homonuclear decoupled NMR analysis.

Similarly to *L*-LA polymerization, the molecular weight determined by NMR is consistent with the propagation of two polymer chains from each metal center. In the case of complexes **1**, **3** & **4** (Table 3.2, entry 1, 3 & 4) the experimental number-average molecular weight determined by SEC (uncorrected with Mark-Houwink correction factor) shows values close to the theoretical ones and the corrected values with correction factor are proportionally lower. This can be attributed to transesterification reactions frequently observed with cyclic esters or to a slow initiation step compared to propagation. Similar kind of results was also found for other catalytic system in the literature³⁵⁻³⁷ although there is deviation in M_n between corrected experimental and theoretical ones; the polymerization occurs in a controlled manner as confirmed from the narrow dispersity values.

Activity of these 1-4-Ti(O^{*i*}Pr)₂ titanium complexes in solution (toluene) condition (> 95% conversion in 22 h) were comparable to the recently reported sulfonamide supported titanium alkoxide complexes under the same reaction condition (90% conversion in 24 h at 70°C)³⁸, amine tris(phenolate) titanium complexes (96% conversion in 24 h, at 80°C)³⁹, titanium salen complexes (97% conversion in 24 h at 70°C)²⁵ and tetranuclear titanium complexes (75% conversion in 24 h at 70°C).³⁴ However, activity of our complexes were found to be lower compare to very recently reported titanium salalen complexes which showed very high activity (98% conversion in 2 h at 80°C).⁴⁰

3.2.1.2. Poly(*L* / *rac*-lactide) characterization

3.2.1.2.1. Determination of molecular weight by SEC with triple detection

In recent years, viscosity and /or light-scattering detectors are very often used to overcome the limitation of conventional SEC in which the true molar masses can only be obtained if the calibration standards and the sample are of the same type. The detectors used in this study are (RI), (viscometer), and (light scattering). The signal of light-scattering detectors is directly proportional to the molecular weight of the polymers.

$$\text{LS signal} = K_{\text{LS}} \cdot (dn/dc)^2 \cdot \text{MW} \cdot c$$

Where K_{LS} is an apparatus-specific sensitivity constant, dn/dc the refractive index increment and c the concentration.

For viscometer detectors, the following equation applies:

$$\text{Visc.signal} = K_{\text{visc}} \cdot [\eta] \cdot c$$

Where $[\eta]$ is the intrinsic viscosity of the polymer

Contradictory results exposed in the literature about the application of Mark-Houwink correction factor, prompted us to evaluate the exact molar mass of some of our polymers. Indeed, in order to have a good agreement between experimental and theoretical molecular weights the Mark-Houwink correction factor is applied or not. In our case, the molecular weight of poly(*rac*-LA) prepared with the complex 4-Ti(OⁱPr)₂ in toluene at 70°C with [M]/[Ti] of 100, was evaluated by SEC with triple detection in THF (dn/dc of polylactide in THF = 0.058 mL.g⁻¹)⁴¹ (Figure 3.1). The observed M_n of 6440 g.mol⁻¹ (6% error) by using multiwavelength light scattering detector was very close to the value observed by SEC using polystyrene standards (RI detector) after applying the correcting factor (M_n(SEC)* = 6650 g.mol⁻¹).

Similarly, PLLA prepared with the complex 4-Ti(OⁱPr)₂ in toluene at 70°C with [M]/[Ti] of 300, was also determined by SEC with triple detection (Figure 3.2). It shows a molecular weight of 16460 g.mol⁻¹ (8% error) by using LS detector and this value is in very good agreement with the value observed by SEC using polystyrene standards (RI detector) after applying the correcting factor (M_n(SEC)* = 16740 g.mol⁻¹) (Table 3.1, Entry 4). These results suggest that to evaluate the exact molecular weight of polylactides by SEC using PS standards and RI detector, the Mark-Houwink correction factor has to be applied, at least in the range of molar masses upto 20000 g.mol⁻¹.

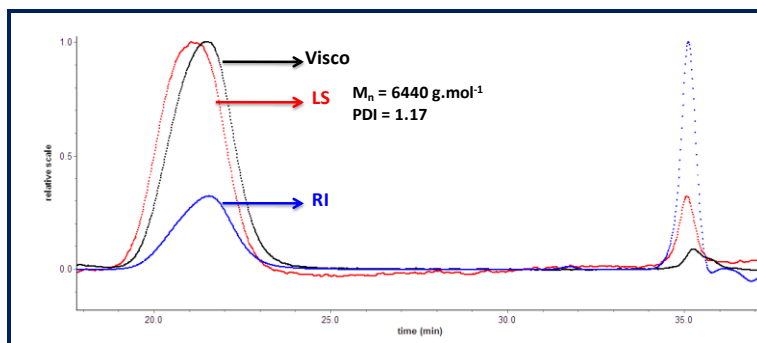


Figure 3.1. SEC chromatogram of PDLLA prepared using 4-Ti(OⁱPr)₂ with [M]/[Ti] = 100.

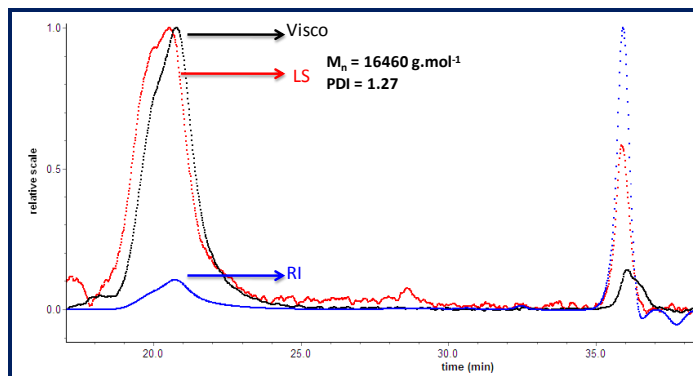


Figure 3.2. SEC chromatogram of PLLA (Table 3.1, entry 4).

3.2.1.2.2. ^1H and ^{13}C NMR analysis

For the end group analysis, polymerizations were carried out in toluene solution at 70°C with a monomer to initiator ratio of 100 using $4\text{-Ti}(\text{O}^i\text{Pr})_2$ as the initiator. The polymerization mixture (after complete monomer conversion) was precipitated in methanol and the white solid obtained was filtered and dried. PLLA was analyzed by ^1H NMR (Figure 3.3). Signals at 5.16 ppm and 1.57 ppm are assigned to the main chain methine proton (**c**) and methyl protons (**b**) respectively. Polymer chain are encapped with acyl-isopropoxide- $\text{COOCH}(\text{CH}_3)_2$ group and hydroxyl methyne- $\text{CH}(\text{CH}_3)\text{OH}$ group which are confirmed by proton signals at 1.15 ppm (doublet of doublets) as proton (**a**), at 4.92 ppm (septet) as proton (**e**) and 4.36 ppm (quartet) for proton (**d**) and 1.40 ppm (doublet) for proton (**f**).

The degree of polymerization (DP_n) of PLLA (Figure 3.3), evaluated from the relative intensity ratio of signals **c** and **a** was shown to be 57, which is nearly equal to half of the initial mole ratio of monomer to initiator (100). Thus, the calculated molecular weight from the NMR spectroscopy ($M_n(\text{NMR}) = 8270 \text{ g}\cdot\text{mol}^{-1}$) is nearly close to the theoretical ones ($M_n(\text{theory}) = 7230 \text{ g}\cdot\text{mol}^{-1}$) calculated assuming that the two O^iPr groups initiates the polymerization. Size Exclusion Chromatography (SEC) analysis of this polymer in THF calibrated using polystyrene standard showed M_n of $11770 \text{ g}\cdot\text{mol}^{-1}$ which is slightly higher than the M_n value observed from the NMR. Nevertheless, if it is corrected by the Mark-Houwink correction factor of 0.58 as discussed before,³² the observed $M_n(\text{SEC})^* = 6830 \text{ g}\cdot\text{mol}^{-1}$ value is in good agreement with $M_n(\text{theory})$.

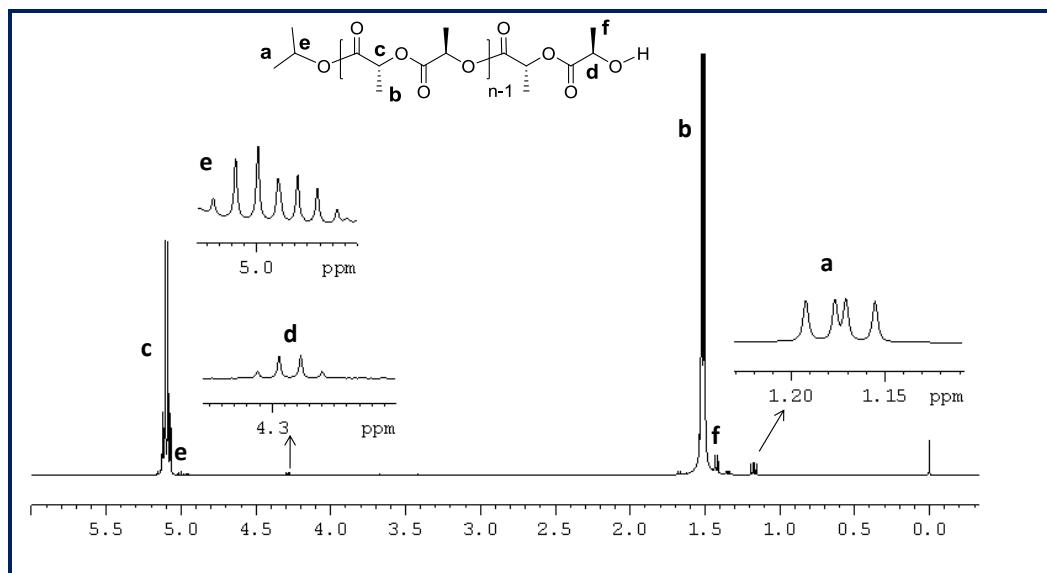


Figure 3.3. ^1H NMR spectrum of PLLA prepared using $4\text{-Ti}(\text{O}^i\text{Pr})_2$.

Poly(*rac*-lactide) was also analyzed by ^1H NMR (Figure 3.4). Similarities are observed, signals at 5.05 ppm (multiplet) and 1.49 ppm (multiplet) are assigned to the main chain methine proton (**c**) and the methyl protons (**b**) respectively. Relatively less intense signals at 1.18 ppm (doublet of doublet) (**a**), 4.94 ppm (septet) (**e**) 4.25 ppm (quartet) (**d**), 1.43 ppm (doublet) (**f**) were assignable to the terminal isopropoxy methyl ($(\text{CH}_3)_2\text{-CH-O}$, methine $(\text{CH}_3)_2\text{-CH-O}$ and hydroxyl methyne and methyl $-\text{CH}(\text{CH}_3)\text{OH}$ group, respectively. However in the ^1H NMR spectrum of poly(*rac*-lactide) the main chain methine and the methyl protons appears as a multiplet which is due to the random placement of either (*R,R*) and (*S,S*) stereosequences in the polymer main chain as compare to the poly(*L*-lactide).

The (DP_n) of Poly(*rac*-lactide), evaluated from the intensity ratio of signals **c** to **a** to be 59, is also nearly equal to half of the initial monomer to initiator ratio 100. Thus, the observed molecular weight from the NMR spectroscopy (M_n (NMR) = $8560 \text{ g}\cdot\text{mol}^{-1}$) was in good agreement with the theoretical one (M_n (theory) = $7230 \text{ g}\cdot\text{mol}^{-1}$). SEC analysis of this polymer using PS standards showed M_n of $11470 \text{ g}\cdot\text{mol}^{-1}$ and again, the observed value after the correction factor (M_n (SEC)* = $6650 \text{ g}\cdot\text{mol}^{-1}$) is in good agreement with M_n (theory).

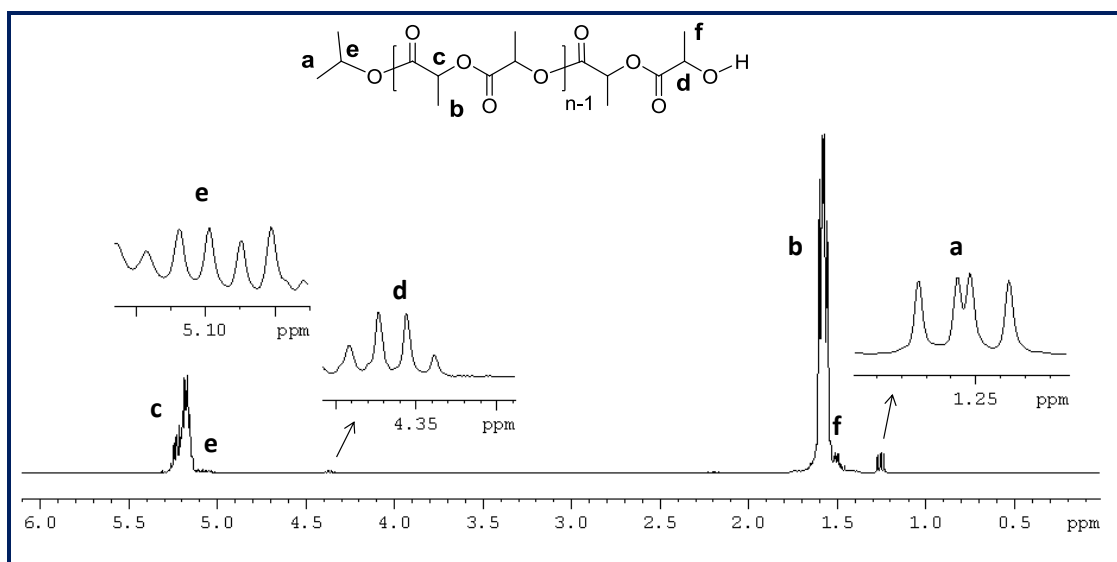


Figure 3.4. ^1H NMR spectrum of PDLLA prepared using $4\text{-Ti}(\text{O}^i\text{Pr})_2$.

^{13}C NMR spectrum of PLLA is presented in Figure 3.5 and displays the peaks corresponding to the chain end isopropoxy methyl and methine carbon chain end at 21.64 ppm (**b**) and 66.7 ppm (**c**) respectively. The peaks at 69.26 ppm (**g**) and 20.5 ppm (**f**) correspond to the other chain end hydroxyl methine and methyl carbons respectively. The main chain methyl and methine carbon resonances appear at 16.6 ppm (**a**) and 69 ppm (**d**) respectively. The carbonyl carbon resonance appears at 169.6 ppm (**e**).

Similarly, the ^{13}C NMR spectrum of the PDLLA is presented in Figure 3.6. Peaks at 21.64 ppm (**b**) and 66.6 ppm (**c**) correspond to the chain end isopropoxy methyl and methine carbon resonance respectively. The peaks at 67.96 ppm (**g**) and 20.5 ppm (**f**) correspond to the other chain end hydroxyl methine and methyl carbons. The main chain methyl and methine carbon resonance appears at 16.6 ppm (**a**) and 69.2 ppm (**d**) respectively. The carbonyl carbon resonance appears at 169.6 ppm (**e**). In this case, the carbonyl, methine and methyl carbon resonance appears as multiplet signals due to the random placement of stereosequences in the polymer.

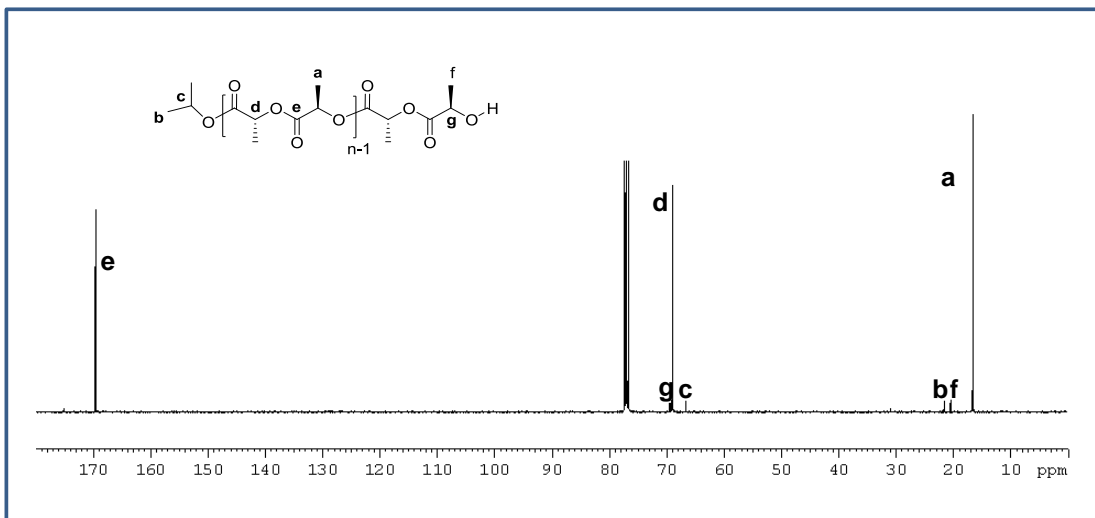


Figure 3.5. ^{13}C NMR spectrum of PLLA prepared using $4\text{-Ti}(\text{O}^i\text{Pr})_2$.

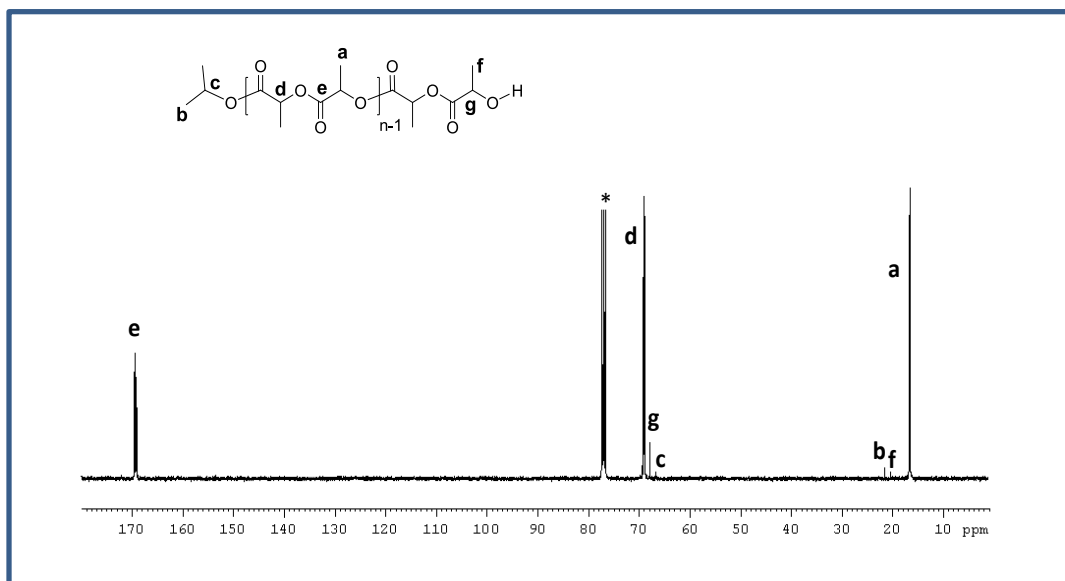
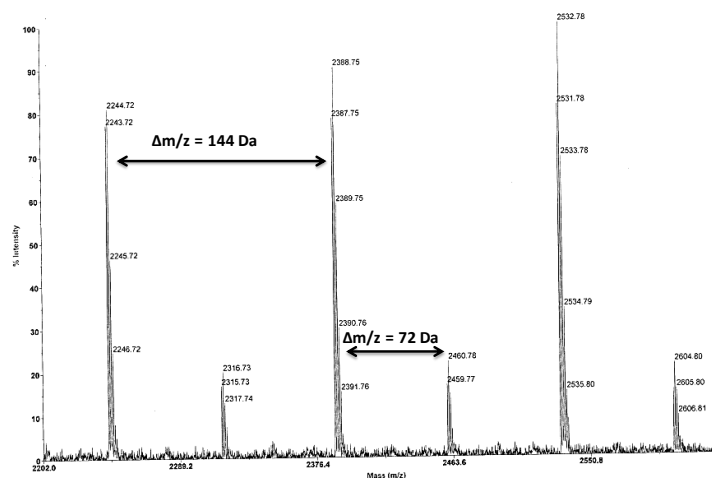
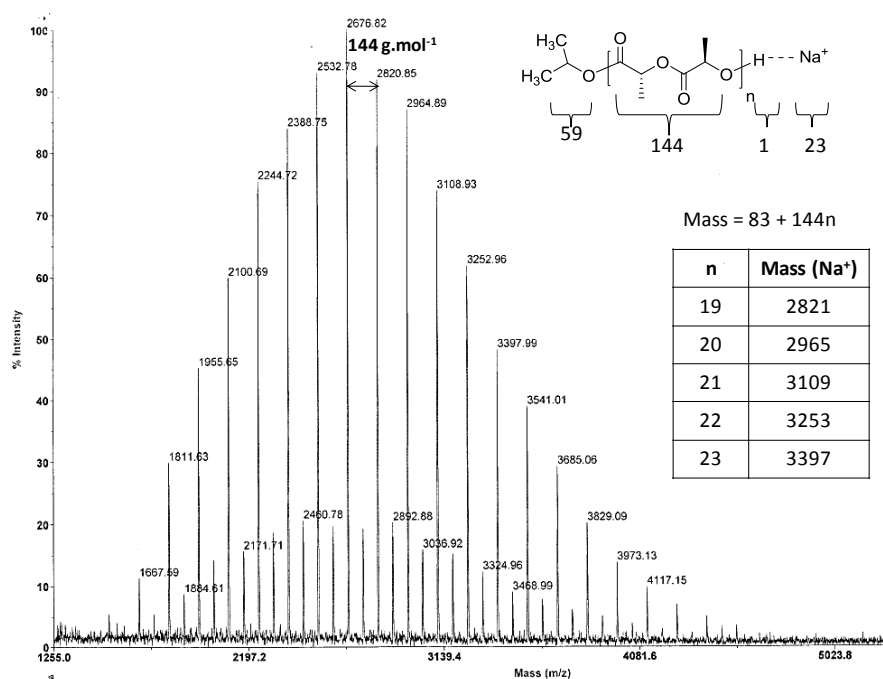


Figure 3.6. ^{13}C NMR spectrum of PDLLA prepared using $4\text{-Ti}(\text{O}^i\text{Pr})_2$.

3.2.1.2.3. MALDI-TOF mass spectrometry analysis

A Poly(L-lactide) produced with the initiator 1-Ti(OⁱPr)₂ with a monomer to initiator ratio of 50 in solution (toluene) at 70°C, was analyzed by MALDI-TOF-mass spectrometry (Figure 3.7). The major set of peaks with a mass difference of $\Delta m/z = 144$ Da corresponds to the expected lactide monomer as the repeating unit [C(O)CH(Me)C(O)CH(Me)] with isopropyl ester and –OH end groups. Minor set of peaks corresponding to a repeating unit of 72 Da, [C(O)CH(Me)] indicates the presence of transesterification reactions occurring during the polymerization process. The formation of macrocyclic polymer due to backbiting is not observed in the spectrum (Scheme 3.4). These results suggest that the polymer initiation occurs through the insertion of lactide into the Ti-O bond *via* coordination insertion mechanism.



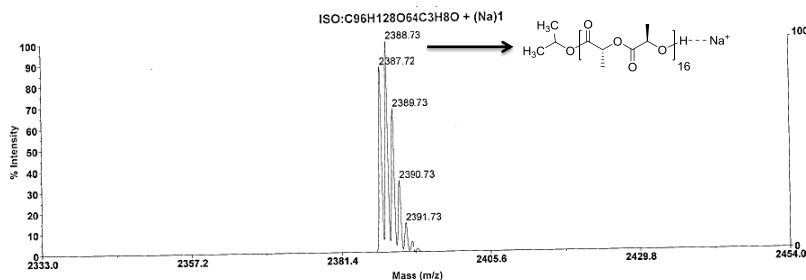
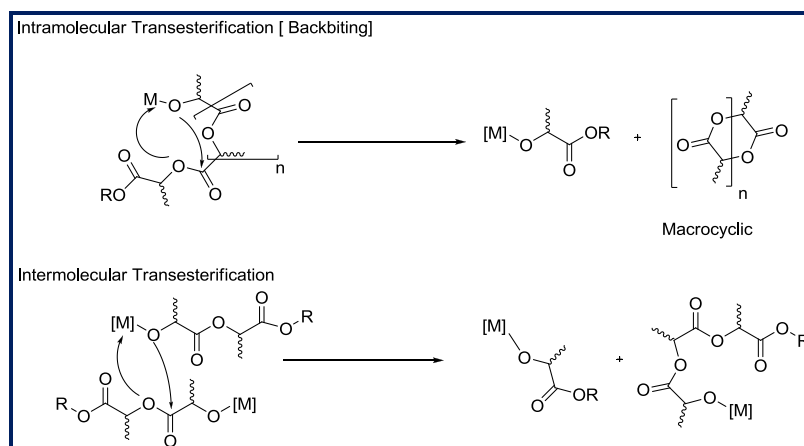


Figure 3.7. MALDI-TOF mass spectrum of PLLA prepared using $1\text{-Ti}(\text{O}^i\text{Pr})_2$ in toluene solution at 70°C .



Scheme 3.4. Transesterification side reactions by coordination insertion mechanism.

A Poly(*rac*-lactide) produced with the initiator $1\text{-Ti}(\text{O}^i\text{Pr})_2$ with a monomer to initiator ratio of 50 in solution (toluene) at 70°C , was analyzed by MALDI-TOF-mass spectrometry (Figure 3.8). The expanded portion of the spectrum shows well resolved signals. Peaks with a difference in mass of ($\Delta m/z = 144$ Da) was observed which corresponds to one lactide monomer unit $[\text{C}(\text{O})\text{CH}(\text{Me})\text{C}(\text{O})\text{CH}(\text{Me})]$ clustered with a Na^+ ion and polymer chains terminated by isopropyl ester and $-\text{OH}$ end groups (red circle). Other peaks with a difference in mass of ($\Delta m/z = 72$ Da) (black circle) are also present and correspond to a repeating unit of $[\text{C}(\text{O})\text{CH}(\text{Me})]$ indicating that intermolecular transesterification side reactions occur to a significant degree during polymerization (Scheme 3.4). Two other minor set of peaks with a difference in mass of ($\Delta m/z = 60$ Da) are observed and are due to the formation of macrocyclic polymer from backbiting reactions either from the expected population or the transesterified one (green circles). As compare to the *L*-lactide polymerization, more side reactions occur in the polymerization of *rac*-lactide under this polymerization condition.

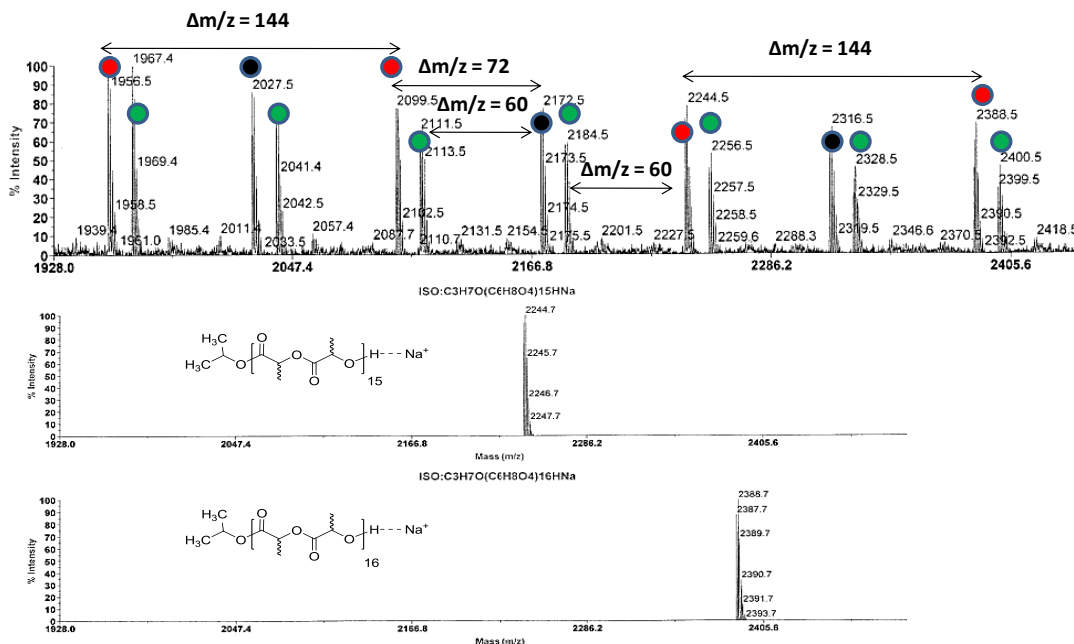
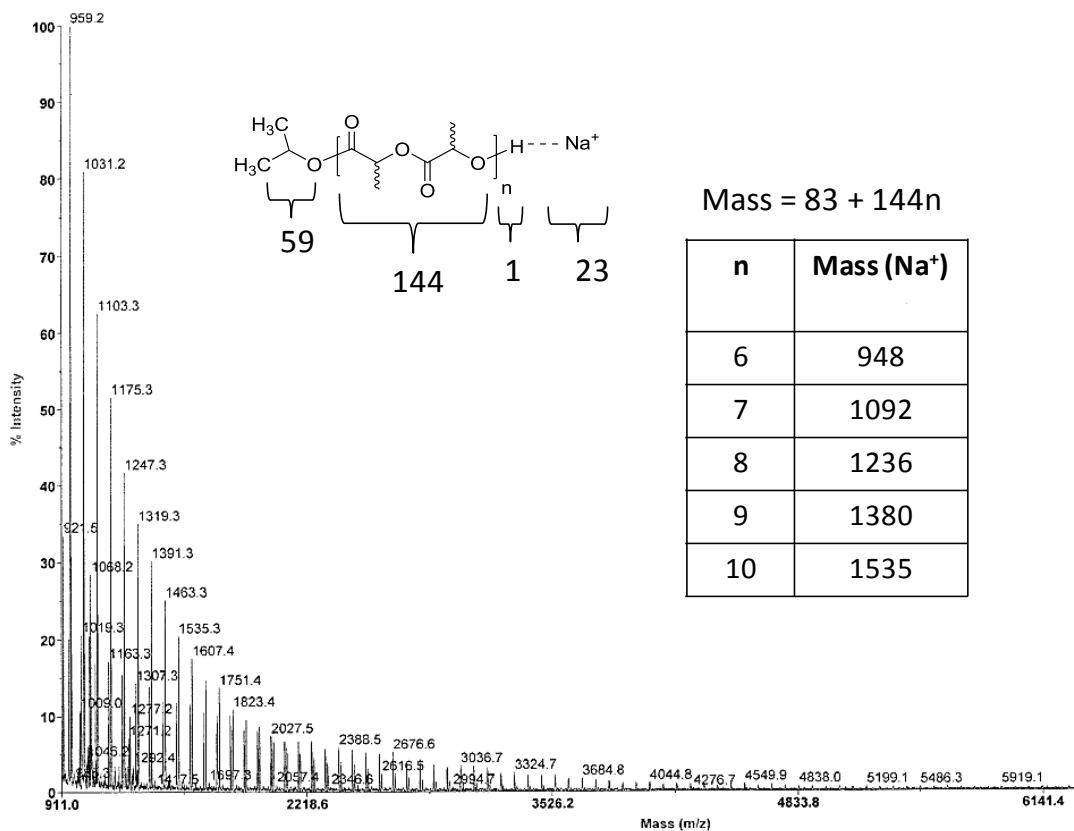


Figure 3.8. MALDI-TOF mass spectrum of PDLLA prepared using 1-Ti(OⁱPr)₂ in toluene solution at 70°C with [M]/[Ti] = 50.

3.2.1.2.4. DSC analysis of PLLA and PDLLA

Thermal analysis of the Poly(*L*-LA) and Poly(*rac*-LA) was carried out by means of differential scanning calorimetry (DSC), in the range of temperature -100 to 200°C. As an illustration, the DSC thermograms obtained during the second heating cycle of PLLA and PDLLA are shown in Figure 3.9. PLLA shows a glass transition temperature (T_g) at 45°C, a crystallization temperature (T_c) at 82°C and a melting temperature (T_m) at 145°C, which is consistent with the formation of optically pure semicrystalline PLLA. For PDLLA, only a glass transition temperature at 47°C is observed consistent with the formation of amorphous atactic polymer.

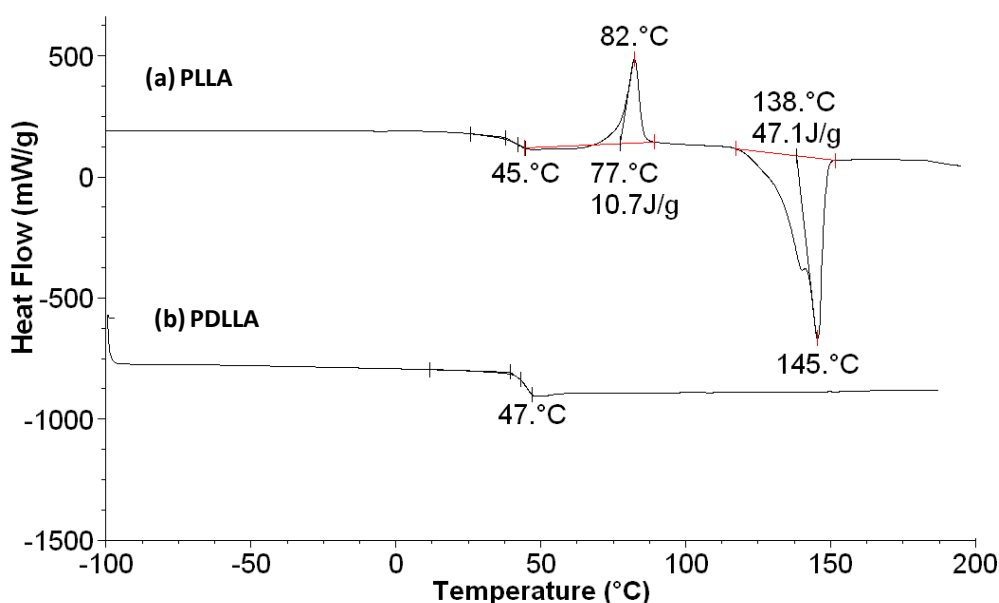
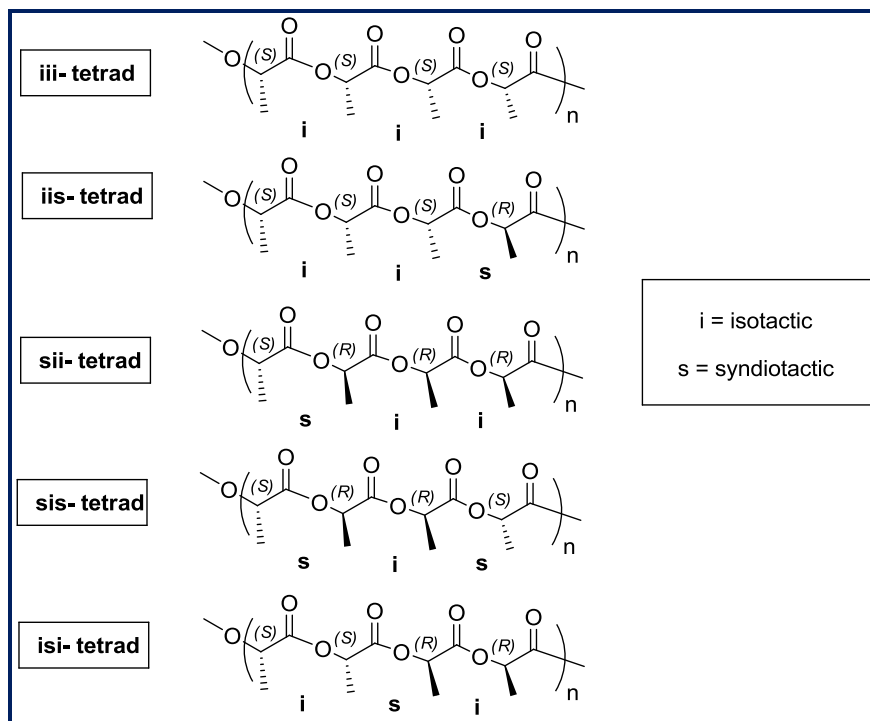


Figure 3.9. DSC thermograms of (a) PLLA and (b) PDLLA prepared using 1-Ti(OⁱPr)₂ in toluene at 70°C with [M]/[Ti] = 100.

3.2.1.2.5. Stereoselectivity of *rac*-LA polymerization with 1-4-Ti(OⁱPr)₂ complexes

In recent years, some group 4 metal complexes derived from multidentate ligands of type N_xO_y (X = Y = 2; X = 1, Y = 2, 3) have been reported to be efficient catalysts for stereocontrolled ring opening polymerization (ROP) of (*rac*-LA).^{20, 24, 25, 27} On the basis of these observations, we anticipated that the titanium complexes derived from the enantiomerically pure, *racemic*, *meso*, and *diastereomeric* mixture of aminodiol ligand of type (X = 1, Y = 2) might be capable of stereochemical control in the polymerization of *rac*-lactide.

According to Bernoullian statistics, PLA derived from the *rac*-lactide can possess five tetrad stereosequences in relative ratios determined by the ability of the catalyst to control *racemic* dyad [$r = s$ dyad; “*r*” stands for *racemic*, “*s*” stands for *syndiotactic*] and *meso* dyad [$m = i$ dyad; “*m*” stands for *meso*, “*i*” stands for *isotactic*] connectivity of the monomer units along the polymer chain (Scheme 3.5, Table 3.3).⁴²



Scheme 3.5. Structures of possible tetrads of Poly(*rac*-lactide).

Table 3.3. Tetrad Probabilities of PDLLA based on Bernoullian Statistics.⁴²

tetrad	probability
[iii]	$P_i^2 + P_i P_s/2$
[iis]	$P_i P_s/2$
[sii]	$P_i P_s/2$
[sis]	$P_s^2/2$
[isi]	$(P_s^2 + P_i P_s)/2$

Stereochemical microstructure of the polymers obtained from *rac*-lactide with the initiators 1-4-Ti(O^{*i*}Pr)₂ is achieved through the inspection of methine and carbonyl region of ¹³C NMR of the polymers (Figure 3.10). Tetrads and Hexads stereosequences were identified using Kasperczyk’s assignments.⁴³

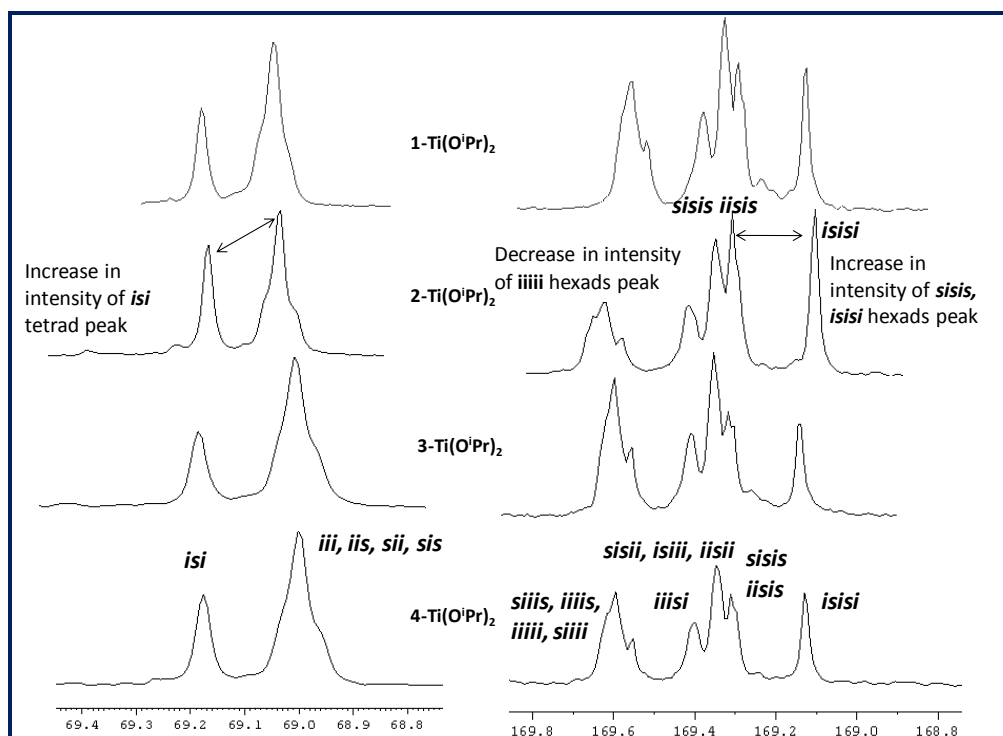


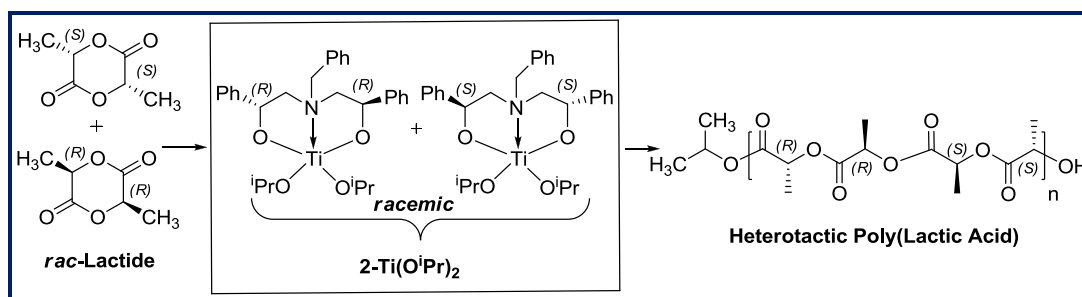
Figure 3.10. $^{13}\text{C}\{^1\text{H}\}$ NMR spectrum of the methine and carbonyl region of PDLLA obtained by using 1-4- $\text{Ti}(\text{O}^i\text{Pr})_2$ at 70°C in toluene.

As seen from Figure 3.10. The methine carbon region in the spectrum exhibits two different lines which corresponds to five different tetrads (*isi*, *iii*, *iis*, *sii*, *sis*) resulting from the pair addition of enantiomers of lactide molecules. Relative intensity between the two resonance is the same for the polymer obtained from the initiators 1- $\text{Ti}(\text{O}^i\text{Pr})_2$, 3- $\text{Ti}(\text{O}^i\text{Pr})_2$, 4- $\text{Ti}(\text{O}^i\text{Pr})_2$. However, a slight increase of the *isi* tetrad peak intensity was observed for the polymer obtained from the initiator 2- $\text{Ti}(\text{O}^i\text{Pr})_2$. This could be due to a better alternative addition of *D* and *L*- lactide with this complex (Scheme 3.6).

The carbonyl region of the NMR spectrum exhibits several lines which correspond to 11 different hexads. Again, an increase in intensities of two hexads peak (*isisi*, *sisis*) is seen accompanied by the decrease in the intensities of the lines due to the remaining hexads for the polymer obtained with 2- $\text{Ti}(\text{O}^i\text{Pr})_2$ as compared to the other initiators. A non typical increase in the intensities of two lines in the methine and carbonyl region of the ^{13}C NMR spectrum suggests a possibility of non-Bernouillian statistics and stereoselection occurred during the polymerization of *rac*-lactide in the presence of 2- $\text{Ti}(\text{O}^i\text{Pr})_2$ as initiator. Kasperczyk reported that LiO^iBu produces the similar results and suggested the formation of predominantly heterotactic PLA from *rac*-lactide.⁴³

Determination of the stereochemical microstructures of the polymers is also achieved through the inspection of the methine region of homonuclear decoupled ^1H NMR spectra of the polymers,⁴⁴⁻⁴⁶ since ^1H NMR spectrum of PLA has a significantly better signal to noise ratio as compared to the ^{13}C NMR and can thus provide better values for quantification of stereosequence probabilities. The homonuclear decoupled ^1H NMR spectrum of PLA obtained with the initiator $2\text{-Ti}(\text{O}^i\text{Pr})_2$ is shown in Figure 3.11. The two resonance peak corresponding to *sis* and *isi* tetrads appear more intense compare to the other tetrads, signifying the formation of heterotactic sequences which contain alternating pairs of stereogenic centers in the main chain (Scheme 3.6).

The probability of the heterotactic enchainment can be calculated from the equations derived from the tetrad probabilities based on Bernoullian statistics (Table 3.3) and it was found to be ($P_r = P_s = 0.65$). It indicates that the probability of a (*R,R*)-lactide unit to be enchainned after a (*S,S*)-lactide unit (or vice versa) is 65% and it also revealed that the complex $2\text{-Ti}(\text{O}^i\text{Pr})_2$ exerts a significant influence on the tacticity of the growing polymer chain.



Scheme 3.6. Preparation of Heterotactic PLA using the catalyst $2\text{-Ti}(\text{O}^i\text{Pr})_2$ in toluene at 70°C .

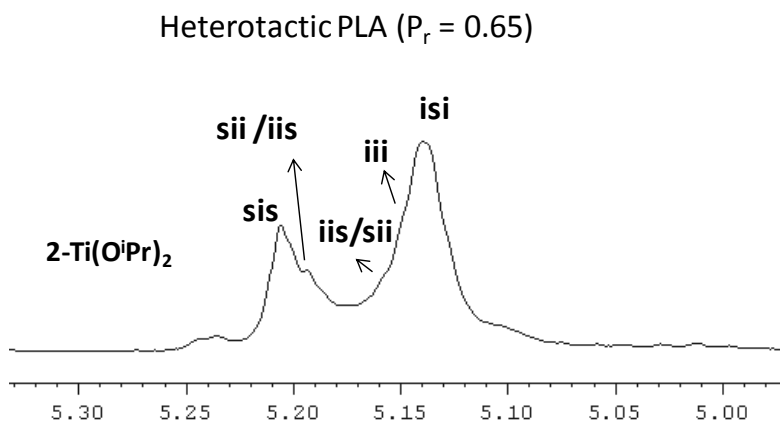


Figure 3.11. Homonuclear decoupled ^1H NMR spectrum of the methine region of PDLLA prepared with $2\text{-Ti}(\text{O}^i\text{Pr})_2$ at 70°C .

Calculation of $P_r = P_s$ (Probability of *racemic* or *disyndiotactic* linkage)

$$[\text{sis}] = \frac{[\text{sis}]}{[\text{sis}] + [\text{iii}] + [\text{isi}] + [\text{iis/sii}] + [\text{sii/iis}]}$$

$$[\text{sis}] = \frac{0.3}{1.4} = 0.21$$

Applying Bernoullian equation,

$$[\text{sis}] = P_s^2 / 2 \quad [\text{sis}] = \text{Intensity observed from the NMR}$$

$$0.21 = P_s^2 / 2$$

$$P_s = 0.65$$

Homonuclear decoupled NMR spectrum of the polymers obtained with all other complexes 1-Ti(OⁱPr)₂ ($P_r = 0.58$), 3-Ti(OⁱPr)₂ ($P_r = 0.5$) and 4-Ti(OⁱPr)₂ ($P_r = 0.58$) shows a five line peaks which corresponds to *isi*, *iii*, *iis/sii*, *sii/iis*, *sis* tetrads signifying the formation of atactic polymers with random placement of either (*R,R*) and (*S,S*) stereosequences in the polymer main chain (Figure 3.12).

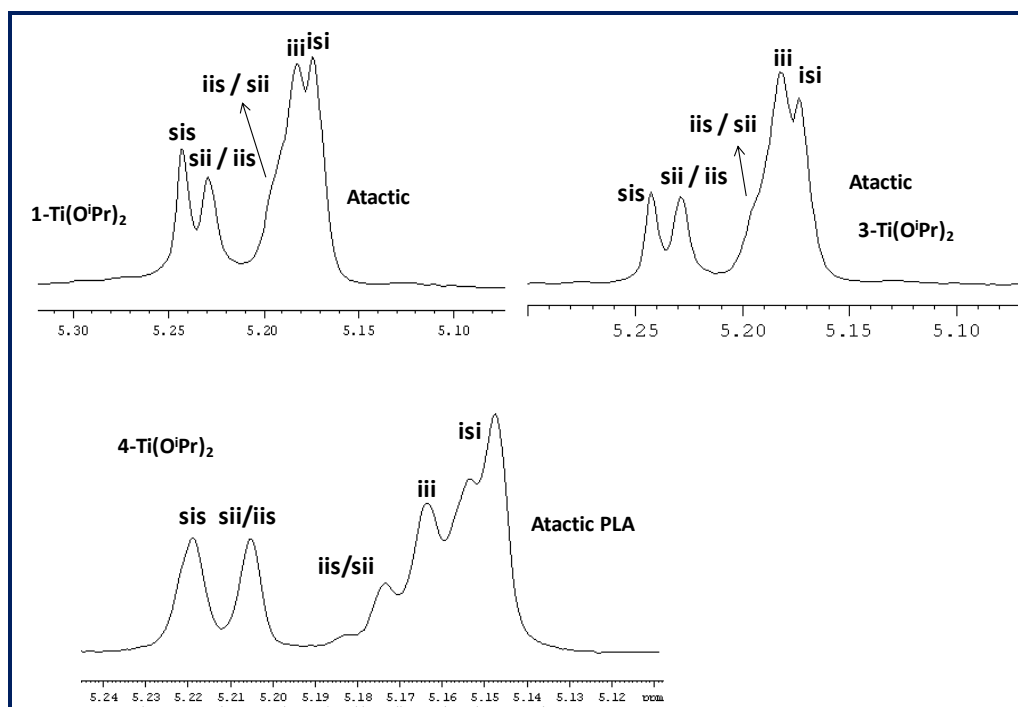


Figure 3.12. Homonuclear decoupled ¹H NMR spectrum of the methine region of PDLLA prepared with 1, 3 & 4-Ti(OⁱPr)₂ at 70°C.

These results suggest that the mixture of two different chiral ligand (*R,R*) and (*S,S*) present in the *racemic* complex 2-Ti(OⁱPr)₂ significantly may influence the heterotactic selectivity, while all other complexes containing enantiomerically pure, *meso*, *diastereomeric* ligand does not influence the stereoselectivity. A possible explanation of enhancement in stereocontrol in case of complex 2-Ti(OⁱPr)₂ compare to other complexes can be due to structural differences in their metal complexes. The difference in selectivity between these complexes suggests that the chirality of the ligand is unimportant, while the growing polymer chain is a significant factor in stereocontrol during polymerization (i.e. if a chain end of *R* stereochemistry selects (*S,S*)-lactide or vice versa forms heterotactic PLA). To the best of our knowledge, among group 4 metal complexes only very few titanium complexes have been reported as efficient initiators for the formation of heterotactic-rich polylactide (PLA) compare to the zirconium and hafnium complexes.^{20, 24, 25, 27} Even polymerization of *rac*-LA initiated with a titanium complex bearing a chiral ligand affords atactic PLA.⁴⁷ From these results, we speculate that the stereoselective polymerization of *rac*-lactide can operate through chain end control mechanism and not site control mechanism.

3.2.1.3. Kinetic studies of *L* / *rac*-lactide polymerization

The kinetics of *L* and *rac*-LA polymerization was investigated in toluene solution at 70°C using the initiator 1-Ti(OⁱPr)₂ with a monomer to initiator ratio of 300. Figures 3.13 & 3.14 show the semi-logarithmic plots of $\ln([LA]_0/[LA]_t)$ versus reaction time for *L*- and *rac*-LA polymerization respectively. $[LA]_0$ is the initial monomer concentration and $[LA]_t$ is the monomer concentration at a given time. The first order kinetic plot of both *L*-LA and *rac*-LA polymerization shows a short induction period of 60-70 min, prior to which no significant polymerization occurs. This can be seen from the Figures 3.13 & 3.14, with extrapolation back to 0% monomer conversion. Similar kind of induction periods have been observed for other LA polymerization initiators notably Al(OⁱPr)₃,⁴⁸ β-diketimate tin(II)-based initiators,⁴⁹ titanium salen initiator,²⁵ sulfonamide supported titanium initiator.⁵⁰ The induction period observed in our catalytic system can be similar to those observed for β-diketimate tin(II)-based initiator, where the introduction of the first lactide unit into one of the Ti-OⁱPr bonds leads to an intermediate transition state followed by a polymerization process that is first order with respect to the monomer concentration.

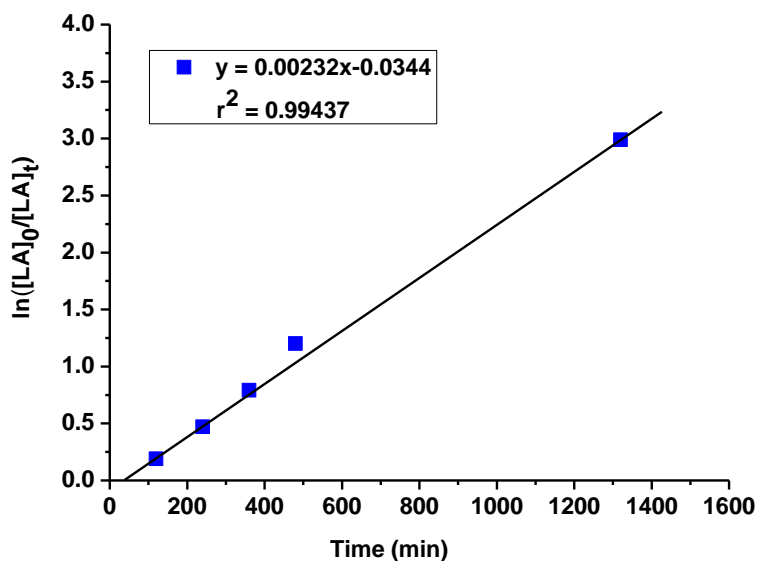


Figure 3.13. First order kinetic plot for *L*-LA consumption vs time using 1-Ti(OⁱPr)₂^a

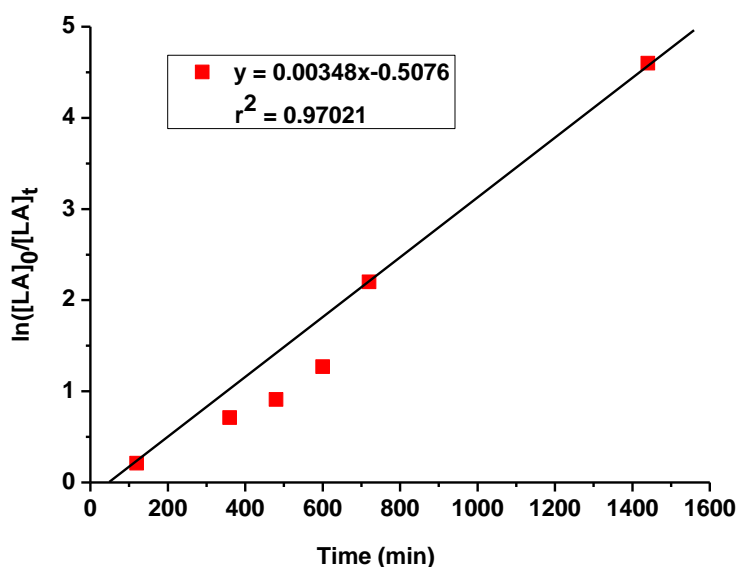


Figure 3.14. First order kinetic plot for *rac*-LA consumption vs time using 1-Ti(OⁱPr)₂^a

^a Polymerization conditions: [M]/[Ti]= 300, 15 mL of toluene, 70°C, 0.2 mL of aliquots was taken at the given intervals. [LA]₀ is the initial concentration of LA and [LA]_t the concentration at time t.

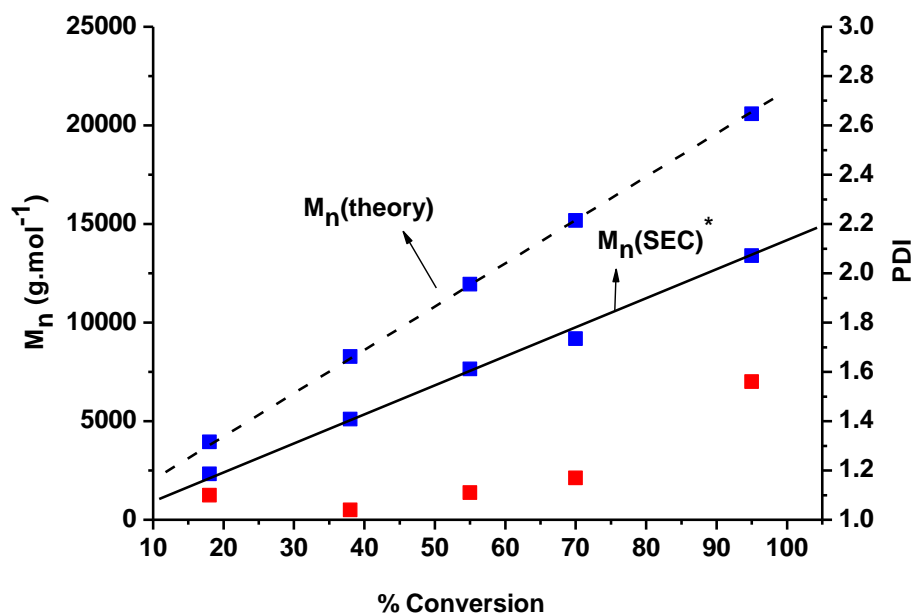
From the slope of the plots, the value of the apparent rate constant (K_{app}) for polymerization of *L*-LA and *rac*-LA were found to be $2.32 \times 10^{-3} \text{ min}^{-1}$ and $3.48 \times 10^{-3} \text{ min}^{-1}$ respectively. This would suggest that polymerization of *L*-LA proceeds at a rate approximately 1.5 times slower than the polymerization of *rac*-LA. The apparent rate of propagation (K_{app}) observed with 1-Ti(OⁱPr)₂ are compared with titanium salen complexes and the values are shown in Table 3.4.

Table 3.4. First Order Propagation Rate Constant (K_{app}) for *L* / *rac*-LA (ROP)

Catalyst	Monomer	$K_{app}(\text{min})^{-1}$	[M]/[I] ; Temp(°C); toluene	ref
Ti(Salen)(O ⁱ Pr) ₂	<i>rac</i> -LA	2.2×10^{-3}	100; 80°C	40
Ti(Salen)(O ⁱ Pr) ₂	<i>L</i> -LA	3.7×10^{-3}	100; 70°C	25
1-Ti(O ⁱ Pr) ₂	<i>rac</i> -LA	3.5×10^{-3}	300; 70°C	-
1-Ti(O ⁱ Pr) ₂	<i>L</i> -LA	2.3×10^{-3}	300; 70°C	-

A plot of M_n values obtained from (SEC)* (values obtained after Mark-Houwink correction factor of 0.58) and M_n (theory) versus % conversion for the polymerization of *L*-LA and *rac*-LA is shown in Figure 3.15 and 3.16 respectively. For both monomers, the M_n values observed from the SEC increase linearly with respect to the monomer conversion indicating that polymerization is well controlled. However the molar mass determined by (SEC)* shows lower value than theoretical ones.

For *L*-LA polymerization, molecular weight distribution observed from the SEC remained very narrow (PDI = 1.1-1.17) until 70% monomer conversion, whereas at higher monomer conversion broader molecular weight distribution was observed (Figure 3.15) which may be due to transesterification side reactions. For *rac*-LA polymerization, the molecular weight distribution remained very narrow (PDI = 1.05 -1.25) even at high monomer conversion (Figure 3.16).

**Figure 3.15.** Plots of $M_n(\text{theory})$, $M_n(\text{SEC})^*$ and PDI vs conversion for the polymerization of *L*-LA using catalyst 1-Ti(OⁱPr)₂.

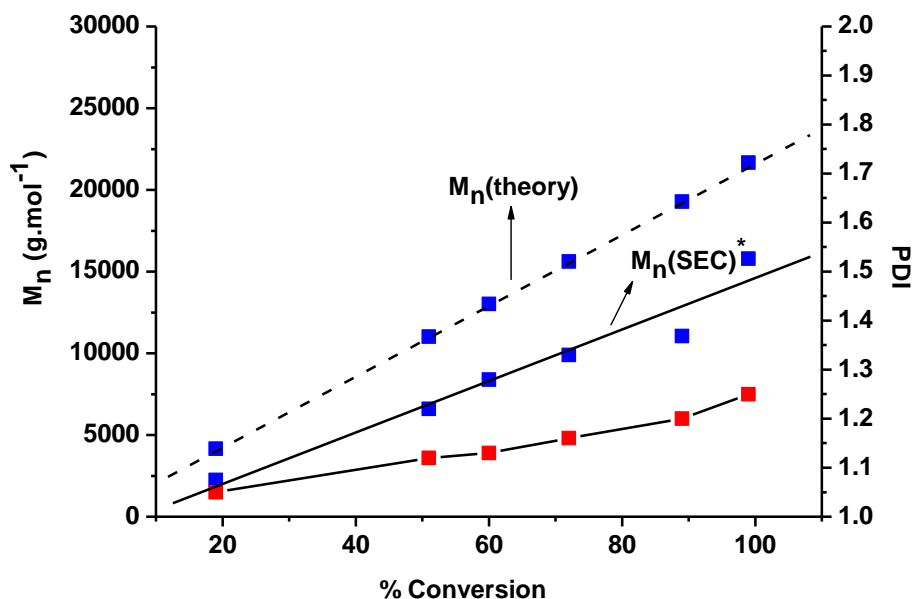


Figure 3.16. Plots of $M_n(\text{theory})$, $M_n(\text{SEC})^*$ and PDI vs conversion for the polymerization of *rac*-LA using catalyst 1-Ti(OⁱPr)₂.

3.2.2. Bulk Polymerization

All complexes were also tested for the polymerization of *L*-LA and *rac*-LA under industrially preferred bulk conditions at 130°C in the absence of solvent with a monomer to initiator ratio of 300. Results are summarized in Table 3.5 & 3.6 respectively.

Table 3.5. Bulk Polymerization of *L*-Lactide ^a

Entry	Catalyst	Conv (%) ^b	M_n (NMR) ^c (g.mol ⁻¹)	M_n (theory) ^d (g.mol ⁻¹)	M_n (SEC) ^e (g.mol ⁻¹)	M_n (SEC) ^f (g.mol ⁻¹)	PDI ^e
1	1-Ti(O ⁱ Pr) ₂	47	13260	10220	21700	12590	1.38
2	2-Ti(O ⁱ Pr) ₂	92	22460	19890	22190	12870	1.33
3	3-Ti(O ⁱ Pr) ₂	58	14690	12590	15400	8930	1.13
4	4-Ti(O ⁱ Pr) ₂	72	16620	15620	27570	15990	1.32

^a Polymerization conditions: 1g of (*L* - LA), temperature = 130°C, [M]/[Ti] = 300, polymerization time = 30 min. ^b Conversion determined by ¹H NMR via the integration of the methine resonance peak of LA and the polymer. ^c Calculated from ¹H NMR (CDCl₃) analysis by integration of the end group of the isopropoxide at 1.24 ppm and the backbone resonance at 5.1 ppm. ^d $M_n(\text{theory})$ was calculated from the formula ((M.W of LA) × (conversion / 100) × [LA]) / 2×[Ti] + 60. ^e Determined from SEC (in THF) relative to polystyrene standards. ^f Determined from SEC (in THF) relative to polystyrene standards and corrected by Mark-Houwink correction factor of 0.58.³²

All complexes were found to be efficient initiators for the polymerization of *L*-LA in bulk condition. 92% monomer conversion was reached within 30 min for the complex 2-Ti(OⁱPr)₂ with relatively narrow molecular weight distribution (PDI = 1.33) indicative of well controlled polymerization even under these drastic conditions. Other complexes revealed less active. The difference in activity among these complexes 1-4-Ti(OⁱPr)₂ is not clear to understand. It may be due to the non homogenous reaction conditions (the mixture becomes viscous in 10 min and stirring stopped) as compared to the solution polymerization condition. The M_n (NMR) and M_n (SEC)^f obtained after applying the correction factor show reasonably good agreement with the calculated M_n (theory) for all the entries in Table 3.5. On the basis of the molecular weight observed for the polymer, we believed that two ⁱPrO⁻ groups could be involved in the initiation as in the case of solution polymerization conditions.

The activity of the complex 2-Ti(OⁱPr)₂ for the polymerization of *L*-LA in bulk condition (92% conversion within 30 min) was found to be higher than that of few titanium complexes reported earlier in the literature under the same polymerization conditions. For example, titanatranes complexes produced PLA with 99% monomer conversion in 24 h at 130°C.¹⁹ Titanium complexes derived from triethanolamine ligands produced PLA with 81% yield in 24 h with [M]/[Ti] ratio of 300 at 130°C.²⁰ Amine-phenolate titanium complexes produced polymer with 55% yield in 26 h under the same polymerization condition.²³ Titanium salan complexes are able to produce PLA with 89% yield in 6 h.⁵¹ However the activity of the complex 2-Ti(OⁱPr)₂ were comparable to the tetranuclear titanium complexes which produced PLA in 94% yield within 30 min with [M]/[Ti] ratio of 300 at 130°C.³³

Table 3.6. Bulk Polymerization of *rac*-Lactide ^a

Entry	Catalyst	Conv (%) ^b	M _n (NMR) ^c (g.mol ⁻¹)	M _n (theory) ^d (g.mol ⁻¹)	M _n (SEC) ^e (g.mol ⁻¹)	M _n (SEC) ^f (g.mol ⁻¹)	PDI ^e	P _r ^g
1	1-Ti(O ⁱ Pr) ₂	94	13060	13600	18520	10740	1.38	0.50
2	2-Ti(O ⁱ Pr) ₂	91	13100	13160	11800	7630	1.63	0.37
3	3-Ti(O ⁱ Pr) ₂	98	14460	14170	26820	15550	1.51	0.46
4	4-Ti(O ⁱ Pr) ₂	94	14270	13600	10420	6040	1.29	0.50

^a Polymerization conditions: 1g of (*DL*-LA), T = 130°C, [M]/[Ti] = 300, polymerization time = 30 min.

^b Conversion determined by ¹H NMR *via* the integration of the methine resonance peak of LA and the polymer. ^c Calculated from ¹H NMR analysis by integration of the end group of the isopropoxide at 1.24 ppm and the backbone resonance at 5.1 ppm. ^d M_n (theory) was calculated from the formula ((M.W of LA) × (conversion / 100) × [LA]) / 2×[Ti] + 60. ^e Determined from SEC (in THF) relative to polystyrene standards. ^f Determined from SEC (in THF) relative to polystyrene standards and corrected by Mark-Houwink correction factor of 0.58.³² ^g P_r (probability of *racemic* linkage) calculated from ¹H Homonuclear decoupled NMR analysis.

For the polymerization of *rac*-LA (proper stirring is maintained in the polymerization mixture within the time period as compare to *L*-LA polymerization), all complexes were found to be efficient initiators. Excellent conversion was reached (91-98%) within 30 min with relatively narrow molecular weight distribution (1.29-1.63) under these polymerization conditions. Molecular weights evaluated by NMR and SEC (corrected values) are in good agreement with the theoretical ones (calculated on the assumption of two chains per metal center) for complexes 1 and 3-Ti(O^{*i*}Pr)₂, whereas molar mass (corrected values) from SEC for the polymer obtained from the complexes 2 and 4-Ti(O^{*i*}Pr)₂ is found to be lower than the theoretical ones.

As for *L*-LA, activity of these complexes was found to be higher than the previously reported titanium complexes for *rac*-LA polymerization in bulk condition. Titanatranes complexes produced PLA with 93% yield with [M]/[Ti] ratio of 300 in 2 h at 130°C.²⁰ Amine tris(phenolate) titanium complexes gave up to 95% monomer conversion in 2 h under the same polymerization condition.³⁹ Amine bisphenolate titanium complexes produced PLA up to 75% conversion in 2 h with [M]/[Ti] mole ratio of 300 at 130°C.²⁴ However, the activity of our complexes is comparable to the tetra nuclear titanium complexes which gave polymer with 92% yield in 30 min.³³ Chiral Schiff base titanium complexes also produced PLA (95% conversion in 30 min with [M]/[Ti] = 300 at 130°C).⁵² Indeed recently reported salalen based titanium complexes were found to be more active (95% conversion in 15 min with [M]/[Ti] = 300 at 130°C).⁴⁰

As in the case of solution polymerization the stereochemical microstructure of the polymers obtained from *rac*-lactide with the initiators 1-4-Ti(O^{*i*}Pr)₂ is achieved through the inspection of methine and carbonyl region of ¹³C NMR of the polymers (Figure 3.17). From these spectra, we observe that the relative intensity of the peaks corresponding to tetrads and hexads stereosequences was found to be same for polymers obtained with all the complexes.

Homonuclear decoupled NMR spectrum presented in Figure 3.18, also revealed that all complexes produced a five line peaks which corresponds to *isi*, *iii*, *iis* / *sii*, *sii* / *iis*, *sis* tetrads and also the calculated (*P_r*) values were shown to be less than 0.5 for all the complexes (Table 3.6) indicating the formation of atactic polymers. To the best of our knowledge very few titanium complexes reported in the literature produced moderate heterotactic PLA under melt polymerization condition, all other complexes produced only atactic PLA.^{19, 20, 24, 27, 28, 52}

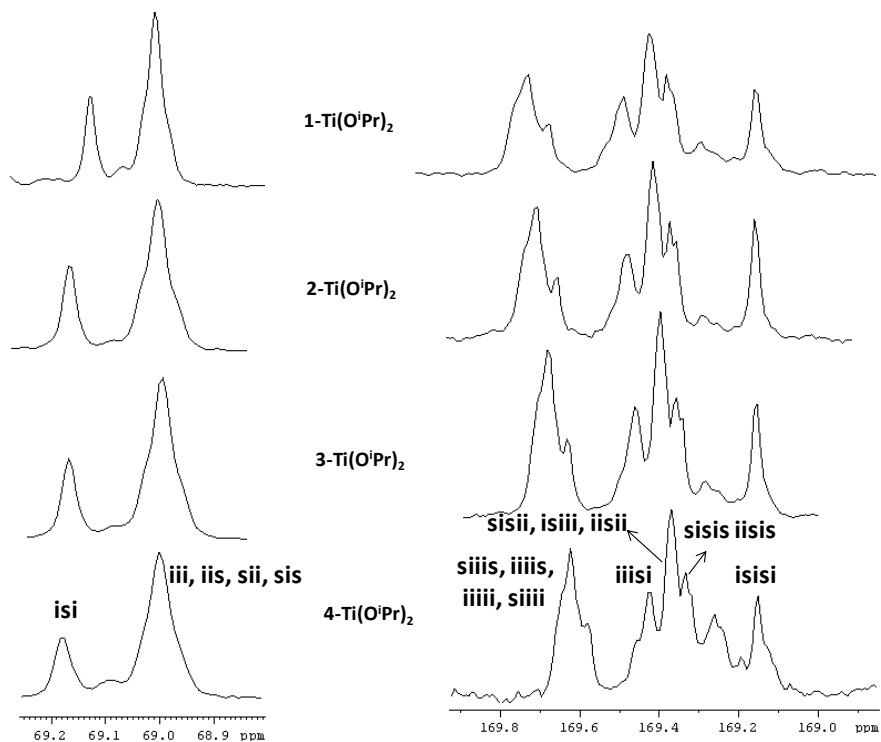


Figure 3.17. $^{13}\text{C}\{^1\text{H}\}$ NMR spectrum of the methine and carbonyl region of PDLLA obtained by using 1-4- $\text{Ti}(\text{O}^i\text{Pr})_2$ at 130°C .

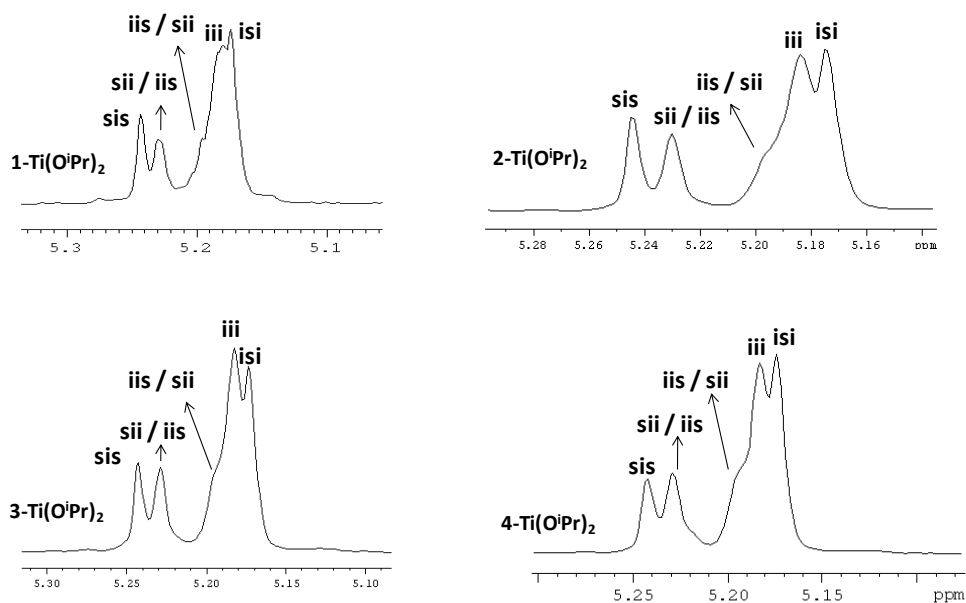


Figure 3.18. Homonuclear decoupled ^1H NMR spectrum of the methine region of PDLLA prepared with 1-4- $\text{Ti}(\text{O}^i\text{Pr})_2$ at 130°C .

3.3. Conclusion

A series of titanium complexes 1-4-Ti(OⁱPr)₂ were tested as initiator for the ring opening polymerization of *L*-LA and *rac*-LA in solution (toluene) at 70°C and bulk conditions at 130°C. All complexes were found to be efficient initiators under both solution and bulk conditions, producing polymers with controlled molecular weights and molecular weight distributions. The activity of these complexes is higher in bulk polymerization (> 95% conversion is achieved within 30 min). To the best of our knowledge only very few titanium complexes were reported in the literature with such high performances.

End group of the polymer were analyzed by ¹H & ¹³C NMR spectrometry and MALDI-TOF mass spectrometry and are in agreement with the insertion of the monomer into the Ti-OⁱPr bond through coordination insertion mechanism with two chains per metal center. Polymerization kinetic studies reveal the “living” nature of the catalyst.

Concerning the stereoselective polymerization of *rac*-lactide, the complex 2-Ti(OⁱPr)₂ could be able to produce heterotactic PLA (*P_r* = 0.65) in solution polymerization condition and atactic PLA in bulk condition. All other complexes produced only atactic PLA either in bulk or in solution polymerization condition. Surprisingly, complex 1-Ti(OⁱPr)₂ derived from an enantiomerically pure ligand does not show any stereoselectivity under both solution and bulk conditions. From this observation, we speculate that the origin of stereocontrol with racemic catalyst could be due to the chain end control mechanism. These results also suggest that the structure of the complex played a key role in stereoselectivity of *rac*-lactide polymerization.

3.4. References

- [1] Auras, R.; Harte, B.; Selke, S. *Macromol. Biosci.* **2004**, 4, 835.
- [2] Rasal, R. M.; Jonorkar, A. V.; Hirt, D. E.; *Prog. Polym. Sci.* **2010**, 35, 338.
- [3] Dechy-Cabaret, O.; Martin-Vaca, B.; Bourissou, D. *Chem. Rev.*, **2004**, 104, 6147.
- [4] Platel, R. H.; Hodgson, L. M.; Williams, C. K. *Polym. Rev.*, **2008**, 48, 11.
- [5] Thomas, C. M.; *Chem. Soc. Rev.* **2010**, 39, 165.
- [6] Spassky, N.; Wisniewski, M.; Pluta, C.; LeBorgne, A. *Macromol.Chem.Phys.* **1996**, 197, 2627.
- [7] Zhong, Z. Y.; Dijkstra, P. J.; Feijen, J. *Angew.Chem. Int. Ed.* **2002**, 41, 4510.
- [8] Zhong, Z. Y.; Dijkstra, P. J.; Feijen, J. *J. Am. Chem. Soc.* **2003**, 125, 11291.
- [9] Ishii, R.; Nomura, N.; Kondo, T. *Polym. J. (Tokyo)* **2004**, 36, 261.
- [10] Hormnirun, P.; Marshall, E. L.; Gibson, V. C.; White, A. J. P.; Williams, D. J. *J. Am. Chem. Soc.* **2004**, 126, 2688.
- [11] Marshall, E. L.; Gibson, V. C.; Rzepa, H. S. *J. Am. Chem. Soc.* **2005**, 127, 6048.
- [12] Cheng, M.; Attygalle, A. B.; Lobkovsky, E. B.; Coates, G. W. *J. Am. Chem. Soc.* **1999**, 121, 11583.
- [13] Chisholm, M. H.; Eilerts, N. W.; Huffman, J. C.; Iyer, S. S.; Pacold, M.; Phomphrai, K. *J. Am. Chem. Soc.* **2000**, 122, 11845.
- [14] Chisholm, M. H.; Gallucci, J.; Phomphrai, K. *Chem. Commun.* **2003**, 48.
- [15] Ovitt, T. M.; Coates, G. W. *J. Am. Chem. Soc.* **1999**, 121, 4072.
- [16] Ovitt, T. M.; Coates, G. W. *J. Polym. Sci., Part A: Polym. Chem.* **2000**, 38, 4686.
- [17] Ovitt, T. M.; Coates, G. W. *J. Am. Chem. Soc.* **2002**, 124, 1316.
- [18] Chamberlain, B. M.; Cheng, M.; Moore, D. R.; Ovitt, T. M.; Lobkovsky, E. B.; Coates, G. W. *J. Am. Chem. Soc.* **2001**, 123, 3229.
- [19] Kim, Y.; Verkade, J. G. *Organometallics.* **2002**, 21, 2395.
- [20] Kim, Y.; Jnaneshwara, G. K.; Verkade, J. G. *Inorg. Chem.* **2003**, 42, 1437.
- [21] Dobrzynski, P. *J. Polym. Sci., Part A: Polym. Chem.* **2004**, 42, 1886.
- [22] Russell, S. K.; Gamble, C. L.; Gibbins, K. J.; Juhl, K. C. S.; Mitchell, W. S.; Tumas, A. J.; Hofmeister, G. E. *Macromolecules.* **2005**, 38, 10336.
- [23] Gendler, S.; Segal, S.; Goldberg, I.; Goldschmidt, Z.; Kol, M. *Inorg. Chem.* **2006**, 45, 4783.
- [24] Chmura, A. J.; Davidson, M. G.; Jones, M. D.; Lunn, M. D.; Mahon, M. F.; Johnson, A. F.; Khunkamchoo, P.; Roberts, S. L.; Wong, S. S. F. *Macromolecules.* **2006**, 39, 7250.
- [25] Gregson, C. K. A.; Blackmore, I. J.; Gibson, V. C.; Long, N. J.; Marshall, E. L.; White, A. J. P.; *Dalton Trans.* **2006**, 3134.
- [26] Atkinson, R. G. J.; Gerry, K.; Gibson, V. C.; Marshall, E. L.; West, L. J. *Organometallics.* **2007**, 27, 316.
- [27] Chmura, A. J.; Davidson, M. G.; Frankis, C. J.; Jones, M. D.; Lunn, M. D. *Chem. Commun.* **2008**, 1293.
- [28] Zelikoff, A. L.; Kopilov, J.; Goldberg, I.; Coates, G. W.; Kol, M. *Chem. Commun.* **2009**, 6804.
- [29] Sergeeva, E.; Kopilov, J.; Goldberg, I.; Kol, M. *Inorg. Chem.* **2010**, 49, 3977.
- [30] Manivannan, R.; Sundararajan, G. *Macromolecules.* **2002**, 35, 7883.

- [31] Piskun, Y. A.; Vasilenko, I. V.; Kostjuk, S. V.; Zaitsez, K. V.; Zaitseva, G. S.; Karlov, S. *J. Polym. Sci., Part A: Polym. Chem.* **2010**, 48, 1230.
- [32] Kowalski, A.; Duda, A.; Penczek, S. *Macromolecules.* **1998**, 31, 2114.
- [33] Kim, Y.; Verkade, J. G. *Macromol. Rapid Commun.* **2002**, 23, 917.
- [34] Kim, Y.; Verkade, J. G. *Macromol. Symp.* **2005**, 224, 105.
- [35] Bonnet, F.; Cowley, A. R.; Mountford, P. *Inorg. Chem.* **2005**, 44, 9046.
- [36] Ma, H.; Okuda, J. *Macromolecules.* **2005**, 38, 2665.
- [37] Wang, J.; Yao, Y.; Zhang, Y.; Shen, Q. *Inorg. Chem.* **2009**, 48, 744.
- [38] Schwarz, A. D.; Herbert, K. R.; Paniagua, C.; Mountford, P. *Organometallics.* **2010**, 29, 4171.
- [39] Whitelaw, E. L.; Jones, M. D.; Mahon, M. F.; Kociok-Kohn, G. *Dalton Trans.* **2009**, 9020.
- [40] Whitelaw, E. L.; Jones, M. D.; Mahon, M. F. *Inorg. Chem.* **2010**, 49, 7176.
- [41] Williams, C. K.; Breyfogle, L. E.; Choi, S. K.; Nam, W.; Young, V. G.; Hillmyer, M. A.; Tolman, W. B. *J. Am. Chem. Soc.* **2003**, 125, 11350.
- [42] Bovey, F. A.; Mirau, P. A. *NMR of Polymers*; Academic Press: San Diego, **1996**.
- [43] Kasperczyk, J. E. *Macromolecules.* **1995**, 28, 3937.
- [44] Thakur, K. A. M.; Kean, R. T.; Zell, M. T.; Padden, B. E.; Munson, E. J. *Chem. Commun.* **1998**, 1913.
- [45] Chisholm, M. H.; Iyer, S. S.; Matison, M. E.; McCollum, D. G.; Pagel, M. *Chem. Commun.* **1997**, 1999.
- [46] Thakur, K. A. M.; Kean, R. T.; Hall, E. S.; Kolstad, J. J.; Lindgren, T. A.; Doscotch, M.A.; Siepmann, J. I.; Munson, E. J. *Macromolecules.* **1997**, 30, 2422.
- [47] Lee, J.; Kim, Y.; Do, Y. *Inorg. Chem.* **2007**, 46, 7701.
- [48] Ropson, N.; Dubois, P.; Jérôme, R.; Teyssié, P. *Macromolecules.* **1995**, 28, 7589.
- [49] Dove, A. P.; Gibson, V. C.; Marshall, E. L.; Rzepa, H. S.; White, A. J. P.; Williams, D.J. *J. Am. Chem. Soc.* **2006**, 128, 9834.
- [50] Schwarz, A. D.; Thompson, A. L.; Mountford, P. *Inorg. Chem.* **2009**, 48, 10442.
- [51] Kim, S. H.; Lee, J.; Kim, D. J.; Moon, J. H.; Yoon, S.; Oh, H.; Do, J. Y.; Ko, Y. S.; Yim, J.-H.; Kim, Y. *J. Organomet. Chem.* **2009**, 694, 3409.
- [52] Chmura, A. J.; Cousins, D. M.; Davidson, M. G.; Jones, M. D.; Lunn, M. D.; Mahon, M. F. *Dalton Trans.* **2008**, 1437.

CHAPTER 4
**Ring Opening Polymerization (ROP) of ϵ -Caprolactone,
rac- β -Butyrolactone and Trimethylene carbonate**

CHAPTER 4

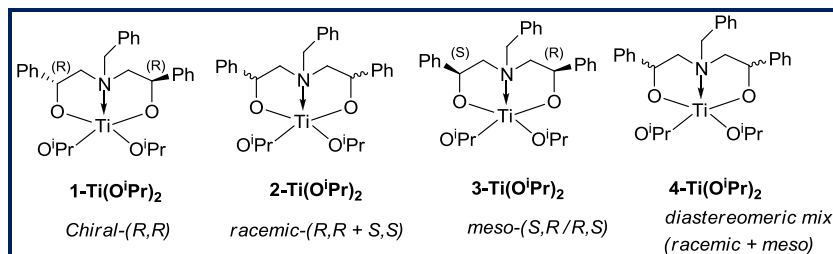
Ring Opening Polymerization (ROP) of ϵ -Caprolactone, *rac*- β -Butyrolactone and Trimethylene carbonate

4.1. Ring Opening Polymerization of ϵ -caprolactone

4.1.1. Introduction

Ring opening polymerization of ϵ -caprolactone using metal based catalysts of different groups has been reviewed recently.¹ Considerable attention has also been paid recently to the utilization of titanium complexes bearing bulky alkoxo,² bis(aryloxo),^{3,4} amine(bisphenolate)⁵ ligands in the polymerization of cyclic esters due to their low toxicity and the possibility to synthesize from medium to high molecular weight polymer with relatively narrow molecular weight distributions. Titanium complexes with different dialkanolamine ligands were briefly investigated recently in the ROP of ϵ -caprolactone.⁶ Despite this, there is exigent need to find out the better catalyst system for ROP of ϵ -CL.

In this connection we have utilized our catalytic system (Scheme 4.1) for ROP of ϵ -CL. The influence of structural changes in the complex on the polymerization activity, molecular weights, and molecular weight distribution was investigated both in solution (toluene) and bulk conditions at different temperatures.



Scheme 4.1. Titanium alkoxide complexes.

4.1.2. Results and Discussion

4.1.2.1. Solution polymerization of ϵ -caprolactone

All the complexes 1-4-Ti(OⁱPr)₂ were tested as initiators for the ROP of ϵ -CL in toluene and the results are summarized in Table 4.1. Polymerizations were performed at two different temperatures (25°C & 70°C) with a monomer to initiator ratio fixed at 300, and a polymerization time of 24 h & 2.5 h corresponding to lower and higher temperature respectively.

Table 4.1. Solution Polymerization of ϵ -Caprolactone ^a

Run	Catalyst	T (°C)	Conv ^b (%)	A ^c	M _n (NMR) ^d	M _n (theory) ^e	M _n ^f	M _n ^g	PDI ^f
1	1-Ti(O ⁱ Pr) ₂	25	97	1.38	14320	16600	24750	14360	1.09
2	2-Ti(O ⁱ Pr) ₂	25	97	1.38	11630	16520	15240	8530	1.25
3	3-Ti(O ⁱ Pr) ₂	25	94	1.24	13070	16090	25460	14760	1.13
4	4-Ti(O ⁱ Pr) ₂	25	96	1.31	11170	15810	20710	11600	1.11
5	1-Ti(O ⁱ Pr) ₂	70	95	12.23	13700	16250	23350	13540	1.12
6	2-Ti(O ⁱ Pr) ₂	70	98	12.63	13870	16780	23980	13910	1.31
7	3-Ti(O ⁱ Pr) ₂	70	99	12.76	13130	16950	30330	16990	1.32
8	4-Ti(O ⁱ Pr) ₂	70	99	12.79	9130	17100	19340	10860	1.21

^a Polymerization conditions: 1 mL of ϵ -CL, [M]/[Ti]=300, toluene = 10 mL, polymerization time; 24 h (for 25°C); 2.5 h (for 70°C). ^b Conversion determined via ¹H NMR. ^c Activity in terms of g_{poly} mmol_{cat}⁻¹ h⁻¹. ^d Calculated from isopropoxy end-group integration in 400-MHz ¹H NMR spectra. ^e M_n (theory) was calculated from the formula (M.W of ϵ -CL) × ([ϵ -CL] / 2 × [Ti]) × (conversion). ^f Determined by SEC (in THF) relative to polystyrene standards. ^g Determined by SEC (in THF) relative to polystyrene standards and corrected by Mark-Houwink correction factor of 0.56.

At 25°C, all complexes were found to be active (> 95% conversion) and to yield controlled polymerizations, as indicated from the observed narrow dispersity values from SEC. For example, the polymerization of ϵ -CL initiated by complex 1-Ti(OⁱPr)₂ at 25°C gave 97% conversion in a period of 24 h to afford PCL with a molar mass of 24,750 g.mol⁻¹ and PDI of 1.09 (Table 4.1, Run 1). All other complexes were shown to have a similar monomer conversion in a respective time period at each temperature, and to produce relatively narrow molecular weight distribution in the range of 1.09 to 1.25. The activity of these titanium complexes at room temperature (25°C) are comparable with previously reported titanium alkoxide polymerization.^{3,7-10} For example, a series of amine bis(phenolate) titanium complexes reported by Davidson *et al.*⁸ was able to achieve >99% (ϵ -CL) conversion in 24 h at room temperature in toluene.

At higher temperature (70°C), all complexes were found to be active and the monomer conversion was > 95% within 2.5 h. Even in this condition, relatively narrow molecular weight distribution PDI in the range of 1.12-1.32 were obtained indicating that the polymerization is pretty well controlled even at higher temperature. Nevertheless, the observed dispersity values were shown to be relatively broader compare to the polymerization carried out at 25°C, indicating that the back-biting and

transesterification reactions are more prevalent at higher temperature. Nonetheless, activity of these initiators is higher than the mononuclear and titanatrane alkoxide complexes (activity in the range of 0.64 to 0.84 $\text{g}_{\text{poly}}\text{mmol}_{\text{cat}}^{-1}\text{h}^{-1}$; $[\text{M}]/[\text{Ti}] = 200$; temperature = 70°C, time = 24 h, in toluene) reported by Verkade *et al.*⁹ All these results suggest that the structure of the complexes does not play a significant role in the polymerization activity.

4.1.2.2. Effect of $[\text{M}]/[\text{Ti}]$ ratio

In order to study the effect of $[\text{M}]/[\text{Ti}]$ molar ratio on the catalyst activity, polymerization was performed with 4-Ti(OⁱPr)₂ in toluene at 70°C by varying the $[\text{M}]/[\text{Ti}]$ molar ratio from 50 to 500, and the results are shown in Table 4.2.

Table 4.2. Polymerization of ϵ -CL at different $[\text{M}]/[\text{Ti}]$ ratio using 4-Ti(OⁱPr)₂^a

Run	$[\text{M}]/[\text{Ti}]$	Yield ^b (%)	A ^c	M _n (NMR) ^d	M _n (theory) ^e	M _n ^f	M _n ^g	PDI ^f
1	50	97	2.31	2510	2850	7270	4070	1.40
2	100	95	4.25	8450	5700	10840	6070	1.46
3	200	92	8.33	11010	11400	16150	9040	1.59
4	300	97	13.29	14250	17120	19400	10860	1.43
5	500	90	20.57	19320	28500	31200	17470	1.41

^a Polymerization conditions: 0.5 mL of ϵ -caprolactone, time; 2.5 h. ^b Isolated yield. ^c Activity in terms of $\text{g}_{\text{poly}}\text{mmol}_{\text{cat}}^{-1}\text{h}^{-1}$. ^d Calculated from isopropoxy end-group integration in 400-MHz ¹H NMR spectra. ^e M_n (theory) was calculated from the formula (M.W of ϵ -CL) × $([\epsilon\text{-CL}] / 2 \times [\text{Ti}]) \times$ (conversion). ^f Determined by SEC (in THF) relative to polystyrene standards. ^g Determined by SEC (in THF) relative to polystyrene standards and corrected by Mark-Houwink correction factor of 0.56.

A plot of M_n (SEC)* (corrected with Mark-Houwink correction factor of 0.56) and M_n (theory) *versus* $[\text{M}]/[\text{Ti}]$ molar ratio is presented in Figure 4.1. From this plot we observed that molar mass of the polymer increases linearly at low $[\text{M}]/[\text{Ti}]$ ratio and the values are comparable to the theoretical ones, whereas at high $[\text{M}]/[\text{Ti}]$ ratio more deviation in molar mass between M_n (theory) and M_n (SEC)* was observed. However, the molecular weight distribution is reasonably well controlled with respect to increase in $[\text{M}]/[\text{Ti}]$ molar ratio and also activity of the catalyst increases with respect to increase in monomer to initiator mole ratio.

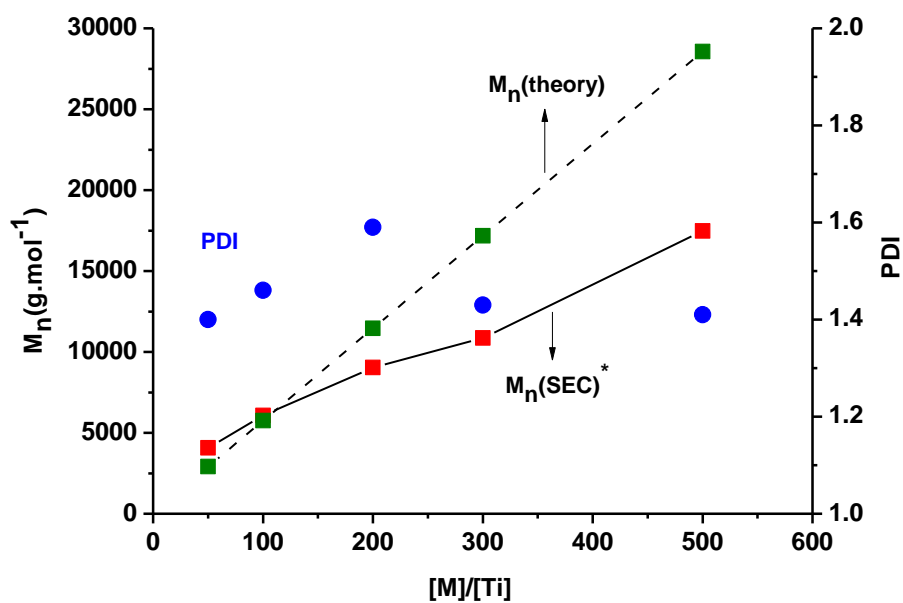


Figure 4.1. Plot of $M_n(\text{theory})$, $M_n(\text{SEC})^*$ and PDI as a function of $[M]/[Ti]$ ratio at 70°C in toluene using 4-Ti(OⁱPr)₂.

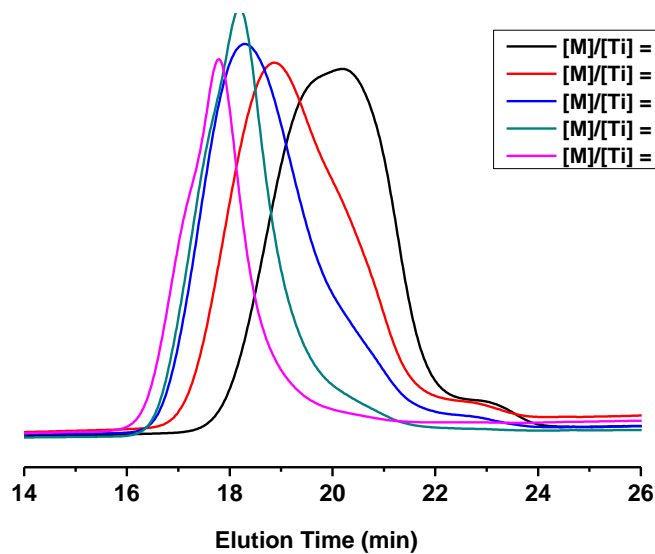


Figure 4.2. SEC overlay of PCL obtained at different $[M]/[Ti]$ mole ratio.

4.1.2.3. Characterization of PCL

Characterization by ^1H & ^{13}C NMR spectroscopy

For the end group analysis of PCL, polymerization was carried out in toluene at 70°C with a monomer to initiator ratio of 50 using the $4\text{-Ti}(\text{O}^i\text{Pr})_2$ complex as the initiator. The polymerization mixture (after complete monomer conversion) was precipitated in methanol and the white solid obtained was filtered and dried. As shown on the ^1H NMR spectrum of such a polymer (Figure 4.3) signals **(a-d)** are due to the repeating $\text{C}(\text{O})(\text{CH}_2)_5\text{O}$ - units, weak signals **e** at 1.14 ppm, **f** at 4.9 ppm and **g** at 3.51 ppm were assignable to the terminal isopropoxide $(\text{CH}_3)_2\text{-CH-O}$, $(\text{CH}_3)_2\text{-CH-O}$ and CH_2OH group respectively.¹¹

The degree of polymerization (DP_n) of the polymer, evaluated from the relative intensities of the main chain $-\text{C}(\text{O})(\text{CH}_2)_5\text{O}$ - signals **d** and the corresponding end group signal **e**, was 25, which is half of the initial mole ratio of monomer to initiator. Thus the estimated molecular weight from the NMR spectroscopy ($M_n(\text{NMR}) = 2910 \text{ g}\cdot\text{mol}^{-1}$) was in good agreement to the $M_n(\text{theory}) = 2910 \text{ g}\cdot\text{mol}^{-1}$ calculated by assuming two chains are grown from each metal center at 100% monomer conversion.

^{13}C NMR of PCL is presented in Figure 4.4 with proper assignments. The main chain methylene carbon signals assigned as **b-f** appear in the region at 24.57 to 62 ppm and the carbonyl carbon appears at 173.53 ppm. The end group carbon resonance is not assigned due to the very less intense signal as compare to the other carbon group.

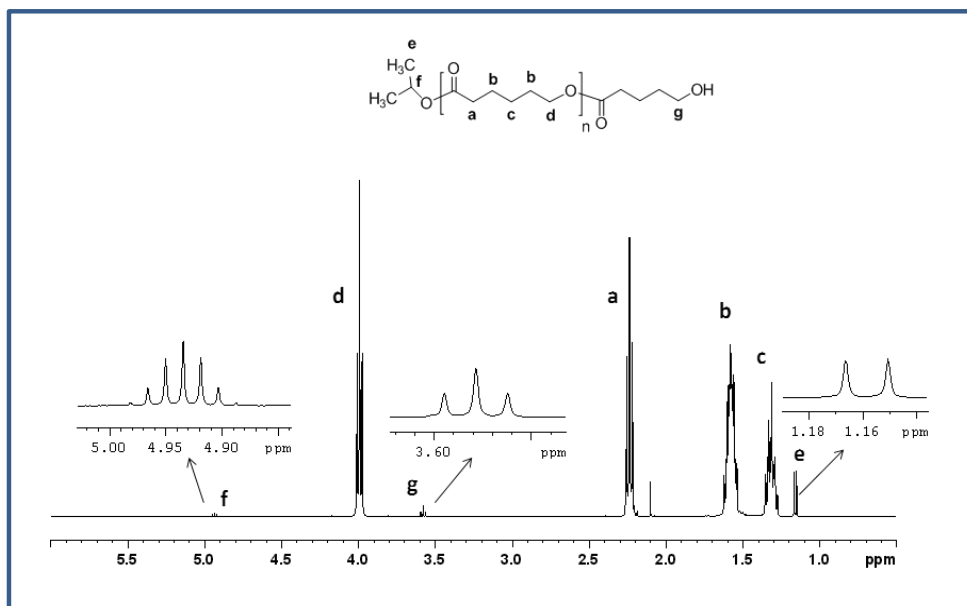


Figure 4.3. ^1H NMR spectrum of PCL prepared using $4\text{-Ti}(\text{O}^i\text{Pr})_2$ at 70°C and $[\text{M}]/[\text{Ti}] = 50$.

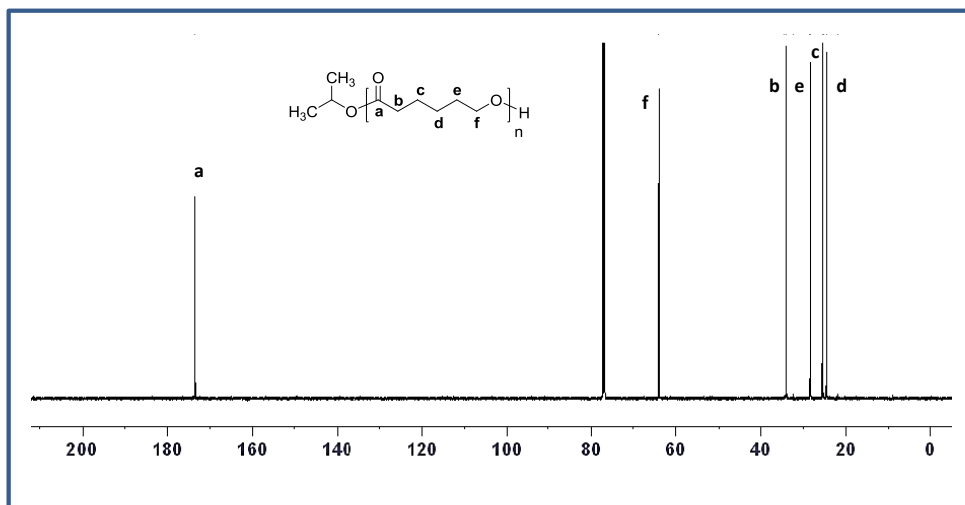


Figure 4.4. ¹³C NMR spectrum of PCL prepared using 4-Ti(OⁱPr)₂ at 70°C and [M]/[Ti] = 50.

Characterization by SEC analysis

PCL prepared with 4-Ti(OⁱPr)₂ at 70°C ([M]/[Ti] = 50) was first analyzed by (SEC) in THF relative to polystyrene standards using RI detector. It shows a molar mass of 6110 g.mol⁻¹ which is two times higher than the M_n value observed from the NMR, this may be due to the over estimation of molecular weight using polystyrene standard but when it was corrected by the Mark-Houwink correction factor of (0.56)¹² the observed (M_n(SEC)* = 3420 g.mol⁻¹) value is in good agreement with M_n (2910 g.mol⁻¹) calculated from the ¹H NMR spectroscopy. The same PCL was also analyzed by triple detection SEC (Figure 4.5) and the molar mass was determined by using viscometry detector, since for low molecular weight polymers, the sensitivity of the viscosity detector is more precise than that of light scattering detector (the signal of light-scattering detectors is directly proportional to the molecular weight of the polymers, signal-to-noise ratio of light scattering is inadequate for low molecular weight polymers). A molar mass of 2870 g.mol⁻¹ (8% error; dn/dc = 0.079) is determined and this value is very close to the M_n calculated theoretically (2910 g.mol⁻¹) and also from NMR (2910 g.mol⁻¹). These results prompted us to determine the molecular weights of few other polymers obtained from the solution polymerization reaction. For instance, PCL prepared with the initiator 4-Ti(OⁱPr)₂ at 25°C ([M]/[Ti] = 300) (Table 4.1, run 4), light scattering detector showed M_n of 13320 g.mol⁻¹ (2% error) (Figure 4.6) which is in good agreement with M_n(theory) (15810 g.mol⁻¹), and M_n(SEC)* (11600 g.mol⁻¹; correction factor employed). Similarly, for PCL obtained from the same initiator at higher temperature 70°C with [M]/[Ti] = 300 (Table 4.1, run 8), LS detector showed M_n of 12590 gmol⁻¹ (3% error) which is in good agreement with M_n(SEC)* (10860 g.mol⁻¹; correction factor employed). These results suggest that to evaluate the exact molecular weight of PCL by SEC using PS standards and RI detector, the Mark-Houwink correction factor of 0.56 has to be applied.

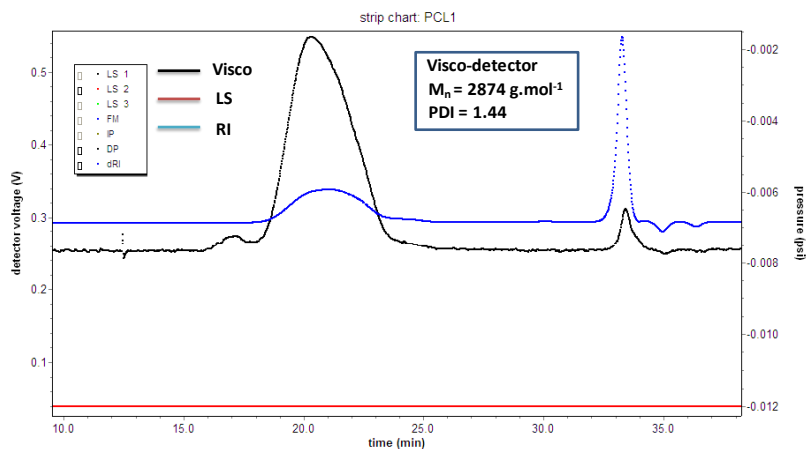


Figure 4.5. SEC chromatogram of PCL prepared using 4-Ti(OⁱPr)₂ at 70°C ([M]/[Ti] = 50).

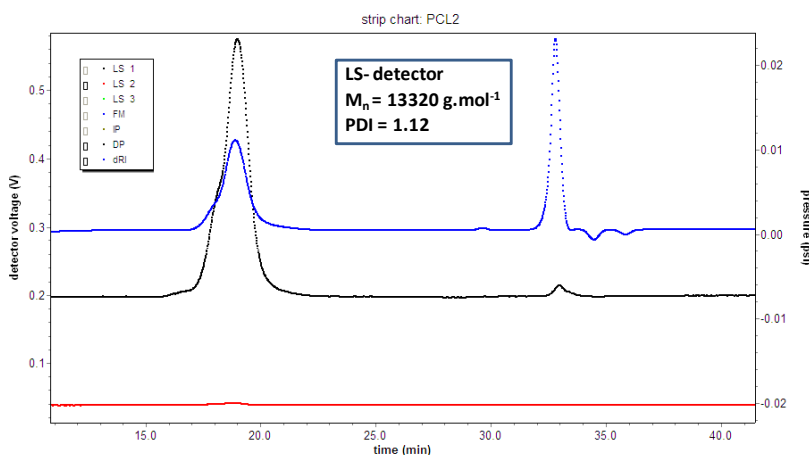


Figure 4.6. SEC chromatogram of PCL prepared using 4-Ti(OⁱPr)₂ at 25°C ([M]/[Ti] = 300).

Characterization by MALDI-TOF- mass spectrometry analysis

The polymer obtained from the initiator 4-Ti(OⁱPr)₂ was analyzed by MALDI-TOF-mass spectrometry, since it shows higher sensitivity to the detection of polymer chains end groups than the ¹H NMR spectroscopy. MALDI-TOF-mass spectrum of PCL (Figure 4.7) gives a major set of peaks with a difference in mass of ($\Delta m/z = 114$ Da) which corresponds to one ϵ -caprolactone unit with a polymer chain terminated by isopropyl ester and $-\text{CH}_2\text{OH}$ groups which is in good agreement with ¹H NMR spectrum. However, in addition to the major population, another minor population was observed in the spectrum, with a difference in mass of ($\Delta m/z = 60$ Da) which is attributed to macrocyclics resulting from intramolecular transesterification reactions occurring during the polymerization process. As it can be seen, those macrocyclics are mainly present in the low molecular weight fraction.

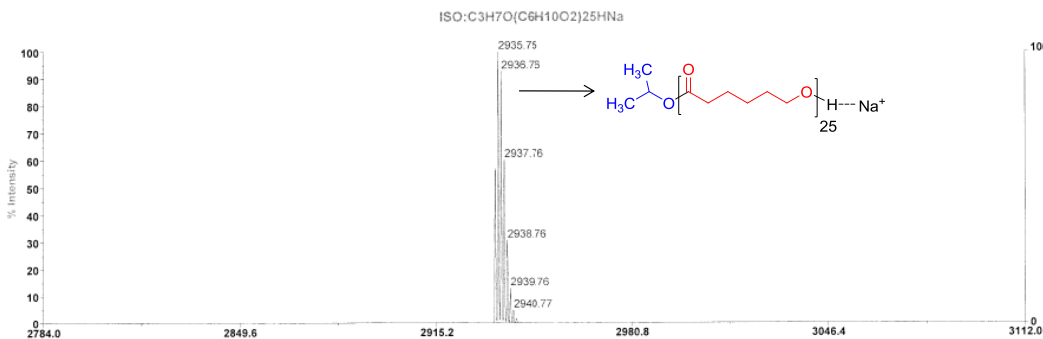
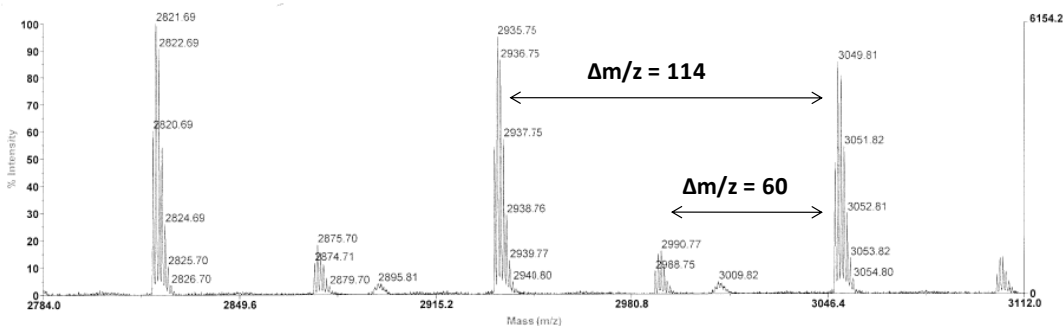
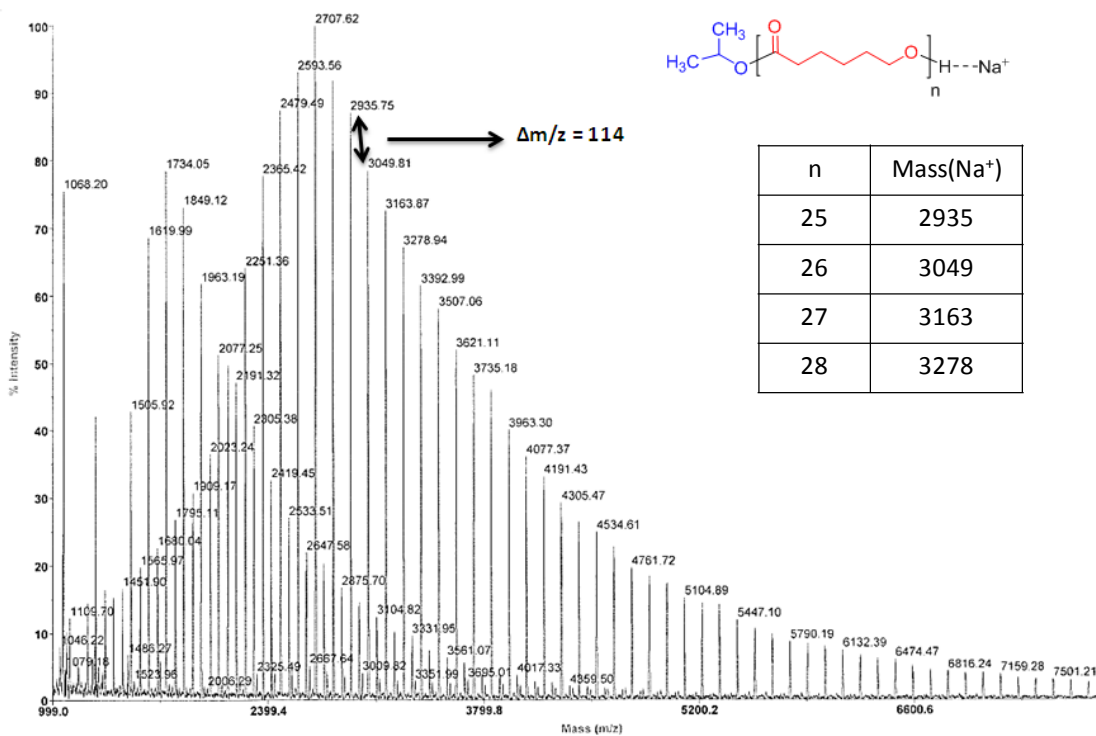
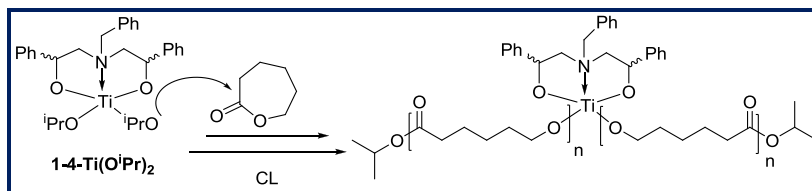


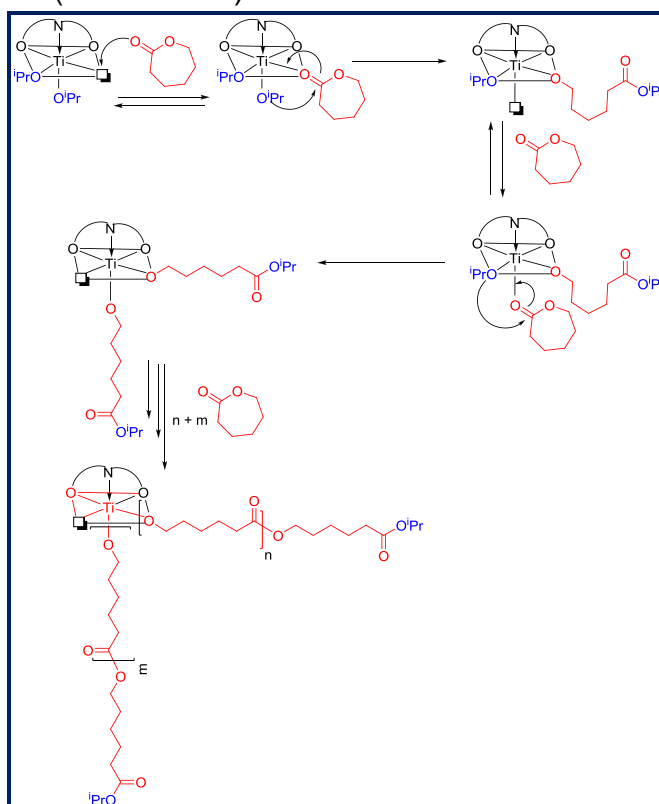
Figure 4.7. MALDI-TOF-MS of PCL prepared using 4-Ti(OⁱPr)₂ at 70°C and [M]/[Ti] = 50.

Overall the end group analysis by NMR, SEC and MALDI-TOF suggest that the initiation occurs through the insertion of monomer (ϵ -CL) into the two Ti-OⁱPr bond (Scheme 4.2), consistent with a polymerization that proceeds *via* a coordination insertion mechanism.¹³



Scheme 4.2. Schematic representation of formation of two growing polymer chains per molecule of the catalyst.

Recently, the plausible mechanism for ROP of ϵ -CL initiated by titanium complexes of dialkanolamine ligands has been proposed by Piskun *et al.*⁶ This mechanism involves the coordination of ϵ -CL to the pentacoordinate titanium atom having one vacant site followed by the ring opening of lactone occurring *via* acyl oxygen bond cleavage in which the growing polymer chain remains attached to the metal center through alkoxide bond, while the alkoxide group of initiator is transferred to the chain end of the polymer molecule. Continuous coordination and insertion of the monomer yield the linear polymer (Scheme 4.3).



Scheme 4.3. Proposed mechanism of ϵ -caprolactone polymerization *via* coordination-insertion mechanism.⁶

DSC Analysis: Thermal analysis of PCL was carried out by differential scanning calorimetry (DSC), in the range of temperature -150°C to 100°C . A glass transition temperature at -61°C and a melting temperature at 56°C are observed in the spectrum (Figure 4.8), they are typical of a PCL.

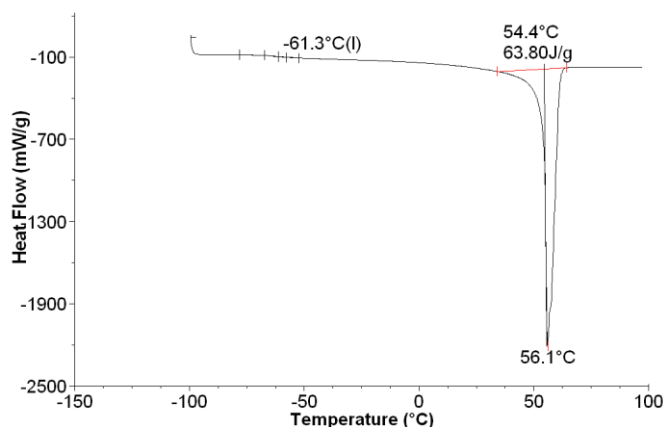


Figure 4.8. DSC analysis of PCL prepared using $4\text{-Ti}(\text{O}^i\text{Pr})_2$ at 70°C and $[\text{M}]/[\text{Ti}] = 50$.

4.1.2.4. Kinetic studies of ϵ -Caprolactone polymerization

Kinetic studies have been performed in order to investigate further in details the mechanism of controlled ROP. The results of the kinetic experiments have been utilized to understand the action of the initiator. The kinetics of ϵ -caprolactone polymerization was investigated in toluene at 25°C and 70°C by using the initiator $4\text{-Ti}(\text{O}^i\text{Pr})_2$. Figure 4.9 shows the semi-logarithmic plots of $\ln([\text{CL}]_0/[\text{CL}]_t)$ versus reaction time at two different temperatures. $[\text{CL}]_0$ is the initial ϵ -caprolactone concentration and $[\text{CL}]_t$ is the ϵ -caprolactone concentration at a time t .

The linearity of the plots shows that the propagation was first order with respect to monomer concentration and the straight line passing through the origin indicates the absence of an induction period, like for Lactide polymerization. Induction period was described to occur with some catalysts and to be due to rearrangement of catalyst aggregates to form the active species.^{5,14,15} From the slope of the plots, the values of the apparent rate constant (K_{app}) were found to be $2.53 \times 10^{-2} \text{ min}^{-1}$ (70°C) and $0.16 \times 10^{-2} \text{ min}^{-1}$ (25°C). This would suggest that the rate of the polymerization at higher temperature (70°C) is 15 times faster than the polymerization conducted at room temperature (25°C). This seems to indicate that the effect of temperature have significant effect on the activation energy of the polymerization and the initiator efficiency. The apparent rate of propagation (K_{app}) observed with our catalytic system are comparable to titanium sulfonamide based complexes used in ϵ -CL solution polymerization at 100°C (Table 4.3).

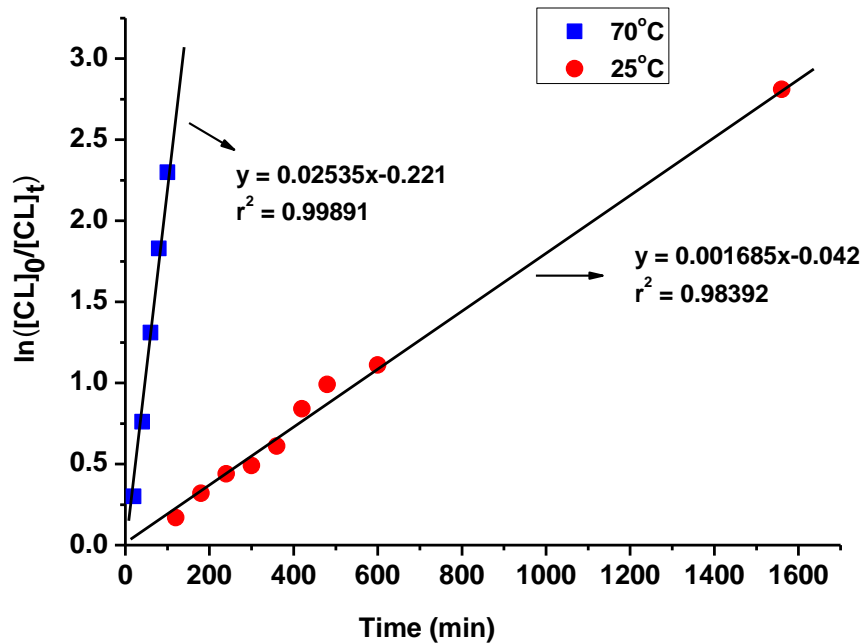


Figure 4.9. First order kinetic plot for ϵ -CL consumption vs time using 4-Ti(OⁱPr)₂ at 25°C & 70°C.

Polymerization conditions: $[\epsilon\text{-CL}]/[\text{Ti}] = 300$, 10 mL of toluene, 0.2 mL of aliquots was taken at the given intervals. $[\text{CL}]_0$ is the initial concentration of ϵ -caprolactone and $[\text{CL}]_t$ the concentration at time t .

Table 4.3. First Order Propagation Rate Constant (K_{app}) for ϵ -CL polymerization

Catalyst	$K_{\text{app}}(\text{min})^{-1}$	$[\text{M}]/[\text{I}]$; Temp(°C); toluene	ref
Ti(sulfonamide 1)	0.75×10^{-2}	100; 100	16
Ti(sulfonamide 2)	6.50×10^{-2}	100; 100	16
Ti(sulfonamide 3)	2.30×10^{-2}	100; 100	17
4-Ti(O ⁱ Pr) ₂	2.53×10^{-2}	300; 70	-
4-Ti(O ⁱ Pr) ₂	0.16×10^{-3}	300; 25	-

A representative plot of conversion *versus* time is shown in Figure 4.10 for the polymerization at 70°C and 25°C, monomer conversion takes place linearly with respect to the polymerization time at least up to 60% conversion.

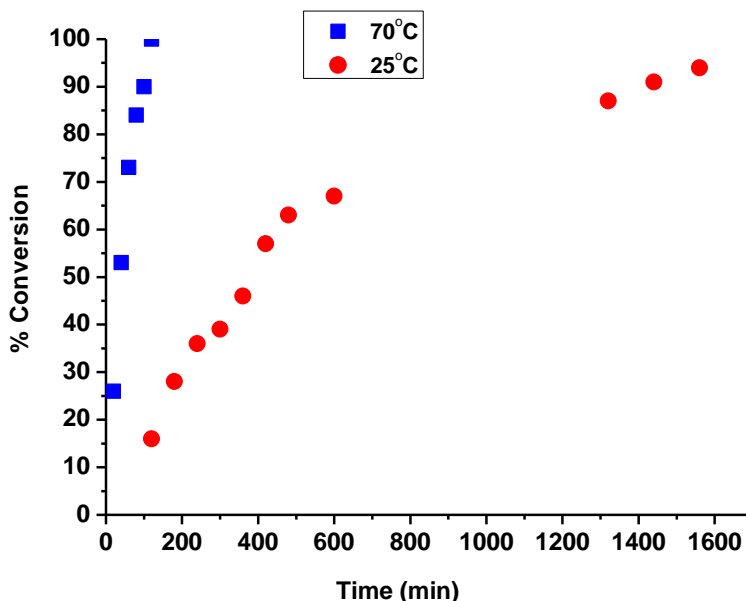


Figure 4.10. Plot for ϵ -CL consumption vs time using 4-Ti(OⁱPr)₂ at 25°C and 70°C.

In Figures 4.11 & 4.12, a plot of M_n (theory) and M_n (SEC)* (correction factor employed) *versus* conversion shows that M_n increases linearly with respect to monomer conversion and it is evidencing the “living” character of the polymerization at both temperatures. At low temperature (25°C) molecular weight distribution remained very narrow (PDI = 1.04-1.08) during the polymerization process until nearly complete monomer conversion (Figure 4.11) and also shows good agreement in molar mass between experimental (SEC)* and theoretical ones even after high monomer conversion. These results indicated that no back biting reaction took place throughout the polymerization over a period of 24 h, whereas at higher temperature (70°C), deviation in molar mass between M_n (SEC)* and M_n (theory) was observed at high monomer conversion. The molecular weight distribution is uniform until 90% conversion (Figure 4.12) and at high monomer conversion the occurrence of transesterification side reactions can lead to a broader molecular weight distribution (PDI = 1.07-1.25).

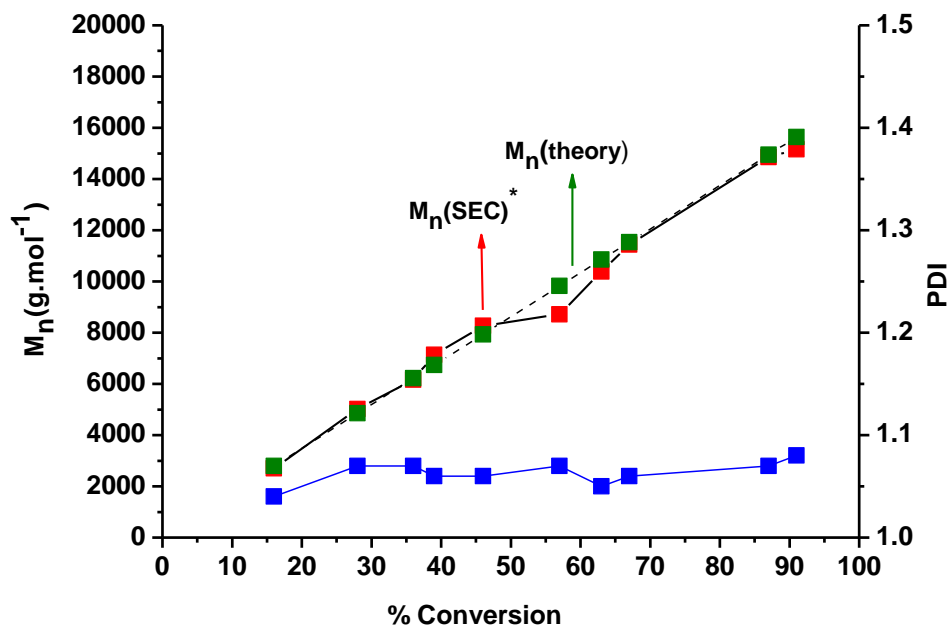


Figure 4.11. Plots of M_n (theory), M_n (SEC)* and PDI vs Conversion for the polymerization of ϵ -CL using catalyst 4-Ti(OⁱPr)₂ at 25°C.

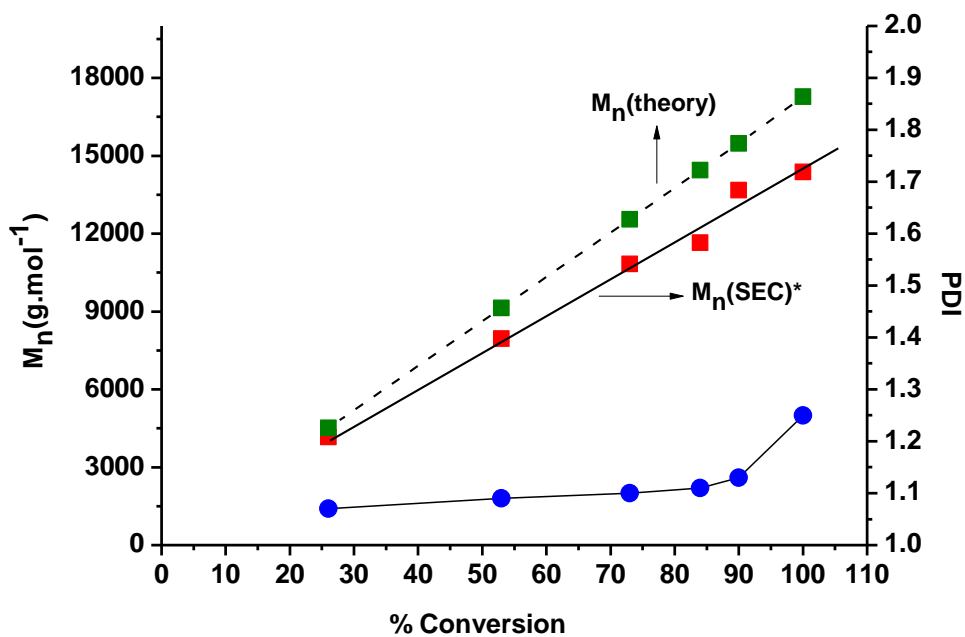


Figure 4.12. Plots of M_n (theory), M_n (SEC)* and PDI vs Conversion for the polymerization of ϵ -CL using catalyst 4-Ti(OⁱPr)₂ at 70°C.

To confirm the living nature of the polymerization, a sequential two stage polymerization was carried out in toluene at 70°C by using complex 4-Ti(OⁱPr)₂ as the initiator. Thus, the first stage of ε-CL polymerization ([M]/[Ti] = 200) proceeds to reach 100% monomer conversion within 2.5 h ($M_n = 13850$, PDI = 1.32), then 200 equiv of ε-CL was newly added to the system, whereupon the second-stage polymerization occurred to attain 100% monomer conversion in 2.5 h to afford a higher molecular weight polymer with a molar mass of 28370 g.mol⁻¹ with PDI of 1.77 (Figure 4.13). This indicated that the polymerization of ε-CL by the initiator proceeded in a controlled manner even if some broadening of the molecular weight distribution is observed for the second monomer feed consumption.

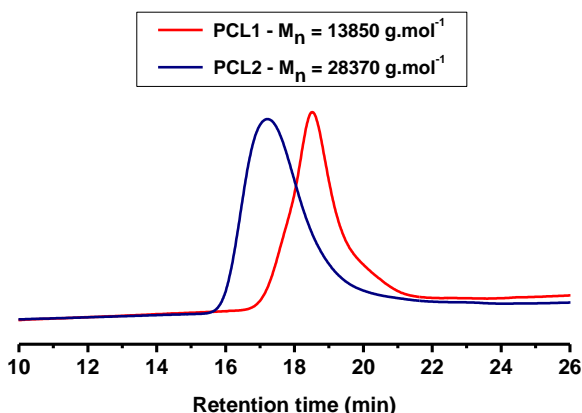


Figure 4.13. Two-stage polymerization of ε-CL initiated by 4-Ti(OⁱPr)₂ in toluene at 70°C.

4.1.2.5. Bulk polymerization of ε-Caprolactone

Polymerization experiments have also been carried out in industrially relevant melt conditions or solvent free conditions, to evaluate the behavior of these catalysts under drastic conditions (Table 4.4). The polymerization was carried out with a monomer to initiator ratio fixed at 300 at two different temperatures 70°C and 100°C. Almost all the complexes acts as fairly active initiators, conversion > 60% was reached within 10 min at 70°C, with relatively narrow molecular weight distribution in the range of 1.14 to 1.30. The experimental molecular weight observed from the $M_n(\text{SEC})^g$ (correction factor employed) is shown to be in good agreement with the theoretical ones. The molecular weights of some polymers have also been analyzed by triple detection SEC. For example, PCL prepared with the initiator 2-Ti(OⁱPr)₂ at 70°C ([M]/[Ti] = 300) (Table 4.4, run 2), LS detector showed M_n of 11910 g.mol⁻¹ which is in good agreement with $M_n(\text{SEC})^g$ (11140 g.mol⁻¹). Similarly, PCL prepared from the initiator 3-Ti(OⁱPr)₂ (Table 4.4, run 3) LS detector showed M_n of 7390 g.mol⁻¹ comparable to $M_n(\text{SEC})^*$ (6810 g.mol⁻¹) and the M_n of PCL prepared from the initiator 4-Ti(OⁱPr)₂ (Table 4.4, run 4) was shown to be 13690 g.mol⁻¹ (LS detector) comparable $M_n(\text{SEC})^*$ (11550 g.mol⁻¹).

Table 4.4. Bulk Polymerization of ϵ -caprolactone ^a

Run	Catalyst	T (°C)	Conv ^b (%)	A ^c	M _n (NMR) ^d	M _n (theory) ^e	M _n ^f	M _n ^g	PDI ^f
1	1-Ti(O ⁱ Pr) ₂	70	80	156.28	9700	13700	17270	9670	1.30
2	2-Ti(O ⁱ Pr) ₂	70	74	140.65	10160	12850	19890	11140	1.16
3	3-Ti(O ⁱ Pr) ₂	70	60	113.30	7190	10270	12160	6810	1.14
4	4-Ti(O ⁱ Pr) ₂	70	68	125.02	11810	11640	20630	11550	1.29
5	1-Ti(O ⁱ Pr) ₂	100	32	62.51	5420	5480	8530	4770	1.16
6	2-Ti(O ⁱ Pr) ₂	100	84	160.18	9620	14380	21330	11950	1.78
7	3-Ti(O ⁱ Pr) ₂	100	71	117.20	8150	12150	23970	13420	1.94
8	4-Ti(O ⁱ Pr) ₂	100	72	128.93	8220	12330	23700	13270	1.95

^a Polymerization conditions: 0.5 mL of ϵ -caprolactone, [M]/[Ti]=300, polymerization time; 10 min. ^b Conversion determined via ¹H NMR. ^c Activity in terms of g_{poly} mmol_{cat}⁻¹ h⁻¹. ^d Calculated from isopropoxy end-group integration in 400-MHz ¹H NMR spectra. ^e M_n (theory) was calculated from the formula (M.W of ϵ -CL)×([ϵ -CL]/ 2×[Ti])×(conversion) + 60 (End group). ^f Determined by SEC (in THF) relative to polystyrene standards. ^g Determined by SEC (in THF) relative to polystyrene standards and corrected by Mark-Houwink correction factor of 0.56.

No significant activity increase could be observe when the polymerization temperature increases from 70°C to 100°C, but molecular weight distribution are rather broader in the range of 1.78 to 1.95. It may be due to undesirable side reaction such as back-biting and also deactivation of the catalyst species at higher temperature. Nonetheless, the activity of these complexes in the range of 62.51 to 160.18 g_{poly}mmol_{cat}⁻¹h⁻¹, which is superior to those of the titanium complexes having tellurium bridged bis(phenolate) systems which gave activity in the range of 1.03 to 3.8 g_{poly}mmol_{cat}⁻¹h⁻¹ under the same reaction temperature with monomer to initiator of 100.⁷ The higher activity of these complexes may be due to the coordination of axial nitrogen atom from the ligand to the titanium metal center reducing the activation energy for the ϵ -caprolactone polymerization. Such kind of interaction was already explained in the literature for the olefin insertion into the metal carbon bond of certain non-metallocene catalysts.¹⁸ It was also explained that the transannular interaction of nitrogen atom of triethanolamine ligand of half sandwich complex to the titanium metal center led to considerable increase of the catalyst activity in the syndiospecific styrene polymerization.¹⁹ Interestingly the coordination of nitrogen atom of the ligand to the

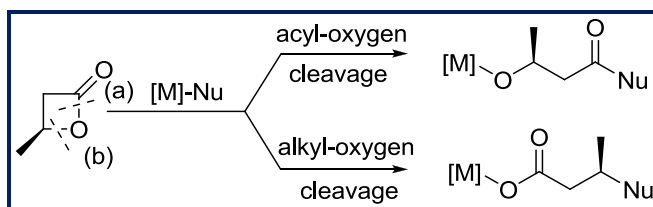
titanium makes it less acidic allowing to suppress undesirable side reactions and led to achieve the controlled ROP of ϵ -caprolactone.

4.2. Ring Opening Polymerization of rac- β -Butyrolactone

4.2.1. Introduction

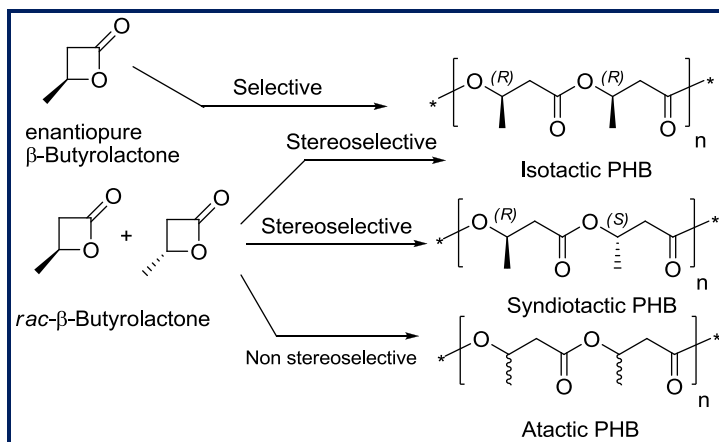
Poly(3-hydroxybutyrate) (PHB) is aliphatic polyesters produced by bacteria and other living organisms and this biodegradable, biocompatible natural polymer is isotactic with all stereocentres in the (*R*) configuration.²⁰ However, high production costs of naturally synthesized poly-(3-hydroxyalkanoates) (PHAs) render it impractical in many applications. Therefore, efficient chemical synthesis pathways for this natural polyester motif are of significant importance.

The polymerization of β -butyrolactone (BBL) can occur *via* different processes, namely anionic, “coordination-insertion”, organo-catalyzed, enzymatic and cationic processes.^{21,22} Some of these processes share common mechanistic characteristics, in which the ring opening of β -lactones can proceed *via* cleavage of either acyl-oxygen bond or alkyl oxygen bond leading respectively to alkoxy and carboxy propagating chain ends (Scheme 4.4). As a matter of fact, this type of mechanism may be often associated with side reactions such as transesterification, chain transfer, and multiple hydrogen transfer reactions. The extent of these undesirable side reactions strongly depends on the nature of the initiating system and the conditions (temperature, solvent, concentration, etc).^{21,22}



Scheme 4.4. Possible modes of ROP of β -butyrolactone (BBL) for anionic/“coordination-insertion” processes (Nu = nucleophile, $[M]$ = metal); (a) Acyl-oxygen cleavage and (b) Alkyl oxygen cleavage.

The most common and convenient method for synthesizing PHAs is the use of metal alkoxide species supported by ancillary ligands which were found to be efficient initiators for controlled (ROP) of β -butyrolactone (BBL), where the relief of ring strain is the driving force for polymerization.²³ Unlike bacteria-mediated polymerization, which gives only isotactic PHB, controlled ROP of BBL allows access to a variety of PHB microstructures. For example highly isotactic (*R*)- or (*S*)-PHB can be obtained when optically pure (*R*)- or (*S*)-BBL is involved,²⁴ while use of a racemic (*rac*) mixture of BBL give rise to atactic PHB,²⁵ and PHB enriched in isotactic²⁶ or syndiotactic²⁷ diads (Scheme 4.5).



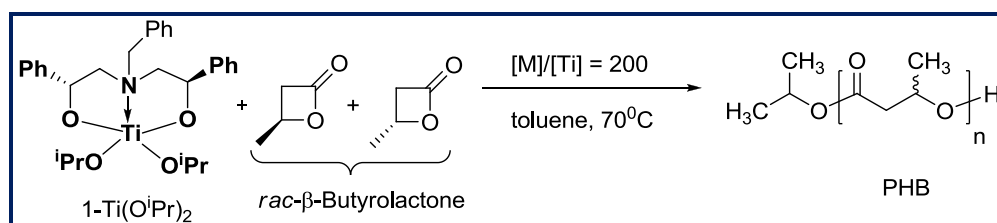
Scheme 4.5. Microstructures of Poly(3-hydroxybutyrate) (PHB).

Although some initiators are able to polymerize *racemic* BBL with good rates under mild conditions to make PHBs in a controlled manner,²⁸ the stereospecific (ROP) of *rac*-BBL remains a challenge among the researcher. More recently, Carpentier and coworkers²⁹ reported a Group 3 metal catalysts that affords a predominantly syndiotactic PHB by a chain end control mechanism.

4.2.2. Results and Discussion

Generally β -butyrolactone (BBL) appears as a reluctant monomer, significantly less reactive than related higher lactones despite having high internal strain four membered ring.²¹ Numerous studies have evidenced that most initiating system are extremely slow and produced low molecular weight PHB.

Our investigation is focused on the ROP of *rac*- β -butyrolactone (BBL) using the titanium alkoxide complex $1\text{-Ti}(\text{O}^i\text{Pr})_2$ which was shown to be effective initiator for the (ROP) of Lactides and ϵ -caprolactone, in the previous chapter and section. The initial polymerization reaction was carried out in toluene at 70°C with a monomer to initiator ratio of 200 (Scheme 4.6). The complete monomer conversion was reached after 20 h. The polymerization was stopped by the addition of methanol and the resulting polymer was characterized by ^1H and ^{13}C NMR spectroscopy (Figure 4.14 & 4.15).



Scheme 4.6. ROP of *rac*- β -butyrolactone (BBL) using $1\text{-Ti}(\text{O}^i\text{Pr})_2$ in toluene at 70°C .

The presence of less intense signals at 4.9 ppm (septet) as proton (**g**) and at 4.12 ppm (broad signal) as proton (**f**), indicates the presence of $-\text{OCH}(\text{CH}_3)_2$ and hydroxyl end group respectively, meaning that the BBL ring is cleaved at the acyl-oxygen bond and inserted into the metal-isopropoxide bond *via* a coordination insertion mechanism (Scheme 4.4). The main chain methylene and methine protons appear at 2.4-2.6 ppm (multiplet) as proton (**d**), and at 5.2-5.3 ppm (multiplet) as proton (**e**) respectively. The main chain and the end group methyl protons appear together as a multiplet in the region 1.1-1.3 ppm. It is noteworthy that *trans*-crotonate (and carboxy) groups, which are often observed due to elimination reaction in the case of anionic mechanism (Scheme 4.7)^{30,31} were not observed in the spectrum (absence of signals at 1.9 and 5.7 ppm) of this PHBs, thus confirming the coordination insertion mechanism. The monomer conversion was evaluated from the crude polymer between the intensity ratios of methine signal at 4.6 ppm (monomer) to that at methine signal at 5.2 ppm (polymer).

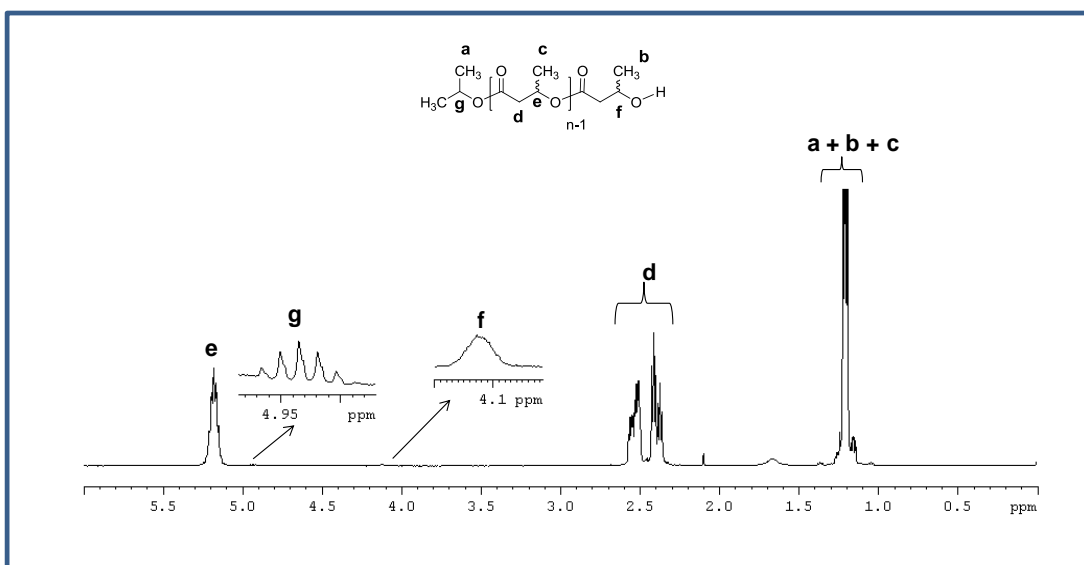
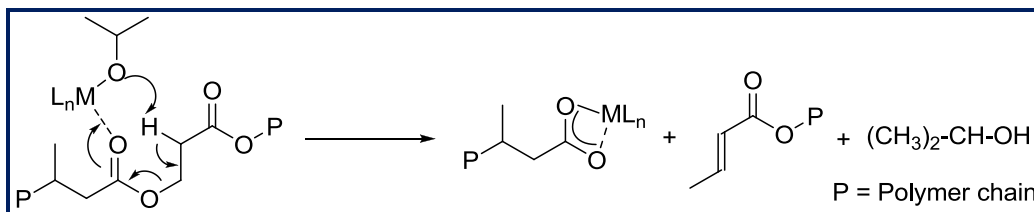


Figure 4.14. ^1H NMR spectrum of PHB prepared using $1\text{-Ti}(\text{O}^i\text{Pr})_2$ in toluene at 70°C .



Scheme 4.7. Elimination reactions of PHBs by metal catalysts.

The (DP_n) of the polymer was evaluated by 1H NMR by the ratio of the integration of the end group hydroxyl methine proton at 4.12 ppm to the main chain methine protons at 5.2 ppm to be 85, which is nearly half of the initial monomer to initiator mole ratio of 200. Thus the estimated molecular weight from the NMR spectroscopy ($M_{n, NMR} = 7370 \text{ g}\cdot\text{mol}^{-1}$) was in close agreement to the theoretically calculated molecular weight ($M_{n, theory} = 8660 \text{ g}\cdot\text{mol}^{-1}$, calculated by assuming two chains are grown from each metal center). The molar mass measured by SEC analysis is also close to the theoretical one ($M_{n, SEC} = 9510 \text{ g}\cdot\text{mol}^{-1}$; $M_w/M_n = 1.44$). These results suggest the polymerization is controlled, and the observed molecular weight distribution indicate the occurrence of small amount of transesterification during the polymerization.

^{13}C NMR data (Figure 4.15) confirmed the presence of carbonyl group at 169.2 ppm (**d**), and the main chain methyl, methylene and methine carbons appear at 19.8 ppm (**a**), 40 ppm (**b**) and 67.6 ppm (**c**) respectively.

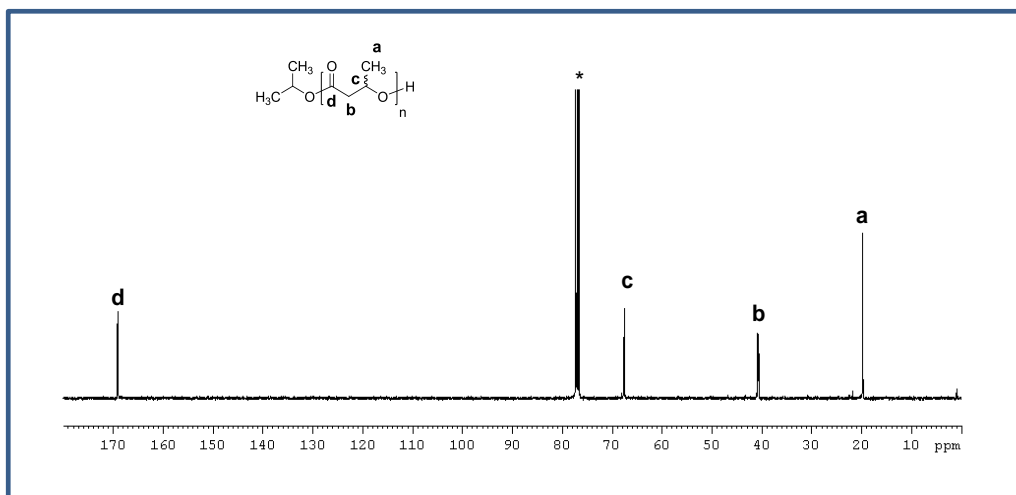


Figure 4.15. ^{13}C NMR spectrum of PHB prepared using $1\text{-Ti}(\text{O}^i\text{Pr})_2$ in toluene at 70°C .

Microstructure analysis of the polymer was done by ^{13}C NMR. Assignments are on the basis of earlier work reported by Carpentier *et al.*²⁹ Expansion of the carbonyl region shows 3 peaks that could be assigned to four different triad stereosequences (Figure 4.16, a). Thus we assigned the resonance at 169.12 ppm to the (*ii/si*) triad, the resonance at 169.22 and 169.24 ppm to the (*ss*) and the (*is*) triads, respectively. The relative intensity of these triad stereosequences is almost equal.

Similarly, the expansion of the methylene resonance shows four peaks of equal intensity, the resonance at 40.65, 40.71, 40.79, and 40.84 ppm were assigned to the (*is*), (*ss*), (*ii*), and (*si*) respectively. The methyl region shows essentially two peaks of equal intensity that correspond to two different diads (*i*) and (*s*). This result implies that the obtained polymer is atactic, and it indicates that the catalyst does not initiate the polymerization in a stereoselective manner.

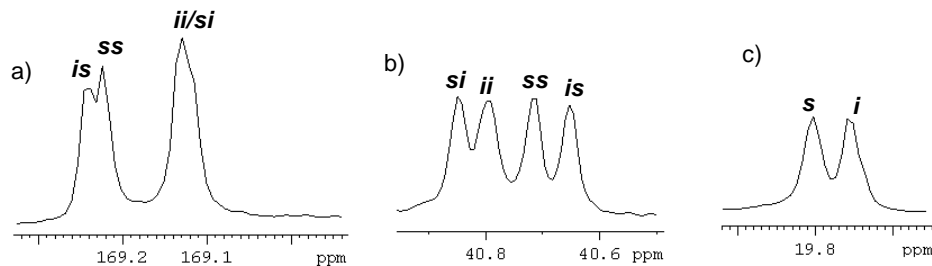


Figure 4.16. a) Carbonyl region, b) Methylene region, c) Methyl region of the $^{13}\text{C}\{^1\text{H}\}$ NMR spectra of PHBs prepared by ROP of *rac*-BBL.

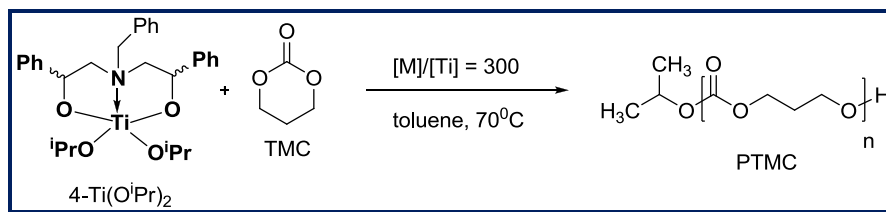
4.3. Ring Opening Polymerization of Trimethylene carbonate

4.3.1. Introduction

Aliphatic polycarbonates, copolymers of cyclocarbonates and lactones are of great potential interest for applications in various areas, such as agriculture and medicine, because of their good biodegradability, biocompatibility, low toxicity and superior mechanical properties compared to those of structurally different polyesters.³²⁻³⁴ They can be prepared from the polycondensation of diols and carbonates, cyclic ethers, and carbondioxide as well as by the ring opening polymerization (ROP) of suitable cyclic carbonates such as trimethylene carbonate (TMC).³⁵ The polycondensation of diol and carbonate presents some limitations intrinsic to step growth techniques, especially polymers with low molar mass and high molecular weight distribution are obtained. ROP of six-membered ring carbonates is a valuable alternative method, leading to better controlled reactions and producing well defined polymers. For cyclic carbonate ROP, cationic,³⁷ anionic,³⁸ coordination-insertion polymerization,³⁹ enzyme catalyst,⁴⁰ and organocatalysts.³⁶ have been described in the literature. Polymerization *via* a coordination–insertion mechanism has been frequently applied for the preparation of poly(trimethylene carbonate) (PTMC) using several initiators/catalysts systems^{35,36} including tin-, bismuth-, and zinc contain species.

4.3.2. Results and Discussion

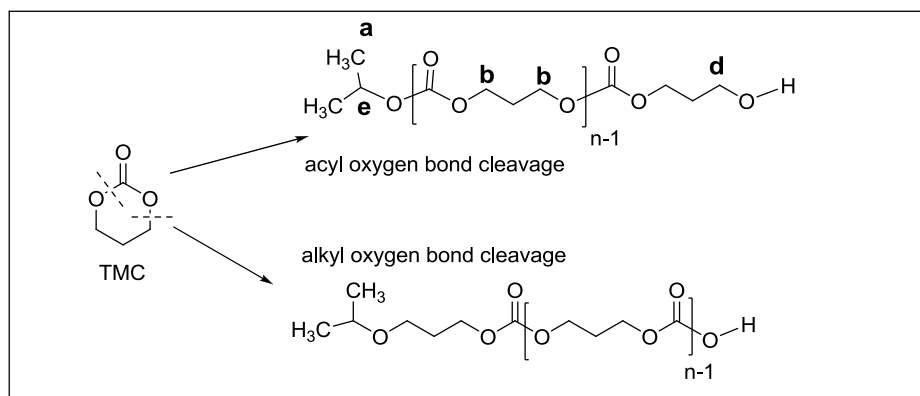
In the previous section and chapters, we have reported that titanium complexes derived from aminodiols ligands has been successfully used as initiators for the ROP of β -butyrolactone, ϵ -caprolactone and *L* / *rac*-LA. To further develop the application of these complexes, we have investigated their potential application as a single component catalyst in polymerization of trimethylene carbonate (TMC) both in solution (toluene) and bulk polymerization condition (Scheme 4.8).



Scheme 4.8. Ring Opening Polymerization of TMC initiated with 4-Ti(OⁱPr)₂ in toluene at 70°C.

4.3.2.1. Solution polymerization of Trimethylene carbonate

The polymerization was first carried out in solution (toluene) using 4-Ti(OⁱPr)₂ with a monomer to initiator ratio of 300 at 70°C. The complete monomer conversion was achieved in 7 h under this condition. It is well known in the literature the mechanism of ROP of cyclic carbonate can proceed by either acyl-oxygen bond cleavage or alkyl-oxygen bond cleavage, as illustrated in Scheme 4.9. To clarify the reaction mechanism, the polymer (PTMC) was characterized by ¹H NMR as shown in Figure 4.17.



Scheme 4.9. Ring Opening modes of Trimethylene carbonate.

The ¹H-NMR spectrum (Figure 4.17) shows signals at 4.7-4.8 ppm (septet, 1H) and at 1.22-1.24 ppm (doublet, 6H) that were assigned to isopropyl methine (**e**) and methyl group (**a**) respectively of one end of PTMC chain. Signal at 3.67 ppm (triplet) corresponds to methylene protons (**d**) of the other end group CH₂OH. The main chain methylene protons signals appear at 4.15-4.18 ppm (triplet) as proton (**b**) and at 1.95-2.0 ppm (quintet) as proton (**c**) of intensity ratio 2:1 respectively. The complete absence of ether linkage (proton resonance at 1.8 and 3.4 ppm) indicates that the poly(TMC)s obtained are free of oxetane units arising from CO₂ elimination.⁴¹ These results suggest that the (ROP) of TMC occurs *via* a coordination mechanism by acyl-oxygen bond cleavage (Scheme 4.9).

The degree of polymerization (DP_n) of the polymer, evaluated by the integration of the end group of the isopropoxide methyl proton at 1.22 ppm and the backbone methylene resonance at 2.0 ppm, was 143, which is almost half of the initial monomer to initiator mole ratio. Thus the estimated molecular weight from the NMR spectroscopy (M_n (NMR) = 14660 g.mol⁻¹) was in good agreement with the theoretical ones (M_n (theory) = 15370 g.mol⁻¹) calculated by assuming two chains are grown from each metal center.

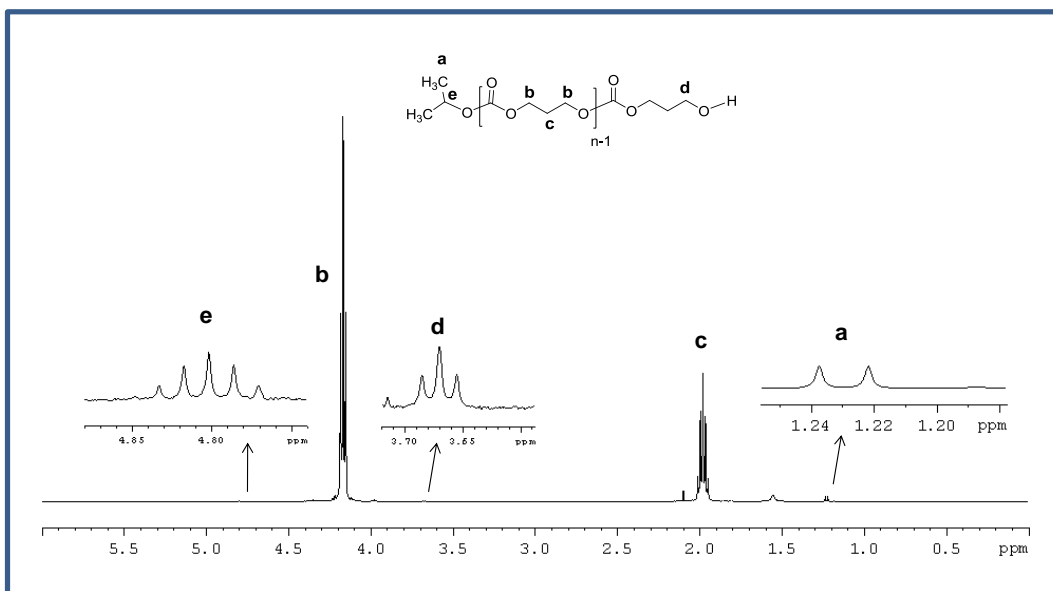


Figure 4.17. ¹H NMR spectrum of PTMC prepared using 4-Ti(OⁱPr)₂ in toluene at 70°C.

The polymer molecular weight and dispersity values were determined from the SEC analysis in THF calibrated with polystyrene standards. The raw value obtained was found to be $M_{n(\text{SEC, raw data})} = 19530 \text{ g.mol}^{-1}$ with M_w/M_n of 1.53. Calibration of SEC with commercial polystyrene standards overestimates the real molar mass of aliphatic polyesters.^{33,42} The molar mass was corrected by using the correction coefficient of (0.88).⁴² The $M_{n(\text{SEC})}$ observed after applying the correction factor (17190 g.mol⁻¹) is in reasonably good agreement with molecular weight calculated from the NMR (14660 g.mol⁻¹) and theoretically (15370 g.mol⁻¹).

¹³C NMR data (Figure 4.18) confirmed the presence of main chain $[-(\text{CH}_2)_3\text{-OC(O)O-}]$ carbonate group at 155 ppm (a), and the main chain methylene carbons at 64 ppm (b) and 28 ppm (c). These NMR analyses also revealed the absence of signals corresponding to ether units (66.5-67.7 ppm)⁴³ thus highlighting the absence of decarboxylation of PTMCs, a trend yet often observed in the ROP of carbonates.³⁵

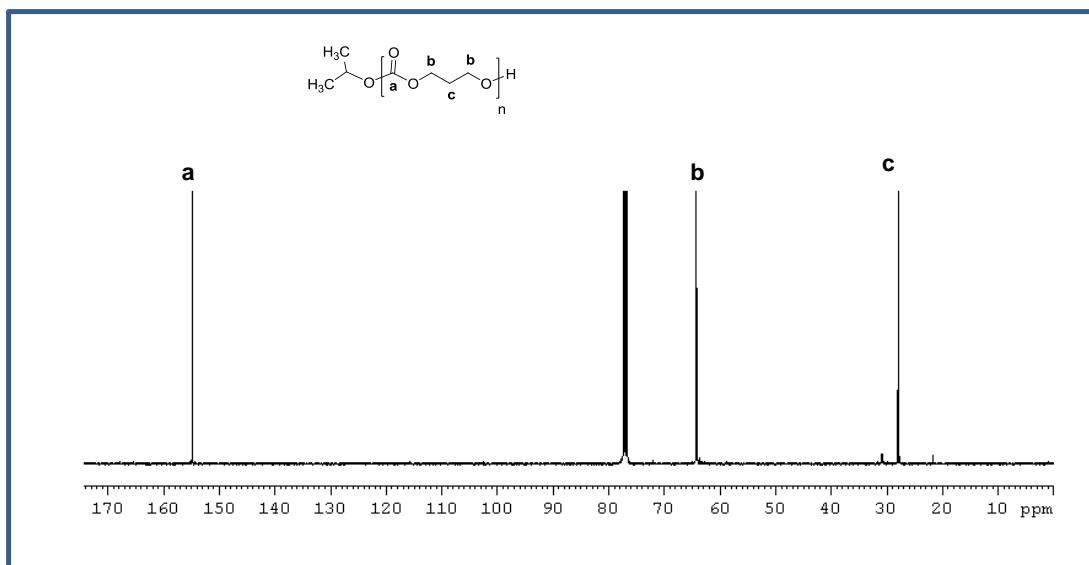
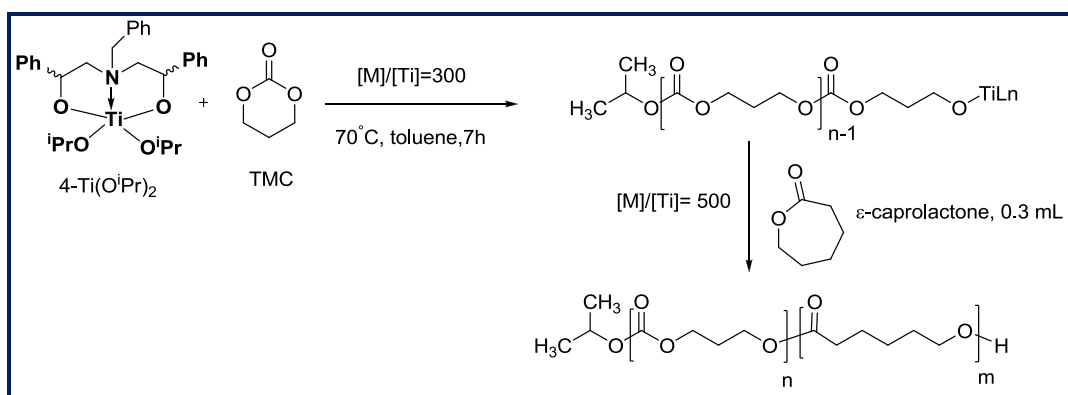


Figure 4.18. ^{13}C NMR spectrum of PTMC prepared using $4\text{-Ti}(\text{O}^i\text{Pr})_2$ in toluene at 70°C .

To confirm the living nature of the polymerization of TMC in toluene at 70°C , a sequential polymerization was performed to yield a block copolymer. A first feed of TMC was polymerized. A second monomer feed ($\epsilon\text{-CL}$, 0.3 mL) was then added into the reaction mixture and the polymerization was continued until complete $\epsilon\text{-CL}$ conversion (3 h) (Scheme 4.10).



Scheme 4.10. Sequential synthesis of block copolymer PTMC-*b*-PCL.

The polymer was first analyzed by SEC (Figure 4.19). As expected, the polymer showed unimodal peak with almost 3-fold increase in molecular weight and relatively controlled molecular weight distribution ($M_{n(\text{SEC})} = 55930 \text{ g}\cdot\text{mol}^{-1}$; PDI = 1.32) compare to the homopolymer PTMC.

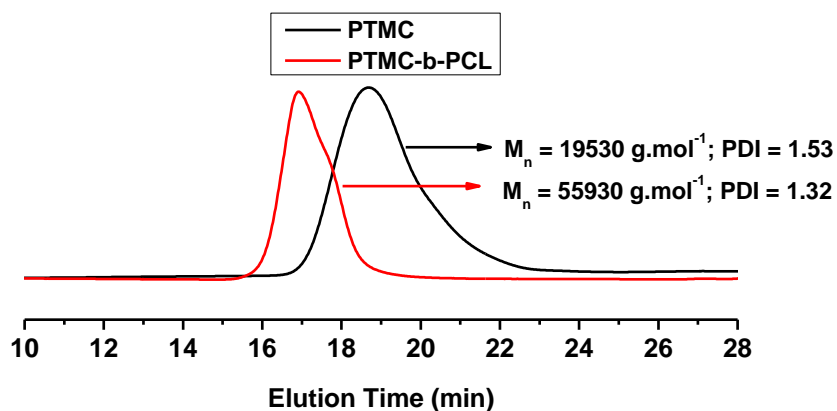


Figure 4.19. SEC traces of PTMC and the corresponding PTMC-b-PCL copolymer prepared using 4-Ti(OⁱPr)₂ in toluene at 70°C.

The copolymer was further characterized by ¹H and ¹³C NMR analysis as shown in Figure 4.20 & 4.21 respectively. The ¹H NMR analysis of the copolymer shows the characteristic signals corresponding to both TMC and ε-CL unit in the polymer. The presence of less intense signals at 1.22 ppm (doublet) as proton (a), 4.8 ppm (septet) as proton (i) and 3.59 ppm (triplet) as proton (h) indicates the presence of isopropyl and hydroxyl end group as chain end. The main chain methylene protons of ε-CL unit appeared as signals d, e, f, g and the main chain methylene protons of TMC unit appeared as signals b and c.

The molar composition of the copolymers was determined by relative intensity ratio of the resonance of PTMC (CH₂CH₂CH₂, at 1.95-2.01 ppm) and PCL (CH₂C(O), at 2.22-2.25 ppm) to the chain end signal at 1.22 ppm. The degree of polymerization (DP_n) of both TMC and ε-CL unit present in the copolymer was found to be 112 and 251 respectively. The molecular weight of the copolymer observed from the NMR was calculated to be 40110 g.mol⁻¹ and this value is in good agreement with the M_n calculated theoretically (M_{n, theory} = 44140 g.mol⁻¹).

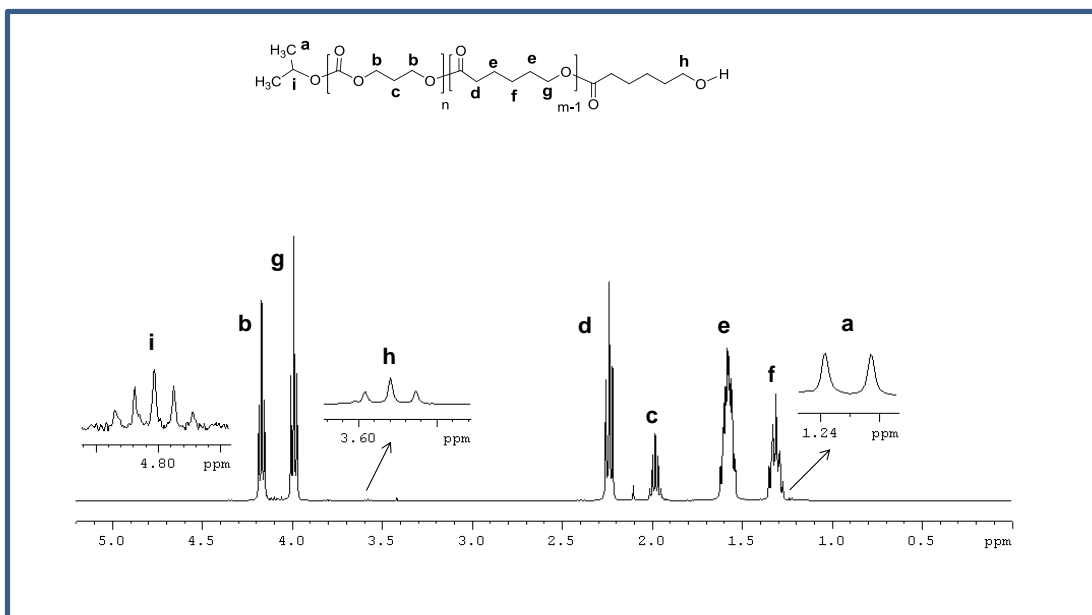


Figure 4.20. ¹H NMR spectrum of PTMC-*b*-PCL prepared using 4-Ti(O^{*i*}Pr)₂ in toluene at 70°C.

¹³C NMR spectrum of the copolymer PTMC₁₁₂-*b*-PCL₂₅₁ (Figure 4.20) shows two carbonyl resonance peaks at 173 ppm (**d**) and 154 ppm (**a**) corresponding to the PCL block and PTMC block respectively. The absence of any other peak between these two carbonyl group resonances clearly indicates the exclusive presence of carbonyl due to the homosequences TMC-TMC and CL-CL, and not any random heterosequences TMC-CL. This observation confirms the formation of truly block copolymer.

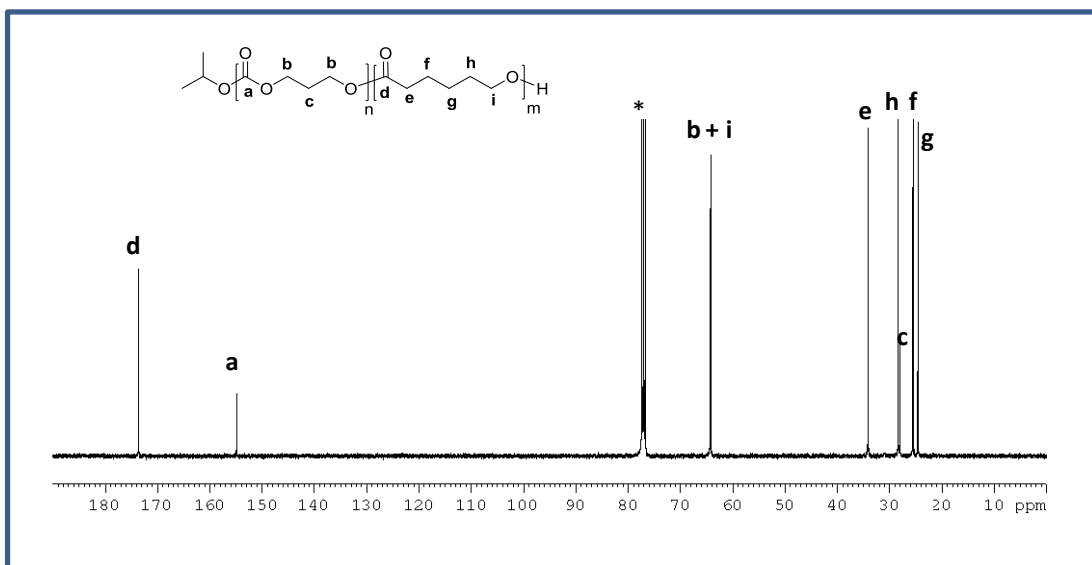


Figure 4.21. ¹³C NMR spectrum of PTMC-*b*-PCL prepared using 4-Ti(O^{*i*}Pr)₂ in toluene at 70°C.

Thermal analysis of both PTMC and PTMC-*block*-PCL was carried out by (DSC) in the range of temperature -60°C to 60°C for PTMC and -100°C to 100°C for the copolymer. The thermograms obtained during second heating scan are presented in Figure 4.22. PTMC shows T_g at -16.5°C , whereas the copolymer shows one melting peaks at 56.8°C corresponding to PCL block and two T_g at -61°C and -15°C corresponding to both PCL and PTMC block present in the copolymers respectively. This observation indicates the formation of purely block copolymer and not any random copolymer.

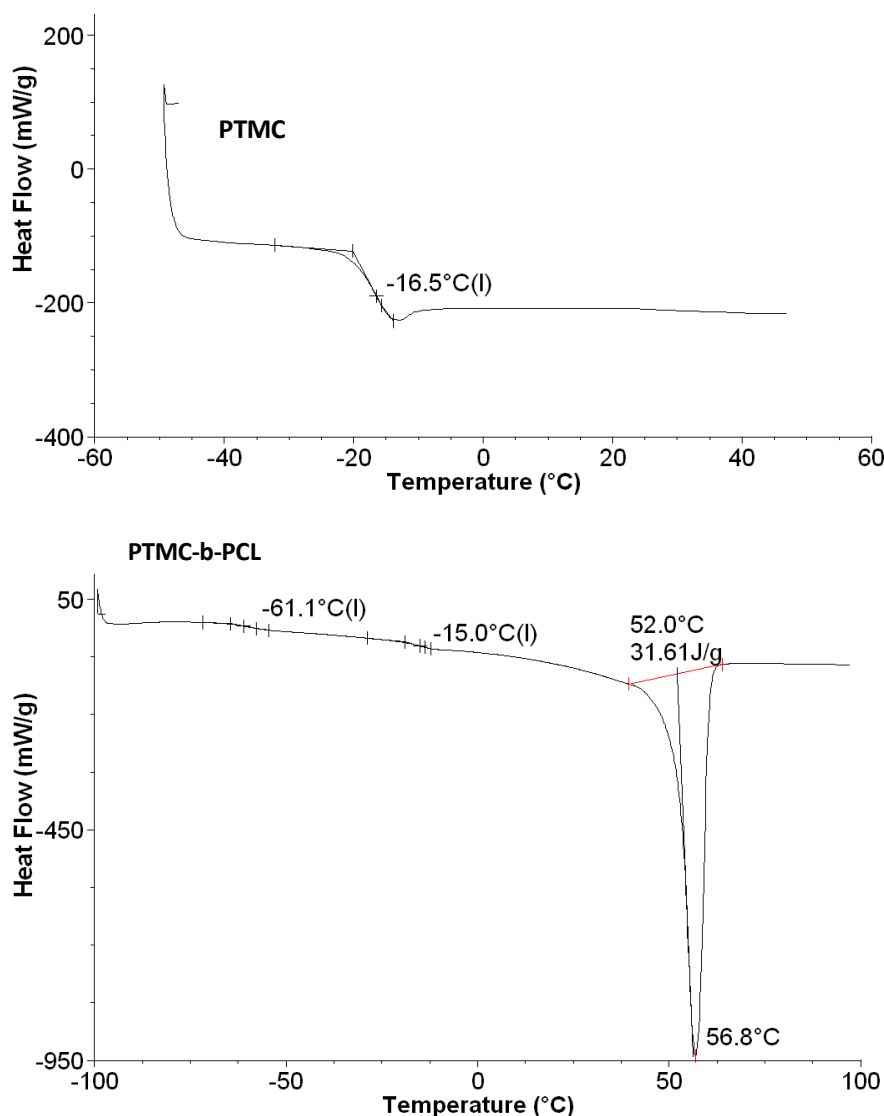


Figure 4.22. DSC thermograms of PTMC and PTMC-*b*-PCL.

4.3.2.2. Bulk polymerization of Trimethylene carbonate

In order to investigate the efficiency of this catalytic system for the polymerization of TMC under solvent free condition at higher temperature, melt polymerization of TMC has been carried out at different monomer to initiator ratio using the initiator 4-Ti(OⁱPr)₂ at 100°C for a period of 10 min. The results of these polymerizations are summarized in Table 4.5.

Table 4.5. Bulk polymerization of TMC using initiator 4-Ti(OⁱPr)₂^a

Run	[M]/[Ti]	Conv ^b (%)	M _n (NMR) ^c	M _n (theory) ^d	M _n (SEC) ^e	M _n (SEC) ^f	PDI ^e
1	100	99	5920	5080	8740	6380	1.62
2	200	87	6430	8910	14230	12520	1.76
3	300	82	9040	12590	17200	15140	1.89
4	400	79	14850	16160	24140	21240	1.70

^a Polymerization conditions: 0.2 g of TMC, polymerization time; 10 min, temperature = 100°C. ^b Conversion as determined via ¹H NMR through the intensity ratio of methylene signal (OCH₂-) at 4.37 ppm (monomer) to that at 4.15 ppm (polymer). ^c Calculated from intensity ratio of end-group isopropoxy methyl protons at 1.22 ppm to that of methylene protons at 2.0 ppm from the ¹H NMR spectra. ^d M_n(theory) was calculated from the formula ;((102.09 g mol⁻¹) × (conversion / 100) × [TMC]) / 2 × [Ti] + 60 (End group). ^e Determined by SEC (in THF) relative to polystyrene standards. ^f Determined by SEC (in THF) relative to polystyrene standards and corrected by correction factor of 0.88 for M_{n,SEC} > 10000, 0.73 for M_{n,SEC} < 10000.⁴³

As indicated in Table 4.5, we observed that the complex 4-Ti(OⁱPr)₂ acts as an efficient initiator (high monomer conversion was reached within 10 min). The percentage of monomer conversion decreases with the increase of the [M]/[Ti] molar ratio. Number average molecular weight of the polymer determined from SEC measurements were corrected, to reflect actual values by multiplication with a correction factor 0.88 for M_{n,SEC} > 10000 g.mol⁻¹ and 0.73 for M_{n,SEC} < 10000 g.mol⁻¹.⁴² The corrected molar mass values are in quite good agreement with the calculated values M_n(theory) at low [M]/[Ti] molar ratio and increases linearly with increasing [M]/[Ti] molar ratio (Figure 4.23), with PDI > 1.6, whereas deviation in molecular weight observed between theoretical and experimental ones increases with higher [M]/[Ti] mole ratio. These results suggest that polymerization is not very well controlled and transfer reactions take place with the occurrence of inter and intramolecular side reactions occurring during the chain propagation at high [M]/[Ti] ratio. The molar mass calculated from the NMR shows relatively good agreement with the M_n (theory). All these results suggest that the level of polymerization control is moderate under this condition.

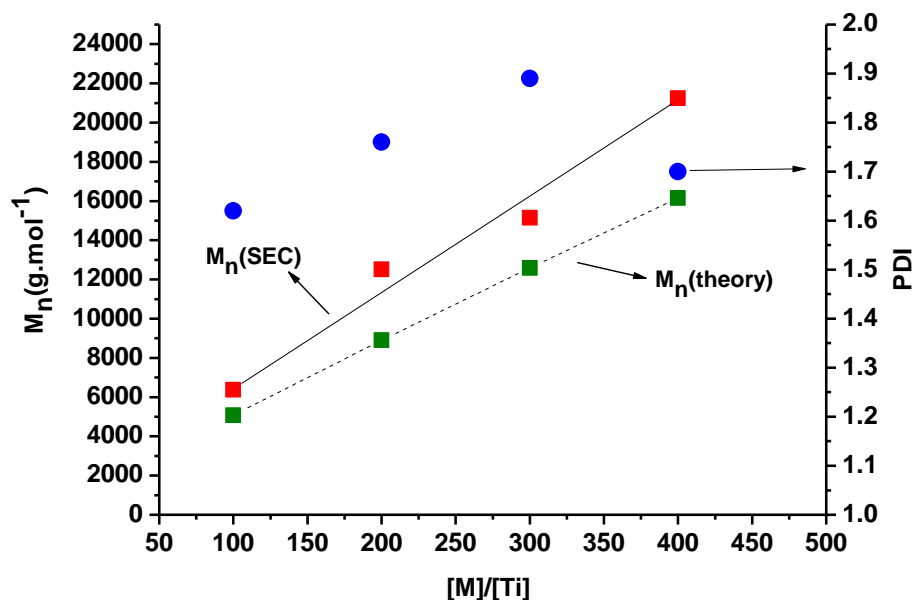


Figure 4.23. Plot of $M_n(\text{theory})$, $M_n(\text{SEC})^*$ and PDI as a function of $[\text{M}]/[\text{Ti}]$ ratio for ROP of TMC in melt at 100°C.

4.4. Conclusions

A series of titanium complexes 1-4-Ti(OⁱPr)₂ derived from aminodiols ligands of different symmetry were tested as initiator for the ring opening polymerization of ϵ -caprolactone. All complexes were shown to be active with good control over molecular weights and low molecular weight distributions both in solution and in bulk polymerization conditions. The end group of the polymer was analyzed by ¹H NMR and MALDI-TOF and indicated that the polymerization occurred through the insertion of monomer into the Ti-OⁱPr bond through a coordination insertion mechanism. Polymerization kinetic study revealed the “living” nature of the catalyst and this behavior was also confirmed from the two stage polymerization resumption experiment. The structure of the complexes does not play a key role in the activity of the polymerization, almost all the complexes were shown to have a similar level of activity. Under bulk polymerization condition, 80% conversion of monomer was reached within 10 min, with relatively narrow molecular weight distribution even under this drastic reaction conditions. The high activity and controlled nature of the polymerization may be due to the transannular interaction of the axial nitrogen atom to the titanium metal center.

Similarly, the same catalytic system has been utilized for ROP of β -BBL and produced polymer with controlled molecular weight distribution and the stereosequence analysis of the polymer suggest the formation of atactic polymer. ROP of TMC (trimethylene carbonate) also been tested by this catalytic system both in solution and bulk condition and produced polymer with reasonably controlled molecular weight distribution. End group analysis of the polymer indicates the coordination insertion mechanism.

4.5. References

- [1] Labet, M.; Thielemans, W. *Chem. Soc. Rev.* **2009**, 38, 3484.
- [2] Perez, Y.; Del Hierro, I.; Sierra, I.; Gómez-Sal, P.; Fajardo, M.; Otero, A. *J. Organomet Chem.* **2006**, 691, 3053.
- [3] Takeuchi, D.; Nakamura, T.; Aida, T. *Macromolecules.* **2000**, 33, 725.
- [4] Takashima, Y.; Nakayama, Y.; Watanabe, K.; Itono, T.; Ueyama, N.; Nakamura, A.; Yasuda, H.; Harada, A.; Okuda, J. *Macromolecules.* **2002**, 35, 7538.
- [5] Chmura, A. J.; Davidson, M. G.; Jones, M. D.; Lunn, M. D.; Mahon, M. F.; Johnson, A. F.; Khunkamchoo, P.; Roberts, S. L.; Wong, S. S. F. *Macromolecules.* **2006**, 39, 7250.
- [6] Piskun, Y. A.; Vasilenko, I. V.; Kostjuk, S. V.; Zaitsez, K. V.; Zaitseva, G. S.; Karlov, S. S. *J. Polym. Sci., Part A: Polym. Chem.* **2010**, 48, 1230.
- [7] Takashima, Y.; Nakayama, Y.; Watanabe, K.; Itono, T.; Ueyama, N.; Nakamura, A.; Yasuda, H.; Harada, A.; Okuda, J. *Macromolecules.* **2002**, 35, 7538.
- [8] Chmura, A. J.; Davidson, M. G.; Jones, M. D.; Lunn, M. D.; Mahon, M. F. *Dalton Trans.* **2006**, 887.
- [9] Kim, Y.; Jnaneshwara, G. K.; Verkade, J. G. *Inorg. Chem.* **2003**, 42, 1437.
- [10] Takashima, Y.; Nakayama, Y.; Hirao, T.; Yasuda, H.; Harada, A. *J. Organomet. Chem.* **2004**, 689, 612.
- [11] Akatsuka, M.; Aida, T.; Inoue, S. *Macromolecules.* **1995**, 28, 1320.
- [12] Barakat, I.; Jérôme, R.; Ph. T. J. *J. Polym. Sci., Part A: Polym. Chem.* **1993**, 31, 505.
- [13] Kricheldorf, H. R.; Berl, M.; Scharnagl, N. *Macromolecules.* **1988**, 21, 286.
- [14] Storey, R. F.; Sherman, J. W.; *Macromolecules.* **2002**, 35, 1504.
- [15] Mata-Mata, J. L.; Gutierrez, J. A.; Paz-Sandoval, M. A.; Madrigal, A. R.; Martinez-Richa, A. *J Polym Sci Part A: Polym Chem.* **2006**, 44, 6926.
- [16] Schwarz, A. D.; Thompson, A. L.; Mountford, P. *Inorg. Chem.* **2009**, 48, 10442.
- [17] Schwarz, A. D.; Herbert, K. R.; Paniagua, C.; Mountford, P. *Organometallics.* **2010**, 29, 4171.
- [18] Froese, R. D. J.; Musaev, D. G.; Matsubara, T.; Morokuma, K. *J. Am. Chem. Soc.* **1997**, 119, 7190.
- [19] Kim, Y.; Han, Y.; Hwang, J.-W.; Kim, M. W.; Do, Y. *Organometallics.* **2002**, 21, 1127.
- [20] Sudesh, K.; Abe, H.; Doi, Y. *Prog. Polym. Sci.* **2000**, 25, 1503.
- [21] Coulembier, O.; Dubois, P. *Handbook of Ring-Opening Polymerization*, Dubois, P.; Coulembier, O.; Raquez, J.-M. Eds., Wiley, Weinheim, **2009**, 227–25;4.
- [22] Thomas, C. M. *Chem. Soc. Rev.* **2010**, 39, 165.
- [23] Carpentier, J.-F.; *Macromol. Rapid Commun.* **2010**, 31, DOI: 10.1002/marc.201000114.
- [24] Yori, Y.; Suzuki, M.; Yamaguchi, A.; Nishishita, T. *Macromolecules.* **1993**, 26, 5533.
- [25] Moeller, M.; Kånge, R.; Hedrick, J. L. *J. Polym. Sci. Part A: Polym. Chem.* **2000**, 38, 2067.
- [26] Wu, B.; Lenz, R. W. *Macromolecules.* **1998**, 31, 3473.
- [27] Kricheldorf, H. R.; Eggerstedt, S. *Macromolecules.* **1997**, 30, 5693.
- [28] Rieth, L. R.; Moore, D. R.; Lobkovsky, E. B.; Coates, G. W. *J. Am. Chem. Soc.* **2002**, 124, 15239.

- [29] Ajellal, N.; Bouyahyi, M.; Amgoune, A.; Thomas, C. M.; Bondon, A.; Pillin, I.; Grohens, Y.; Carpentier, J.-F. *Macromolecules*. **2009**, *42*, 987 and references there in.
- [30] Rieth, L. R.; Moore, D. R.; Lobkovsky, E. B.; Coates, G. W. *J. Am.Chem. Soc.* **2002**, *124*, 15239.
- [31] Kurcok, P.; Dubois, P.; Jérôme, R. *Polym. Int.* **1996**, *41*, 479.
- [32] Andronova, N.; Albertsson, A. C. *Biomacromolecules*. **2006**, *7*, 1489.
- [33] Kricheldorf, H. R.; Rost, S. *Macromolecules*. **2005**, *38*, 8220.
- [34] Al-Azemi, T. F.; Harmon, J. P.; Bisht, K. S. *Biomacromolecules*. **2000**, *1*, 493.
- [35] Rokicki, G. *Prog. Polym. Sci.* **2000**, *25*, 259.
- [36] Helou, M.; Miserque, O.; Brusson, J.-M.; Carpentier, J.-F.; Guillaume, S. M. *Chem. Eur. J.* **2010**, *16*, 13805.
- [37] Ariga, T.; Takata, T.; Endo, T. *Macromolecules*. **1997**, *30*, 737.
- [38] Matsuo, J.; Aoki, K.; Sanda, F.; Endo, T. *Macromolecules*. **1998**, *31*, 4432.
- [39] Dobrzynski, P.; Kasperczyk, J. *J. Polym. Sci., Part A: Polym. Chem.* **2006**, *44*, 3184.
- [40] Varma, I. K.; Albertsson, A.-C.; Rajkhowa, R.; Srivastava, R. K.; *Prog. Polym. Sci.* **2005**, *30*, 949.
- [41] Koinuma, H.; Hirai, H. *Makromol. Chem.* **1977**, *178*, 241.
- [42] Palard, I. Schappacher, Belloncle, M.; Soum, B. A.; Guillaume, S. M. *Chem. Eur. J.* **2007**, *13*, 1511.
- [43] Ariga, T.; Takara, T.; Endo, T. *J. Polym. Sci. Part A: Polym. Chem.*, **1993**, *31*, 581.

CHAPTER 5

Living Ring Opening Block and Random copolymerization of ϵ -Caprolactone, *L*- and *rac*-Lactide

Living Ring Opening Block and Random copolymerization of ϵ -Caprolactone, *L*- and *rac*-Lactide

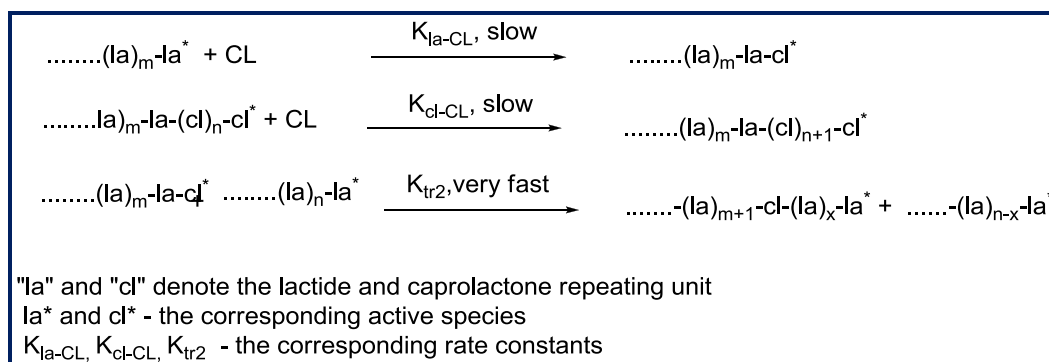
5.1. Introduction

Aliphatic polyesters such as ϵ -caprolactone (PCL) and polylactide (PLA) and their copolymers have received considerable interest in the medical field because of their biodegradable and biocompatible properties.¹⁻³ PCL is a semicrystalline polymer exhibiting remarkable drug permeability, elasticity, and thermal properties but poor mechanical properties. On the contrary PLA exhibits good mechanical properties but poor elasticity.^{4,5} Because the glass transition temperature of poly(*rac*-lactide) and poly(*L*-lactide) is above body temperature ($T_g \approx 60^\circ\text{C}$), these materials are stiff with poor elasticity in the human body. PCL is in the rubbery state at room temperature, exhibiting a glass transition temperature of -60°C . Moreover, PCL degrades much slower (half-life of about one year *in vivo*) than PLA which exhibits degradation with a half-life of about few weeks *in vivo*. Among the PLA, Poly(*L*-LA) degradation rate is much slower than that of Poly(*rac*-LA).⁶ Even though PLLA exhibits relatively good mechanical properties, its commercial products are limited by its brittleness and stiffness. Therefore, copolymerization or blending of PLA and PCL could allow the fabrication of a variety of biodegradable materials with improved properties (elasticity and degradability) compared with those of the parent homopolymers.^{7,8} Nevertheless, such high molecular weight PLLA/PCL blends are reported to be immiscible,⁹⁻¹² and thus desirable mechanical properties for specific applications may not be anticipated. If block copolymers of LA and CL are produced, then macrophase separation is avoided and a better control on the composition and morphology can be obtained.¹³

Moreover the combination of PCL drug permeability and the rapid degradation rate of PLA present in the copolymer may lead to a wide range of drug delivery devices with adjustable properties depending on the composition. By varying the copolymer composition, monomer sequencing, and molecular weight, the copolymer properties can be tailored to meet the requirements of various applications. These types of polyesters copolymers are commonly prepared from the ROP of cyclic esters. When two or more monomers of comparable reactivity can be polymerized in a living manner according to the same mechanism, their sequential polymerization leads to block copolymers. Therefore, the synthesis of block copolymers using different metal initiators such as Zn, Sn, Mg¹⁴⁻¹⁷ and random copolymers of ϵ -CL / LA using $\text{Al}(\text{O}^i\text{Pr})_3$, Lanthanides, $\text{Al}(\text{acac})_3$, Zn, $\text{Ti}(\text{OBu})_4$, Sn has been widely studied in recent years.¹⁸⁻²³ For example, Jérôme and *coll.* investigated the living sequential block copolymerization of ϵ -CL and other lactones or lactides using aluminium alkoxide as an initiator.^{24,25}

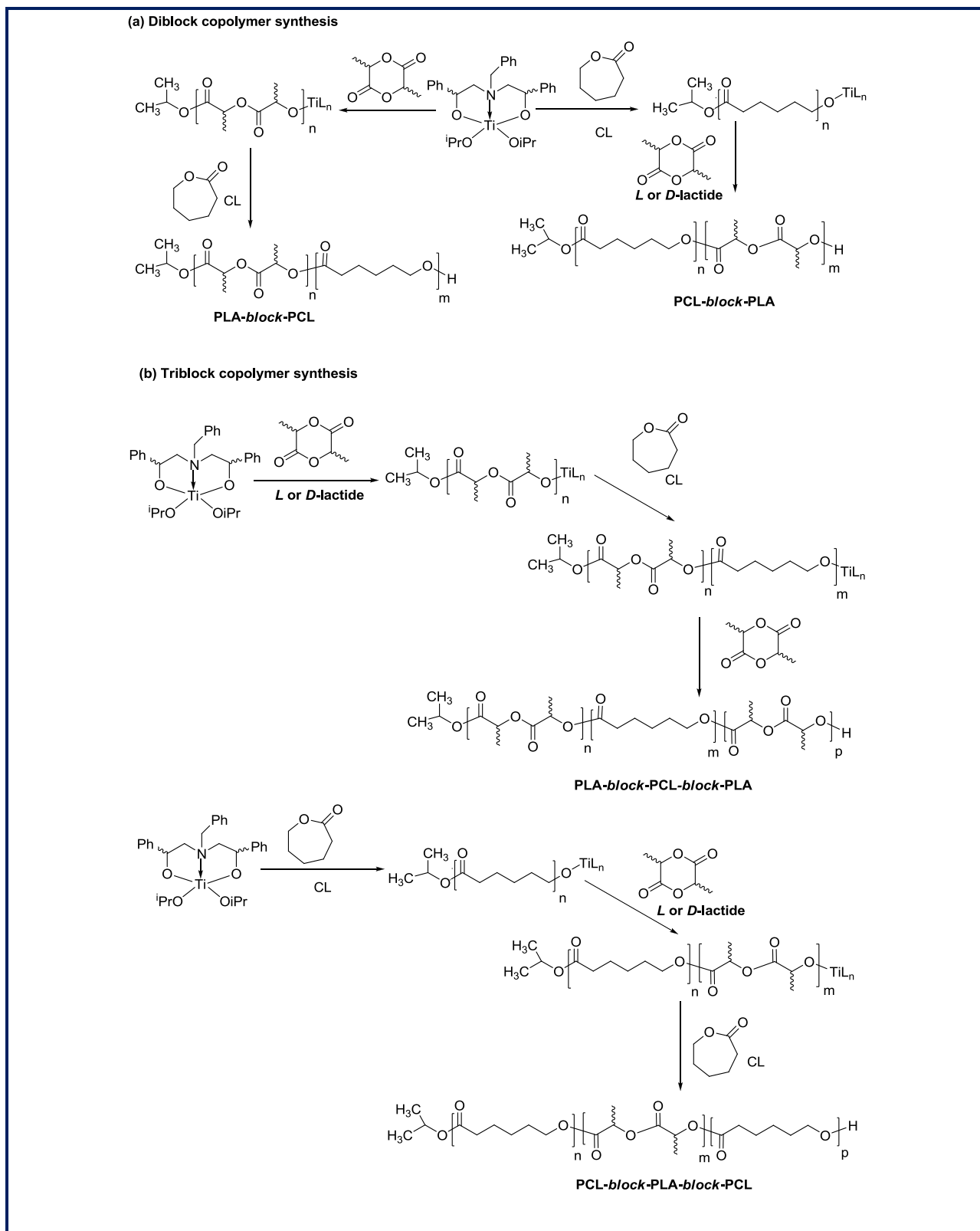
Feijen and *coll.* and Kim *et al.* reported the synthesis and crystallization behavior of linear PCL-*b*-PLA copolymer using a SnOct₂ catalyst.^{26,27} Recently salicylaldiminato aluminium complexes has been explored as a effective living initiator for the synthesis of block and random copolymerization of ε-CL and LA.¹³ On the contrary, only very few group 4 metal complexes used as initiators for the living ROP block copolymerization of cyclic esters have been reported in the literature.²⁸

Generally for sequential block copolymer synthesis of PCL and PLLA, the order of addition of monomers was critical. A series of papers has been reported in the literature using different metal based initiators (Al, Sm, Sn, La, Ti)²⁸⁻³⁴ claiming that CL could not be polymerized with the living polylactide (PLA*) i.e. when the LA monomer was polymerized first, the living PLA* does not initiate the PCL chain growth, because the PLA*+CL cross-propagation rate was lower than that of the PLA-CL*+PLA transesterification (Scheme 5.1).³⁵ However, recently few reports revealed that the living PLA* does initiate CL polymerization and diblock PLLA-*b*-PCL, PDLLA-*b*-PCL and triblock PLLA-*b*-PCL-*b*-PLLA copolymers were synthesized by using bulky Schiff's base as well as salicylaldiminato aluminium complexes.^{35,13}



Scheme 5.1. Sequential polymerization of LA and CL accompanied by the bimolecular transesterification.³⁵

Our interest is to further explore the use of group 4 metal based initiator for these types of block and random copolymer synthesis. We first attempted to synthesize diblock as well as triblock copolymers *via* sequential polymerization techniques (Scheme 5.2) using titanium alkoxide complexes 1-4-Ti(OⁱPr)₄ as initiators, since these complexes were found to be effective initiators for the homopolymerization of ε-caprolactone, *L* and *rac*-lactide, producing polymers with controlled molecular weight and molecular weight distribution (discussed in the previous chapters). Subsequently random copolymerization of ε-CL / LA was also performed by using the same initiators.



Scheme 5.2. Schematic representation of sequential diblock and triblock copolymer synthesis.

5.2. Results and Discussion

5.2.1. Diblock copolymer synthesis

5.2.1.1. PCL-*block*-PLLA

First, block copolymers were prepared by polymerizing first ϵ -CL at (70°C) in solution (toluene) using the initiator 1-Ti(OⁱPr)₂ with a monomer to initiator ratio of 300, to almost complete monomer conversion (3 h), then the second monomer (*L*-LA) was added to the polymerization medium with [M]/[Ti] = 117 and the polymerization was continued until complete monomer conversion (24 h) at the same temperature (Scheme 5.2). The polymerization was stopped by the addition of methanol. Similarly using the same initiator ϵ -CL was polymerized first at low temperature (25°C) and then the temperature was raised to (70°C) after adding the second monomer and the results are summarized in Table 5.1.

Table 5.1. Synthesis of Diblock copolymer PCL-*block*-PLLA^a

Entry	Mono/Di	M _n (theory)	M _n (NMR) ^e	M _n (SEC) ^f	PDI ^f	Yield (%)
	Block	(g.mol ⁻¹)	(g.mol ⁻¹)	(g.mol ⁻¹)		
1	PCL	17160 ^c	14500	35180	1.43	-
	PCL- <i>b</i> -PLLA	25660 ^d	24080	44210	1.46	91
2 ^b	PCL	17160	12490	27410	1.11	-
	PCL- <i>b</i> -PLLA	25440	23520	32970	1.17	93

^a Polymerization conditions: [CL] = 18 mmol; [*L*-LA] = 7 mmol; [Ti] = 6 × 10⁻² mmol; solvent : toluene = 15 mL; Temperature = 70°C. ^b Polymerization conditions: [CL] = 18 mmol; [*L*-LA] = 7 mmol; [Ti] = 6 × 10⁻² mmol; solvent : toluene = 15 mL; Temperature = 25°C (1st block) & 70°C (2nd block). ^c M.W_{CL} × [CL] / 2 [Ti] + 60 (End group). ^d M.W_{CL} × [CL] / 2 [Ti] + M.W_{L-LA} × [*L*-LA] / 2 [Ti] + 60. ^e Determined on the basis of the relative intensities ratio of the main chain methine proton of PLLA and the methylene protons of PCL to the corresponding end group proton. ^f Determined from SEC (in THF) relative to polystyrene standards.

The polymer was analyzed by SEC, ¹H & ¹³C NMR, and DSC measurements. As expected in the SEC profile (Figure 5.1) the block copolymer showed a unimodal peak with an increase in molecular weight (M_n = 44210 g.mol⁻¹; PDI = 1.46) compare to the homo polymer PCL with (M_n = 35180 g.mol⁻¹; PDI = 1.41). In addition, the unimodal SEC profile also implies that there is no homopolymer detected in the copolymer sample with a controlled molecular weight distribution.

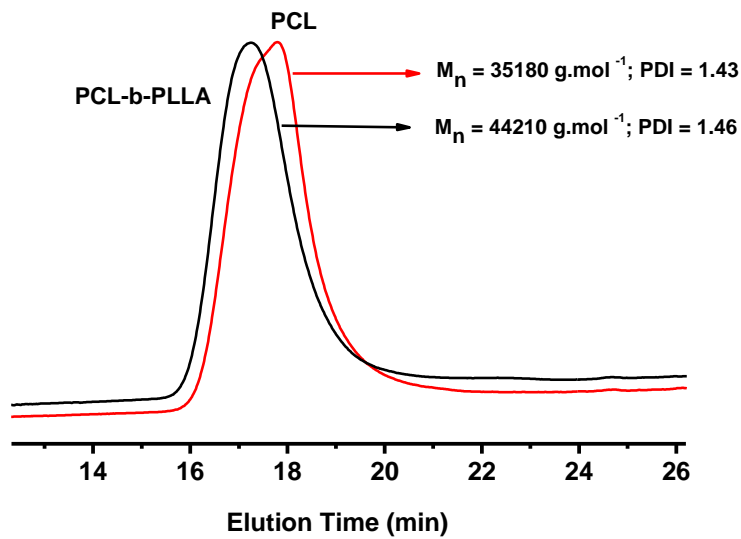


Figure 5.1. SEC traces of PCL and the corresponding PCL-*block*-PLLA copolymer prepared using 1-Ti(OⁱPr)₂ (Table 5.1, Entry 1).

The ¹H NMR spectrum of Poly(CL-*block*-PLA) copolymer (Figure 5.2) shows signals at 5.08 ppm and 4.05 ppm assigned to the main chain methine protons (**h**) and the methylene protons (**f**) of L-LA and ε-CL respectively. The two polymer chain ends which should be acyl-isopropoxide-COOCH(CH₃)₂ group and hydroxyl methylene-CH(CH₃)OH group are confirmed by proton signals at 1.15 ppm (doublet) as proton (**a**) and at 4.29 ppm (quartet) as proton (**i**). The absence of signals at 3.57 ppm suggests that the absence of ε-CL prepolymer chain. While all other signals corresponding to both ε-CL and L-LA is observed in the spectrum.

The $M_{n,NMR}$ of the block copolymer was calculated from the relative intensity of signals at 5.08 ppm (main chain methine proton of PLLA block) and at 4.05 ppm (main chain methylene proton of PCL block) with the corresponding end group signal at 1.15 ppm and 4.29 ppm. The M_n of the PCL segment is found to be 15810 g.mol⁻¹ and that of PLLA segment found to be 8210 g.mol⁻¹. These values are in good agreement with theoretical molecular weight ($M_{n,PCL} = 17100$ g.mol⁻¹; $M_{n,PLLA} = 8500$ g.mol⁻¹) calculated by assuming two polymer chains were grown per metal center taking 100% conversion into account (Table 5.1).

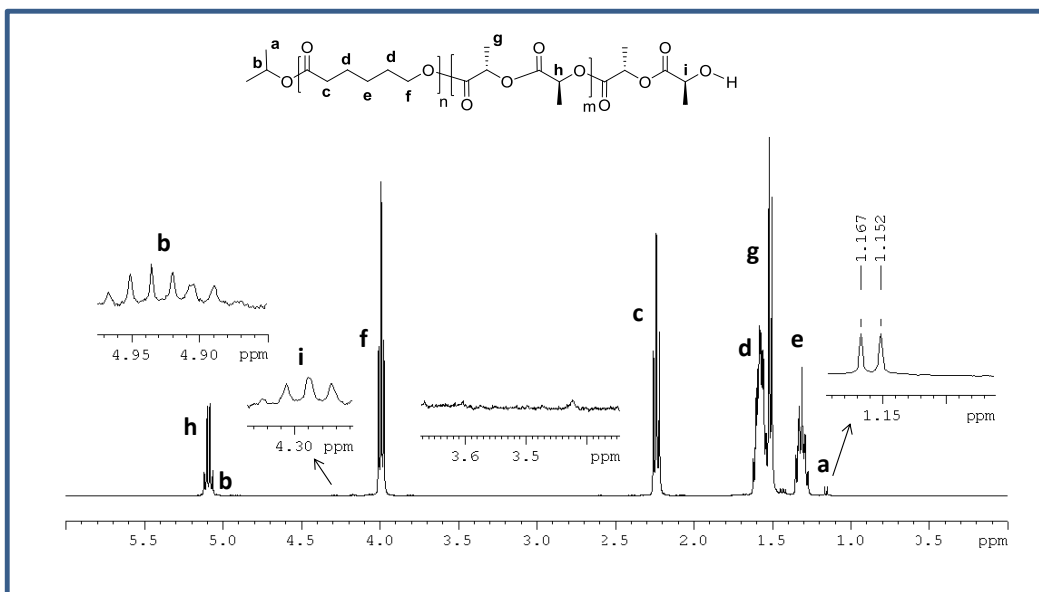


Figure 5.2. ^1H NMR spectrum of PCL-*block*-PLLA copolymer synthesized using $1\text{-Ti}(\text{O}^i\text{Pr})_2$.

The formation of block copolymer was also confirmed from the ^{13}C NMR spectrum (Figure 5.3) showing two carbonyl resonance peaks at 173.5 ppm and 169.6 ppm corresponding to the PCL and PLLA block respectively. The absence of any other peak between these two carbonyl groups revealed the exclusive presence of carbonyl due to the homosequences CL-CL and LA-LA, and not any random heterosequences CL-LA which normally arises due to transesterification reaction. This observation confirms the formation of truly block copolymers and not any random copolymer.¹⁸ The respective carbon group resonance are properly assigned in the spectrum and the end group carbon resonance is not assigned due to the very less intense signal as compare to the other carbon group.

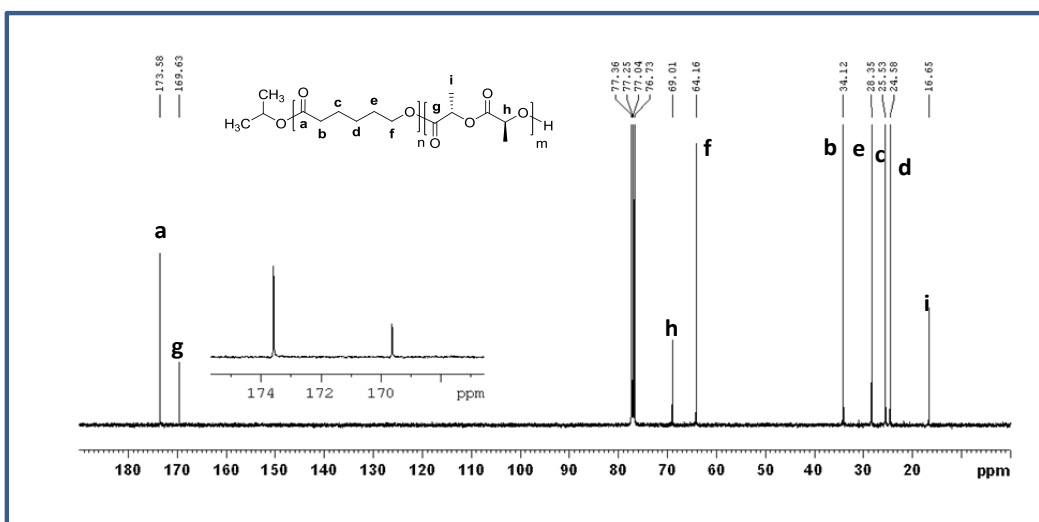


Figure 5.3. ^{13}C NMR spectrum of PCL-*block*-PLLA copolymer synthesized using $1\text{-Ti}(\text{O}^i\text{Pr})_2$.

Thermal analysis of the copolymers was carried out by means of differential scanning calorimetry (DSC), in the range of temperature -100°C to 200°C . Figure 5.4 presents the DSC thermograms of PCL-*b*-PLLA copolymer obtained during the second heating. It displayed two melting peaks (T_m) at 55°C and 158°C , and a glass transition temperature (T_g) at -56°C belonging to PCL (T_g of PLLA is difficult to assign, since (T_m) of PCL and (T_g) of PLLA are in the same temperature range). These results again indicate the formation of block copolymers because in the case of random copolymers or racemization only one melting point with a value between those of PLA and PCL would be observed. These results demonstrate that a pure diblock copolymer has been synthesized successfully.

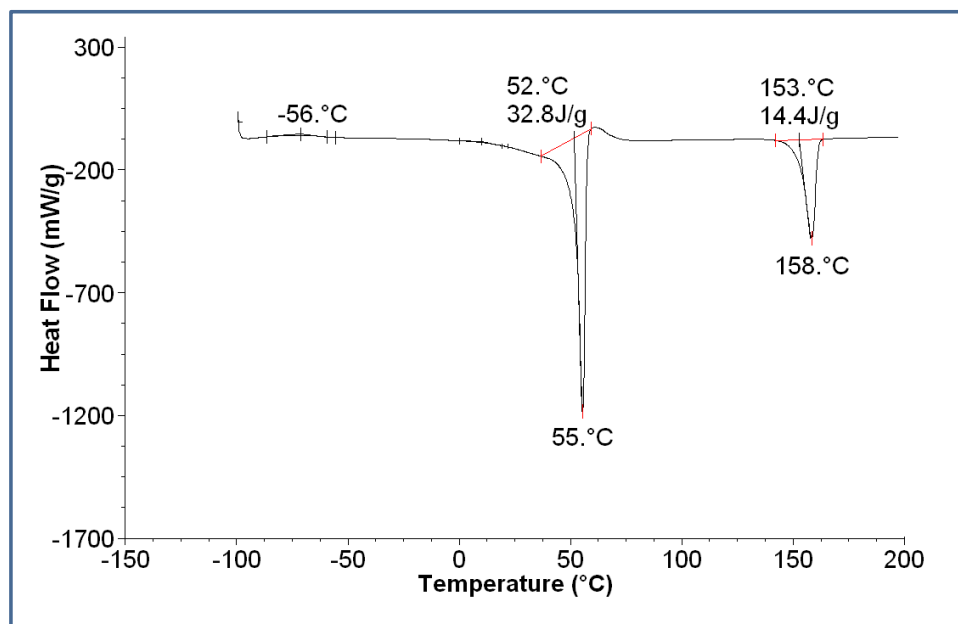


Figure 5.4. DSC analysis of PCL-*block*-PLLA copolymer synthesized using $1\text{-Ti}(\text{O}^i\text{Pr})_2$.

5.2.1.2. PLLA-*block*-PCL

In order to explore further the formation of diblock copolymers, the 'Poly(*L*-LA) block first' route was examined using group 4 metal complexes. We attempted to synthesize the diblock copolymer PLLA-*b*-PCL using the initiator $1\text{-Ti}(\text{O}^i\text{Pr})_2$ in solution (toluene) at 70°C (Scheme 5.2). To start with this approach, polymerization of *L*-LA was performed in toluene solution at 70°C until complete monomer conversion (24 h) (Table 5.2, Entry 1). Then the second monomer $\epsilon\text{-CL}$ was added at the same temperature, the polymerization was continued until complete monomer conversion (3 h).

Table 5.2. Synthesis of Diblock copolymer PLLA-*block*-PCL^a

Entry	Catalyst	Mono/Di	M _n (theory)	M _n (NMR) ^d	M _n (SEC) ^e	PDI ^e	Yield (%)
		Block	(g.mol ⁻¹)	(g.mol ⁻¹)	(g.mol ⁻¹)		
1	1-Ti(O ⁱ Pr) ₂	PLLA	21660 ^b	27130	30480	1.58	-
		PLLA- <i>b</i> -PCL	43950 ^c	30410	56880 40900 ^f	1.48 1.31	91
2	2-Ti(O ⁱ Pr) ₂	PLLA	21660	28480	45650	1.34	-
		PLLA- <i>b</i> -PCL	43950	32080	58880	1.36	89
3	3-Ti(O ⁱ Pr) ₂	PLLA	21660	27080	35660	1.36	-
		PLLA- <i>b</i> -PCL	43950	31770	41910	1.43	85
4	4-Ti(O ⁱ Pr) ₂	PLLA	21660	22240	28870	1.31	-
		PLLA- <i>b</i> -PCL	43950	31850	34980 ^f	1.33	81

^a Polymerization conditions: [L-LA] = 6.9 mmol; [CL] = 9 mmol, [Ti] = 2.3 × 10⁻² mmol; solvent : toluene = 15 mL; Temperature = 70°C. ^b M.W_{L-LA} × [L-LA] / 2 [Ti] + 60 (End group). ^c M.W_{L-LA} × [L-LA] / 2 [Ti] + M.W_{CL} × [CL] / 2 [Ti] + 60. ^d Determined on the basis of the relative intensities ratio of the main chain methine proton of PLLA and the methylene protons of PCL to the corresponding end group proton. ^e Determined from SEC (in THF) relative to polystyrene standards. ^f Determined from triple detection SEC (in THF) using light scattering detector (dn / dc = 0.065, calculated from the molar composition of each block from the NMR).

The obtained polymer was first analyzed by SEC (Figure 5.5). As expected, block copolymer showed unimodal peak with an increase in molecular weight and relatively controlled molecular weight distribution (M_n = 56880 g.mol⁻¹; PDI = 1.48) compare to the homo polymer PLLA (M_n = 30480 g mol⁻¹; PDI = 1.58). M_ns determined by SEC with an RI detector are typically higher compared to the actual values, since polystyrene standards were used for the calibration.³⁶

The same polymer was then analyzed by triple detection (SEC) in THF in order to find out the accurate molar mass of the block copolymer. To this end, the dn/dc value is required. Since dn/dc depends on the sample type and on the composition, for copolymers dn/dc value is often not constant within the copolymer, whereas the molar mass determination of the block copolymers with a narrow molar mass distribution can be assumed to be give values close to the true molar masses.^{37,38} The dn/dc of the polymer PLLA(x)-*block*-PCL(y)- was calculated from the molar composition of both PCL (dn/dc = 0.079 × x) and PLLA (dn/dc = 0.058 × y) observed from the NMR.

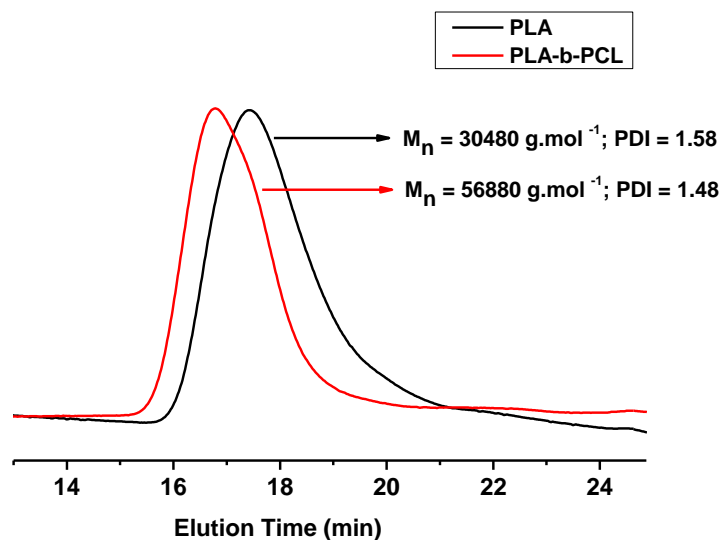


Figure 5.5. SEC traces of PLLA and the corresponding PLLA-*block*-PCL copolymer prepared using 1-Ti(OⁱPr)₂ (Table 5.2, Entry 1).

Chromatograms of the polymer PLLA-*b*-PCL presented in Figure 5.6 showed M_n of 40900 g.mol⁻¹ (2% error) by using light scattering detector ($dn/dc = 0.065$) and this value is close to the M_n calculated theoretically (43950 g.mol⁻¹) (Table 5.2, Entry 1).

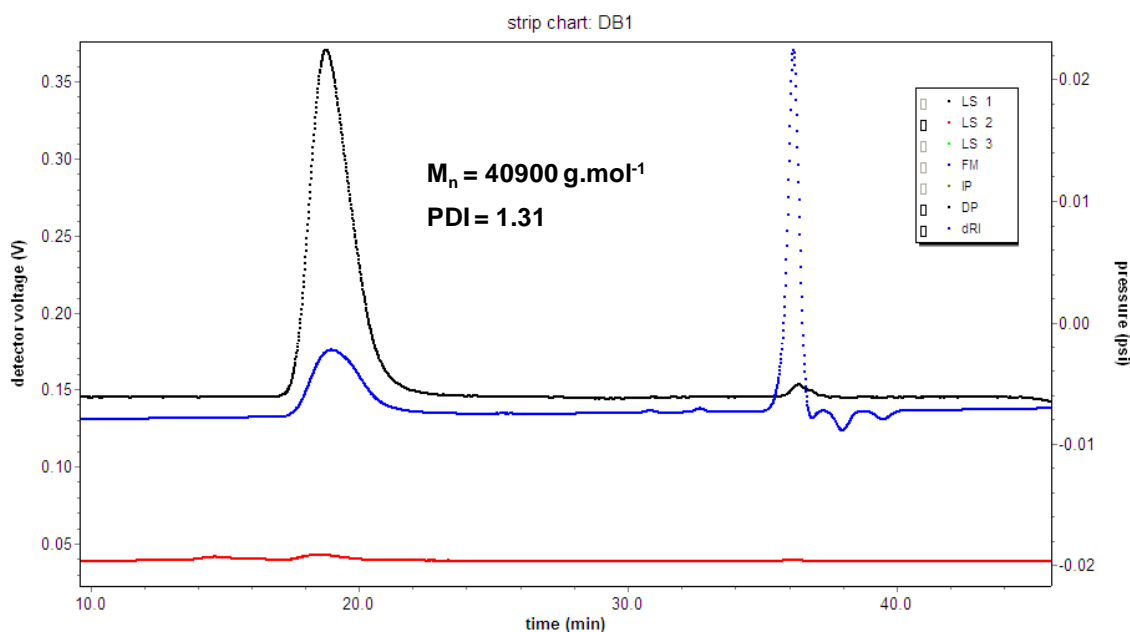


Figure 5.6. Triple chromatogram of PLLA-*block*-PCL copolymer prepared using 1-Ti(OⁱPr)₂.

Further evidence for the formation of block copolymers is also provided from the analysis of ^1H & ^{13}C NMR spectroscopy (Figure 5.7 and 5.8). It is observed from the ^1H NMR spectrum that the signals at 5.09 ppm and 3.99 ppm should be assigned to the main chain methine protons (**g**) and methylene protons (**f**) of *L*-LA and ϵ -CL respectively. The presence of less intense peaks at 1.17 ppm (doublet of doublet) as proton (**a**), at 3.57 ppm (triplet) as proton (**h**) corresponding to the polymer chain end groups of isopropoxy methyl and hydroxyl methylene protons respectively. The expanded spectrum shows signals at 4.28 ppm which could be due to chains terminated by LA unit, coming either from unreacted “first block” macroinitiators or from transesterification reactions. All other signals corresponding to both ϵ -CL and *L*-LA are observed in the spectrum.

The $M_{n,\text{NMR}}$ of the copolymer was calculated from the relative intensity of signals at 5.09 ppm (main chain methine proton of PLLA block) and at 3.99 ppm (main chain methylene proton of PCL block) with the corresponding end group signal at 1.17 ppm and 3.57 ppm. The M_n of the PLLA segment is found to be $18720 \text{ g}\cdot\text{mol}^{-1}$ which is reasonably in good agreement with theoretical molecular weight ($M_{n,\text{theory, PLLA}} = 21600 \text{ g}\cdot\text{mol}^{-1}$), whereas for PCL segment the molecular weight observed from the NMR $11630 \text{ g}\cdot\text{mol}^{-1}$ is lower than the theoretical molecular weight ($M_{n,\text{theory, PCL}} = 17100 \text{ g}\cdot\text{mol}^{-1}$). This also indicates that ϵ -CL is not consumed completely in the copolymerization.

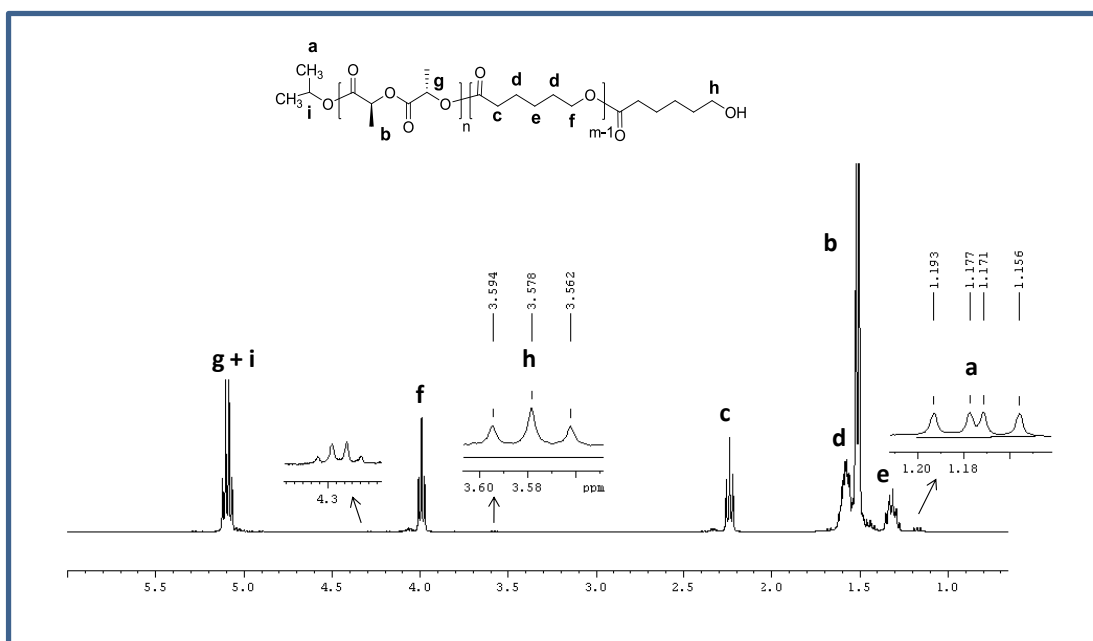


Figure 5.7. ^1H NMR spectrum of PLLA-*block*-PCL copolymer synthesized using $1\text{-Ti}(\text{O}^i\text{Pr})_2$.

^{13}C NMR spectrum of the polymer PLLA-*block*-PCL is presented in Figure 5.8 with proper assignments. It also confirms the formation of block copolymer due to the absence of peaks in the carbonyl region due to CL-LA heterosequences.

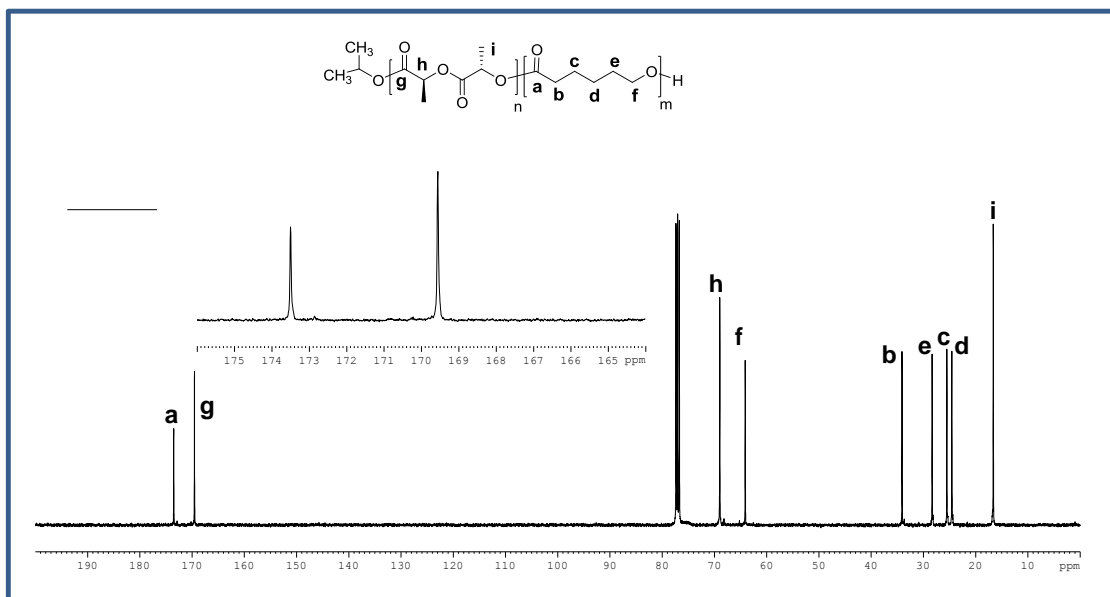


Figure 5.8 ^{13}C NMR spectrum of PLLA-*block*-PCL copolymer synthesized using 1-Ti(O^{*i*}Pr)₂.

This type of block copolymer was also synthesized with other titanium complexes 2-4-Ti(O^{*i*}Pr)₂ adopting the same polymerization conditions (Table 5.2). From the Table, we observe an increase of the molecular weight of the block copolymer relative to that of the first PLLA block. These results suggest that all complexes were found to be efficient initiator and could be able to produce block copolymers (starting with LA for the first block) with reasonably controlled molecular weight distribution, whereas the molar mass observed from the NMR is comparatively less than M_n (theory).

Thermal analysis of the PLLA-*b*-PCL copolymers (Table 5.2) obtained from the initiators 1, 3, and 4-Ti(O^{*i*}Pr)₂ was carried out by DSC in the range of temperature -100°C to 200°C. All initiators gave a copolymer with similar thermal properties. The thermograms obtained during the second heating scan are presented in Figure 5.9, and it shows two melting peaks (T_m) at (46-48°C, PCL) and (164-167°C, PLLA), and a glass transition temperatures (T_g) at (-49 to -61°C, PCL) belonging to PCL block present in each copolymer, whereas T_g of PLLA block is difficult to assign. This result indicates that the two different phase structure exist in the copolymer. Additionally crystallization temperature (T_c) at 76°C belonging to PLLA block was observed for the copolymer obtained from the initiator 4-Ti(O^{*i*}Pr)₂. Again, the presence of two different melting temperatures indicates the absence of random copolymer.

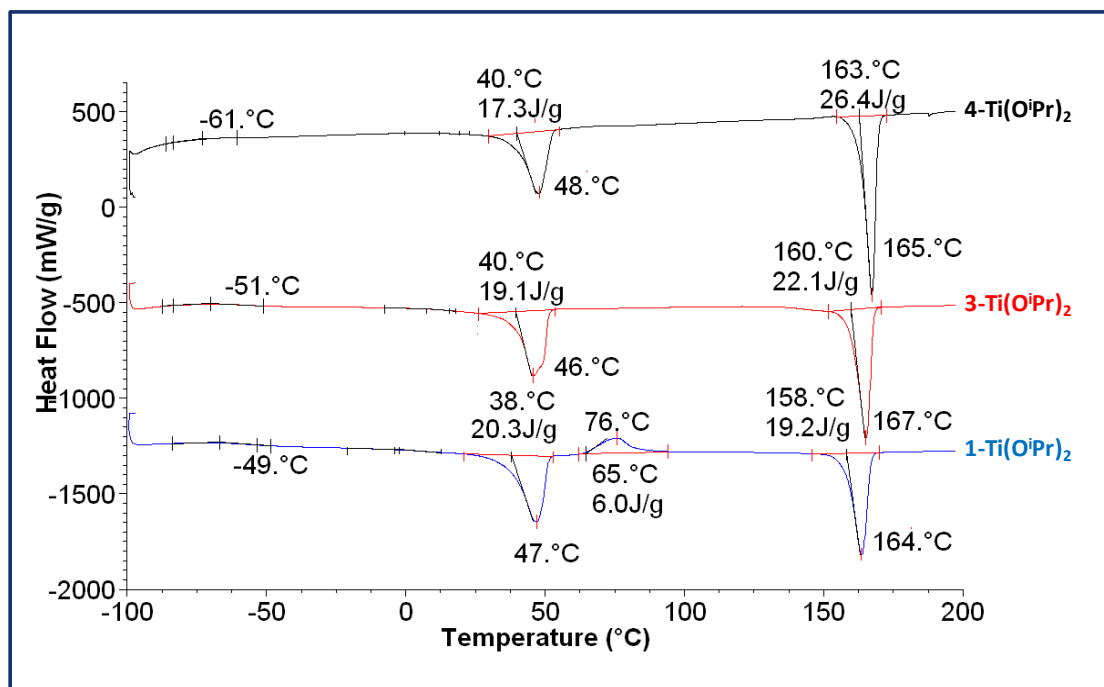


Figure 5.9. DSC analysis of PLLA-*block*-PCL copolymer prepared using 1, 3, 4-Ti(OⁱPr)₂.

5.2.1.3. PDLLA-*block*-PCL

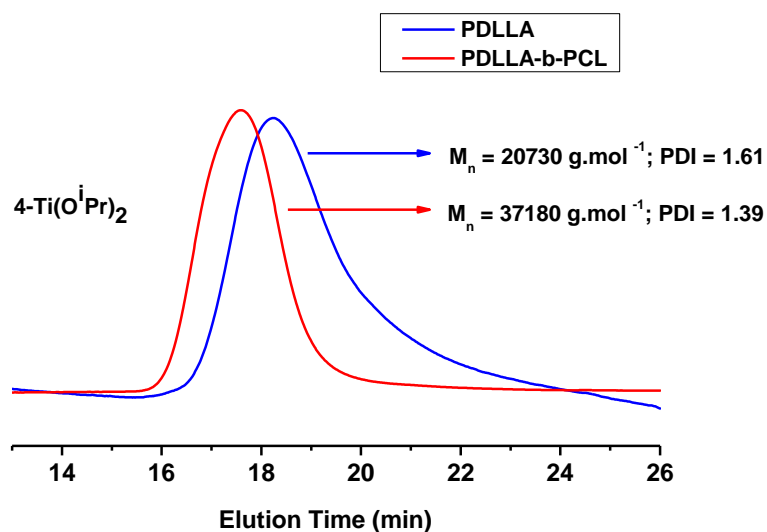
Block copolymers of the type Poly(*DL*-LA-*block*- ϵ -CL) was also prepared by sequential polymerization technique starting with *DL*-LA as the first monomer in solution (toluene) condition at 70°C with a monomer to initiator ratio of 300 using the initiators 2-4-Ti(OⁱPr)₂ (Table 5.3). After complete conversion of *DL*-LA, second monomer (ϵ -CL) was added and the polymerization was continued until complete conversion of ϵ -CL.

Copolymers obtained from all the initiators were shown increase in molecular weight with unimodal molar mass distribution from SEC analysis. For example, the copolymer obtained with the initiator 4-Ti(OⁱPr)₂ shows an expected shift to higher molar masses ($M_n = 37180 \text{ g}\cdot\text{mol}^{-1}$; PDI = 1.39) for PDLLA-*b*-PCL copolymer compared to the homopolymer PDLLA ($M_n = 20730 \text{ g}\cdot\text{mol}^{-1}$; PDI = 1.61) (Figure 5.10). In order to find out the true molar mass, the polymer synthesized with 2-Ti(OⁱPr)₂ was analyzed by SEC using LS detector. The molar mass determined by LS detector was evaluated at $20120 \text{ g}\cdot\text{mol}^{-1}$ (2% error), which is much less than the theoretical molecular weight of $38760 \text{ g}\cdot\text{mol}^{-1}$ whereas M_n calculated from the NMR ($38500 \text{ g}\cdot\text{mol}^{-1}$) is in good agreement with the theoretical one. The observed low molecular weight from SEC analysis is not clear, same tendency is observed for the copolymer obtained from the initiator 3-Ti(OⁱPr)₂.

Table 5.3. Synthesis of Diblock copolymer PDLLA-*block*-PCL^a

Entry	Catalyst	Mono/Di	M _n	M _n	M _n	PDI ^e	Yield (%)
		Block	(theory)	(NMR) ^d	(SEC) ^e		
			(g.mol ⁻¹)	(g.mol ⁻¹)	(g.mol ⁻¹)		
1	2-Ti(O ⁱ Pr) ₂	PDLLA	21660 ^b	26090	26790	1.39	
		PDLLA- <i>b</i> -PCL	38760 ^c	38500	32770 20120 ^f	1.39 1.28	79
2	3-Ti(O ⁱ Pr) ₂	PDLLA	21660	31300	14300	1.54	-
		PDLLA- <i>b</i> -PCL	38760	34990	24100 25560 ^f	1.30 1.36	83
3	4-Ti(O ⁱ Pr) ₂	PDLLA	21660	20990	20730	1.61	-
		PDLLA- <i>b</i> -PCL	38760	30330	37180	1.39	86

^a Polymerization conditions: [DL-LA] = 6.9 mmol; [CL] = 6.9 mmol, [Ti] = 2.3 × 10⁻² mmol; solvent : toluene = 15 mL; Temperature = 70°C. ^b M.W_{L-LA} × [L-LA] / 2 [Ti] + 60. ^c M.W_{L-LA} × [L-LA] / 2 [Ti] + M.W_{CL} × [CL] / 2 [Ti] + 60. ^d Determined on the basis of the relative intensities ratio of the main chain methine proton of PLLA and the methylene protons of PCL to the corresponding end group proton. ^e Determined from SEC (in THF) relative to polystyrene standards. ^f Determined from triple detection SEC (in THF) using light scattering detector (dn/dc = 0.065, calculated from the molar composition of each block from the NMR).

**Figure 5.10.** SEC traces of PDLLA and the corresponding PDLLA-*block*-PCL copolymer prepared using 4-Ti(OⁱPr)₂.

^1H & ^{13}C NMR spectra of diblock copolymer PDLLA-*b*-PCL were shown in Figures 5.11 & 5.12 respectively. As it can be seen on the ^1H NMR spectrum, the signals due to the isopropoxy methyl chain end group appeared at 1.17 ppm as proton (a) and hydroxyl methylene group appeared at 3.57 ppm as proton (h). The signals at 5.12 ppm (multiplet) and at 1.5 ppm (multiplet) are due to the main chain methine (g) and methyl protons (b) of PDLLA respectively. The presence of the PCL block in the copolymer was confirmed by the signals at 4.00 ppm (triplet) as proton (f), 2.22 ppm (triplet) as proton (c), 1.6 ppm (multiplet) as proton (b) and 1.3 ppm (multiplet) as proton (e) for the methylene protons of the backbone. However, the expanded spectrum shows signals at 4.29 ppm which could be due to chains terminated by LA unit, coming either from unreacted “first block” macroinitiators or from transesterification reactions. All other signals corresponding to both ϵ -CL and *DL*-LA are observed in the spectrum.

The molecular weight of each block was calculated from ^1H NMR through the relative intensity of signals due to the main chain methine and methylene proton of PDLLA and PCL respectively ($M_{n, \text{PDLLA}} = 26350 \text{ g.mol}^{-1}$; $M_{n, \text{PCL}} = 12080 \text{ g.mol}^{-1}$). These values are reasonably comparable to the theoretical molecular weight ($M_{n, \text{PDLLA}} = 21600 \text{ g.mol}^{-1}$; $M_{n, \text{PCL}} = 17100 \text{ g.mol}^{-1}$) (Table 5.3).

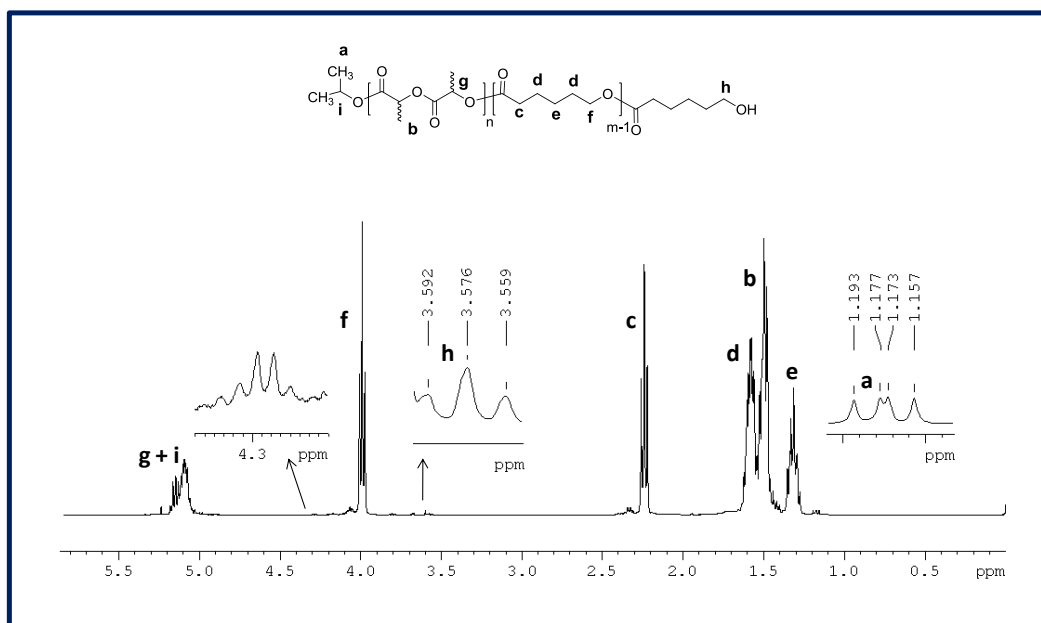


Figure 5.11. ^1H NMR spectrum of PDLLA-*block*-PCL copolymer synthesized using $2\text{-Ti}(\text{O}^i\text{Pr})_2$.

From the ^{13}C NMR spectroscopy, two pairs of signals in the area of the carbonyl region at 173.5 ppm (a) and 169.1-169.6 ppm (g) (multiplet due to random stereo sequences of carbonyl group in the PDLLA backbone) and methylene and methine carbon resonance at 64.1 ppm (f) & 68.2 ppm (h) proves the presence of PCL and PDLLA block respectively.

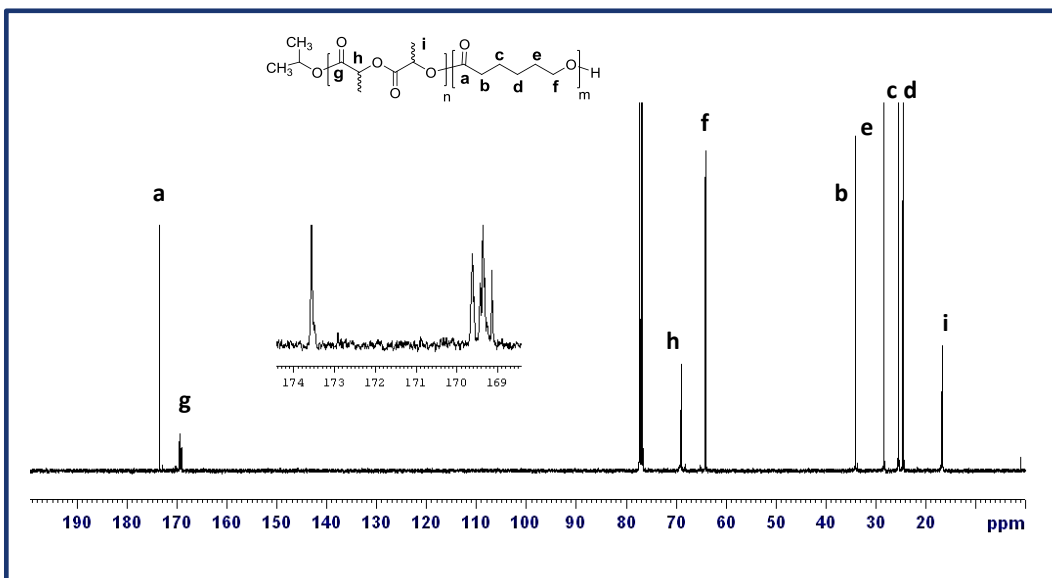


Figure 5.12. ^{13}C NMR spectrum of PDLLA-*block*-PCL copolymer synthesized using 4-Ti(OⁱPr)₂.

Thermal analysis of the PDLLA-*b*-PCL copolymer was carried out by means of differential scanning calorimetry (DSC), in the range of temperature -100°C to 200°C (Figure 5.13). The copolymer shows only one melting peaks (T_m) at 51°C corresponding to PCL block, and a glass transition temperatures (T_g) at -52°C belonging to PCL. The T_g of PDLLA block is difficult to determine accurately, because T_g of PDLLA and the T_m of PCL are in the same range in the copolymer.

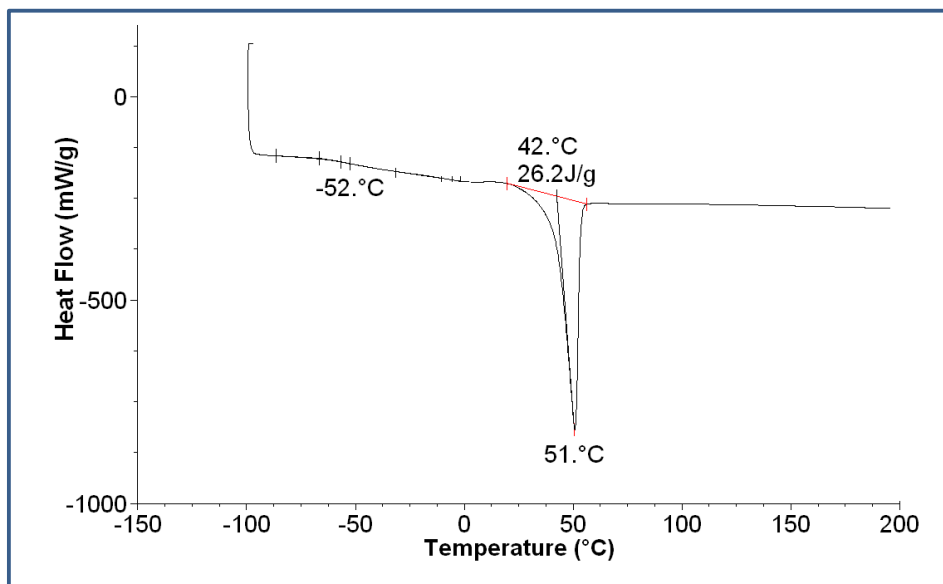


Figure 5.13. DSC analysis of PDLLA-*block*-PCL copolymer prepared using 2-Ti(OⁱPr)₂.

5.2.2. Triblock copolymer synthesis

5.2.2.1. PCL-*b*-PLLA-*b*-PCL

Synthesis of diblock copolymer with controlled molecular weight distribution confirmed the living nature of the polymerization for both lactide and caprolactone. Taking advantage of this “living” behavior, we attempted to synthesize triblock copolymer of the type PCL-*b*-PLLA-*b*-PCL in a similar manner by sequentially polymerizing ϵ -CL, L-LA and ϵ -CL again using the initiator 1-Ti(OⁱPr)₂ in toluene solution at 70°C (Scheme 5.2) and the results are summarized in Table 5.4. Aliquots were taken from the reaction mixture at each stage of the polymerization after complete monomer conversion in order to characterize the first and the second block, the triblock copolymer was then characterized by ¹H & ¹³C NMR, SEC and DSC analysis. The final copolymer yield is 91%.

Table 5.4. Synthesis of Triblock copolymer PCL-*b*-PLLA-*b*-PCL^a

Entry	M _n (theory)	M _n (NMR) ^e	M _n (SEC) ^f	PDI ^f
	(g.mol ⁻¹)	(g.mol ⁻¹)	(g.mol ⁻¹)	
PCL	17160 ^b	15850	28970	1.27
PCL- <i>b</i> -PLLA	25550 ^c	28810	38290	1.27
PCL- <i>b</i> -PLLA- <i>b</i> -PCL	42660 ^d	40870	55710 40880 ^g	1.56 1.50

^a Polymerization conditions: [CL]₁ = 9 mmol; [L-LA]₀ = 3.5 mmol; [CL]₂ = 9 mmol; [Ti] = 3 × 10⁻² mmol ; solvent: toluene = 15 mL; Temperature = 70°C. ^b M.W_{CL} × [CL]₁ / 2 [Ti] + 60; ^c M.W_{CL} × [CL]₁ / 2 [Ti] + M.W_{L-LA} × [L-LA]₀ / 2 [Ti] + 60. ^d M.W_{CL} × [CL]₁ / 2 [Ti] + M.W_{L-LA} × [L-LA]₀ / 2 [Ti] + M.W_{CL} × [CL]₂ / 2 [Ti] + 60. ^e Determined on the basis of the relative intensities ratio of the main chain methylene protons of PCL and the methine proton of PLLA to the corresponding end group protons. ^f Determined from SEC (in THF) relative to polystyrene standards. ^g Determined from triple detection SEC (in THF) using light scattering detector (dn/dc = 0.069, calculated from the molar composition of each block from the NMR).

On the SEC profile (Figure 5.14), an increase of the molecular weight with unimodal distribution going from first block (PCL of M_n = 28970 g.mol⁻¹) to diblock (PCL-*b*-PLLA of M_n = 38280 g.mol⁻¹) and to triblock (PCL-*b*-PLLA-*b*-PCL of M_n = 55710 g.mol⁻¹) was observed (Table 5.4). The same polymer was also analyzed by triple detection SEC in THF. The molar mass determined by LS detector was shown to be M_n = 40880 g.mol⁻¹ (2% error) and is comparable to molar mass determined from the NMR (40870 g.mol⁻¹) and theoretically (42660 g.mol⁻¹).

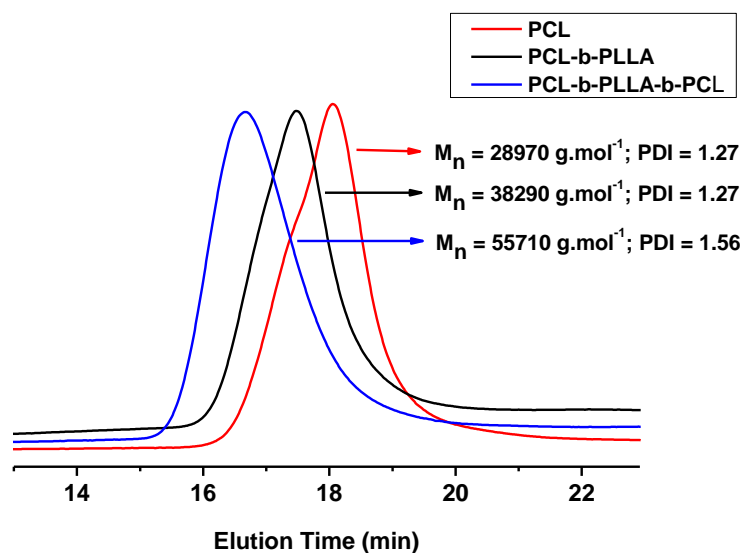


Figure 5.14. SEC traces of PCL, PCL-*b*-PLLA and the corresponding PCL-*b*-PLLA-*b*-PCL triblock copolymer.

Figure 5.15 illustrates the ^1H NMR spectrum of PCL-*b*-PLLA-*b*-PCL copolymer. End group signals at 1.15 ppm of proton (**a**) and 3.57 ppm of proton (**h**) are observed, while a signal corresponding to hydroxyl methyne-CH(CH₃)OH proton signal at 4.3 ppm of the PCL-*b*-PLLA prepolymer is also observed in the spectrum. This probably implies that few PCL-*b*-PLLA prepolymer chains do not initiate the polymerization of the third CL block. The degree of polymerization (DP_n) of ϵ -CL and *L*-LA unit present in the copolymer was found to be 267 and 72 respectively. The total molecular weight calculated from the NMR spectroscopy ($M_{n,\text{NMR}} = 40870 \text{ g. mol}^{-1}$) was reasonably in good agreement with theoretical molecular weight ($M_{n,\text{theory}} = 42660 \text{ g. mol}^{-1}$) (Table 5.4).

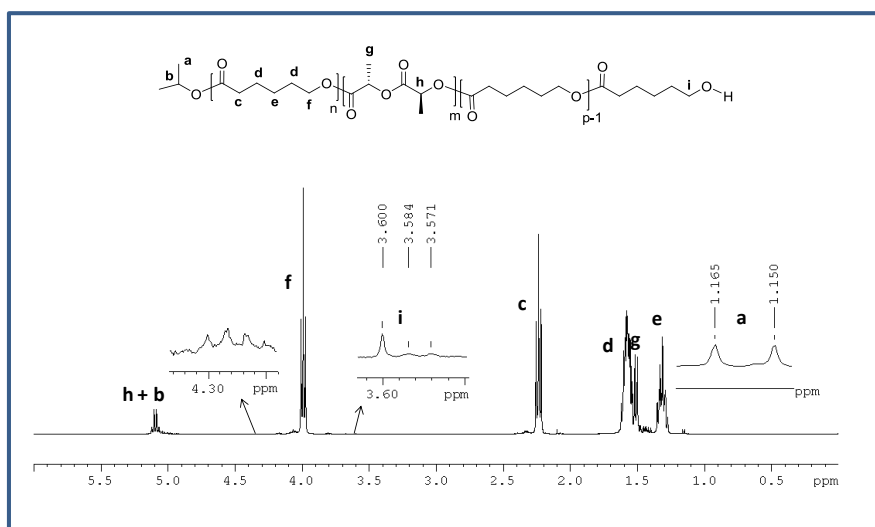


Figure 5.15. ^1H NMR spectrum of PCL-*block*-PLLA-*block*-PCL triblock copolymer.

^{13}C NMR spectrum of PCL-*b*-PLLA-*b*-PCL (Figure 5.16) shows two carbonyl resonance peaks at 173.5 ppm and 169.6 ppm corresponding to the PCL block and PLLA block respectively. The absence of any other peak between the two carbonyl group resonances, as seen in the expanded spectrum, indicates the formation of homosequences CL-CL and LA-LA unit, while the peaks corresponding to random heterosequences were not observed. Thus the formation of truly block copolymer can be assumed.

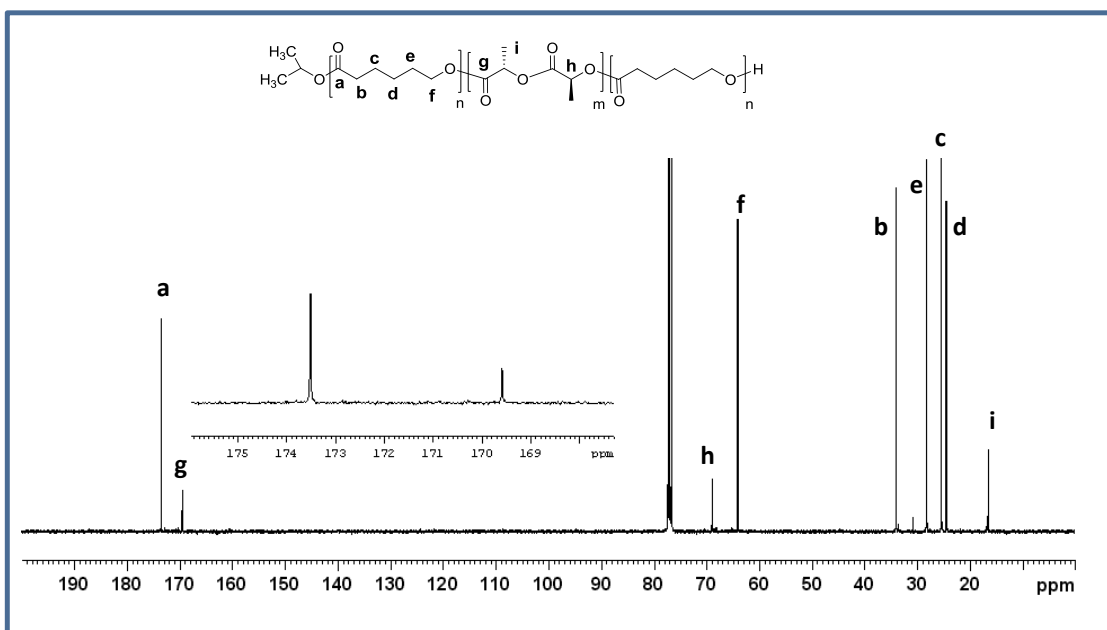


Figure 5.16. ^{13}C NMR spectrum of PCL-*block*-PLLA-*block*-PCL triblock copolymer.

The formation of block copolymer was also confirmed from the DSC analysis (Figure 5.17). As in the case of diblock copolymer PCL-*b*-PLLA, the copolymer PCL-*b*-PLLA-*b*-PCL also shows two melting peaks (T_m) at 52°C and 137°C, and two glass transition temperatures (T_g) at -43°C and 22°C, belonging to PCL and PLLA respectively. However the melting temperature as well as glass transition temperature of PLLA unit was found to be less than that of the pure homopolymer PLLA, and this could be due to the effect of increased composition of PCL block in the copolymer or to the fact that the PLLA is the central block in the copolymer. Nonetheless these results indicate the formation of triblock copolymer which exhibited two different phases in the polymer.

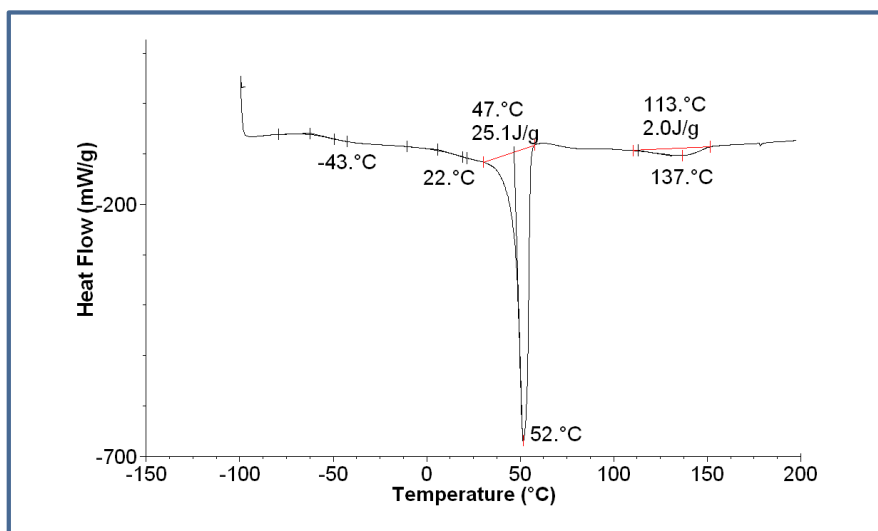


Figure 5.17. DSC analysis of PCL-*block*-PLLA-*block*-PCL triblock copolymer.

5.2.2.2. PLLA-*block*-PCL-*block*-PLLA

Triblock copolymer of the type PLLA-*b*-PCL-*b*-PLLA was also synthesized by sequential polymerization technique. The polymerization was started with *L*-LA as the first monomer using the initiator 1-Ti(O^{*i*}Pr)₂ with a monomer to initiator ratio of 100 in toluene solution at 70°C, followed by successive addition of ε-CL and *L*-LA (Scheme 5.2). Results are summarized in Table 5.5. Aliquots were taken from the reaction mixture at each stage of the polymerization after complete monomer conversion in order to characterize the first and the second block. The final copolymer yield is 89%.

Table 5.5. Synthesis of Triblock copolymer PLLA-*b*-PCL-*b*-PLLA^a

Entry	M _n (theory)	M _n (NMR) ^e	M _n (SEC) ^f	PDI ^f
	(g.mol ⁻¹)	(g.mol ⁻¹)	(g.mol ⁻¹)	
PLLA	7260 ^b	8060	15410	1.29
PLLA- <i>b</i> - PCL	37410 ^c	26710	82830	1.26
PLLA- <i>b</i> - PCL- <i>b</i> - PLLA	44670 ^d	35420	93000 40180 ^g	1.25 1.47

^a Polymerization conditions: [L-LA]₁ = 3.4 mmol; [CL] = 18 mmol; [L-LA]₂ = 3.4 mmol; [Ti] = 3.4 × 10⁻² mmol; solvent: toluene = 15mL; Temperature = 70°C. ^b M.W._{L-LA} × [L-LA]₁ / 2 [Ti] + 60. ^c M.W._{L-LA} × [L-LA]₁ / 2 [Ti] + M.W._{CL} × [CL] / 2 [Ti] + 60. ^d M.W._{L-LA} × [L-LA]₁ / 2 [Ti] + M.W._{CL} × [CL] / 2 [Ti] + M.W._{L-LA} × [L-LA]₂ / 2 [Ti] + 60. ^e Determined on the basis of the relative intensities ratio of the main chain methine proton of PLLA and the methylene protons of PCL to the corresponding end group proton. ^f Determined from SEC (in THF) relative to polystyrene standards. ^g Determined from triple detection SEC (in THF) using light scattering detector (dn/dc = 0.074, calculated from the molar composition of each block from the NMR).

In the SEC profile (Figure 5.18) an expected shift to higher molar masses with unimodal distribution was observed after the formation of each block. The first PLLA block showed M_n of 15410 g.mol^{-1} with PDI of 1.29, the diblock copolymer PLLA-*b*-PCL shifts to M_n of 82830 g.mol^{-1} with PDI of 1.26 and the triblock copolymer PLLA-*b*-PCL-*b*-PLLA showed M_n of 93000 g.mol^{-1} with PDI of 1.25. This observation shows the formation of triblock copolymer, however M_n value obtained from conventional SEC analysis found to be higher than the theoretical molecular weight and those calculated from the NMR spectroscopy (Table 5.4). The polymer was analyzed by triple detection SEC using LS detector and show M_n of 40180 g.mol^{-1} (1% error) which is comparable to molar mass determined from the NMR (35420 g.mol^{-1}) and theoretically (44670 g.mol^{-1}).

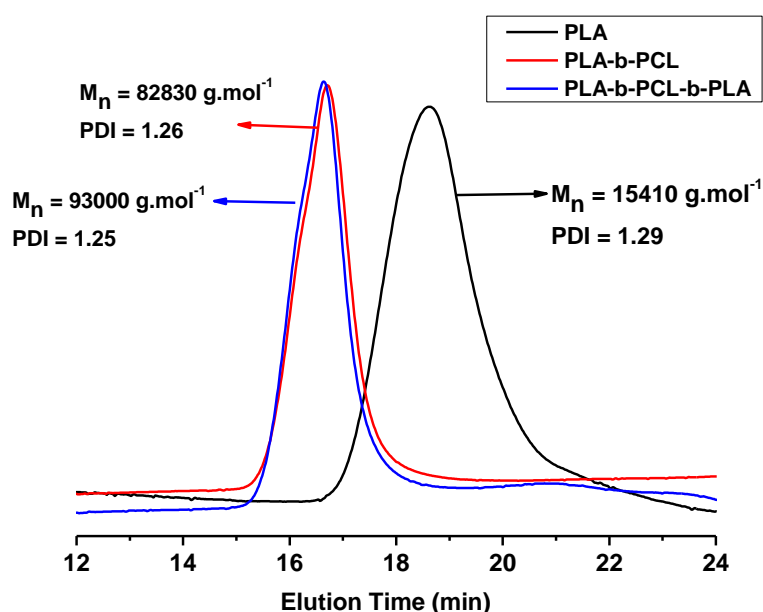


Figure 5.18. SEC traces of PLLA, PLLA-*b*-PCL, and the corresponding PLLA-*b*-PCL-*b*-PLLA triblock copolymer.

On the ^1H NMR spectrum of PLLA-*block*-PCL-*block*-PLLA copolymer presented in Figure 5.19, end group signals at 1.17 ppm for protons (**a**) and at 4.29 ppm for proton (**h**) are observed. The absence of signal at 3.57 ppm indicates that PLLA-*b*-PCL prepolymer can initiate the third block more efficiently than the PCL-*b*-PLLA prepolymer. The degree of polymerization (DP_n) of *L*-LA unit and ϵ -CL unit present in the copolymer PLLA-*b*-PCL-*b*-PLLA calculated from the ^1H NMR spectroscopy was found to be 79 and 163 respectively. The total molecular weight calculated from the NMR spectroscopy ($M_{n,\text{NMR}} = 35420 \text{ g.mol}^{-1}$) was found to be less than the theoretical molecular weight ($M_{n,\text{theory}} = 44670 \text{ g.mol}^{-1}$) (Table 5.5).

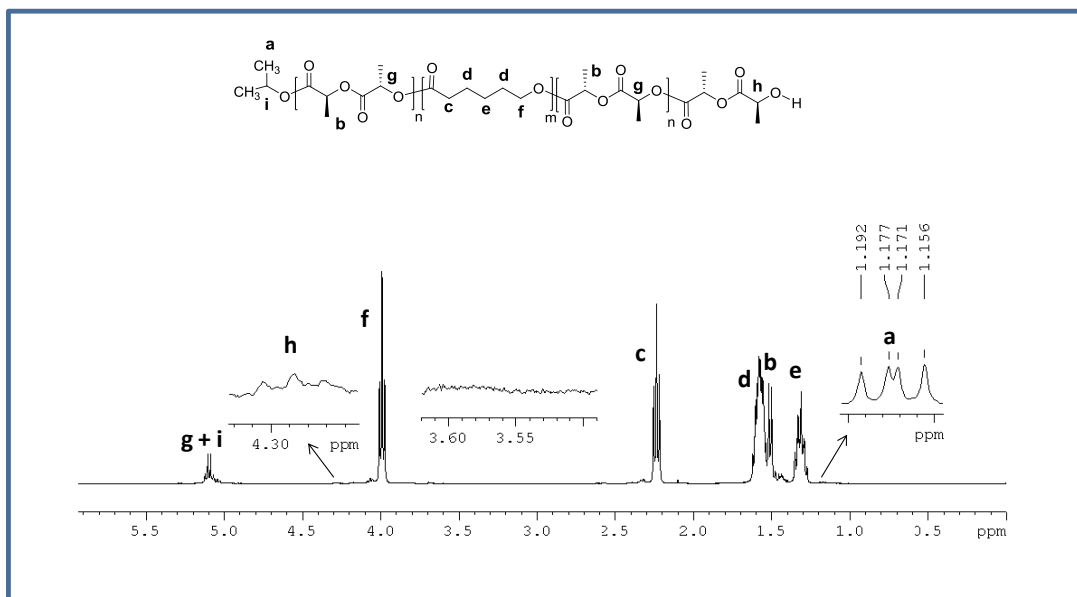


Figure 5.19. ^1H NMR spectrum of PLLA-*block*-PCL-*block*-PLLA triblock copolymer.

^{13}C NMR spectrum of PLLA-*b*-PCL-*b*-PLLA (Figure 5.20) shows two carbonyl resonance peaks at 173.5 ppm and 169.5 ppm corresponding to the PCL block and PLLA block respectively. The absence of any other peak between these two carbonyl group resonances as seen in the expanded spectrum, indicate the formation of truly block copolymer without any transesterification reactions.

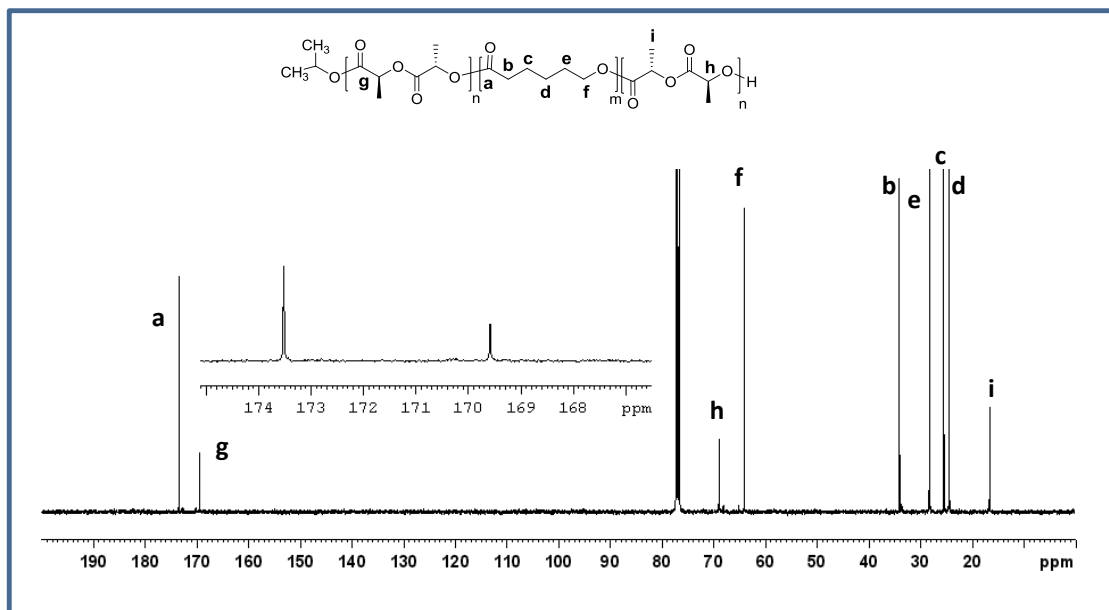


Figure 5.20. ^{13}C NMR spectrum of PLLA-*block*-PCL-*block*-PLLA triblock copolymer.

The formation of block copolymer was also confirmed from the DSC analysis (Figure 5.21). As in the case of diblock copolymers PLLA-*b*-PCL, the copolymer PLLA-*b*-PCL-*b*-PLLA also shows two melting peaks (T_m) at 52°C and 159°C, and a glass transition temperature (T_g) at -49°C belonging to PCL. A crystallization temperature (T_c) at 79°C belonging to PLLA unit was also observed in the spectrum. The effect of composition of PCL units present in the copolymer decreases the T_m of PLLA units as compare to the homopolymer of L-LA. It also indicates the existence of two different phase system present in the copolymer. All these results suggest that the formation of triblock copolymer PLLA-*b*-PCL-*b*-PLLA has been achieved using the initiator 1-Ti(O^{*i*}Pr)₂.

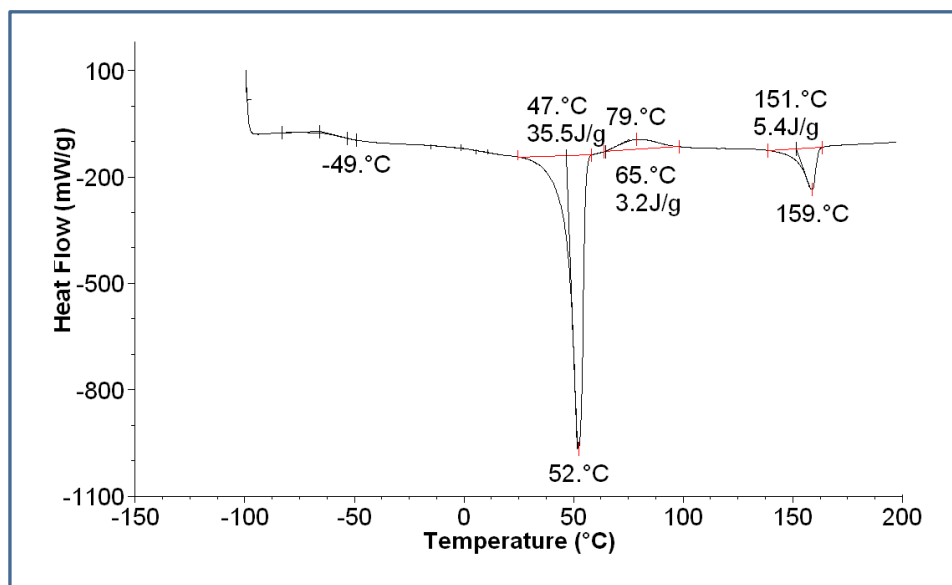
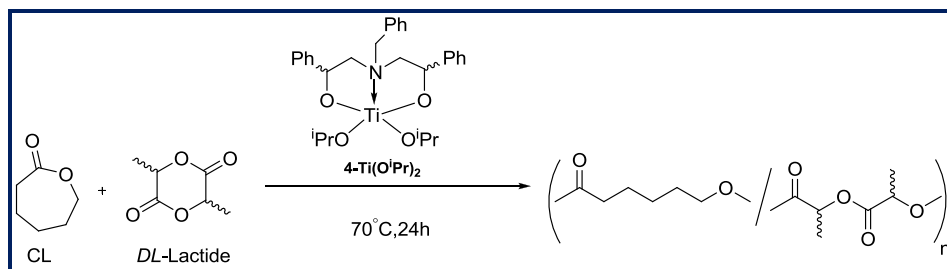


Figure 5.21. DSC analysis of PLLA-*block*-PCL-*block*-PLLA copolymer.

5.2.3. Random copolymerizations

In order to gain further insight into the ROP of cyclic esters by these titanium complexes 1-4-Ti(O^{*i*}Pr)₂, their behavior in the random copolymerization of *DL* / L-LA and ϵ -caprolactone was investigated both in melt and solution conditions.

To start with, random copolymerization of *D,L*-LA and ϵ -CL was carried out at various molar ratio of ϵ -CL / *DL*-LA in toluene at 70°C using the initiator 4-Ti(O^{*i*}Pr)₂ (Scheme 5.3). The copolymerization was started by mixing the appropriate proportion of the two monomers and the catalyst, in conditions similar to those used for the preparation of the parent homopolymers in solution condition for a period of 24 h. The copolymers were characterized by ¹H and ¹³C NMR spectroscopy, SEC and DSC analysis. The results are summarized in Table 5.6.



Scheme 5.3. Copolymerization of ϵ -caprolactone with *D,L*-Lactide using the initiator 4-Ti(OⁱPr)₂.

Table 5.6. Copolymerization of ϵ -CL and *D,L*-Lactide with 4-Ti(OⁱPr)₂ in solution

Run	[ϵ -CL] (mmol)	[LA] (mmol)	CL/LA in copolymer ^b (mol %)	L _{CL} ^c	L _{LA} ^d	T _g (°C)	Yield (%)	M _n ^e (g.mol ⁻¹)	PDI ^e
1	1.73	3.46	15/85	1.4	3.3	25	64	17480	1.22
2	3.46	3.46	34/66	2.3	1.5	-nd-	57	23580	1.50
3	3.46	1.73	53/47	3.1	0.5	-nd-	60	18720	1.28
4*	1.73	3.46	20/80	1.7	2.8	28	68	36170	1.52

^a Polymerization conditions: [Ti] = 20 μ mol; temperature = 70°C; time = 24 h, run 4* = L-LA / CL. ^b CL / LA mole ratio in the copolymer determined by ¹H NMR. ^c Average sequence length of the caproyl unit in the copolymer as determined by ¹³C NMR. ^d Average sequence length of the lactidyl unit in the copolymer as determined by ¹³C NMR. ^e As determined by SEC in THF using polystyrene standards.

The copolymer was analyzed by ¹H NMR spectroscopy in CDCl₃ (Figure 5.22). The methylene protons of polycaprolactone close to the carbonyl group (-COO-CH₂-) and (-CH₂-C=O) is observed around 4.00 ppm (triplet) and 2.2 ppm (triplet) respectively as proton (a) and (e), and the same kinds of methylene protons corresponding to the caprolactone-lactide (CL-LA) heterosequences appears in the down field region around 4.1 ppm (multiplet) and 2.3 ppm (multiplet) as proton (b) and (f). The methine signal of polylactide (-COO-CHCH₃) appears around 5.15 ppm as proton (c) and the methine protons corresponding to the LA-CL heterosequences appears in the higher field region around 5.0 ppm (multiplet) as proton (d). The methyl and methylene protons of lactide and caprolactone together appear as a multiplet in the region of 1.25 to 1.6 ppm. The methyl protons of the isopropoxy end group appear as a doublet in the region 1.15 ppm.

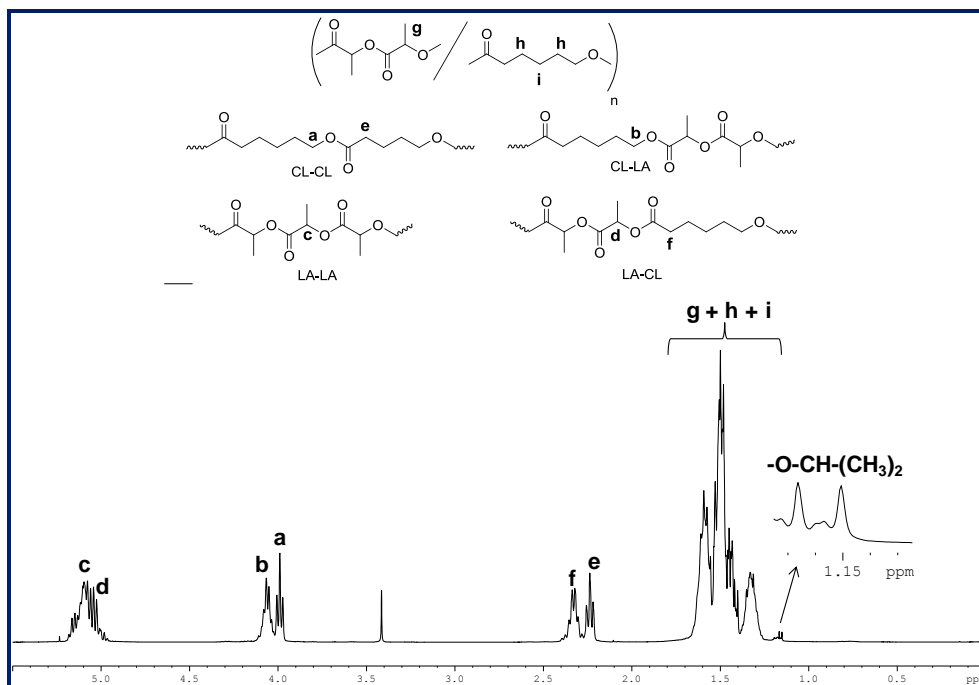


Figure 5.22. ¹H NMR spectrum of PCL-co-PDLLA (run 2, table 5.6).

The percentage of each monomer incorporated into polymer chains were determined by ¹H NMR spectroscopy, through the ratio of the integrated values of the methine proton of the LA segment (-COO-CHCH₃) around 5-5.2 ppm, and the methylene signal of the CL segment (-COO-CH₂-) around 4-4.1 ppm. Experimental observations revealed that the percentage of caprolactone units in the polymer chain is always reduced in comparison to the percentage of monomer feed ratios. This implies that the reactivity of ε-CL is lower than that of LA and this is in sharp contrast to the results of the homopolymerization of CL and LA (ROP of CL is much faster than the ROP of LA) under the same polymerization condition. Nevertheless, such a behavior seems to be a common feature for the random copolymerization of ε-CL and LA and it has been reported in the literature earlier.^{13,18-23}

As illustrated in Table 5.6 and Figure 5.23, the percentage of CL-LA heterodiads were calculated by comparing, in the ¹H NMR spectrum, the relative intensity of the signals corresponding to methylene protons assigned to α(CL-LA) and ε(CL-LA) heterosequences to that of the same methylene protons for the α(CL-CL) and ε(CL-CL) homosequences which appear at higher field. As seen in Figure 5.23, the intensities of the resonances assigned to CL-CL homosequences increases upon increasing the amount of ε-CL/LA mole ratio in the feed. The obtained copolymer had random sequences, with percentage of heterodiads higher than 50% for run1 (a) in Figure 5.23.

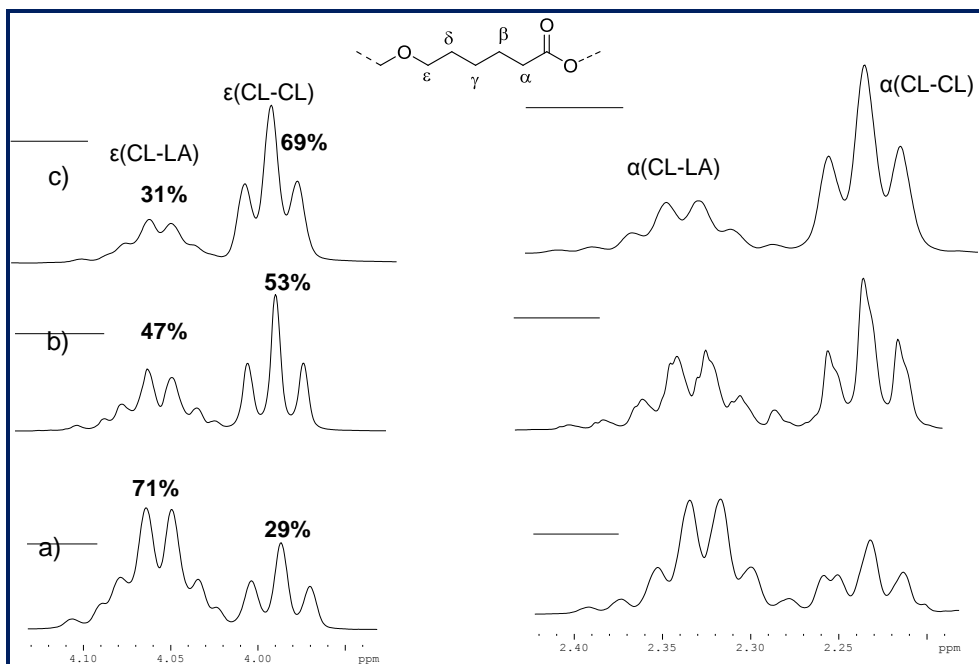


Figure 5.23. ^1H NMR spectrum of ϵ - and α -methylene protons of PCL-co-PDLLA of run 1 (a), run 2 (b), run 3 (c) in Table 5.6.

The microstructure of the copolymers was studied by ^{13}C NMR spectroscopy (between 165 and 175 ppm) since this technique is very sensitive to monomer sequencing and is therefore a powerful tool for determining the average sequence length for each type of monomer unit present in the copolymer. Spectra of the carbonyl regions of the random ϵ -CL/*D,L*-LA copolymers are shown in Figure 5.24.

According to the general case of binary copolymerization, eight different triads are observed; the peaks were assigned according to the literature.¹⁸ The average monomer sequence lengths of ϵ -CL segment (L_{CL}) and LA segment (L_{LA}) can be calculated from the integrated values of triads by the following equations (I = Intensity of triad signal) and the results are summarized in table 5.6.

$$L_{\text{CL}} = \frac{[I_{\text{CL-CL-CL}} + I_{\text{LA-CL-CL}}]}{[I_{\text{CL-CL-LA}} + I_{\text{LA-CL-LA}}]} + 1$$

$$L_{\text{LA}} = \left[\frac{I_{\text{LA-LA-LA}} + (I_{\text{LA-LA-CL}} + I_{\text{CL-LA-LA}}) / 2}{(I_{\text{LA-LA-CL}} + I_{\text{CL-LA-LA}}) / 2 + I_{\text{CL-LA-CL}}} + 1 \right] 0.5$$

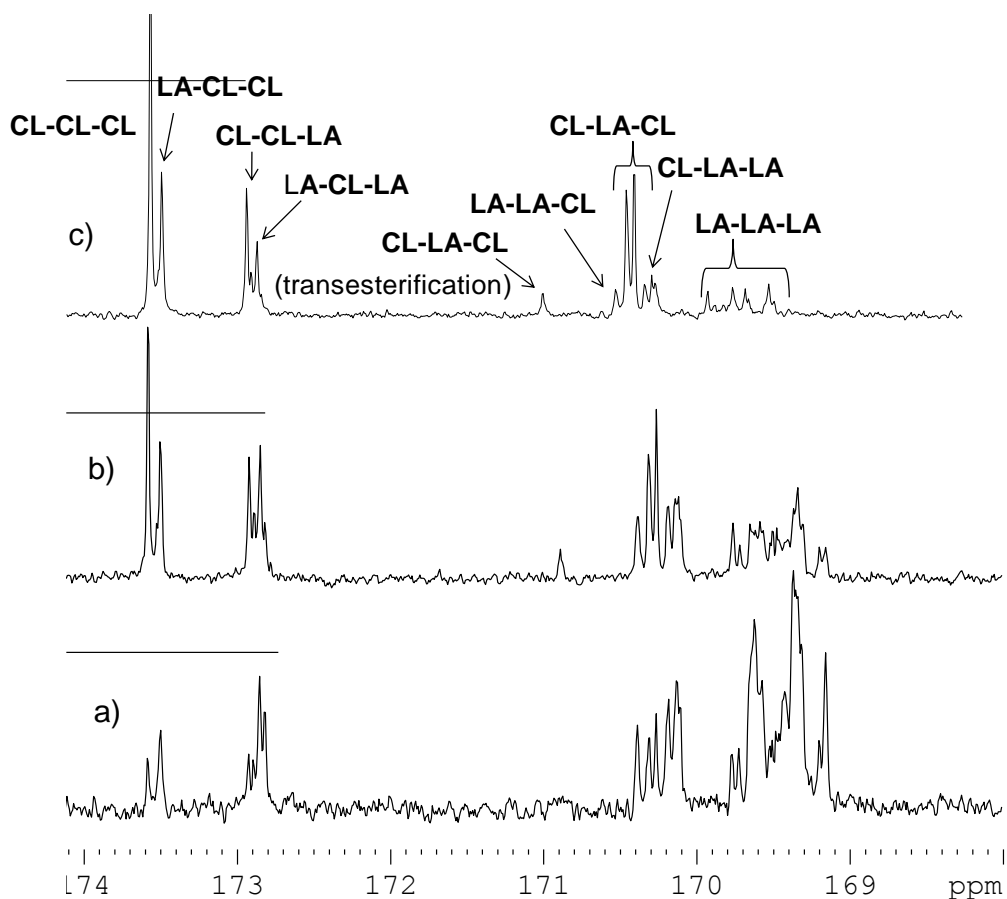


Figure 5.24. ^{13}C NMR spectrum of PCL-co-PDLLA of run 1 (a), run 2 (b), run 3 (c) in Table 5.6 (CL = caprolactone unit, LA = Lactide unit).

The calculated sequence lengths (L_{CL}) and (L_{LA}) increased as the relative proportion of their respective monomers increased. Obviously, the copolymer composition has a profound influence on the values of L_{CL} and L_{LA} . As seen in Figure 5.24, the carbonyl signal relative to the triad CL-CL-CL homosequences increases upon the increasing amount of ϵ -CL/LA mole ratio in the feed. It is worth noting that the appearance of a signal at 170.9 ppm (run 2 (b), run 3 (c)) in Figure 5.24, related to the triad (CL-LA-CL) having one single “lactic” ester unit between the two CL units is indicative of transesterification occurring during the copolymerization process when the $[\text{CL}]/[\text{LA}]$ monomer feed ratio increases.

The copolymerization of ϵ -CL and *L*-LA was also conducted in solution (toluene) condition with [ϵ -CL/*L*-LA] mole ratio of 0.5. The copolymer was characterized by ^1H and ^{13}C NMR spectroscopy (Figure 5.25 & 5.26). The percentage of ϵ -CL and the average monomer sequence lengths of ϵ -CL segment (L_{CL}) present in the copolymer is slightly higher compare to the ϵ -CL/*D,L*-LA copolymerization under the same reaction condition (run 4, table 5.6). As in the case of ϵ -CL/*D,L*-LA copolymerization, the signal at 170.9 ppm was not observed in ^{13}C NMR spectra with the same mole ratio of 0.5.

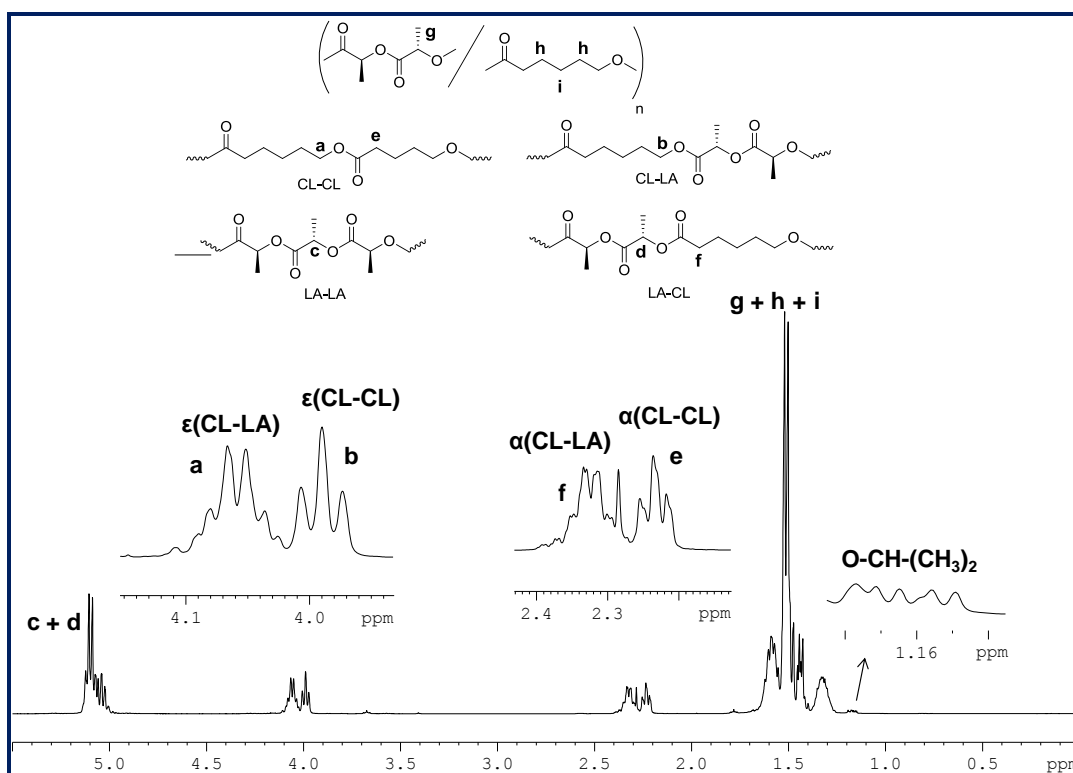


Figure 5.25. ^1H NMR spectrum of PCL-*co*-PLLA (run 4, table 5.6).

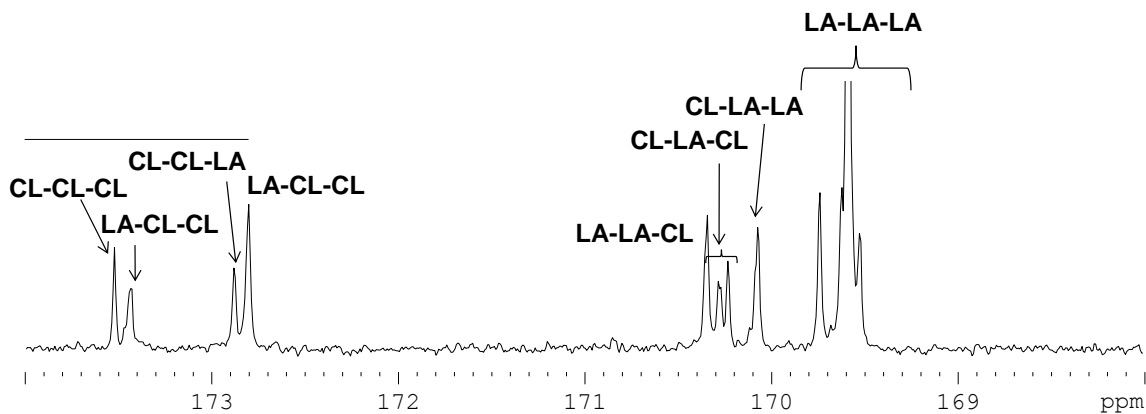


Figure 5.26. ^{13}C NMR spectrum carbonyl carbon of PCL-*co*-PLLA (run 4, table 5.6).

Thermal analysis of the copolymers was carried out by differential scanning calorimetry (DSC), in the range of temperature -100 to 150°C for (ϵ -CL-co-DL-LA) and -100 to 200°C for (ϵ -CL-co-L-LA). The thermograms recorded after second heating cycle for the samples of run1 and run 4 (Table 5.6, Figure 5.27) exhibits a unique glass transition temperature (T_g) at 25°C and 28°C for each copolymer, on the contrary to the block copolymer which normally exhibits two (T_g) values corresponding to both the PCL and PLA block present in the copolymer. The absence of melting transitions indicates amorphous nature of both copolymers. On the contrary, experimental (T_g) values are not in good agreement with the theoretical one, calculated by the Fox equation as shown below.

$$1/T_g = W_1/T_{g1} + W_2/T_{g2}$$

Where T_g is the glass transitions temperature of the copolymer, T_{g1} and T_{g2} are those of two homopolymers by following the literature values: PCL = -60°C; PDLLA = 45°C; PLLA = 57°C and W_1 and W_2 are the corresponding weight fractions of those two components present in the copolymer.

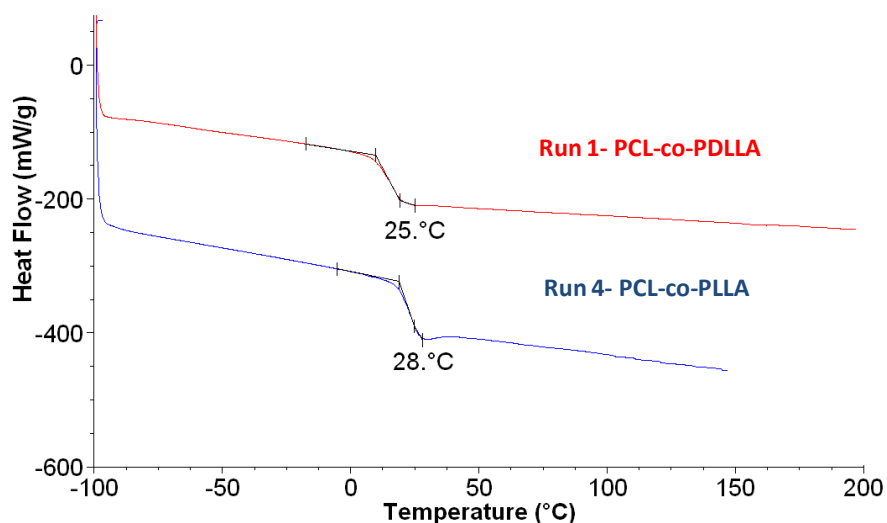


Figure 5.27. DSC thermograms of PCL-co-PDLLA (Table 5.6, run 1) and PCL-co-PLLA (Table 5.6, run 4) in solution condition.

The copolymerization of ϵ -CL/D,L-LA was also investigated in bulk polymerization condition at 130°C. The results are summarized in Table 5.7. Similar kinds of results as in solution condition are observed. The percentage of caprolactone in the copolymer was always reduced as compare to the initial monomer feed ratio. The incorporation of ϵ -CL and the percentage of [CL-CL] homosequences present in the copolymer increases by increasing the [ϵ -CL/LA] mole ratio as observed from the ^1H NMR spectrum.

The average monomer sequence lengths of ϵ -CL segment (L_{CL}) and LA segment (L_{LA}) segment can be calculated from the ^{13}C NMR spectrum (Figure 5.28) in a similar manner as mentioned above for solution condition. In this condition, the value of L_{CL} and L_{LA} is also strongly dependent on the composition and the monomer feed ratio (Table 5.7). Transesterification reactions are more important as compared to the solution condition as observed from the ^{13}C NMR spectrum.

Table 5.7. Copolymerization of ϵ -CL and *D,L*-Lactide with 4-Ti(O^{*i*}Pr)₂ in Bulk ^a

Run	[ϵ -CL] (mmol)	[LA] (mmol)	CL/LA in copolymer ^b (mol %)	L_{CL} ^c	L_{LA} ^d	T_g (°C)	Yield (%)	M_n ^e (g.mol ⁻¹)	PDI ^e
1	1.73	3.46	18/82	1.4	3.5	19	64	22670	1.42
2	3.46	3.46	27/73	1.7	2.2	3	57	26790	1.49
3	3.46	1.73	46/54	2.8	1.2	-23	60	23440	1.47

^a Polymerization conditions: [Ti] = 20 μmol ; temperature = 130°C; time = 30 min. ^b CL/LA mole ratio in the copolymer determined by ^1H NMR. ^c Average sequence length of the caprolyl unit in the copolymer as determined by ^{13}C NMR. ^d Average sequence length of the lactidyl unit in the copolymer as determined by ^{13}C NMR. ^e As determined by size-exclusion chromatography in THF using polystyrene standards.

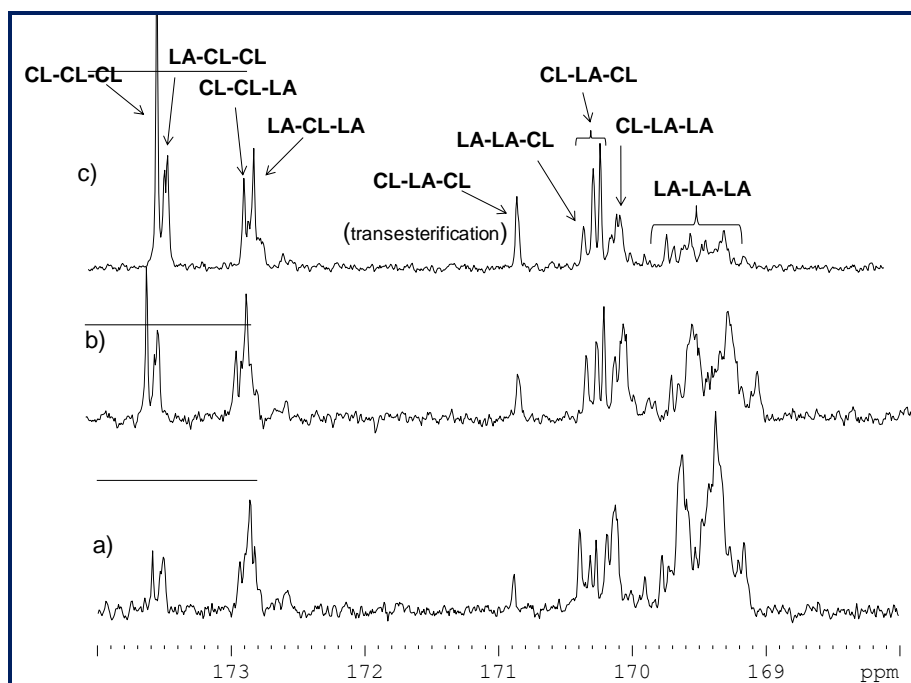


Figure 5.28. ^{13}C NMR spectrum of PCL-co-PDLLA of run 1 (a), run 2 (b), run 3 (c) in Table 5.7 (CL = caprolactone unit, LA = Lactide unit).

Thermal analysis of the copolymers PCL-co-PDLLA obtained from the bulk polymerization condition was also carried out by (DSC), in the range of temperature -80 to 80°C. The thermograms recorded after second heating cycle for all the copolymers of varying composition are plotted in Figure 5.29 (Table 5.7). As in the case of solution polymerization condition, copolymers exhibit a unique glass transition temperature (T_g) which decreases with an increase in the [CL]/[LA] mole ratio. For instance the samples of run 1 with [CL]/[LA] mole ratio of 0.5 showed a T_g at 19°C, run 2 with [CL]/[LA] mole ratio of 1 showed a T_g at 3°C and run 3 with [CL]/[LA] mola ratio of 2 showed a T_g at -23°C. These results suggest that the copolymer composition and chain microstructure have a profound influence on the thermal properties of the obtained copolymers. As in the case of solution polymerization, experimental T_g are not in good agreement with the theoretical values calculated by Fox equation.

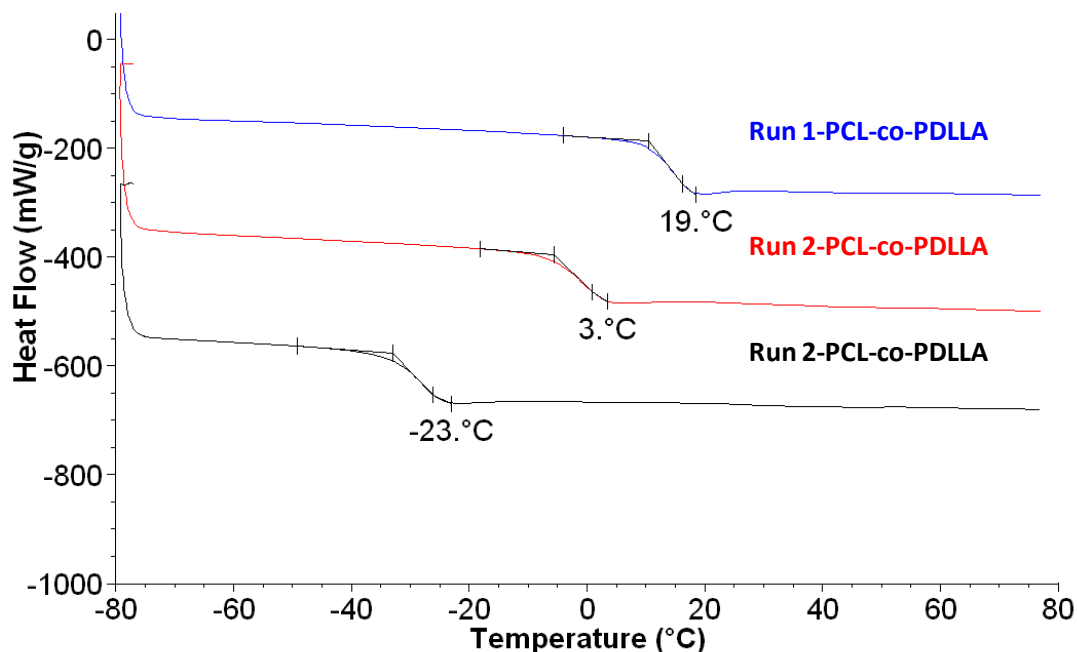


Figure 5.29. DSC thermograms of PCL-co-PDLLA copolymers (Table 5.7, run 1, 2, 3) in bulk condition.

5.3. Conclusion

All complexes 1-4-Ti(OⁱPr)₂ were able to initiate the ring opening polymerization of ε-CL, L/D,L-LA in a controlled manner. Such a feature allowed the preparation of high molecular weight diblock copolymers PCL-*b*-PLLA, PLLA-*b*-PCL, PDLLA-*b*-PCL and triblock copolymers PCL-*b*-PLLA-*b*-PCL, PLLA-*b*-PCL-*b*-PLLA, with controlled molecular weight distribution. The block copolymers were characterized by ¹H, ¹³C NMR, SEC and DSC analysis. Differential scanning calorimetry revealed the thermal properties of the copolymers to be highly dependent upon the monomer compositions.

The random copolymers of ε-CL/D,L-LA with various compositions were successfully prepared both in solution and bulk condition using the initiator 4-Ti(OⁱPr)₂ with the different monomer feed ratio. The amount of ε-CL present in the copolymer is lower than its initial concentration in the feed, indicating lower reactivity of ε-CL in the copolymerization compare to the homopolymerization. The percentage of CL-CL homosequences and the average sequence length of L_{CL} in the copolymer increases by increasing the amount of ε-CL/D,L-LA mole ratio in the feed. Nonetheless, all the obtained copolymers had percentage of heterodiads (CL-LA) almost higher than 50% at low monomer concentration of ε-CL, indicative of highly random copolymerization. The random copolymer of ε-CL/L-LA was also successfully prepared in the solution condition and produces the same kind of results as ε-CL/D,L-LA copolymerization.

5.4. References

- [1] Scott, G.; Gilead, D. In *Degradable polymers. Principles and Applications*; Chapman&Hall: London, **1995**.
- [2] Jarrett, P.; Benedict, C.; Bell, J. P.; Cameron, J. A.; Huang, S.J. In *Polymers as Biomaterials*; Shalaby, S. W., et al., Eds.; Plenum Press: New York, **1984**.
- [3] Mecking, S. *Angew. Chem., Int. Ed.* **2004**, 43, 1078.
- [4] Ge, H.; Hu, Y.; Yang, S.; Jiang, S. X.; Yang, C. *J Appl Polym Sci*, **2000**, 75, 874.
- [5] Kasperczyk, J. *Macromol Symp.* **2001**, 175, 19.
- [6] Schindler, A.; Jeffcoat, R.; Kimmel, G. L.; Pitt, C. G.; Wall, M. E.; Zweidinger, R. In *Contemporary Topics in Polymer Science*; Pearce, E. M.; Schaefgen, J. R. Eds.; Plenum Press: New York, **1977**; Vol. 2, p 251.
- [7] Grijpma, D. W.; Hofslot, R. D. A.; Super, H.; Nijenhuis, A. J.; Pennings, A. J. *Polym. Eng. Sci.*, **1994**, 34, 1674.
- [8] Corbin, P. S.; Webb, M. P.; McAlvin, J. E.; Fraser, C. L. *Biomacromolecules.* **2001**, 2, 223.
- [9] Dell'Erba, R.; Groeninckx, G.; Maglio, G.; Malinconico, M.; Migliozi, A. *Polymer.* **2001**, 42, 7831.
- [10] Na, Y. -H.; He, Y.; Shuai, X.; Kikkawa, Y.; Doi, Y.; Inoue, Y. *Biomacromolecules.* **2002**, 3, 1179.
- [11] Yang, J. M.; Chen, H. L.; You, J. W.; Hwang, J. C. *Polym. J.* **1997**, 29, 657.
- [12] Sakai, F.; Nishikawa, K.; Inoue, Y.; Yazawa, K. *Macromolecules.* **2009**, 42, 8335.
- [13] Pappalardo, D.; Annunziata, L.; Pellecchia, C. *Macromolecules.* **2009**, 42, 6056.
- [14] Huang, M. H.; Li, S. M.; Coudane, J.; Vert, M. *Macromol. Chem. Phys.* **2003**, 204, 1994.
- [15] Jeon, O.; Lee, S.-H.; Kim, S. H.; Lee, Y. M.; Kim, Y. H. *Macromolecules.* **2003**, 36, 5585.
- [16] Wang, J. L.; Dong, C. M. *Macromol. Chem. Phys.* **2006**, 207, 554.
- [17] Wie, Z.; Liu, L.; Yu, F.; Wang, P.; Qu, C.; Qi, M. *Polym. Bull.* **2008**, 61, 407.
- [18] Vanhoorne, P.; Dubois, Ph.; Jérôme, R.; Teyssié, Ph. *Macromolecules*, **1992**, 25, 37.
- [19] Shen, Y.; Zhun, K. J.; She, Z.; Yao, K.-M. *J. Polym. Sci., Part A: Polym. Chem.* **1996**, 34, 1799.
- [20] Bero, M.; Kasperczyk, J. *Macromol. Chem. Phys.* **1996**, 197, 3251.
- [21] Kister, G.; Cassanas, G.; Bergounhon, M.; Hoarau, D.; Vert, M. *Polymer.* **2000**, 41, 925.
- [22] Fay, F.; Renard, E.; Langlois, V.; Linossier, I.; Vallée-Rhel, K. *Eur. Polym. J.* **2007**, 43, 4800.
- [23] Calandrelli, L.; Calarco, A.; Laurienzo, P. Malinconico, M.; Petillo, O.; Peluso, G. *Biomacromolecules.* **2008**, 9, 1527.
- [24] Barakat, I.; Dubois, P.; Jérôme, R.; Teyssié, P.; Mazurek, M. *Macromol. Symp.* **1994**, 88, 227.
- [25] Tian, D.; Dubois, P.; Jérôme, R. *Macromolecules.* **1997**, 30, 1947.
- [26] IntVeld, P. J. A.; Velner, E. M.; Witte, P. V. D.; Hamhuis, J.; Dijkstra, P. J.; Feijen, J. *J. Polym. Sci. Polym. Chem.*, **1997**, 35, 219.
- [27] Kim, J. K.; Park, D. J.; Lee, M. S.; Ihn, K. J. *Polymer.* **2001**, 42, 7429.

- [28] Chmura, A. J.; Davidson, M. G.; Jones, M. D.; Lunn, M. D.; Mahon, M. F.; Johnson, A. F.; Khunkamchoo, P.; Roberts, S. L.; Wong, S. S. F. *Macromolecules*. **2006**, 39, 7250.
- [29] Song, C. X.; Feng, X. D. *Macromolecules*. **1984**, 17, 2764.
- [30] Jacobs, C.; Dubois, Ph.; Jérôme, R.; Teyssié, P. *Macromolecules*. **1991**, 24, 3027.
- [31] Deng, X.; Zhu, Z.; Xiong, Ch.; Zhang, L. *J. Polym. Sci., Part A: Polym. Chem.*, **1997**, 35, 703.
- [32] Cui, D.; Tang, T.; Bi, W.; Cheng, J.; Chen, W.; Huang, B. *J. Polym. Sci., Part A: Polym. Chem.*, **2003**, 41, 2667.
- [33] Stassin, F.; Jérôme, R.; *J. Polym. Sci., Part A: Polym. Chem.*, **2005**, 43, 2777.
- [34] Fan, L.; Xiong, Y.-B.; Xu, H.; Shen, Z. Q. *Eur. Polym. J.* **2005**, 41, 1647.
- [35] Florczak, M.; Libiszowski, J.; Mosnacek, J.; Duda, A.; Penczek, S. *Macromol. Rapid Commun.* **2007**, 28, 1385.
- [36] Biela, T.; Duda, A.; Penczek, S. *Macromol. Symp.* **2002**, 183, 1.
- [37] Gores, F.; Kliz, P. *Chromatography of Polymers*, ACS Symp. Ser 521, **1993**, 122.
- [38] Kratochvil, P. *Classical Light Scattering from Polymer Solutions*, Elsevier, New York, USA (**1987**).
- [39] Ye, W. P.; Du, F. S.; Jin, W. H.; Yang, J. Y.; Xu, Y. *Funtional. Polym.* **1997**, 32, 161.

CHAPTER 6
Experimental Section

CHAPTER 6

EXPERIMENTAL SECTION

6.1. General Experimental Details

For the preparation and characterization of all metal complexes and for all polymerization, reactions manipulations were performed under an inert atmosphere of argon using standard Schlenk or glove box techniques. All solvents were freshly distilled from suitable drying agents and degassed prior to use.

6.1.1. Chemical Materials

(R)-(+)-styrene oxide, (*racemic*)-styrene oxide, Benzylamine, Methyl Iodide, sodium hydride (60% dispersion in oil) were purchased from Aldrich and used as received. 2N ammonia solution in methanol (98%) was obtained from Acros organics. $\text{Ti}(\text{O}^i\text{Pr})_4$ (98%) was obtained from Acros Organics Chemicals and was purified by vacuum distillation prior to use. $\text{Zr}(\text{O}^t\text{Bu})_4$ (99%) was purchased from strem chemicals and used as received. $\text{C}_p^*\text{TiCl}_3$ (99%, Aldrich) and C_pTiCl_3 (99%, Aldrich) were used as received without further purification. ϵ -Caprolactone (99%, Aldrich), *L*-lactide (98%, Aldrich), *rac*-lactide (98%, Aldrich), β -Butyrolactone (98%, Aldrich) and Trimethylene carbonate (Boehringer Ingelheim, Germany) were purified as indicated in 6.1.3.

6.1.2. Purification of solvents

Toluene and pentane was first dried by refluxing over CaH_2 and distilled, then a small amount of styrene and *sec*-BuLi (1.3 M in cyclohexane) was added and stirred until the characteristic red color of the polystyryl anion was obtained, meaning that all the protonic impurities have been consumed. The desired volume of toluene was then distilled off from the polystyryl solution just before use. DCM (dichloromethane) was dried by refluxing over calcium hydride and distilled under reduced pressure, stored in a solvent reservoir under argon atmosphere. CDCl_3 was dried over CaH_2 for 24 hours, distilled under reduced pressure and stored in a Schlenk tube with 4 Å molecular sieves under argon atmosphere in a glove box.

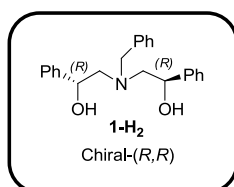
6.1.3. Purification of Monomers.

L and *rac*-lactide were recrystallized twice from dry toluene and stored in glove box. ϵ -caprolactone, β -butyrolactone was dried over calcium hydride for a minimum of 24 hours, then distilled under vacuum and stored in a Schlenk flask under argon atmosphere. Trimethylene carbonate (TMC, 1,3-dioxane-2-one) was dissolved in THF and stirred over CaH_2 for 2 days and filtered, followed by recrystallization twice from cold THF, dried and stored in a glove box.

6.2. Synthesis and Characterization of Ligands

6.2.1. Synthesis and Characterization of Ligand 1-H₂

To a cooled solution of benzyl amine (2 g , 19 mmol) in 10 mL of methanol, (*R*)-styrene epoxide (4.5 g, 37 mmol), in 8 mL methanol solution at 0°C was added and let stirred for an hour. The contents were then refluxed for 6 h. After the completion of the reaction, the solvent was removed under vacuum. The crude product was obtained as a colorless syrupy liquid. The product was then purified by flash column chromatography using 80:20 cyclohexane:ethyl acetate as eluent mixture. The major isomer is a colorless syrupy liquid (Yield 82%).



(1) Properties of Chiral aminodiol-1-H₂

Formula: C₂₃H₂₅NO₂

Nature: Colourless shiny solid

Mol.Wt: 348 g/mol

Yield: 82%

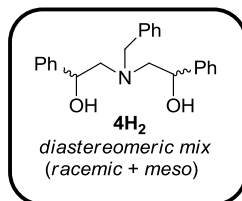
¹H-NMR (400 MHz, CDCl₃): 2.64 (dd, J = 13.2 & 3.6 Hz, 2H), 2.69 (dd, J = 13.6 & 3.6 Hz, 2H), 3.1 (s, 2H, OH), 3.58 (d, J = 13.6 Hz, 1H, N-CH₂Ph), 3.88 (d, J = 13.6 Hz, 1H, N-CH₂Ph), 4.65 (dd, J= 9.6 & 3.6 Hz, 2H, -CH-Ph), 7.1-7.3 (m, 15H, Ar-H).

¹³C-NMR (100 MHz, CDCl₃): 59.74 (N-CH₂), 62.53 (N-CH₂-Ph), 70.77 (-CH-Ph), 125.86, 127.41, 127.53, 128.33, 128.50, 129.14, 138.03, 142.10 (Ar).

6.2.2. Synthesis and Characterization of Ligand 4-H₂, 2-H₂, 3-H₂

To a cooled solution of benzyl amine (1.07 g , 10 mmol) in 4 mL of methanol, racemic styrene epoxide (2.4 g, 20 mmol), in 8 mL methanol solution at 0 °C was added and let stirred for an hour. The contents were then refluxed for 6 h. After the completion of the reaction, the solvent was removed under vacuum. The crude product was obtained as a colorless syrupy liquid. The product was then purified by flash column chromatography using 80:20 cyclohexane:ethyl acetate as eluent mixture. The major isomer (**4-H₂**) is a colorless syrupy liquid (Yield 85%). The obtained aminodiol was dissolved in 80:20 = CH₃OH:H₂O for semi-preparative HPLC. The resulted product in CH₃OH/H₂O was extracted with CH₂Cl₂. About 100 mg of the aminodiol dissolved in 1 mL of the Eluent gave 45 mg of pure separated aminodiol.

(2) Properties of *diastereomeric* aminodiol-**4-H₂**



Formula: C₂₃H₂₅NO₂

Nature: Colourless syrupy liquid

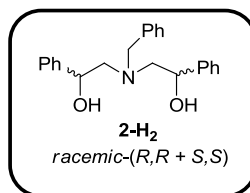
Mol.Wt: 348 g/mol

Yield: 85%

¹H-NMR (400 MHz, CDCl₃): 2.63-2.80 (m, 4H, N-CH₂), 3.47 (s, 2H, OH), 3.59 (d, J = 13.2 Hz, N-CH₂Ph, 1H), 3.72 (s, 2H, N-CH₂Ph), 3.86 (d, J = 13.7 Hz, N-CH₂Ph, 1H), 4.58 (dd, J = 8.8 & 4 Hz, 1H, -CH-Ph), 4.65 (dd, J = 9.6 & 3.6 Hz, 1H, -CH-Ph), 7.14-7.25 (m, 15H, Ar-H).

¹³C-NMR (100 MHz, CDCl₃): 59.78, 59.87 (N-CH₂), 62.63, 63.50 (N-CH₂-Ph), 70.84, 72.03, (-CH-Ph), 125.96, 126.04, 127.48, 127.58, 127.64, 127.68, 128.44, 128.55, 128.61, 129.22, 129.31, 137.92, 138.07, 142.17, 142.32 (Ar).

(3) Properties of *racemic* aminodiol **2-H₂**



Formula: C₂₃H₂₅NO₂

Nature: Colourless shiny solid

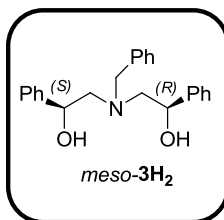
Mol.Wt.: 348 g/mol

Yield: 42%

¹H-NMR (400 MHz, CDCl₃): 2.66 (dd, J = 13.2 & 3.6 Hz, 2H), 2.72 (dd, J = 13.6, & 3.6 Hz, 2H), 3.46 (s, 2H, OH), 3.59 (d, J = 13.6 Hz, 1H, N-CH₂Ph), 3.86 (d, J = 13.6 Hz, 1H, N-CH₂Ph), 4.65 (dd, J = 13.6 & 3.2 Hz, 2H, -CH-Ph), 7.15-7.28 (m, 15H, Ar-H).

¹³C-NMR (100 MHz, CDCl₃): 59.85 (N-CH₂), 62.64 (N-CH₂-Ph), 70.84 (-CH-Ph), 125.97, 127.53, 127.60, 128.42, 128.59, 129.29, 137.99, 142.23 (Ar).

(4) Properties of *meso* aminodiol-**3-H₂**



Formula: C₂₃H₂₅NO₂

Nature: Colourless syrupy liquid

Mol. Wt.: 348 g/mol

Yield: 45%

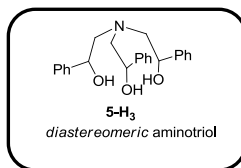
¹H-NMR (400 MHz, CDCl₃): 2.67 (dd, J = 13.2 & 3.6 Hz, 2H, N-CH₂), 2.77 (dd, J = 13.6 & 4 Hz, 2H, N-CH₂), 3.55 (s, 2H, OH), 3.70 (s, 2H, N-CH₂Ph), 4.56 (dd, J = 8.8 & 4 Hz, 2H, -CH-Ph), 7.2-7.4 (m, 15H, Ar-H).

¹³C-NMR (100 MHz, CDCl₃): 59.74 (N-CH₂), 63.49 (N-CH₂-Ph), 72.00 (-CH-Ph), 126.05, 127.45, 127.65, 128.42, 128.53, 129.21, 138.13, 142.38 (Ar).

6.2.3. Synthesis and Characterization of Ligand **5-H₃**

To 2.0 M ammonia in methanol solution (14 mL, 28.0 mmol) was added dropwise styrene epoxide (10.0 g, 84 mmol) at -78°C. The mixture was stirred overnight at room temperature and then refluxed at 80°C for 3 days. After the completion of the reaction, the solvent was removed under vacuum. The crude product was obtained as a colorless syrupy liquid. The product was then purified by flash column chromatography using 70:30 cyclohexane:ethyl acetate as eluent mixture.

(5) Properties of *diastereomeric* [Tris(2-phenylethanol)amine]-**5-H₃**



Formula: C₂₄H₂₇NO₃

Nature: Colourless syrupy liquid

Mol.Wt.: 377 g/mol

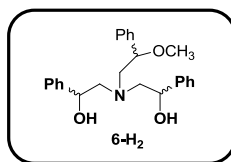
Yield: 53%

¹H-NMR (400 MHz, CDCl₃): 2.61-2.90 (m, 6H, N-CH₂-), 4.30 (s, 3H, OH), 4.65-4.85 (m, 3H, O-CH-), 7.23-7.38 (m, 15H, Ar-H).

6.2.4. Synthesis and Characterization of Ligand 6-H₂

A solution of aminotriol 5-H₃ (4 g, 10.6 mmol) in dry THF (30 mL) was added dropwise *via* syringe to NaH (0.25 g, 10.6 mmol) in THF (40 mL) at -78°C. The mixture was stirred for 3h at 0°C and then stirred at room temperature (20°C) for 2 h. The reaction mixture turns colorless to pale yellow. To this solution CH₃I (1.5 g, 10.6 mmol) was added at 0°C. The reaction mixture was then allowed to stir at room temperature for 6 hours. After completion of reaction, the product was then extracted with ethylacetate, followed by washing with water and brine solution. The solvent was removed under vacuum and the crude product was purified by flash column chromatography using 80:20 cyclohexane:ethyl acetate as eluent mixture. The pure product was obtained as a colorless syrupy liquid.

(6) Properties of *diastereomeric* aminodiol-6-H₂



Formula: C₂₅H₂₉NO₃

Nature: Colourless syrupy liquid

Mol.Wt: 391 g/mol

Yield: 43%

¹H-NMR (400 MHz, CDCl₃): 2.67-3.11 (m, 6H, N-CH₂-), 3.32 (s, 1H, CH₂-H), 3.34 (s, 1H, CH₂-H), 3.37 (s, 1H, CH₂-H), 4.15 (s, 2H, OH), 4.35-4.45 (m, 1H, CH-Ph-OCH₃), 4.69-4.83 (m, 2H, CH-Ph-OH), 7.19-7.43 (m, 15H, Ar-H).

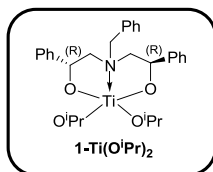
6.3. Synthesis and Characterization of Complexes

6.3.1. Synthesis and Characterization of Titanium and Zirconium alkoxide complexes

6.3.1.1. Synthesis and Characterization of Complex 1-Ti(OⁱPr)₂

Ti(OⁱPr)₄ (0.85 g, 3 mmol) in 5 mL of dry toluene was cooled to -30°C. Then the required aminodiol 1-H₂ (1.05 g, 3 mmol) in 10 mL of dry toluene was added dropwise to the reaction mixture. The mixture was stirred at room temperature (25°C) for 6 h to give a clear yellow solution. The solvent was removed under vacuum to yield titanium isopropoxide complex (1.41g, 91% yield) as a crystalline yellow solid.

Properties of titanium isopropoxide complex 1-Ti(OⁱPr)₂



Formula: C₂₉H₃₇NO₄Ti

Nature: Crystalline yellow solid

Mol.Wt: 512 g/mol

Yield: 91%

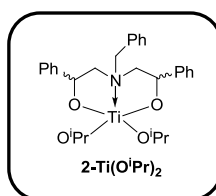
¹H-NMR (400 MHz, CDCl₃): 1.17 (d, J = 6.0 Hz, 3H, CH₃), 1.24 (d, J = 6.4 Hz, 3H, CH₃), 1.30 (d, J = 6 Hz, 3H, CH₃), 1.32 (d, J = 5.6 Hz, 3H, CH₃), 2.81-3.07 (m, 4H, N-CH₂), 4.13 (d, J = 14.8 Hz, 1H, N-CH₂Ph), 4.44 (d, J = 14.8 Hz, 1H, N-CH₂Ph), 4.70 (sept, J = 6.0 Hz, 2H, CH-(CH₃)₂), 5.48 (dd, J = 10.8 & 4.0 Hz, 1H, -CH-Ph), 5.87 (dd, J = 10.4 & 3.6 Hz, 1H, -CH-Ph), 7.24 (m, 15H, ArH).

¹³C-NMR (100 MHz, CDCl₃): 26.01, 26.09, 26.51, 26.57, (-CH₃-), 57.61 (NCH₂), 59.10 (PhCH₂), 65.68 (-CH-Ph), 80.49 (CH-(CH₃)₂), 80.73 (CH-(CH₃)₂), 125.20, 125.44, 127.30, 128.29, 128.58, 131.08, 133.63, 143.40, 143.65 (Ar).

6.3.1.2. Synthesis and Characterization of complex 2-Ti(OⁱPr)₂

The desired complex 2-Ti(OⁱPr)₂ was obtained as a crystalline yellow solid with an isolated yield of 96% (1.19 g) (with the same procedure as for 1-Ti(OⁱPr)₂) using **2-H₂** (*racemic* aminodiols) ligand (0.84 g, 2.4 mmol) and Ti(OⁱPr)₄ (0.68 g, 2.4 mmol).

Properties of titanium isopropoxide complex 2-Ti(OⁱPr)₂



Formula: C₂₉H₃₇NO₄Ti

Nature: Crystalline yellow solid

Mol.Wt.: 512 g/mol

Yield: 96%

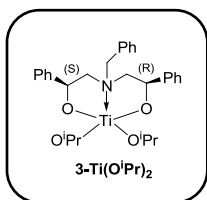
¹H-NMR (400 MHz, CDCl₃): 1.17 (d, J = 6.0 Hz, 3H, CH₃), 1.24 (d, J = 6.4 Hz, 3H, CH₃), 1.30 (d, J = 6 Hz, 3H, CH₃), 1.32 (d, J = 5.6 Hz, 3H, CH₃), 2.80-3.06 (m, 4H, N-CH₂), 4.13 (d, J = 14.8 Hz, 1H, N-CH₂Ph), 4.44 (d, J = 14.8 Hz, 1H, N-CH₂Ph), 4.70 (sept, J = 6.4 Hz, 2H, CH-(CH₃)₂), 5.49 (dd, J = 10.8 & 4.0 Hz, 1H, -CH-Ph), 5.87 (dd, J = 10.4 & 3.2 Hz, 1H, -CH-Ph), 7.23 (m, 15H, ArH).

^{13}C -NMR (100 MHz, CDCl_3): 26.01, 26.08, 26.50, 26.69, (CH_3), 57.63 (NCH_2), 59.11 (PhCH_2), 65.69 ($-\text{CH}-\text{Ph}$), 80.50 ($\text{CH}-(\text{CH}_3)_2$), 80.74 ($\text{CH}-(\text{CH}_3)_2$), 125.20, 125.43, 127.28, 128.19, 128.57, 131.07, 133.65, 143.41, 143.66.

6.3.1.3. Synthesis and Characterization of complex 3-Ti(OⁱPr)₂

The desired complex 3-Ti(OⁱPr)₂ was obtained as a crystalline yellow solid with an isolated yield of 90% (1.85 g) (with the same procedure as for 1-Ti(OⁱPr)₂) using 3-H₂ (*meso* aminodiol) ligand (1.4 g, 4 mmol) and Ti(OⁱPr)₄ (1.14 g, 4 mmol).

Properties of titanium isopropoxide complex 3-Ti(OⁱPr)₂



Formula: $\text{C}_{29}\text{H}_{37}\text{NO}_4\text{Ti}$

Nature: Crystalline yellow solid

Mol.Wt.: 512 g/mol

Yield: 90%

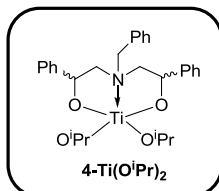
^1H -NMR (400 MHz, CDCl_3): 1.36 (d, $J = 6.0$ Hz, 6H, CH_3), 1.46 (d, $J = 6.0$ Hz, 6H, CH_3), 2.49 (dd, $J = 12.8$ & 8.8 Hz, 2H, NCH_2), 3.45 (dd, $J = 12.8$ & 8.4 Hz, 2H, NCH_2), 4.42 (s, 2H, $\text{N}-\text{CH}_2\text{Ph}$), 4.77 (sept, $J = 6.0$ Hz, 1H, $\text{CH}-(\text{CH}_3)_2$), 4.89 (sept, $J = 6.0$ Hz, 1H, $\text{CH}-(\text{CH}_3)_2$), 5.82 (dd, $J = 8.4$ & 4.4 Hz, 2H, $\text{CH}-\text{Ph}$), 7.27 (m, 15H, ArH).

^{13}C -NMR (100 MHz, CDCl_3): 26.05, 26.41 ($-\text{CH}_3-$), 56.34 (NCH_2), 61.1 (PhCH_2), 65.11 ($-\text{CH}-\text{Ph}$), 81.12 ($\text{CH}-(\text{CH}_3)_2$), 125.26, 125.94, 127.0, 128.14, 128.63, 131.35, 133.52, 143.60, 144.10 (Ar).

6.3.1.4. Synthesis and Characterization of complex 4-Ti(OⁱPr)₂

The complex 4-Ti(OⁱPr)₂ was obtained as a crystalline yellow solid with an isolated yield of 83% (1.06 g) (with the same procedure as for 1-Ti(OⁱPr)₂) using 4-H₂ (*diastereomeric* aminodiols) ligand (0.87 g, 2.5 mmol) and Ti(OⁱPr)₄ (0.71 g, 2.5 mmol).

Properties of titanium isopropoxide complex 4-Ti(OⁱPr)₂



Formula: C₂₉H₃₇NO₄Ti

Nature: Crystalline yellow solid

Mol.Wt.: 512 g/mol

Yield: 83%

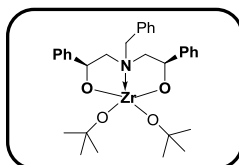
¹H-NMR (400 MHz, CDCl₃): 1.17 (d, J = 6.0 Hz, 3H, CH₃), 1.24 (d, J = 6.0 Hz, 3H, CH₃), 1.32 (d, J = 6.0 Hz, 3H, CH₃), 1.35 (d, J = 6.0 Hz, 3H, CH₃), 2.39 (dd, J = 12.0 & 8.8 Hz, 1H, NCH₂), 2.81 (m, 2H, NCH₂), 3.35 (dd, J = 12.4 & 8.8 Hz, 1H, NCH₂), 4.13 (d, J = 14.8 Hz, 1H, N-CH₂Ph, *racemic*), 4.32 (s, 2H, N-CH₂Ph, *meso*), 4.48 (d, J = 14.8 Hz, 1H, N-CH₂Ph, *racemic*), 4.67 (sept, J = 6.0 Hz, 1H, CH-(CH₃)₂), 4.77 (sept, J = 6.0 Hz, 1H, CH-(CH₃)₂), 5.48- 5.87 (dd, J = 10.4 & 4.0 Hz, 2H, -CH-Ph), 7.11 (m, 15H, ArH).

¹³C-NMR (100 MHz, CDCl₃): 26.07, 26.42, 26.55, 26.69 (CH₃), 56.35, 57.65 (NCH₂), 59.12 (PhCH₂), 65.11, 65.70 (-CH-Ph), 80.51, 80.74, 81.12 (CH-(CH₃)₂), 125.20, 125.27, 125.43, 127.05, 127.27, 128.15, 128.28, 128.57, 128.64, 131.05, 131.36, 133.67, 143.42, 143.60, 143.67 (Ar-H).

6.3.1.5. Synthesis and Characterization of complex 3-Zr(O^tBu)₂

Zr(O^tBu)₄ (0.44 g, 0.45 mL, 1.15 mmol) in 5 mL of dry toluene was cooled to -30°C. Then the required aminodiols **3-H₂** (0.4 g, 1.15 mmol) in 5 ml of dry toluene was added dropwise to the reaction mixture. The mixture was stirred at room temperature (25°C) for 6 h to give a clear yellow solution. The solvent was removed under vacuum, and the resulting yellow solid was washed with cold pentane. The final yield was 73% (0.52 g).

Properties of Zirconium tert-butoxide complex 3- $Zr(O^tBu)_2$



Formula: $C_{31}H_{41}NO_2Zr$

Nature: Crystalline yellow solid

Mol.Wt.: 619 g/mol

Yield: 73%

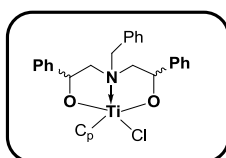
1H -NMR (400 MHz, $CDCl_3$): 0.62 (s, 3H, $OC(CH_3)_3$), 0.91 (s, 3H, $OC(CH_3)_3$), 1.15 (s, 3H, $OC(CH_3)_3$), 1.21 (d, $J = 4$ Hz, 9H, $OC(CH_3)_3$), 2.55-3.32 (m, 4H, N- CH_2), 4.19-5.34 (d, $J = 14.2$ Hz, 15.2 Hz, 2H, N- CH_2 -Ph), 5.96-6.41(m, 2H, CH -Ph), 7.1-7.7 (m, 15H, ArH).

6.3.2. Synthesis and Characterization of Half-sandwich Titanium complexes

6.3.2.1. Synthesis and Characterization of complex 4- $C_pTiCl[O,O,N]$

A yellowish solution of C_pTiCl_3 (0.65 g, 3 mmol) in dry CH_2Cl_2 (40 mL) was added dropwise to a solution of **4-H₂** (1 g, 3 mmol) and triethylamine (1.3 mL, 9 mmol) in CH_2Cl_2 (40 mL) at $-78^\circ C$. The reaction mixture was allowed to warm to room temperature ($20^\circ C$) and stirred for 14 h. The solvent was removed under vacuum, and the resulting reddish brown residue was redissolved in dry toluene (15 mL), the precipitated solid was filtered through a sintered crucible under N_2 atmosphere. The removal of solvent from the yellow filtrate gave the complex 4- $C_pTiCl[O,O,N]$ as pale yellow solid with a yield of 86% (1.2 g).

Properties of 4- $C_pTiCl[O,O,N]$ complex



Formula: $C_{29}H_{28}ClNO_2Ti$

Nature: Yellow solid

Mol.Wt: 493 g/mol

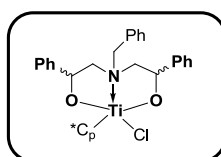
Yield: 86%

1H -NMR (400 MHz, $CDCl_3$): 2.60-3.23 (m, 4H, N- CH_2), 4.05-4.34 (m, 2H, N- CH_2 -Ph), 6.30-6.59 (s, 5H, C_5H_5), 2.83-3.31 (m, 4H, N- CH_2), 4.10-4.71 (m, 2H, N- CH_2 -Ph), 5.32 (dd, $J = 9.6$ Hz, 2.8 Hz, 1H, CH -Ph), 5.62-5.95 (m, 1H, CH -Ph), 7.24-7.61 ((m, 15H, ArH).

6.3.2.2. Synthesis and Characterization of complex 4- $C_p^*TiCl[O,O,N]$

A reddish solution of $C_p^*TiCl_3$ (1.4 g, 5 mmol) in dry CH_2Cl_2 (40 mL) was added dropwise to a solution of **4-H₂** (1.7 g, 5 mmol) and triethylamine (2 ml, 15 mmol) in CH_2Cl_2 (40 ml) at $-78^\circ C$. The reaction mixture was allowed to warm to room temperature ($20^\circ C$) and stirred for 14 h. The solvent was removed under vacuum, and the resulting reddish brown residue was redissolved in dry toluene (15 mL), the precipitated solid was filtered through a sintered crucible under N_2 atmosphere. The removal of solvent from the yellow filtrate gave the complex 4- $C_p^*TiCl[O,O,N]$ as reddish orange solid with a yield of 82% (2.2 g).

Properties of 4- $C_p^*TiCl[O,O,N]$ complex



Formula: $C_{33}H_{38}ClNO_2Ti$

Nature: Reddish brown solid

Mol.Wt.: 563 g/mol

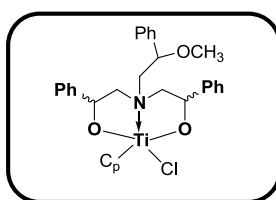
Yield: 82%

1H -NMR (400 MHz, $CDCl_3$): 2.35 (s, 15H, C_5Me_5), 2.83-3.31 (m, 4H, N- CH_2), 4.10-4.71 (m, 2H, N- CH_2 -Ph), 5.64-5.68 (m, 1H, CH-Ph), 7.11-7.37 (m, 15H, ArH).

6.3.2.3. Synthesis and Characterization of complex 6-C_pTiCl[O,O,N]

A yellowish solution of C_pTiCl₃ (0.45 g, 2 mmol) in dry CH₂Cl₂ (40 mL) was added dropwise to a solution of **6-H₂** (0.8 g, 2 mmol) and triethylamine (0.8 mL, 6 mmol) in CH₂Cl₂ (40 mL) at -78°C. The reaction mixture was allowed to warm to room temperature (20°C) and stirred for 14 h. The solvent was removed under vacuum, and the resulting reddish brown residue was redissolved in dry toluene (15 mL), the precipitated solid was filtered through a sintered crucible under N₂ atmosphere. The removal of solvent from the yellow filtrate gave the complex 6-C_pTiCl[O,O,N] as yellow solid with a yield of 75% (0.8 g).

Properties of 6-C_pTiCl[O,O,N] complex



Formula: C₃₀H₃₂ClNO₂Ti

Nature: Yellow solid

Mol.Wt.: 536 g/mol

Yield: 75%

¹H-NMR (400 MHz, CDCl₃): 2.55-3.08 (m, 4H, N-CH₂), 3.10-3.23 (s, 3H, OCH₃), 3.30-3.58 (m, 2H, N-CH₂-Ph), 4.43-4.57 (m, 1H, CH-OMe), 5.44-5.99 (m, 1H, CH-Ph), 6.46-6.50 (s, 5H, C₅H₅), 7.17-7.37(m, 15H, ArH).

6.4. General procedure for solution polymerization

All polymerization reactions were carried out under a dry and inert atmosphere using vacuumed flame-dried Schlenk apparatus. In a typical polymerization, a magnetically stirred flame dried reaction vessel (50 (or) 100 cm³) was charged with the respective monomer in dry toluene. The solution was thermostated at the required temperature, to which a required catalyst solution was added. After the required polymerization time, the polymerization was terminated by the addition of 5 mL of methanol solution, and the solvent was evaporated to dryness. The crude polymer obtained was dissolved in dichloromethane, and precipitated with excess of methanol; the white solid obtained was then filtered and washed with copious amount of methanol to remove any unreacted monomer, dried in vacuum, to yield the polymers.

6.4.1. Solution polymerization of Lactides

In a typical polymerization, a magnetically stirred flame dried reaction vessel (50 cm³) was charged with the monomer (L-LA or rac-LA, 1 g, 6.9 mmol) in dry toluene (10 mL) and the solution was thermostated at 70°C. A solution of complex **1-Ti(OⁱPr)₂** (11.7 mg, 0.023 mmol) in toluene (5 mL) was added to the preheated solution of L-LA and the polymerization was continued until the required polymerization time (22h). The polymerization was terminated by the addition of 5 mL of methanol solution. The polymer so obtained was dissolved in dichloromethane, and an excess of methanol was added. The resulting reprecipitated polymer (white solid) was filtered, washed with methanol, dried in vacuum, and weighed for calculating the yield. The polymer was characterized by ¹H & ¹³C NMR spectroscopy and SEC analysis.

Characterization of Poly(L-lactide): ¹H NMR analysis of PLLA (400 MHz, CDCl₃, 25°C): 1.15 (dd, J = 6Hz, CH(CH₃)₂ end group), 1.40 (d, J = 6.8 Hz, 3H, CH₃CH(OH) end group), 1.57 (d, J = 6.8 Hz, 3H, C(O)CHCH₃), 4.36 (q, J = 6.8 Hz, 1H, CH₃CH(OH) end group), 4.92 (sept, J = 6 Hz, 1 H, CH(CH₃)₂ end group), 5.16 (q, J = 6.8 Hz, 1H, C(O)CHCH₃).

¹³C NMR analysis of PLLA (100 MHz, CDCl₃, 25°C): 16.6 (C(O)CHCH₃), 20.5 (CH₃CH(OH) end group), 21.64 (CH(CH₃)₂ end group), 66.7 (CH(CH₃)₂ end group), 69.26 (CH₃CH(OH) end group), 69 (C(O)CHCH₃), 169.6 (C(O)CHCH₃).

Characterization of Poly(DL-lactide): ¹H NMR analysis of PDLLA (400 MHz, CDCl₃, 25°C): 1.18 (dd, J = 6 Hz, CH(CH₃)₂ end group), 1.43 (d, J = 6.8 Hz, 3H, CH₃CH(OH) end group), 1.49 (m, 3H, C(O)CHCH₃), 4.25 (q, J = 6.8 Hz, 1H, CH₃CH(OH) end group), 4.94 (sept, J = 6 Hz, 1 H, CH(CH₃)₂ end group), 5.05 (m, 1H, C(O)CHCH₃).

¹³C NMR analysis of PDLLA (100 MHz, CDCl₃, 25°C): 16.6 (C(O)CHCH₃), 20.5 (CH₃CH(OH) end group), 21.64 (CH(CH₃)₂ end group), 66.6 (CH(CH₃)₂ end group), 67.96 (CH₃CH(OH) end group), 69.2 (C(O)CHCH₃), 169.6 (C(O)CHCH₃).

6.4.2. Solution polymerization of ε-caprolactone

In a typical polymerization, a magnetically stirred flame dried reaction vessel (50 cm³) was charged with the monomer (ε-CL, 1 mL, 9 mmol) in dry toluene (8 mL) and the solution was thermostated at 70°C. A solution of complex **1-Ti(OⁱPr)₂** (15 mg, 0.03 mmol) in toluene (2 mL) was added to the preheated solution of ε-CL and the polymerization was continued until the required polymerization time (2.5 h). The polymerization was terminated by the addition of 5 mL of methanol solution. The polymer so obtained was dissolved in dichloromethane, and an excess of methanol was added. The resulting reprecipitated polymer (white solid) was filtered, washed with methanol, dried in vacuum, and weighed for calculating the yield. The polymer was characterized by ¹H & ¹³C NMR spectroscopy and SEC analysis.

Characterization of Polycaprolactone: ^1H NMR analysis of PCL (400 MHz, CDCl_3 , 25°C): 1.15 (d, $J = 6\text{ Hz}$, 6H, $\text{CH}(\text{CH}_3)_2$ end group), 1.29 (m, 2H, CH_2 backbone), 1.53 (m, 4H, CH_2 backbone), 2.2 (m, 2H, CH_2 backbone), 3.57 (t, $-\text{CH}_2\text{OH}$ end group), 3.97 (t, 2H, OCH_2 backbone), 4.9 (sept, $J = 6\text{ Hz}$, $\text{CH}(\text{CH}_3)_2$ end group).

^{13}C NMR analysis of PCL (100 MHz, CDCl_3 , 25°C): 21.85 ($\text{CH}(\text{CH}_3)_2$ end group), 24.57, 25.53, 28.35 (CH_2 backbone), 34.12 (CH_2CO), 62.62 ($-\text{CH}_2\text{OH}$ end group), 64.14 (OCH_2 backbone), 67.47 ($\text{CH}(\text{CH}_3)_2$ end group), 173.53 ($-\text{C}(\text{O})-\text{O}(\text{CH}_2)_5-$).

6.4.3. Solution polymerization of β -butyrolactone

In a typical polymerization, a magnetically stirred flame dried reaction vessel (50 cm^3) was charged with the monomer (β -BL, 1 mL, 12.2 mmol) in dry toluene (8 mL) and the solution was thermostated at 70°C . A solution of complex **1-Ti(OⁱPr)₂** (31.2 mg, 0.061 mmol) in toluene (2 mL) was added to the preheated solution of β -BL and the polymerization was continued until the required polymerization time (20 h). The polymerization was terminated by the addition of 5 mL of methanol solution. The polymer so obtained was washed with methanol, yielding poly(β -Butyrolactone) as a viscous liquid. The polymer was characterized by ^1H & ^{13}C NMR spectroscopy and SEC analysis.

Characterization of Poly(β -butyrolactone): ^1H NMR analysis of PBL (400 MHz, CDCl_3 , 25°C): 1.15 (dd, $J = 6.0\text{ Hz}$, $\text{CH}(\text{CH}_3)_2$ end group), 1.19-1.22 (m, 6H, $\text{C}(\text{O})\text{CH}_2\text{CH}(\text{CH}_3)$, $\text{C}(\text{O})\text{CH}_2\text{CH}(\text{CH}_3)-\text{OH}$ end group), 2.4-2.6 (m, 2H, $-\text{C}(\text{O})\text{CH}_2-\text{CH}(\text{CH}_3)$), 4.12 (br(m), 1H, $-\text{CH}(\text{CH}_3)-\text{OH}$ end group), 4.93 (sept, $J = 6\text{ Hz}$, 1H, $\text{CH}(\text{CH}_3)_2$ end group), 5.15-5.21 (m, 1H, $-\text{C}(\text{O})\text{CH}_2-\text{CH}(\text{CH}_3)$).

^{13}C NMR analysis of PBL (100 MHz, CDCl_3 , 25°C): 19.8 ($-\text{C}(\text{O})\text{CH}_2-\text{CH}(\text{CH}_3)$), 21.7 ($\text{CH}(\text{CH}_3)_2$ end group), 67.6 ($-\text{C}(\text{O})\text{CH}_2-\text{CH}(\text{CH}_3)$), 169.2 ($-\text{C}(\text{O})\text{CH}_2-\text{CH}(\text{CH}_3)$).

6.4.4. Solution polymerization of Trimethylene carbonate

In a typical polymerization, a magnetically stirred flame dried reaction vessel (50 cm^3) was charged with the monomer (TMC, 0.25 g, 2.44 mmol) in dry toluene (3 mL) and the solution was thermostated at 70°C . A solution of complex **4-Ti(OⁱPr)₂** (4 mg, 0.0081 mmol) in toluene (1 mL) was added to the preheated solution of TMC and the polymerization was continued until the required polymerization time (7h). The polymerization was terminated by the addition of 5 mL of methanol solution. The polymer so obtained was dissolved in dichloromethane, and an excess of methanol was added. The resulting reprecipitated polymer (white solid) was filtered, washed with methanol, dried in vacuum. The polymer was characterized by ^1H & ^{13}C NMR spectroscopy and SEC analysis.

Characterization of Poly(TMC): ^1H NMR analysis of PTMC (400 MHz, CDCl_3 , 25°C): 1.22 (d, $J = 6$ Hz, $\text{CH}(\text{CH}_3)_2$ end group), 1.95 (quintet, $J = 6.4$ Hz, 2H, $-\text{OCH}_2\text{CH}_2\text{CH}_2\text{O}$), 3.65 (t, 2H, $J = 6$ Hz, $-\text{CH}_2\text{OH}$ end group), 4.15 (t, $J = 6$ Hz, 4H, $-\text{OCH}_2\text{CH}_2\text{CH}_2\text{O}$), 4.7-4.8 (sept, $J = 6$ Hz, 1H, $\text{CH}(\text{CH}_3)_2$ end group).

^{13}C NMR analysis of PTMC (100 MHz, CDCl_3 , 25°C): 21.5 ($\text{CH}(\text{CH}_3)_2$ end group), 28 ($-\text{OCH}_2\text{CH}_2\text{CH}_2\text{O}$), 64.2 ($-\text{OCH}_2\text{CH}_2\text{CH}_2\text{O}$), 155 ($\text{C}(\text{O})-\text{OCH}_2$).

6.5. General procedure for kinetic studies on Lactide and ϵ -CL polymerization

Kinetic studies of polymerizations were carried out in toluene solution under a dry and inert atmosphere using vacuumed flame-dried special Schlenk apparatus equipped with a withdrawal vial on the side of the main flask. In a typical procedure, a 50 mL flame-dried special schlenk apparatus was charged with the monomer in toluene, and the solution was thermostated at the required temperature (25°C or 70°C), and the polymerization reaction was initiated by the addition of catalyst solution. At precise time intervals, aliquots were withdrawn through vacuum flame-dried withdrawal vial attached to the flask. A droplet of MeOH was then introduced, and the aliquot was removed from the withdrawal vial. The sample was quenched with methanol, dried and analyzed by ^1H NMR and SEC analysis.

6.6. Synthesis and Characterization of Block copolymers

6.6.1. Synthesis of Poly(ϵ -caprolactone-*block*-L-lactide)

In a typical polymerization, a magnetically stirred flame dried reaction vessel (100 cm^3) was charged with the first monomer (ϵ -CL, 2 mL, 18 mmol) in dry toluene (10 mL) and the solution was thermostated at 70°C . A solution of complex $1\text{-Ti}(\text{O}^i\text{Pr})_2$ (30.7 mg, 0.06 mmol) in toluene (2 mL) was added to the preheated solution of ϵ -CL and the polymerization was continued until the required polymerization time (3 h). Aliquot (0.5 mL) was taken from the polymerization mixture and quenched with methanol; completion of reaction was deduced from the ^1H NMR analysis and the molar mass were determined from the SEC analysis. Subsequently, the second monomer (L-LA, 1 g, 6.9 mmol) was added to the polymerization mixture and thermostated at the same temperature (70°C). The polymerization was continued until the complete monomer conversion for a period of (24h). The polymerization was terminated by the addition of 5 mL of methanol solution. The polymer so obtained was dissolved in dichloromethane, and an excess of methanol was added. The resulting reprecipitated polymer (white solid) was filtered, washed with methanol, dried in vacuum, and weighed for calculating the yield. The polymer was characterized by ^1H & ^{13}C NMR spectroscopy and SEC analysis.

Characterization of PCL-*b*-PLLA: ^1H NMR analysis of PCL-*b*-PLLA (400 MHz, CDCl_3 , 25°C): 1.15 (d, $J = 6$ Hz, 6H, $\text{CH}(\text{CH}_3)_2$ end group), 1.29 (m, 2H, CH_2 backbone), 1.52 (d, $J = 7.2$ Hz, 3H, $\text{C}(\text{O})\text{CHCH}_3$), 1.53-1.62 (m, 4H, CH_2 backbone), 2.22 (m, 2H, CH_2 backbone), 4.05 (t, 2H, OCH_2 backbone), 4.29 (q, 1H, $\text{CH}_3\text{CH}(\text{OH})$ end group), 4.92 (sept, $J = 6$ Hz, 1 H, $\text{CH}(\text{CH}_3)_2$ end group), 5.08 (q, $J = 7.2$ Hz, 1H, $\text{C}(\text{O})\text{CHCH}_3$). ^{13}C NMR analysis of PCL-*b*-PLLA (100 MHz, CDCl_3 , 25°C): 16.6 ($\text{C}(\text{O})\text{CHCH}_3$), 24.5, 25.5, 28.3 (CH_2 backbone), 34.1 (CH_2CO), 64.1 (OCH_2 backbone), 69.0 ($\text{C}(\text{O})\text{CHCH}_3$), 169.6 ($\text{C}(\text{O})\text{CHCH}_3$), 173.5 ($-\text{C}(\text{O})-\text{O}(\text{CH}_2)_5-$).

6.6.2. Synthesis of Poly(L-lactide-*b*- ϵ -caprolactone)

In a typical polymerization, a magnetically stirred flame dried reaction vessel (100 cm^3) was charged with the first monomer (L-LA, 1 g, 6.9 mmol) in dry toluene (10 mL) and the solution was thermostated at 70°C . A solution of complex $1\text{-Ti}(\text{O}^i\text{Pr})_2$ (11.7 mg, 0.023 mmol) in toluene (2 mL) was added to the preheated solution of L-LA and the polymerization was continued until the required polymerization time (24 h). Aliquot (0.5 mL) was taken from the polymerization mixture and quenched with methanol; completion of reaction was deduced from the ^1H NMR analysis and the molar mass were determined from the SEC analysis. Subsequently, the second monomer (ϵ -CL, 1 mL, 9 mmol) was added to the polymerization mixture and thermostated at the same temperature (70°C). The polymerization was continued until the complete monomer conversion for a period of (3 h). The polymerization was terminated by the addition of 5 mL of methanol solution. The polymer so obtained was dissolved in dichloromethane, and an excess of methanol was added. The resulting reprecipitated polymer (white solid) was filtered, washed with methanol, dried in vacuum, and weighed for calculating the yield. The polymer was characterized by ^1H & ^{13}C NMR spectroscopy and SEC analysis.

Characterization of PLLA-*b*-PCL: ^1H NMR analysis of PLLA-*b*-PCL (400 MHz, CDCl_3 , 25°C): 1.17 (dd, $J = 6$ Hz, 6H, $\text{CH}(\text{CH}_3)_2$ end group), 1.27 (m, 2H, CH_2 backbone), 1.51 (d, $J = 7.2$ Hz, 3H, $\text{C}(\text{O})\text{CHCH}_3$), 1.55-1.62 (m, 4H, CH_2 backbone), 2.22 (m, 2H, CH_2 backbone), 3.57 (t, $-\text{CH}_2\text{OH}$ end group), 3.99 (t, 2H, OCH_2 backbone), 4.92 (sept, $J = 6$ Hz, 1 H, $\text{CH}(\text{CH}_3)_2$ end group), 5.08 (q, $J = 7.2$ Hz, 1H, $\text{C}(\text{O})\text{CHCH}_3$). ^{13}C NMR analysis of PLLA-*b*-PCL (100 MHz, CDCl_3 , 25°C): 16.6 ($\text{C}(\text{O})\text{CHCH}_3$), 24.5, 25.5, 28.3 (CH_2 backbone), 34.0 (CH_2CO), 64.1 (OCH_2 backbone), 68.9 ($\text{C}(\text{O})\text{CHCH}_3$), 169.5 ($\text{C}(\text{O})\text{CHCH}_3$), 173.5 ($-\text{C}(\text{O})-\text{O}(\text{CH}_2)_5-$).

6.6.3. Synthesis of Poly(*DL*-lactide-*block*- ϵ -caprolactone)

In a typical polymerization, a magnetically stirred flame dried reaction vessel (100 cm³) was charged with the first monomer (*DL*-LA, 1 g, 6.9 mmol) in dry toluene (10 mL) and the solution was thermostated at 70°C. A solution of complex **1-Ti(OⁱPr)₂** (11.7 mg, 0.023 mmol) in toluene (2 mL) was added to the preheated solution of L-LA and the polymerization was continued until the required polymerization time (24 h). Aliquot (0.5 mL) was taken from the polymerization mixture and quenched with methanol; completion of reaction was deduced from the ¹H NMR analysis and the molar mass were determined from the SEC analysis. Subsequently, the second monomer (ϵ -CL, 0.8 mL, 6.9 mmol) was added to the polymerization mixture and thermostated at the same temperature (70°C). The polymerization was continued until the complete monomer conversion for a period of (3 h). The polymerization was terminated by the addition of 5 mL of methanol solution. The polymer so obtained was dissolved in dichloromethane, and an excess of methanol was added. The resulting reprecipitated polymer (white solid) was filtered, washed with methanol, dried in vacuum, and weighed for calculating the yield. The polymer was characterized by ¹H & ¹³C NMR spectroscopy and SEC analysis.

Characterization of PDLLA-*block*-PCL: ¹H NMR analysis of PDLLA-*b*-PCL (400 MHz, CDCl₃, 25°C): 1.17 (dd, J = 6 Hz, 6H, CH(CH₃)₂ end group), 1.27-1.35 (m, 2H, CH₂ backbone), 1.47-1.52 (m, 3H, C(O)CHCH₃), 1.55-1.62 (m, 4H, CH₂ backbone), 2.22 (m, 2H, CH₂ backbone), 3.57 (t, -CH₂OH end group), 3.99 (t, 2H, OCH₂ backbone), 4.92 (sept, J = 6 Hz, 1 H, CH(CH₃)₂ end group), 5.04-5.18 (m, 1H, C(O)CHCH₃).

¹³C NMR analysis of PLLA-*b*-PCL (100 MHz, CDCl₃, 25°C): 16.6 (C(O)CHCH₃), 24.4, 25.4, 28.3 (CH₂ backbone), 34.1 (CH₂CO), 64.1 (OCH₂ backbone), 68.9 (C(O)CHCH₃), 169.1-170.3 (C(O)CHCH₃), 173.5 (-C(O)-O(CH₂)₅-).

6.6.4. Synthesis of Poly(TMC-*block*- ϵ -caprolactone)

In a typical polymerization, a magnetically stirred flame dried reaction vessel (50 cm³) was charged with the first monomer (TMC, 0.2 g, 1.95 mmol) in dry toluene (3 mL) and the solution was thermostated at 70°C. A solution of complex **1-Ti(OⁱPr)₂** (4 mg, 0.0065 mmol) in toluene (1 mL) was added to the preheated solution of TMC and the polymerization was continued until the required polymerization time (7 h). Aliquot (0.2 mL) was taken from the polymerization mixture and quenched with methanol; completion of reaction was deduced from the ¹H NMR analysis and the molar mass were determined from the SEC analysis. Subsequently, the second monomer (ϵ -CL, 0.5 mL, 4.38 mmol) was added to the polymerization mixture and thermostated at the same temperature (70°C). The polymerization was continued until the complete monomer conversion for a period of (3 h). The polymerization was terminated by the addition of 5 mL of methanol solution. The polymer so obtained was dissolved in

dichloromethane, and an excess of methanol was added. The resulting reprecipitated polymer (white solid) was filtered, washed with methanol, dried in vacuum, and weighed for calculating the yield (76%). The polymer was characterized by ^1H & ^{13}C NMR spectroscopy and SEC analysis.

Characterization of PTMC-*b*-PCL: ^1H NMR analysis of PTMC-*b*-PCL (400 MHz, CDCl_3 , 25°C): 1.22 (d, $J = 6.4$ Hz, $\text{CH}(\text{CH}_3)_2$ end group), 1.27-1.35 (m, 2H, CH_2 backbone), 1.53-1.62 (m, 4H, CH_2 backbone), 1.95 (quintet, $J = 6.4$ Hz, 2H, $-\text{OCH}_2\text{CH}_2\text{CH}_2\text{O}-$), 3.58 (t, 2H, $-\text{CH}_2\text{OH}$ end group), 3.99 (t, 2H, OCH_2 backbone), 4.17 (t, $J = 6.4$ Hz, 4H, $-\text{OCH}_2\text{CH}_2\text{CH}_2\text{O}-$), 4.7-4.8 (sept, $J = 6$ Hz, 1H, $\text{CH}(\text{CH}_3)_2$ end group). ^{13}C NMR analysis of PTMC-*b*-PCL (100 MHz, CDCl_3 , 25°C): 24.5, 25.5 (CH_2 backbone), 28 ($-\text{OCH}_2\text{CH}_2\text{CH}_2\text{O}-$), 28.3 (CH_2 backbone of PCL), 34.1 (CH_2CO), 64.1 ($-\text{OCH}_2\text{CH}_2\text{CH}_2\text{O}-$), 155 ($\text{C}(\text{O})-\text{OCH}_2-$), 173.5 ($-\text{C}(\text{O})-\text{O}(\text{CH}_2)_5-$).

6.6.5. Synthesis of Poly(ϵ -CL-*b*-L-LA-*b*- ϵ -CL)

In a typical polymerization, a magnetically stirred flame dried reaction vessel (100 cm^3) was charged with the first monomer (ϵ -CL, 1 mL, 9 mmol) in dry toluene (10 mL) and the solution was thermostated at 70°C . A solution of complex **1-Ti(O^{*i*}Pr)₂** (15.3 mg, 0.03 mmol) in toluene (2 mL) was added to the preheated solution of ϵ -CL and the polymerization was continued until the required polymerization time (3 h). Aliquot (0.5 mL) was taken from the polymerization mixture and quenched with methanol; completion of reaction was deduced from the ^1H NMR analysis and the molar mass were determined from the SEC analysis for first block (PCL). Subsequently, the second monomer (L-LA, 0.5 g, 3.5 mmol) was added to the polymerization mixture and thermostated at the same temperature (70°C). The polymerization was continued until the complete monomer conversion for a period of (24h). Aliquot (0.5 mL) was taken from the polymerization mixture and quenched with methanol; completion of reaction was deduced from the ^1H NMR analysis and the molar mass were determined from the SEC analysis for second block (PLLA). The third monomer (ϵ -CL, 1 mL, 9 mmol) was subsequently added to the polymerization mixture and the polymerization was continued at the same temperature for a period of 3h. The polymerization was terminated by the addition of 5 mL of methanol solution. The polymer so obtained was dissolved in dichloromethane, and an excess of methanol was added. The resulting reprecipitated polymer (white solid) was filtered, washed with methanol, dried in vacuum, and weighed for calculating the yield. The polymer was characterized by ^1H & ^{13}C NMR spectroscopy and SEC analysis.

6.6.6. Synthesis of Poly(L-LA-*block*- ϵ -CL-*block*-L-LA)

In a typical polymerization, a magnetically stirred flame dried reaction vessel (100 cm³) was charged with the first monomer (L-LA, 0.5 g, 3.45 mmol) in dry toluene (10 mL) and the solution was thermostated at 70°C. A solution of complex **1-Ti(OⁱPr)₂** (17.4 mg, 0.034 mmol) in toluene (2 mL) was added to the preheated solution of L-LA and the polymerization was continued until the required polymerization time (24 h). Aliquot (0.5 mL) was taken from the polymerization mixture and quenched with methanol; completion of reaction was deduced from the ¹H NMR analysis and the molar mass were determined from the SEC analysis of the first block (PLLA). Subsequently, the second monomer (ϵ -CL, 2 mL, 18 mmol) was added to the polymerization mixture and thermostated at the same temperature (70°C). The polymerization was continued until the complete monomer conversion for a period of (3 h). Aliquot (0.5 mL) was taken from the polymerization mixture and quenched with methanol; completion of reaction was deduced from the ¹H NMR analysis and the molar mass were determined from the SEC analysis for second block (PCL). The third monomer (L-LA, 0.5 g, 3.45 mmol) was subsequently added to the polymerization mixture and the polymerization was continued at the same temperature for a period of 24 h. The polymerization was terminated by the addition of 5 mL of methanol solution. The polymer so obtained was dissolved in dichloromethane, and an excess of methanol was added. The resulting reprecipitated polymer (white solid) was filtered, washed with methanol, dried in vacuum, and weighed for calculating the yield. The polymer was characterized by ¹H & ¹³C NMR spectroscopy and SEC analysis.

6.7. General procedure for Bulk polymerization

A magnetically stirred flame dried Schlenk flask was charged with the required catalyst and the respective monomer at the desired metal to initiator ratio and heated to the required temperature 70°C or 100°C for respective time period 10 or 30 min with stirring (solution becomes viscous within 10 min). The mixture was cooled to room temperature, and the polymerization reaction was quenched by adding 5 mL of methanol, and the resulting solution was evaporated to dryness to give the crude polymer. The crude polymer was dissolved in dichloromethane, and the polymer was precipitated with excess of methanol, white solid obtained was filtered and dried in vacuum.

6.8. Random copolymerization

6.8.1. Synthesis of Poly(ϵ -caprolactone-*co*-DL-lactide)

In a typical polymerization, a magnetically stirred flame dried reaction vessel (50 cm³) was charged sequentially with *rac*-D,L-LA (0.5 g, 3.46 mmol), ϵ -CL (0.4 g, 3.46 mmol), in 7 mL of toluene. The mixture was thermostated at 70°C, and 1 mL of a solution (toluene) of complex 4-Ti(O^{*i*}Pr)₂ (20 μ mol) was added. After 24h, the polymerization mixture was quenched with 5 mL of methanol. The copolymer was purified by redissolving in CH₂Cl₂ and precipitating from rapidly stirring methanol solution. The polymer was recovered by filtration, dried in vacuum to give a highly viscous liquid. The polymer was then characterized by ¹H & ¹³C NMR spectroscopy.

Characterization of PCL-*co*-PDLLA: ¹H NMR analysis of PCL-*co*-PDLLA (400 MHz, CDCl₃, 25°C): 1.16 (d, 6H, CH(CH₃)₂ end group), 1.31-1.33 (m, 2H, CH₂ backbone), 1.44-1.52 (m, 3H, C(O)CHCH₃), 1.55-1.60 (m, 4H, CH₂ backbone), 2.21 (t, 2H, C(O)CH₂), 2.3 (m, 2H, C(O)CH₂), 3.99 (t, 2H, C(O)O-CH₂), 4.1 (t, 2H, C(O)O-CH₂), 5.0-5.18 (m, 1H, C(O)CHCH₃).

¹³C NMR analysis of PCL-*co*-PLLA (100 MHz, CDCl₃, 25°C): 16.6-16.9 (C(O)CHCH₃), 24.2-24.5, 25.1-25.5, 28.17, 28.33, 33.6-34.1, 64.1, 65.3, 68.2 (O-CO-(CH₂)₅-), 69.0-69.2 (C(O)CHCH₃), 169.2-169.7 (C(O)CHCH₃), 170.12-17.18 (C(O)O, CL-LA-LA), 170.26-170.31 (C(O)O, CL-LA-CL), 170.38 (C(O)O, LA-LA-CL), 170.88 (C(O)O, CL-LA-CL, trans esterification), 172.84 (C(O)O, LA-CL-LA), 172.91 (C(O)O, CL-CL-LA), 173.49 (C(O)O, LA-CL-CL), 173.57 (C(O)O, CL-CL-CL).

6.8.2. Synthesis of Poly(ϵ -caprolactone-*co*-L-lactide)

In a typical polymerization, a magnetically stirred flame dried reaction vessel (50 cm³) was charged sequentially with L-LA (0.5 g, 3.46 mmol), ϵ -CL (0.2 g, 1.73 mmol), 7 mL of toluene. The mixture was thermostated at 70°C, and 1 mL of a solution (toluene) of complex 4-Ti(O^{*i*}Pr)₂ (20 μ mol) was added. After 24h, the polymerization mixture was quenched with 5 mL of methanol. The copolymer was purified by redissolving in CH₂Cl₂ and precipitating from rapidly stirring methanol solution. The polymer was recovered by filtration, dried in vacuum to give a highly viscous liquid. The polymer was then characterized by ¹H & ¹³C NMR spectroscopy.

Characterization of PCL-co-PLLA: ^1H NMR analysis of PCL-co-PLLA (400 MHz, CDCl_3 , 25°C): 1.15-1.17 (dd, 6H, $\text{CH}(\text{CH}_3)_2$ end group), 1.32-1.45 (m, 2H, CH_2 backbone), 1.50 (d, 3H, $\text{C}(\text{O})\text{CHCH}_3$), 1.55-1.60 (m, 4H, CH_2 backbone), 2.23 (t, 2H, $\text{C}(\text{O})\text{CH}_2$), 2.31 (m, 2H, $\text{C}(\text{O})\text{CH}_2$), 3.99 (t, 2H, $\text{C}(\text{O})\text{O}-\text{CH}_2$), 4.05 (m, 2H, $\text{C}(\text{O})\text{O}-\text{CH}_2$), 5.0-5.18 (m, 1H, $\text{C}(\text{O})\text{CHCH}_3$).

^{13}C NMR analysis of PCL-co-PLLA (100 MHz, CDCl_3 , 25°C): 16.6-16.8 ($\text{C}(\text{O})\text{CHCH}_3$), 24.29-24.57, 25.18-25.52, 28.14, 28.34, 33.61-34.11, 64.13, 65.28, 68.2 ($\text{O}-\text{CO}-\text{CH}_2$), 69.0-69.2 ($\text{C}(\text{O})\text{CHCH}_3$), 169.52-169.74 ($\text{C}(\text{O})\text{CHCH}_3$), 170.0 ($\text{C}(\text{O})\text{O}$, CL-LA-LA), 170.23-170.28 ($\text{C}(\text{O})\text{O}$, CL-LA-CL), 170.34 ($\text{C}(\text{O})\text{O}$, LA-LA-CL), 172.80 ($\text{C}(\text{O})\text{O}$, LA-CL-LA), 172.88 ($\text{C}(\text{O})\text{O}$, CL-CL-LA), 173.43 ($\text{C}(\text{O})\text{O}$, LA-CL-CL), 173.52 ($\text{C}(\text{O})\text{O}$, CL-CL-CL).

6.9. Instrumentation and Characterization methods

- ^1H NMR (400 MHz) and ^{13}C NMR (100 MHz) spectra were recorded using Brüker Avance 400 ultra shield spectrometer at room temperature. The chemical shifts are referenced to the residual peaks of CDCl_3 (7.26 ppm, ^1H NMR; 77.0 ppm, ^{13}C $\{^1\text{H}\}$ NMR). Coupling constants are given in Hertz.
- Semi-preparative separation of ligand regioisomers were done in HPLC instrument equipped with Detector Varian 2550 at 254 nm and ODS column (Chromasil silice 10 micron, 100 angstroms), using $\text{CH}_3\text{OH}:\text{H}_2\text{O} = 80:20$ solvent system at a flow rate of 10 mL/min. Pump Prepstar 210 Varian, Injector Vanne Rhéodyne.
- Matrix-assisted laser desorption ionization time-of-flight (MALDI-TOF) mass spectrometry of the samples PLA and PCL was performed using a Voyager-DE STR (Applied Biosystems) spectrometer equipped with a nitrogen laser (337 nm), a delay extraction, and a reflector. The MALDI-TOF mass spectra represent averages over 100 laser shots. This instrument operated at an accelerating potential of 20 kV. Polymer (2 μL) and matrix (20 μL , dithranol) solutions in CH_2Cl_2 (10 $\text{g}\cdot\text{L}^{-1}$) were mixed with 2 μL of a sodium iodide solution (10 $\text{g}\cdot\text{L}^{-1}$ in methanol), which favors ionization. The final solution (1 μL) was deposited onto the sample target and dried in air at room temperature.

- Molar masses were determined by size exclusion chromatography (**SEC**) using a three column set of TSK gel TOSOH (G4000, G3000, G2000 with pore sizes of 20, 75, and 200 Å respectively, connected in series) calibrated with polystyrene standards, THF as eluent (1 mL/min) and trichlorobenzene as a flow marker at 25°C, using both refractometric and UV detectors (Varian). The molecular weights and molecular weight distributions of few polymers were determined by triple detector (SEC) in THF. Separation was achieved by three TSK gel columns with pore sizes of 10^3 , 10^4 , 10^5 Å. An interferometric refractometer (Wyatt Technology OPTILAB) and a multiangle light scattering detector equipped with a 632.8 nm laser (Wyatt Technology DAWN) positioned downstream of the columns enabled the determination of molecular weight based on dn/dc value of 0.058 mL g^{-1} for PLAs and 0.079 mL g^{-1} for PCL.
- Differential scanning calorimetry (**DSC**) measurements were performed on a DSC Q100 apparatus from TA Instruments. Data were recorded during the second run for temperatures ranging from -150°C to 100°C at a heating rate of $10^\circ\text{C min}^{-1}$. The cooling rate between the first and second runs was also equal to $10^\circ\text{C min}^{-1}$. The glass transition temperature (T_g) was given by the inflection point of the transition.

General Conclusions

General Conclusions

Poly(lactides (PLA), Poly(ϵ -caprolactone) and other related polyesters are of great interest since a couple of decades, due to their applications in the medical field thanks to their biodegradable, biocompatible, and permeable properties. They are also found to be good alternatives to non-biodegradable polymers. Ring-opening polymerization (ROP) of cyclic esters is the major polymerization method employed to synthesize these polymers. Even if many metal complexes have been used as initiators for the ROP of cyclic esters *via* coordination-insertion mechanism, group 4 metal complexes were less explored whereas they offer great opportunities to tune catalytic activity and stereoregularity. We have then developed new group 4 (Ti, Zr) metal alkoxide complexes containing aminodiols as the supporting ligand.

The aminodiol ligands were easily prepared under mild reaction conditions and assess to prepare ligands with variable structure (enantiomerically pure, racemic, meso and the diastereomeric mixture). Metal complexes were then easily synthesized by the reaction of proteo ligands with the corresponding metal precursor. The prepared complexes were characterized by ^1H and ^{13}C NMR analysis and utilized as initiators for the ROP of different cyclic esters. These titanium alkoxide complexes were found to be efficient initiators for the polymerization of L-lactide and rac-lactide under different polymerization conditions. In solution polymerization condition, the activity of complexes were comparable to some of the previously reported titanium alkoxide complexes derived from amine tris(phenolate) ligands, sulfonamide ligands, SALEN ligands and superior to titanium complexes derived from triethanolamine ligands. Under bulk polymerization condition at 130°C , catalysts exhibited a high activity (>95% conversion in 30 min) along with controlled molecular weight distribution as compare to few other titanium complexes (based on ligand type titanatranes, triethanolamine, amine-phenolate, salan) reported in the literature. End group analysis of polymers by ^1H NMR and MALDI-TOF mass spectrometry suggests the polymerization occurs *via* coordination insertion mechanism. For rac-LA polymerization, complex with racemic aminodiol ligand as an ancillary ligand produced PLA with 65% heterotactic selectivity in solution polymerization condition, whereas the same complex produced atactic PLA in bulk condition. Surprisingly, the complex derived from the chiral aminodiol ligand does not play a key role in the stereoselective polymerization in accordance with our expectations. All other complexes produced atactic PLA under both polymerization conditions. From this observation, we speculate that the origin of stereoselective in rac-lactide polymerization could be due to the chain end controlled mechanism (CEM).

These titanium complexes were also tested as initiators for the ROP of ϵ -CL under solution and bulk polymerization conditions. All complexes showed to be efficient initiators. For instance, under bulk polymerization condition at 70°C, monomer conversion higher than 60% was reached within 10 min. Activity of these complexes is comparable and also superior to other group 4 metal complexes reported in the literature. Similar to LA polymerization, end group analysis of PCL by ^1H NMR and MALDI-TOF mass spectrometry suggests the polymerization occurs *via* coordination insertion mechanism. Kinetic studies also revealed that the polymerization is first order with respect to monomer conversion. Preliminary polymerization was carried out with another class of lactone (*rac*- β -butyrolactone) and the activity was found to be less than that of ROP of ϵ -CL. Again, the end group analysis by ^1H NMR suggests coordination insertion mechanism, ring opening occurring *via* acyl-oxygen cleavage. Microstructure analysis by ^{13}C NMR confirms the synthesis of atactic PBL. ROP of TMC (trimethylene carbonate) has also been carried with our catalytic systems under solution and bulk conditions. Reasonably good activity and controlled molecular weight distribution were obtained. End group analysis by ^1H NMR suggests coordination insertion mechanism.

The control nature of the homopolymerization allowed us to synthesize diblock and triblock copolymers of ϵ -CL, L-LA, *rac*-LA and TMC by sequential polymerization techniques. The blocky nature of all the polymers was confirmed from the ^1H & ^{13}C NMR, SEC and DSC analysis. Diblock and triblock copolymers of type PCL-*b*-PLA, PCL-*b*-PLA-PCL were successfully synthesized by starting with ϵ -CL as “first monomer”, whereas synthesis of block copolymers of type PLA-*b*-PCL and PLLA-*b*-PCL-*b*-PLLA (starting with LA as “first monomer” sequencing) is associated with problem of reinitiation with few PLA macroinitiator as deduced from the ^1H NMR spectrum. Random copolymers of ϵ -CL/L-LA/*rac*-LA with various monomer compositions were successfully prepared both in bulk and solution conditions. Whereas, ϵ -CL is more reactive in homopolymerization than LA, a reverse reactivity order is observed during random copolymerization.

To conclude, titanium complexes based on aminodiols act as efficient initiators for the ROP of cyclic esters and carbonates and exhibited higher activity and better control over the molecular weight and molecular weight distribution than some other titanium alkoxide complexes reported in the literature. This could be due to the coordination of axial nitrogen atom from the ligand to the titanium metal center, making it less acidic, allowing to suppress side reactions and leading to good controlled polymerizations. The stereoselective nature of our catalytic system could also be improved either by changing the ligand substitution or incorporating the chiral center on the benzylic carbon. The corresponding zirconium and hafnium alkoxide complexes could also act as efficient initiators, especially for the stereoselective polymerization of *rac*-lactide and it should be studied in the near future.

